Cryogen Based Energy Storage: Process Modelling and Optimisation

Yongliang Li

Submitted in accordance with the requirements for the degree of
Doctor of Philosophy

The University of Leeds
Institute of Particle Science and Engineering
School of Process, Environmental & Materials Engineering

September 2011

The candidate confirms that the work submitted is his own and that appropriate credit has been given where reference has been made to the work of others.

Acknowledgements

I would like to express profound gratitude to my academic supervisor, Prof. Yulong Ding, for his invaluable support, endless encouragement, enthusiastic supervision and useful suggestions throughout this research work. His wide knowledge and his logical way of thinking have been of great value for me. His moral support and continuous guidance enabled me to process my work successfully. Going over the concepts with him again and again was always a distinct pleasure. I am also deeply indebted to Prof. Haisheng Chen (now with the Institute of Engineering Thermophysics of Chinese Academy of Sciences) for his detailed and constructive comments, and for his important support throughout this work.

I wish to express my warm and sincere thanks to Prof. Chunqing Tan from Institute of Engineering Thermophysics, Chinese Academy of Sciences, who introduced me to the field of thermodynamics. His ideals and concepts have had a remarkable influence on my entire career in the research field.

I gratefully acknowledge UK Highview Power Storage Ltd and UK Engineering and Physical Sciences Research Council (EPSRC) for their three and a half years financial support through the scheme of a Dorothy Hodgkin Postgraduate Award. I greatly appreciate the support received through the collaborative work undertaken with Highview Power Storage Ltd. Very special thanks are also due to the Institute of Particle Science and Engineering for the provision of a fantastic research environment. My colleagues in Prof. Ding's research group have supported me in various aspects of my research work and living. I want to thank them for all their help, support, interest and valuable comments. Expressly I am obliged to Dr. Lingling Zhang, Dr. Yunhong Jiang, Mrs. Hui Cao, Dr. Jianguo Cao, Mr. Yanping Du, Dr. Sanjeeva Witharana, Mr. Xinjing Zhang and Dr. Christopher Hodges.

Last but not least, a big thank you to my family. My parents Xiumei Fan and Gao Li are the two most special persons in my life. They, not only gave me life, but also fill it with all the love and affection one can wish for. A big thank you to my wife Janet Hong who accomplished without complaints the endless errands that I asked her to do, even when she was on peaks of stress and lack of sleep because of her studies. Without her I would be a very different person today, and it would have been much

harder to finish a PhD. Still today, learning to love her and to receive her love makes me a better person. I also would like to thank my son, Sean, simply for his existence. One day, he may be able to and inclined to understand what I have written here.

Abstract

Reliable operation of large scale electric power networks requires a balance of generation and end-user. The electricity markets mainly depend on the real-time balance of supply and demand because no sufficient power storage is available at present. As the difference between the peak and off-peak loads is significant, it is very expensive for the power companies to deal with the demand-supply mismatch. The situation is getting more challenging with the increasing use of renewable energy sources particularly wind and solar, which are intermittent and do not match the actual energy demand. This makes the large scale energy storage and power management increasingly important.

This thesis studies a Cryogen based Energy Storage (CES) technology which uses cryogen (or more specifically liquid air/nitrogen) as an energy carrier for large scale applications in Supply Side Management (SSM). The aim of this research is to seek the best routes and optimal operation conditions for the use of the CES technology. A systematic optimisation strategy is established by extending the concept of 'superstructure' and combining with Pinch Technology and Genetic Algorithm. Based on this strategy a program named Thermal System Optimal Designer (TSOD) is developed to evaluate or optimise both the thermodynamic and economic performances of thermal systems. Three types of CES systems are proposed and optimised for the applications of load levelling, peak-shaving and cryogenic energy extraction.

In the load levelling system it is found that the integration of air liquefaction and energy releasing process gives a remarkable improvement of the round trip efficiency. If the expander cycle is used to supply cold energy and the waste heat with a temperature higher than 600K is available, the round trip efficiency attains to 80 - 90% under rather reasonable conditions. Economic analyses reveal that such a CES system is very competitive with the current energy storage technologies if the operation period of the energy releasing unit is longer than 4 hours a day.

In the peak-shaving system CES is integrated with Natural Gas Combined Cycle (NGCC) to form oxy-fuel combustion for CO_2 capture. The optimisation of such systems gives an exergy efficiency of 70% and electricity storage efficiency of 67%

while using helium or oxygen as the blending gas. Economic analyses show that both the capital and peak electricity costs of the peak-shaving systems are comparable with the NGCC which are much lower than the oxy-NGCC if the operation period is relatively short. And the use of helium as the blending gas gives the lowest costs due to the lowest combustion pressure and mass flowrate.

A new solar-cryogen hybrid power system is proposed to extract cryogenic energy and to make use of solar radiation for power generation. The system is compared with a solar thermal power system and a cryogen fuelled power system. Thermodynamic analyses and optimisation show that the hybrid system provides over 30% more power than the summation of the power outputs of the other two systems. The results also suggest that the optimal hot end temperature of the heat carrier heated by the solar collectors be about 600K for the hybrid system.

Although interesting and promising results are obtained in this study, practical applications of CES technology meet a number of challenges including the dynamic operation and economic optimisation of the system in the simulation aspect and related experimental demonstration for both the key components and the integrated systems.

Table of Contents

List of Figures

List of Tables

Abbreviations

ASU:	Air Separasion (Liquefaction) Unit
BOG:	Boil-Off Gas
CAES:	Compressed Air Energy Storage
CES:	Cryogen based Energy Storage
DLL:	Dynamic Link Library
DMR:	Dual Mixed Refrigerant
DSM:	Demand Side Management
ECS:	Extended Corresponding State
EDU:	Energy Utilitization Diagram
EHTF:	Effective Heat Transfer Factor
GA:	Genetic Algorithm
HRSG:	Heat Recovery Steam Generator
LHV:	Low Heating Value
LNG:	Liquified Natural Gas
MAT:	Minimum Approach Temperature
MINLP:	Mixed-Integar Non-Linear Programming
MFC:	Mixed Fluid Cascade
MGT:	Mirror Gas Turbine
MRC:	Mixed Refrigerant Cycle
NGCC:	Natural Gas Combined Cycle
NIST:	National Institute of Standards and Technology
ORC:	Organic Rankine Cycle
PEM:	Proton Exchange Membrane
PHS:	Pumped Hydro Storage
TES:	Thermal Energy Storage
TIT:	Turbine Inlet Temperature
TSOD:	Thermal System Optimal Designer
SSM:	Supply Side Management
STPP:	Solar Thermal Power Plant

Nomenclature

A	surface area of a heat exchanger (m^2)
AL	energy level
C	capital cost of the system (US$/kW)
CE	electricity price (US$/kWh)
CF	fuel price (US$/kg)
CP	construction period (year)
C_p	Isobaric heat capacity (kJ/kg·K)
C_{SC}	concentration ratio of solar collector
D	density (kg/m^3)
E	exergy (kJ/kg)
${}^{S}E$	global irradiance of the solar energy
${}^{S}E_b$	direct radiation of the solar energy
${}^{S}E_d$	diffusion radiation of the solar energy
EXL	exergy loss in a process
f	annuity factor
f_S	dilution factor of solar irradiance
h	heat transfer coefficient ($W/(m^2 \cdot K)$)
H	enthalpy (kJ/kg)
in	interest rate (%/year)
I	component investment (US$)
IR	total irradiance energy of the solar collector (kJ)
k	amortization period (years)
$\dot{m}$	mass flowrate (kg/s)
O	operation period per day (hours)
P	pressure (kPa)
q	heat flow (kJ/kg)
Q	heat load (kJ)
ri	rate of inflation (%/year)
S	entropy (kJ/kg·K)

T	temperature (°C)
T_{CSC}	cover temperature of solar collector (°C)
T_S	the effective solar temperature (°C)
UF_{SC}	convection heat loss coefficient of solar collector ($Wm^{-2}K^{-1}$)
W	consumed/generated power (kW/kg)
ΔT_{MAT}	minimum approach temperature difference (°C)
ΔT_{pi}	pinch temperature difference (°C)
ΔA	average difference of A
x	liquid fraction
$(\alpha\tau)F_{SC}$	absorption term coefficient of solar collector
$(\alpha\varepsilon)F_{SC}$	emission term coefficient of solar collector
$(\varepsilon\overline{\rho})F_{SC}$	absorber loss term coefficient of solar collector
η	proportion/efficiency
σ	Stefan-Boltzmann constant ($W/(m^2 \cdot K^4)$)
γ	operation period ratio
η_e	exergy efficiency
η_s	electricity storage efficiency
φ	maintenance factor
$\overline{A}$	normalised value of A

subscripts

a	ambient condition
AC	adiabatic compressor
b	boiling point
c	carbon dioxide flow
C	cold flow
CF	cryogen fuelled power system
CP	compressor
ea	energy acceptor
ed	energy donor
EP	expender
f	fuel flow

g	gaseous phase
GEN	electricity generator
GT	gas turbine
H	hot flow
i	the i^{th} flow
IC	isothermal compressor
ie	isentropic process
it	isothermal process
I	flow inlet
l	liquid phase
n	liquid nitrogen flow
net	net value
o	oxygen flow
O	flow outlet
opk	off-peak hours
oxy	oxy-fuel combustion
P	pump
pi	pinch point
pk	peak hours
PS	peak-shaving system
r	real process
SC	solar collector
SCH	solar-cryogen hybrid power system
si	solar irradiance
SP	solar thermal power system
wh	waste heat

Chapter 1 Background and Motivation

1.1 Demand for Energy Storage

An electricity market consists of six primary elements, source, generation, storage, transmission and marketing, distribution and services, where the storage element ensures smooth operation of both generation and end-user. Unfortunately, no sufficient power storage is currently available and the electricity markets mainly depend on the real-time balance of supply and demand. This leads to a tremendous weakness: electricity must always be used precisely when it is produced. As a result, the current electric power market suffers from uncertainty, and both producers and consumers are experiencing and will continue to experience the consequence if the storage issue is not resolved.

1.1.1 Characteristics of End-users' Electric Demands

The end-users of a power system consist of these consumer groups: industrial, domestic and commercial including public lighting. The demand for electricity from these consumers is constantly changing, but broadly within the following categories:

- Seasonal (during dark winters more electric lighting and heating is required, while hot weather conditions boost the requirement for air conditioning)
- Weekly (many industrial operations close at weekends, and hence lowering the demand)
- Daily (peak hours when everyone arrives home and switches on the domestic applications)
- Hourly (for example towards a working day superposition of commercial, industrial, public lighting and residential uses occurs)
- Transient (fluctuations due to individual's actions and difference in power transmission efficiency etc)

In electricity supply side the transient fluctuations could be smoothed out by rapid-response energy storage technologies such as supercapacitors, rechargeable batteries and flywheel [1]. These technologies are generally of high rating and relatively small content and not suitable to be used to cope with high amount

outages. The other changes of electricity demand can be found from Figure 1.1, which shows the UK electricity demand as a function of time over a 24-hour period, metered half hourly by the National Grid [2]. One can see significant differences between summer and winter, weekday and weekend, and more significantly between the peak-load and off-peak load in a day. Currently the global demand for electric power increases about 2% each year and peak demand grows even faster than the average demand especially due to rapid increase in the use of large air conditioning systems [3]. As a consequence, the electrical industry must develop technologies to meet the highest peak of the year at any given moment and operate within a "just-in-time" framework that is dependent on variable end-use demands. This requirement is currently dealt with through the use of mixed generation, namely, base-load generation (e.g. coal-fired and nuclear) and peak-load (e.g. gas turbine) [4].

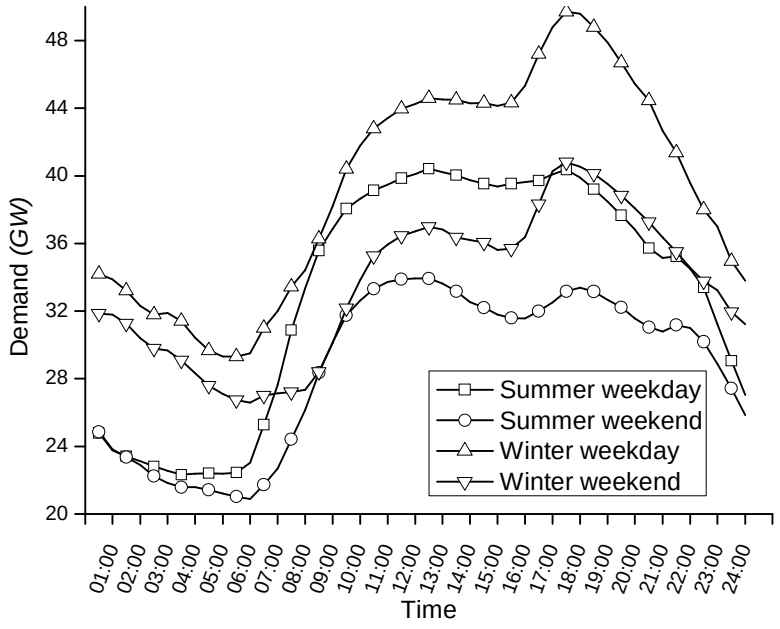

Figure 1.1 Typical electrical demand profile of UK in 2009

The base-load generation unit provides a steady flow of power regardless of total power demand by the grid. It runs all days and even all seasons except for scheduled maintenance and unscheduled repairs. The base-load plants usually run on low-cost fuels such as nuclear or coal so that they have fairly low operating costs but take several days to reach full scale operation.

The peak-load generation unit is made up of dispatchable power sources, including small scale gas turbines, diesel generators, and hydroelectric dams. It can operate on demand, supplementing the base-load to meet the peak time requirements. Gas turbines can go from standby to full power in less than 10 min, whereas diesel engines and turbines of hydro power plants require even less time [5]. Hydroelectric plants are not generally operated as base-load plants because the amount of operating time is restricted by the amount of water stored in the upper reserve. Peak electricity generation using gas turbines and diesel generators is very expensive, not only due to the high fuel costs (for example the fuel cost is some 3 to 5 times the cost of coal in the US, see Figure 1.2 [6]), but also because the expensive generating equipments are unused most of the time. On the other hand as the base-load capacity is much higher than the off-peak demand, the base-load generators often run below their maximum outputs and hence not at their best efficiencies. It is reported that the base-load power facilities in USA are used only 55% of the time on average, with the peak-load units going unused even 90% of the time, resulting in an inefficient use of investor, consumer and capital resources [3].

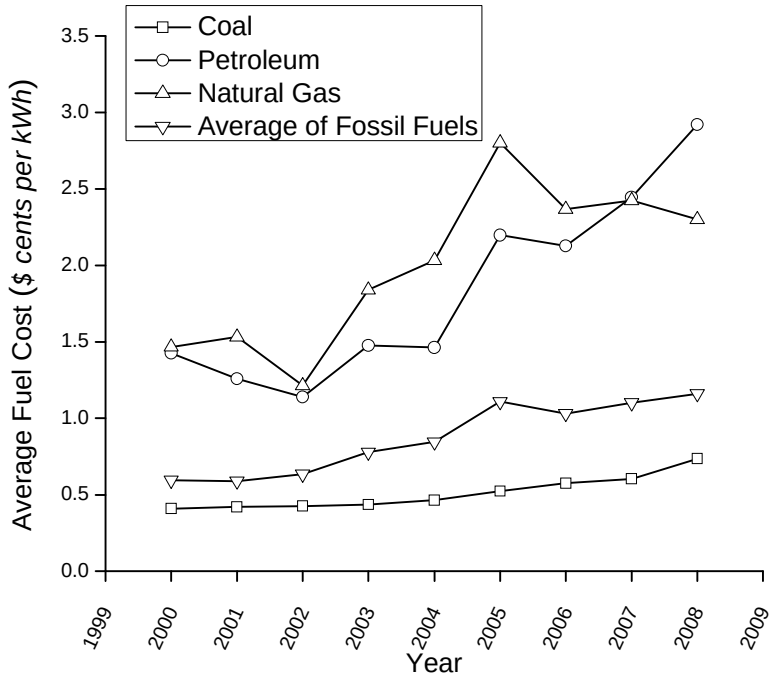

Figure 1.2 Electric power industry fuel costs in USA

In the electricity market, peak-load pricing often reflects the high investment made to meet the peak demand. Take the UK as an example, the growing electricity demand is straining the available power generation and transmission infrastructure, and meeting the peak demands in winter is increasingly expensive and high price spikes is often seen (Figure 1.3 [7]). In the USA extremely high cost has to be paid for peak demands in both winter and summer; see Figure 1.4 [8]. The great price difference makes the energy storage technologies attractive for shifting load from peak to off-peak hours, thus enabling the base-load generators to run closer to their best efficiencies for much of the time.

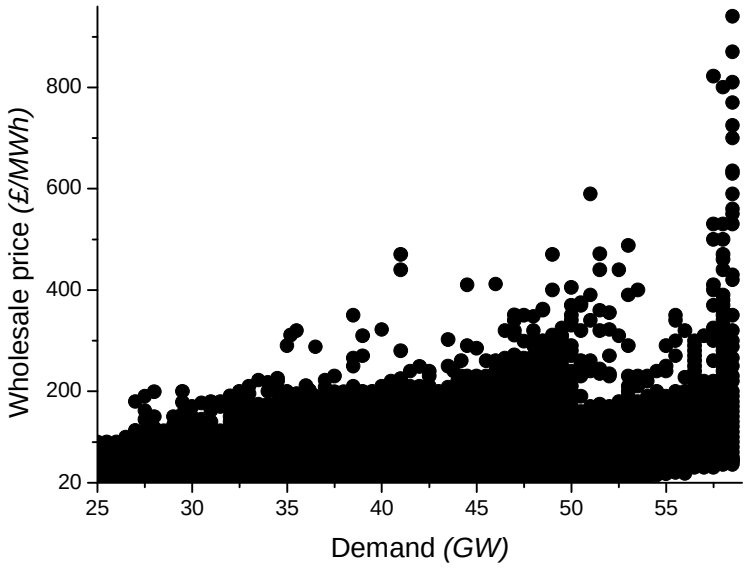

Figure 1.3 Wholesale price of UK electricity at different demand levels

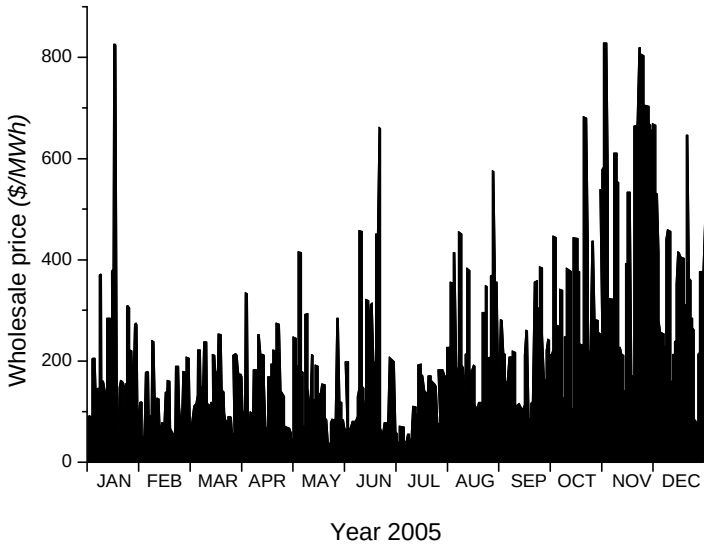

Figure 1.4 Wholesale price of USA electricity at different times

1.1.2 Characteristics of Renewable Energy Resources

Burning of fossil fuels has long been recognized as the main cause for some serious environmental issues including greenhouse effect, ozone layer depletion and acid rains [9]. An obvious (and also hard) solution is to replace the fossil fuels with renewable ones such as wind, solar and ocean energy etc [10]. Currently, the renewable energy resources account for about 5% of global power capacity and 3.4% of global power generation excluding large hydropower stations (which is about 15% of the global power generation capacity) [11]. Like a number of other countries, the UK government has set a target for increasing electricity generation from renewable resources from about 4.6% at present to 20% by 2020, and EU proposed recently an even higher goal of between 30 and 40% [12]. As a consequence, significant efforts have been made in the renewable energy research on solar, wind, biomass, ocean sources and geothermal sources.

However the use of renewable energy resources presents a number of challenges. First, renewable energy resources often have an unpredictability of supply, as they rely on the weather. Hydro generators need rain to fill dams to supply flowing water. Wind turbines need wind to turn the blades, and solar collectors need a clear sky and sunshine to harvest heat and generate electricity. Second, the time of availability of the renewable resources does not match the time-dependent demand of end-users. Third, the intermittent nature of the renewable resources can cause big issue

to the power transmission system, particularly when the amount exceeds 10-20% of the total load [13, 14].

Another issue associated with the renewable energy utilization is the remote locations of the resources. For example, the tidal potential resource in the Kimberly region of Australia is about eight times the current demand of the nation, whereas the tidal potential of the Shelikhov Gulf in the Okhotsk Sea in eastern Russia is about 80GW [15]. These locations are far away from any population areas or industry. As a result, harvest of the immense amount of renewable energy resources and deliver them in a useable form as a high-value product is another great challenge. Conventional electricity transmission and distribution approaches could be an option but it requires very high capital, operation and maintenance costs.

Energy storage technologies have a great potential to provide solutions to meet these challenges. Such technologies can not only help mitigate the issues of unpredictability of renewable energy resources but also provide an alternative transportation method if the energy carrier (e.g. hydrogen) used in the technology can be detached easily and completely from the generation and release devices. Figure 1.5 shows the overall requirements of energy storage together with their power and capacities [16]. By using suitable energy storage technologies, one would expect a more efficient market that costs less to operate, more responsive to market changes, and more reliable in the event of a disruption.

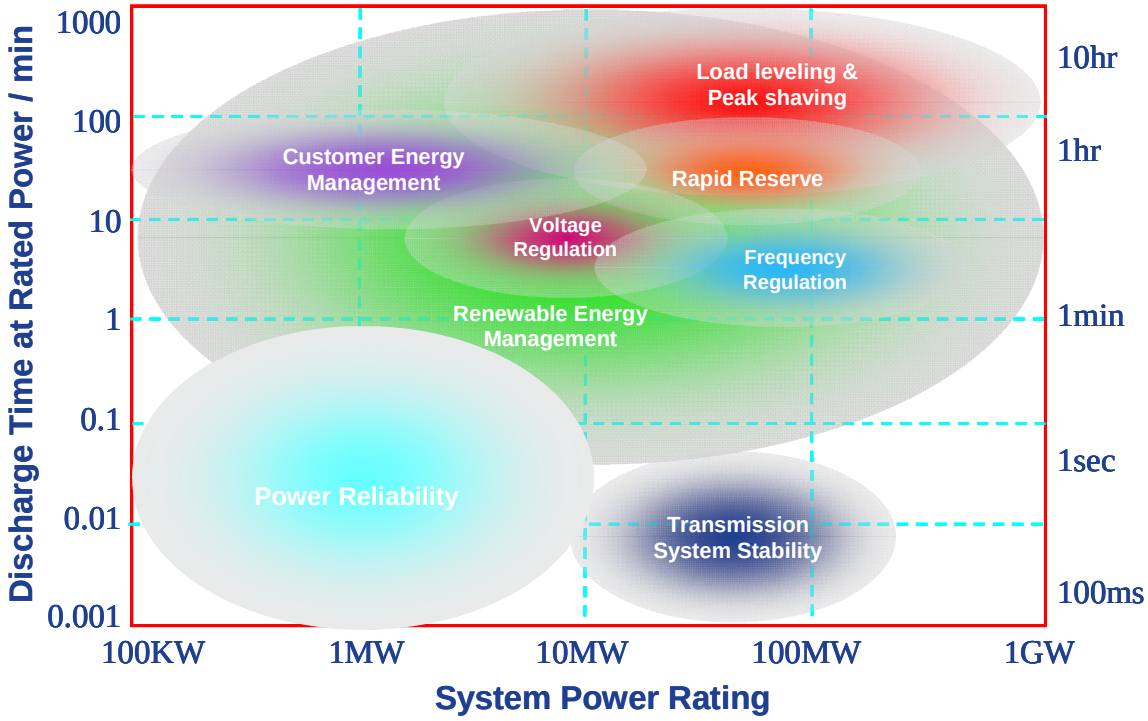

Figure 1.5 Overall requirements of energy storage technologies

1.2 Principles and Classifications of Energy Storage Technologies

Energy storage refers to a process of storing some forms of energy to perform some useful operations at a later time [17]. This work aims at electricity storage which can be done in the following forms:

- Electric & magnetic forms: (i) Electrostatic energy storage (capacitors and supercapacitors); (ii) Magnetic/current energy storage (Superconducting Magnetic Energy Storage).

- Mechanical form: (i) Kinetic energy storage (flywheels); (ii) Potential energy storage (Pumped Hydroelectric Storage and Compressed Air Energy Storage).

- Chemical form: (i) Electrochemical energy storage (conventional batteries such as lead-acid, nickel metal hydride, lithium ion and flow-cell batteries such as zinc bromine and vanadium redox); (ii) Chemical energy storage (hydrogen and Metal-Air batteries); (iii) Thermo-chemical energy storage (solar metal, solar ammonia dissociation–recombination and solar methane dissociation–recombination).

- Thermal form: (i) Low temperature energy storage (aquiferous cold energy storage, cryogenic energy storage); (ii) High temperature energy storage (sensible heat systems such as steam or hot water accumulators, graphite, hot rocks and concrete, latent heat systems such as phase change materials).

The present progress and possible development paths to the future of these technologies have been reviewed in detail by the research team at Leeds University [1]. In terms of the function, these technologies can be categorised into those that are intended firstly for high power ratings with a relatively small energy content making them suitable for power quality or reliability; and those designed for energy management, as shown in Figure 1.6. The energy management technologies could be used either as demand side management (DSM) tools for electrical and/or heat loads, or as supply side management (SSM) tools for efficient and economical power production.

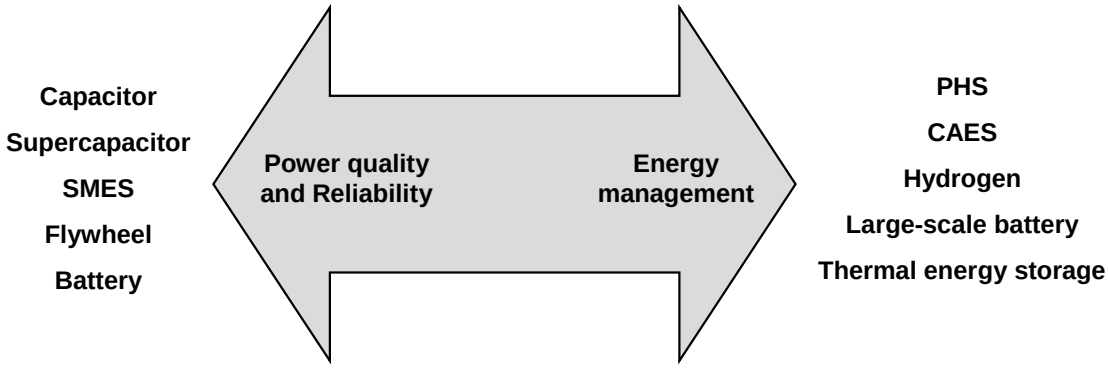

Figure 1.6 Classification of energy storage technologies with respect to function

As an effective SSM technology, bulk energy storage stores electrical energy during times when production (from power plants) exceeds consumption and the stores are used at times when consumption exceeds production. In this way, electricity production need not be drastically scaled up and down to meet momentary consumption – instead, production is maintained at a more constant level. This has the advantage that fuel-based power plants can be more efficiently and easily operated at constant production levels. In particular, the use of large scale intermittent renewable energy sources can benefit from bulk energy storage. Thus, bulk energy storage is one method that the operator of an electrical power grid can use to adapt energy production to energy consumption, both of which can vary randomly over time. However at present pumped hydro storage (PHS) and compressed air energy storage (CAES) are the only commercially available technologies capable of providing very large energy storage deliverability (above 100 MW with single unit), see Figure 1.7.

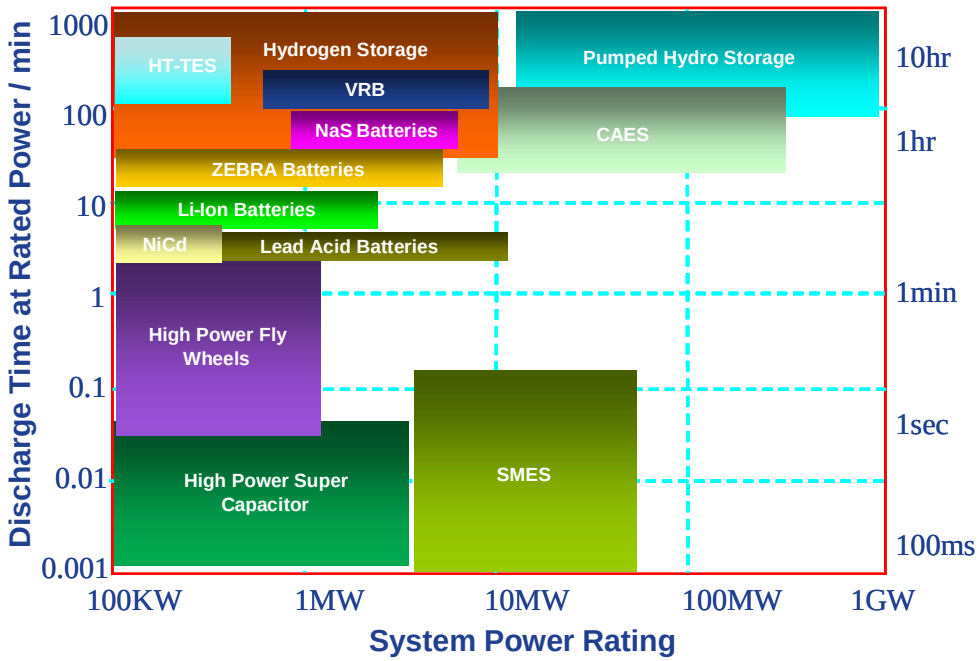

Figure 1.7 The power rating and capacities of current energy storage technologies

PHS works through pumping water to an elevated position (storing energy in the form of potential energy of water). Release of the energy occurs through flowing of water downwards to drive a hydro-turbine. PHS is a mature technology for large capacity and long period storage. The storage period of PHS can be varied from hours to days and even years. Taking into account the evaporation and conversion losses, the PHS has a round trip efficiency of about 60% to 85%. PHS was first used in Italy and Switzerland in the 1890s whereas the first large-scale commercial use was in the USA in 1929 (Rocky River PHS plant, Hartford). There is currently about 100 GW of PHS in operation worldwide with ~32 GW installed in Europe, ~21 GW in Japan, ~19.5 GW in the USA and others in Asia and Latin America. The PHS accounts for about 3% of global generation capacity [1]. As the most implemented bulk energy storage technology, future prospects of PHS is regarded as limited because there are less and less suitable sites for PHS. In addition, there are environmental and cost issues associated with PHS development [18].

CAES works on the basis of conventional gas turbine technology. It decouples the compression and expansion cycles of a conventional gas turbine generation process into two separated processes and stores the energy in the form of elastic potential energy of compressed air. CAES systems are designed to cycle on a daily basis and to operate efficiently during partial load conditions. This design approach allows

CAES units to swing quickly from generation to compression modes. Utility systems that benefit from the CAES include those with load varying significantly during the daily cycle and with costs varying significantly with the generation level or time of day. There are two CAES plants in operation in the world. The first CAES plant is in Huntorf, Germany, and has been in operation since 1978. The unit couples with 60 MW compressors providing a maximum pressure of 10 MPa and runs on a daily cycle with 8 hours of charging and can generate 290 MW for 2 hours. The plant has shown an excellent performance with 90% availability and 99% starting reliability. The second plant is in McIntosh, Alabama, USA, which has been in operation since 1991. The unit compresses air to up to ~7.5 MPa and has a generating capacity of 110 MW with a working duration of about 26 hours [18]. There are several large scale CAES units being planned or under construction such as the Norton, Ohio Project (9×300 MW) developed by Haddington Ventures Inc., Markham, Texas Project (4×135 MW) developed jointly by Ridege Energy Services and EI Paso Energy, Iowa Project (200 MW) developed by the Iowa Association of Municipal Utilities in the United States, and some other projects, e.g. Chubu Electric Project in Japan and Eskom Project in South Africa [1, 18]. Similar to the PHS, the major barrier to the implementation of large scale CAES is that the technology relies on suitable geological locations. It is only economically feasible for power plants that have nearby rock mines, salt caverns, aquifers or depleted gas fields.

Other site-free bulk energy storage methods of providing several MWh or higher capacity that have been demonstrated or proposed include hydrogen fuel storage, large-scale battery storage and flow batteries [1, 19-21]. The applications of hydrogen as an electrical energy storage medium strongly rely on the hydrogen storage technologies and chemical energy extraction methods, in particularly the development of fuel cell technology. This will be discussed in details in Chapter 2.

Rechargeable/secondary battery is the oldest and most developed form of electricity storage which stores electricity in the form of chemical energy. Batteries are in some ways ideally suited for electrical energy storage applications as they usually have very low standby losses and can respond very rapidly to load changes. However, large-scale utility battery storage (including NaS batteries, Li-Ion batteries, Lead Acid batteries etc.) has been rare up until fairly recently because of low energy densities, small power capacity, high maintenance costs, a short cycle life and a limited

discharge capability. In addition, most batteries contain toxic materials. Hence the ecological impact from uncontrolled disposal of batteries must always be considered.

A flow battery is a special type of rechargeable battery in which the electrolyte contains one or more dissolved electroactive species flowing through a power cell/reactor in which the chemical energy is converted to electricity. Additional electrolyte is stored externally, generally in tanks, and is usually pumped through the cell (or cells) of the reactor. In contrast to conventional batteries, flow batteries store energy in the electrolyte solutions. The power and energy ratings are independent of the storage capacity determined by the quantity of electrolyte used and the power rating by the active area of the cell stack. Flow batteries are distinguished from fuel cells by the fact that the chemical reaction involved is often reversible and they can be recharged without replacing the electroactive material. On the negative side, flow batteries are rather complicated in comparison with standard batteries as they may require pumps, sensors, control units and secondary containment vessels. The energy densities vary considerably but are, in general, rather low compared to portable batteries, such as the Li-ion. Some flow batteries (for example Vanadium Redox Battery and Zinc bromine battery) are technically developed and commercially available. However, the actual applications, especially for large-scale utility, are still not widespread. Their competitiveness and reliability still need more trials by the electricity industry and the market.

1.3 Cryogenic Energy Storage

Storing energy in the form of heat/cold is a physical process and therefore is benign to the environment. Thermal Energy Storage (TES) refers to a number of technologies that store energy in a thermal storage medium for later and/or suitable uses (time and/or location shifting). Applications of the TES technologies in the SSM often involve the use of a working temperature of the storage media that deviates (either increases or decreases) significantly from the ambient temperature. As an example of high temperature TES, high grade heat can be generated by solar energy to produce steam at 250-300°C [22-24]. Another example is the Archimedes project, where a binary mixture of molten salts (40% KNO_3, 60% $NaNO_3$) is used as a sensible heat storage medium, which is the world's first solar energy system integrated with a gas-fired combined cycle power plant and the working temperature ranges from 290 to 550°C [25].

Different from high temperature TES, the energy in low temperature TES is stored in a medium through decreasing its internal energy while increasing its exergy. Using cryogen as the energy storage medium was first proposed by E.M. Smith in 1977 [26] and has attracted lots of attention recently due to its potential for the SSM applications [27-30]. Such a method is also termed Cryogen based Energy Storage (CES).

A cryogen is normally defined as a liquid (liquefied gas) that boils at a temperature below about -150°C [28]. Examples of the cryogen include liquid nitrogen, liquid oxygen, liquid hydrogen, liquid helium and liquefied natural gas. Cryogenic engineering, a discipline dealing with production, storage and utilization of cryogen, went through a rapid development since 1940s when large scale air and helium liquefaction processes became practical. The cryogenic engineering enables rapid developments in numerous scientific fields including physics (superconducting), chemistry (cryogenic synthesis), biology (long terms storage of biological cells), analytic sciences (Cryo-TEM and SEM), and instrumentations (thermocouple calibration). In the energy field, liquefied natural gas (LNG) has become popular for large scale storage of natural gas and its transportation from the production sites to countries and cities thousands miles away [29]. It is anticipated that similar operations would occur for liquid hydrogen if the hydrogen economy become a reality [30]. Over the past decade or so, liquid nitrogen/air as a combustion free and non-polluting ‘fuel’ has attracted lots of attention [31]. In the following, fundamental aspects associated with cryogen as an energy carrier will be discussed and compared using liquefied nature gas, liquid hydrogen and liquid nitrogen as examples.

1.3.1 Exergy Density of Cryogens

Cryogens carry high grade cold energy, which according to the second law of thermodynamics, is a more valuable energy source than heat. The appropriate parameter to quantify the energy in terms of usefulness is exergy, which is defined as the maximum theoretical work obtainable by bringing the fluid into equilibrium with the environment. Assuming heat/cold is stored in a material with a constant specific heat, C_p, an increase or a decrease in its temperature by ΔT from the ambient temperature, T_a, will lead to an amount of heat, ΔQ, being charged or discharged into the material:

$$\Delta Q = C_p \Delta T \tag{1.1}$$

In a reversibly infinitesimal heat transfer process the exergy change of the material dE could be calculated as:

$$dE = dH - T_a \cdot \frac{\delta Q}{T} = C_p dT - T_a \cdot \frac{C_p dT}{T} \tag{1.2}$$

The exergy, ΔE, stored in the material therefore could be obtained by integrating Equation (1.2) from T_a to ($T_a + \Delta T$):

$$\Delta E = \int_{T_a}^{T_a+\Delta T} C_p \cdot \left(1 - \frac{T_a}{T}\right) dT = C_p(\Delta T - T_a \cdot \ln(\frac{T_a + \Delta T}{T_a})) \tag{1.3}$$

The combination of equations (1.1) and (1.3) gives the proportion of the available energy stored in the material (*η: the ratio of stored exergy and stored thermal energy*) as follow:

$$\eta = \frac{\Delta E}{|\Delta Q|} = \frac{\Delta T - T_a \cdot \ln(\frac{T_a + \Delta T}{T_a})}{|\Delta T|} \tag{1.4}$$

Equation (1.4) is illustrated in Figure 1.8 where the ambient temperature is assumed to be 25 ^{o}C. One can see from Figure 1.8 that, given a temperature difference, the stored cold is more valuable than the stored heat particularly at large temperature differences. It is also noted that the ratio of stored exergy and stored thermal energy may be greater than 1 while decreasing the temperature to an extreme low temperature.

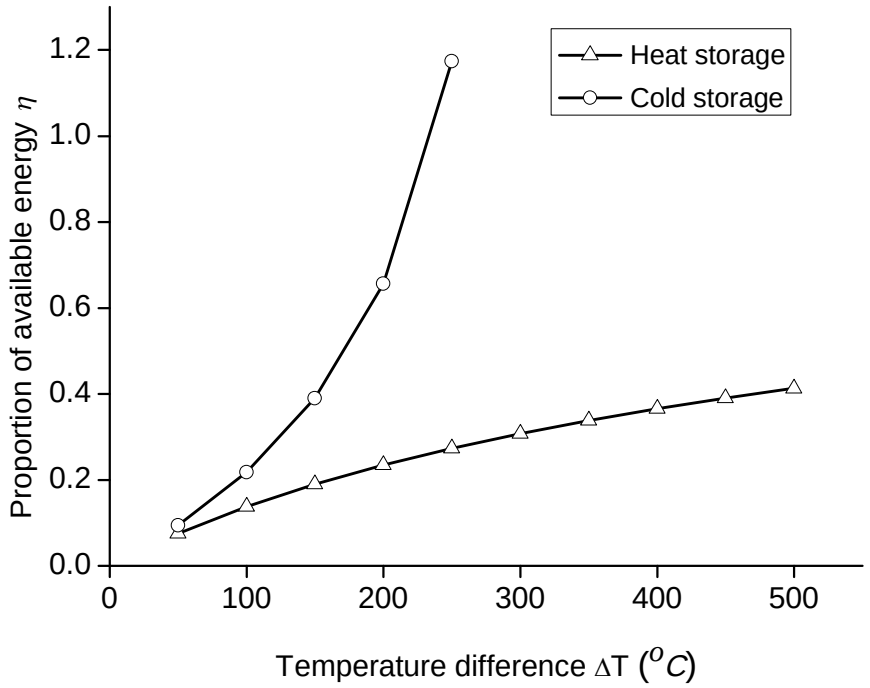

Figure 1.8 The proportion of the available energy as a function of temperature difference for heat and cold storage

The energy stored in a cryogen is in the form of both sensible and latent heat. Table 1.1 [25, 32] compares the specific heat, latent heat and exergy density of three typical cryogens with some commonly used heat storage media. One can see that, although the specific heat and phase change heat of the cryogens are of similar order of magnitude to these of the heat storage materials, the exergy density of cryogens is much greater. Among the cryogens listed, liquefied hydrogen has the highest exergy density (about an order of magnitude higher than the other materials). Liquid nitrogen has the lowest exergy density, but it is still much higher than high temperature thermal energy storage media. Note that the high exergy density of methane and hydrogen is mainly due to their chemical exergy; see below for more discussion.

Table 1.1 Comparison of specific heat, latent heat and exergy density of cryogens and some commonly used heat storage materials

Media components	Storage method [a]	Specific heat (kJ/kgK)	Phase-changing/Working temperature (℃)	Fusion/Latent heat (kJ/kg)	Exergy density (kJ/kg)
Rock	S	0.84 ~ 0.92	1000	N	455 ~ 499
Aluminum	S	0.87	600	N	222
Magnesium	S	1.02	600	N	260
Zinc	S	0.39	400	N	52
N_2 (liquid)	S+L	1.0 ~ 1.1	-196	199	762
CH_4 (liquid)	S+L	2.2	-161	511	1081
H_2 (liquid)	S+L	11.3 ~ 14.3	-253	449	11987
$NaNO_3$	L	N [b]	307	182	89
KNO_3	L	N	335	191	97
40% KNO_3+ 60% $NaNO_3$	S	1.5	290 ~ 550	N	220
KOH	L	N	380	150	82
$MgCl_2$	L	N	714	452	316
NaCl	L	N	801	479	346
Na_2CO_3	L	N	854	276	203
KF	L	N	857	425	313
K_2CO_3	L	N	897	236	176
38.5% MgCl+61.5% NaCl	L	N	435	328	190

[a] 'S' indicates thermal energy is stored in the form of sensible heat while 'L' stands for latent heat.
[b] 'N' refers to cases where data are not available.

1.3.2 Storage and Delivery of Cryogens

As mentioned above, cryogens can contain both physical (thermal) and chemical exergies. Table 1.2 shows a comparison between the three cryogens listed in Table 1.1. One can see that the density of the chemical exergy of liquid hydrogen and liquid methane are respectively ~10 times and 48 times their physical exergies. Liquid nitrogen does not have chemical exergy.

Cryogens are in liquid form, which are much easier to store and transport particularly when there are no pipelines. For example, for a given mass, liquefied methane (main component of natural gas) takes about 1/643 the volume of the gaseous methane at the ambient condition, whereas liquefied hydrogen takes about 1/860 the volume of gaseous hydrogen. It is anticipated that storage and transportation of liquid hydrogen will play a crucial role in the use of renewable energy to produce the energy carrier.

Table 1.2 Comparison of physical and chemical exergies of the cryogens

Cryogen	Thermal exergy (kJ/kg)	Chemical exergy (kJ/kg)	Gas density (kg/m^3)	Liquid density (kg/m^3)
Liquid H_2	11,987	116,528	0.0824	70.85
Liquid N_2	762	0	1.1452	806.08
Liquid CH_4	1,081	51,759	0.6569	422.36

Although liquid nitrogen contains no chemical exergy, its thermal exergy density is still highly competitive to the current battery technologies [1]. Therefore liquid nitrogen is regarded not only as an energy storage medium [27] but also as a potential combustion-free fuel for transportation [31].

Bulk cryogen storage is a developed technology with the development of LNG industry. The cryogenic tank with the single unit capacity of 150, 000 m^3 is currently in operation for the storage of LNG [33]. If such a container is used to store liquid nitrogen, the exergy capacity reaches about 25.5GWh. Considering that the market potential of bulk energy storage in the UK is about 80 to 100GWh, the storage of

cryogen is technically not an issue if liquid air or liquid nitrogen is used as the energy carrier for large scale energy management.

1.3.3 Thermodynamic Properties of Cryogens

In a power generation system, the working fluid of a thermal cycle, such as water/steam in a Rankine cycle or nitrogen/air in a Brayton cycle, is normally involved in the energy extraction process from the thermal storage media and the thermal energy storage media work only as the heat/cold sources in the cycle. In the cold energy extraction process, the cryogen, which serves as the cold source, can also be used as the thermal cycle working fluid through direct expansion cycles [31, 34]. Thermodynamically, the use of cryogen as the working fluid in thermal cycles can be very efficient in terms of recovering low grade heat. Currently low to medium grade heat is often recovered by steam cycles in which water/steam is the working fluid. For example, such an approach has been widely used to recover waste heat from the Brayton cycle with a Combined Cycle Gas Turbine (CCGT) technology. The approach has also been investigated for the use of low grade solar heat [24, 25, 35]. However, steam is not an idea working fluid for utilizing low grade heat as the critical temperature of water (374^{o}C) is much higher than the ambient temperature and its critical pressure (22.1MPa) is extremely high. Therefore in subcritical or even trans-critical cycles great proportion of heat is consumed for the vaporisation of the water during phase change. In these heat transfer processes a great portion of exergy is lost due to temperature glide mismatching between the heat source and the working fluid - the so-called pinch limitations [36, 37].

To compare the properties of thermal cycle working fluids in using a low grade heat source, a heat transfer process between the heat source and the working fluid is taken as an example. It is assumed that the working fluids are heated from ambient temperature, T_a, to T_H = 400^{o}C. A normalised heat, $\overline{Q}$, is used, which is defined as the ratio of heat load at a certain temperature, T, to the total heat exchange amount during the whole process.

$$\overline{Q}(T) = \frac{H(T) - H(T_a)}{H(T_H) - H(T_a)} \tag{1.5}$$

In equation (1.5) H is the enthalpy. The calculation results of equation (1.5) are shown in Figure 1.9 which compares the working fluid temperature dependence of the normalised heat of water with three cryogens, where the ambient temperature is

assumed to be 25^{o}C. One can see that, given a working pressure, the specific heat (the slope of the lines) for the three cryogens (hydrogen, methane and nitrogen) is approximately the same. However, different behaviour occurs to water. If the working pressure is lower than its critical value (22.1MPa), the specific heat of water changes greatly due to phase change. This leads to inefficient use of the heat source considering that the heat sources (hot-side working fluids) are mostly fluids with a constant specific heat (e.g. flue gases or hot air). Although water behaves similarly to the cryogens under supercritical conditions (e.g. the case with pressure of 300 bar in Figure 1.9), the high working pressure increases the technical difficulties in realizing the process.

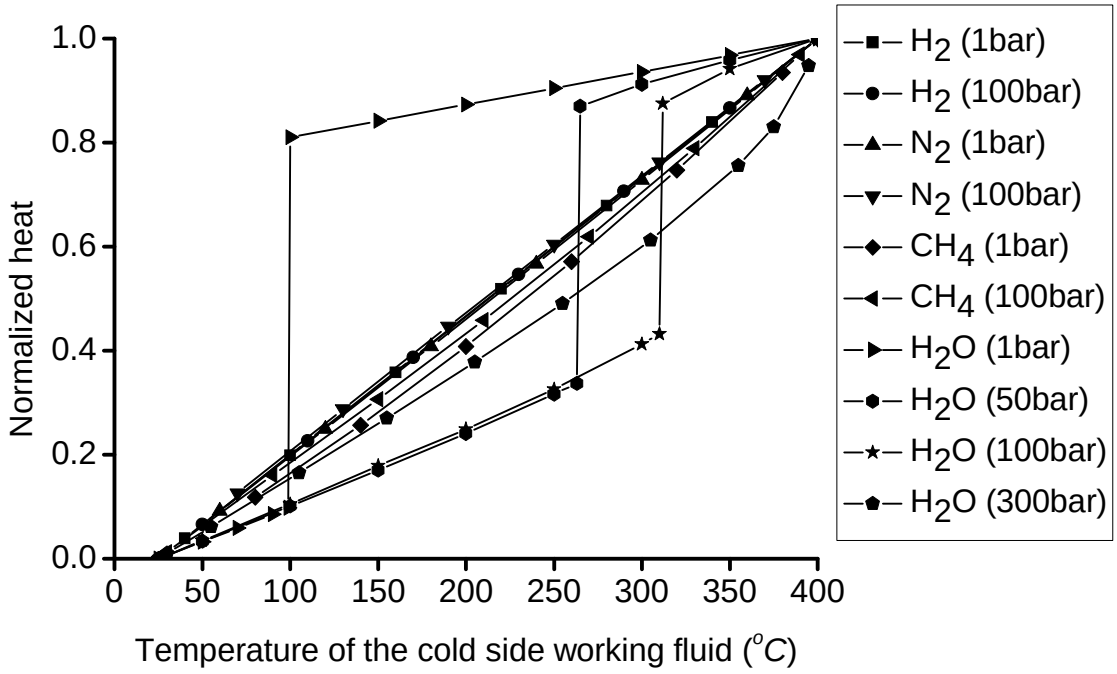

Figure 1.9 Normalised heat vs. cold side working fluid temperature diagram of some working fluids

Cryogens have a relatively high energy density in comparison with other thermal energy storage media and they can be efficient working media for recovering low grade heat due to their low critical temperature. These properties make the CES technology more attractive for large scale SSM. The CES process could be subdivided into three processes: gas liquefaction (cryogen production) for energy storage, cryogen storage and transportation and cryogenic energy extraction process. From this point of view, the current LNG industry is a CES process although

it mainly aims at the transportation of natural gas and the cryogenic energy is wasted in most LNG terminals.

1.4 Aim of This Research

The aim of this research is to seek the best routes and optimal operation conditions for the use of the CES technology. The main barrier for the use of CES is the low exergy efficiency of cryogen production process which is lower than ~ 50% with the current liquefaction technology as will be mentioned in the next chapter. It is therefore less attractive for the use of CES technology independently for large scale energy storage as lots of exergy loss during the process. However, in many cases when there are waste heat and renewable heat sources, CES can be integrated with other technologies to make it applicable. As a result, the first task of this work is to find out under what conditions the CES is applicable and why. The second task is on the thermodynamic modelling and optimisation of the specific systems to attain a suitable configuration and the best operational parameters together with an economic analysis.

1.5 Structure of This Dissertation

This thesis is structured into eight chapters. Chapter Two reviews two important technologies closely related to CES technology: gas liquefaction and cryogenic energy extraction. Another popular energy carrier, hydrogen, is also briefly reviewed and compared with cryogen in terms of production, transportation and energy extinction processes using the ocean energy exploitation as an example.

Chapter Three focuses on thermodynamic modelling and optimisation of complex power/thermal systems. A generalized technique combining Superstructure, Pinch Technology and Genetic Algorithms is proposed for the global optimisation including both configuration selection and parametric optimisation.

Chapter Four analyses the integration of the CES system with air liquefaction for electricity load levelling with industrial waste heat. The integrated system is optimised using the new method proposed in Chapter Three.

Chapter Five considers a peak-shaving power system which combines the CES, oxy-fuel combustion technologies with a natural gas fuelled power system and CO_2 capture. The global optimisation is carried out for the system. An economic analysis is also carried out.

Chapter Six presents a solar-cryogen hybrid power system aimed for use in large scale LNG terminals with good solar energy resources. A EUD method is used to analyse the results.

In Chapter Seven, a modelling and optimisation program is developed and the procedures of the software are introduced. An example is given to use the software for designing a large scale liquefaction system.

Chapter Eight summarises the key conclusions of this work. Recommendations for future work are also given based on the conclusions.

Chapter 2 Literature Review

2.1 Large Scale Gas Liquefaction

Gas liquefaction is a process of refrigerating a gas to a temperature below its critical temperature so that the liquid phase can be formed at a suitable pressure below its critical value. Many gases can be turned into a liquid state either at the normal atmospheric pressure or at a pressurized state by simple cooling. These processes are widely used for scientific, industrial and commercial purposes, for example in the medical and biological fields, in superconductivity research and in aerospace engineering [38, 39]. As the liquefaction plants use large amounts of process energy, it is vital for the overall energy chain performance that efficient liquefaction processes are developed.

Although many methods can be used to liquefy a gas, they operate on the same basic principle as shown in Figure 2.1. The feed gas is first compressed to an elevated pressure in an ambient-temperature compressor. This high-pressure gas is passed through a countercurrent heat exchanger to a decompressor (typically a Joule-Thomson valve). Upon expanding to a lower pressure, cooling takes place, and some liquid may form in the reservoir. The cool, low-pressure gas returns to the compressor inlet to repeat the cycle. The purpose of the countercurrent heat exchanger is to warm the low-pressure gas prior to recompression, and simultaneously to cool the high-pressure gas to the lowest temperature possible prior to expansion. This is the simplest cycle of gas liquefaction known as Linde-Hampson liquefier which was independently filed for patent by Hampson and Linde in 1895. The advantage of Linde-Hampson cycle is that it has no moving parts at the cold end. However, as the cooling load is supplied solely by the low-pressure returning gas, only a very small fraction of the main flow mass could be liquefied to give the end product. The actual exergy efficiencies are therefore under about 10% [40, 41].

The poor thermodynamic performance of Linde-Hampson cycle is caused by two main reasons: the exergy loss in irreversible throttling process and the poor match temperature profiles in the countercurrent heat exchanger as illustrated in Figure 2.2 where an example is taken for nitrogen liquefaction at 3.5 MPa. The large temperature differences in the heat transfer processes moves the system away from thermodynamic reversibility, and hence, leading to a low thermodynamic efficiency.

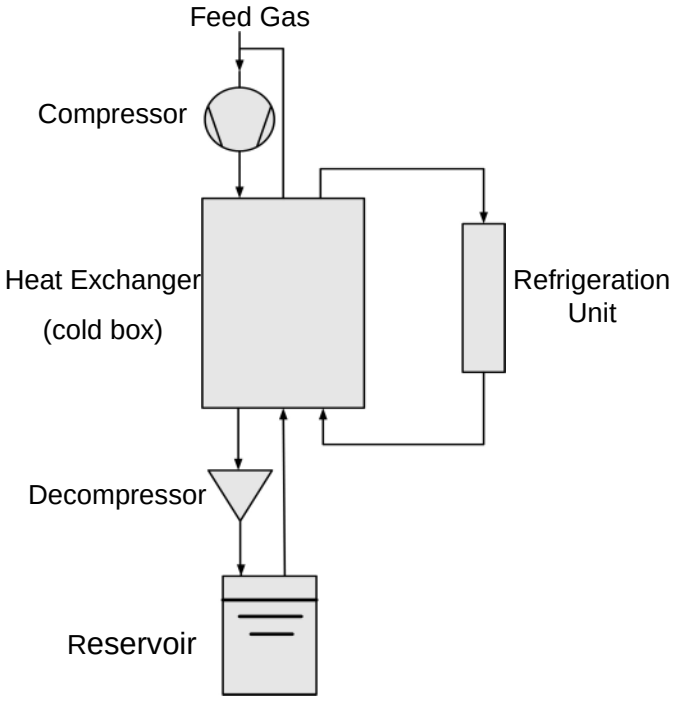

Figure 2.1 Principal process of gas liquefaction

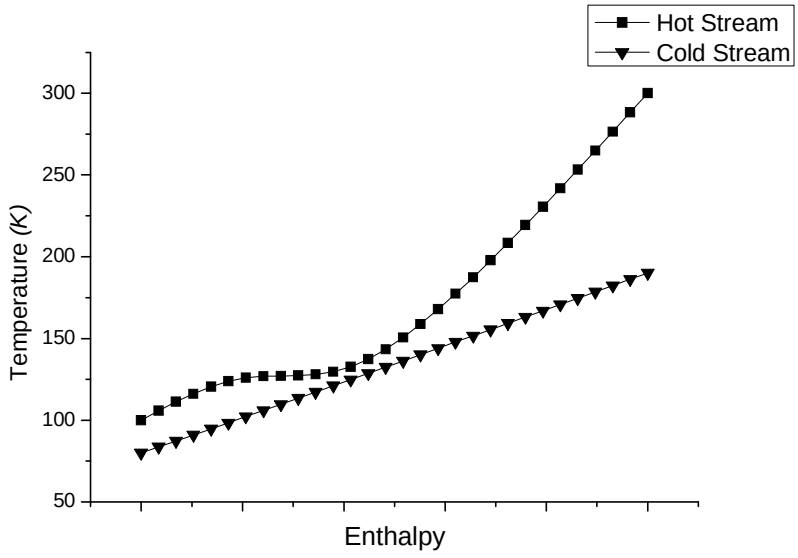

Figure 2.2 Temperature profiles of nitrogen liquefaction in a Linde-Hampson liquefier

In actual liquefaction systems an additional refrigeration unit is usually involved to produce cold energy for a better matched temperature profile and therefore an enhanced performance. According the configurations of the refrigeration unit the

liquefaction methods could be grouped into three main types, namely, the cascade cycle, the mixed refrigerant cycle (MRC) and the expander cycle [42-44]. The former two employ throttle valves with multiple or mixed refrigerants for the cold production while the third one uses compression and expansion machines with a single gas-phase refrigerant to generate cold power.

2.1.1 Cascade Refrigerant Cycle

The liquefaction processes feature the refrigeration cycles with the purpose of removing heat from hot streams. In a simple closed refrigeration cycle shown in Figure 2.3, the heat is removed by vaporization of a low pressure refrigerant in the evaporator which is then compressed and condensed at a higher pressure against a warmer cold utility or heat sink. External cold sources generally play the roles of heat sinks although part of the cooling power may be supplied by the refrigerant after evaporation in a self-cooling system. A major limitation of the simple refrigerant cycle that makes use of pure components as refrigerants is that refrigeration is provided at a constant temperature while the cold refrigerant is evaporating.

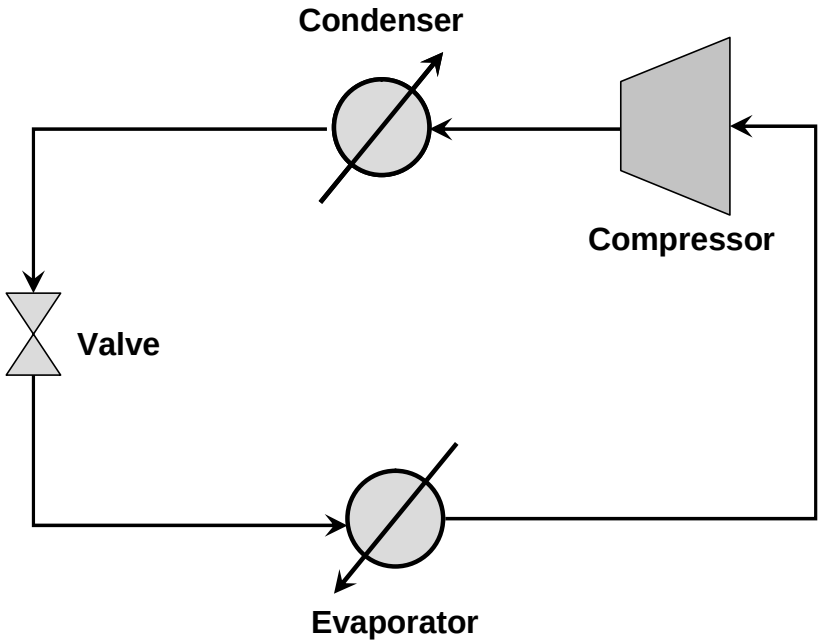

Figure 2.3 Flowsheet of a simple refrigerant cycle

To enable the refrigerant cycle supply the cooling power along a wide temperature range, a multilevel pure refrigerant system is likely to be implemented as seen in Figure 2.4 (a) where a three level configuration is shown as an example. In such a

system different pressure levels are used to provide refrigeration at different temperature levels; see Figure 2.4 (b) for the corresponding temperature profiles. It should be noted that both heat transfer area and complexity would increase as a consequence.

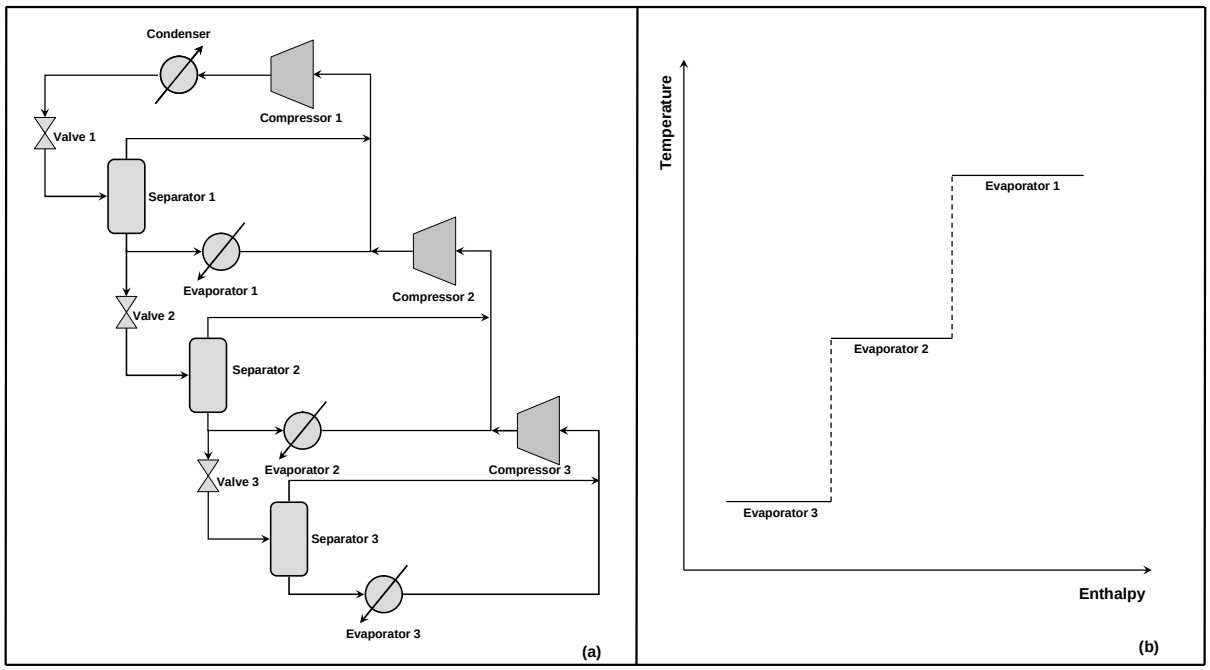

Figure 2.4 A three-level pure refrigerant cycle

Although multilevel pure refrigerant system could provide different levels of refrigeration, the temperature range of the cooling is still limited by the properties of the refrigerant. If the hot streams (streams that need cooling) demand the cooling task to be carried out along a wider temperature range, different sub-cycles using different refrigerants are integrated to improve the thermodynamic efficiency. Figure 2.5 (a) shows a multistage cascade refrigeration cycle for LNG production that uses three different refrigerants namely propane, ethane and methane in their individual refrigeration cycles. From the figure one can see that the propane cycle provide the low grade refrigeration (233-203K) for ethane condensing, methane pre-cooling and natural gas pre-cooling. The medium grade cold (193-163K) producer ethane cycle supplies refrigeration for methane condensing and natural gas further-cooling and the high grade cooling power (118-113K) is provided by the methane cycle for natural gas super-cooling [45]. In other words, in a cascade system the colder cycles reject heat to the warmer ones and eventually the warmest cycle rejects heat to an ambient utility. If each of the cycles operates at three evaporating temperature levels

as mentioned above, the cooling curve of natural gas and evaporation stages of the refrigerants could be charted in Figure 2.5 (b).

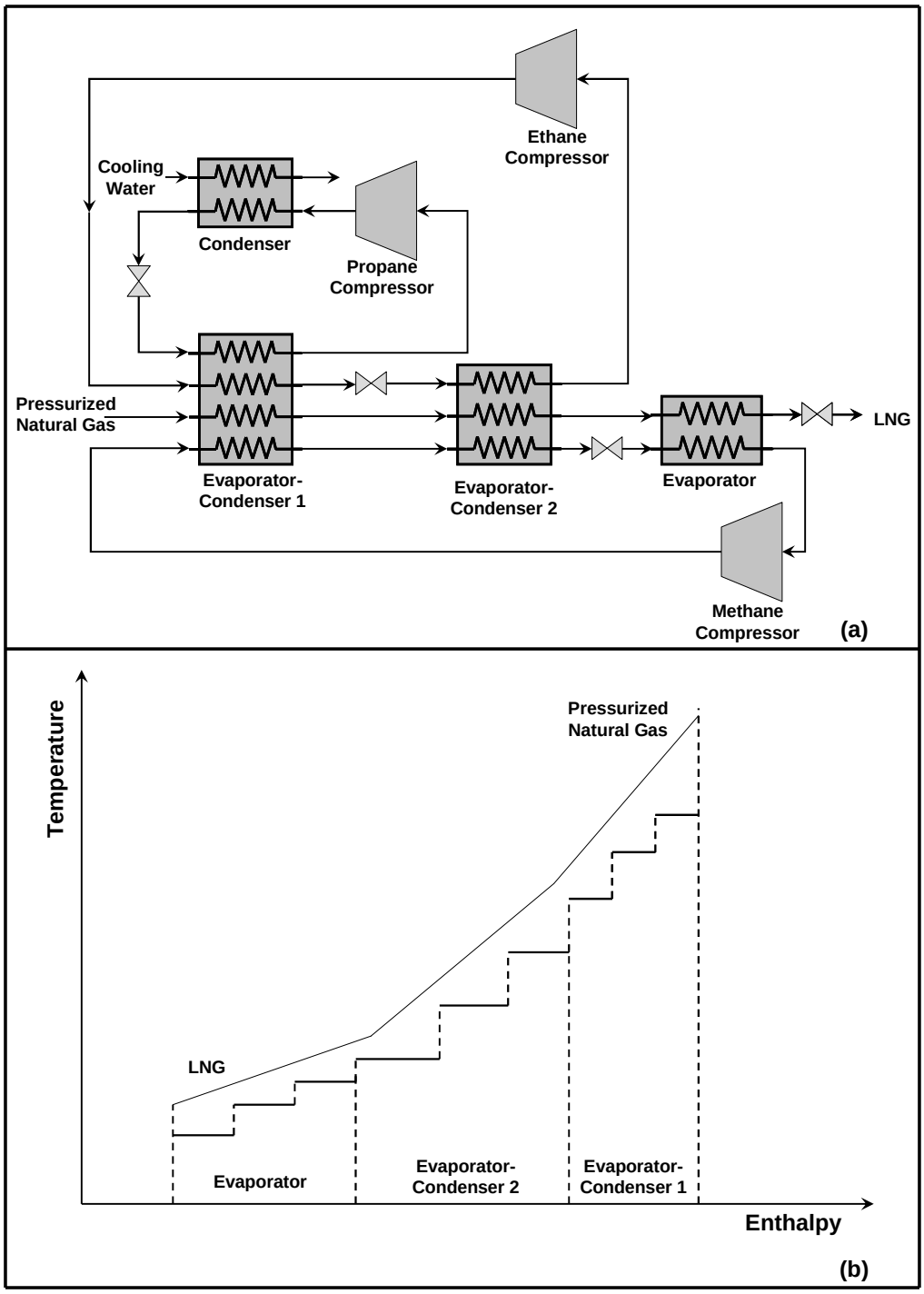

Figure 2.5 A schematic diagram of a cascade cycle for LNG production

The cascade cycle requires much less amount of power than the Linde-Hampson process, mainly because the flow of high grade refrigeration is lower and the mean temperature differences between the composite warming curve and cooling curve are smaller. It is reported the exergy efficiency of the multistage cascade

refrigeration cycle for nitrogen and natural gas liquefaction processes ranges from 40% to 55% [46-48]. Meanwhile, as the heat transfer occurs mainly in the evaporator and condenser, the cascade cycle has a comparatively low heat exchanger surface area requirement.

The major disadvantage of the cascade cycle is the relatively high capital cost due to the numbers of refrigeration compression circuits, each requiring its own compressor and refrigerant storage. Maintenance and spare equipment costs tend to be comparatively high due to the large number of machines [49]. Furthermore, as the refrigeration temperature range is limited by the properties of the refrigerants, the cascading cycle is not applicable for liquefying very low boiling point gases such as hydrogen and helium which are often done through the expander cycle [50]. Economic analyses show that the cascade cycle is most suited for large train sizes of offshore LNG production.

2.1.2 Mixed Refrigerant Cycle

The mixed refrigerant cycle (MRC) uses a single mixed refrigerant instead of the multiple pure refrigerants in the cascade cycle. The mixed refrigerants undergo isobaric phase change in the cycle through a range of temperatures between the dew and bubble points of the mixture. This is similar to liquefying process of the natural gas [51]. A mixture of nitrogen and hydrocarbons is normally used to provide optimal refrigeration characteristics. Table 2.1 shows an example of a refrigerant consisting of various components, typical for LNG production [52]. The temperature profiles of the mixed refrigerant are illustrated in Figure 2.6 together with that of their corresponding pure refrigerants. One can see that the mixed refrigerant can smooth the cooling curve via a non-constant temperature phase change process. Given a suitable pressure and a composition, a good match between the process and refrigerant temperature profiles can be obtained with a simple configuration.

Table 2.1 Mass fraction of components for mixed refrigerants

Components	CH_4	C_2H_6	C_3H_8	C_4H_{10}	C_5H_{12}	N_2
Mass fraction	0.12	0.40	0.09	0.04	0.26	0.09

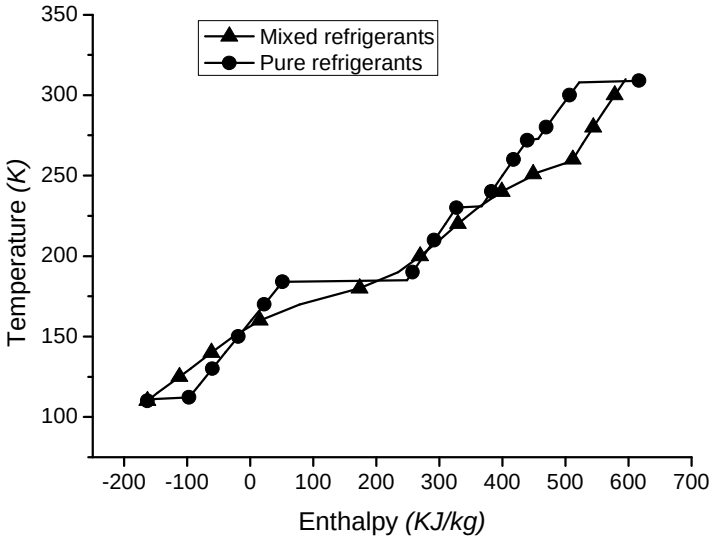

Figure 2.6 Temperature profiles of mixed refrigerants and their corresponding pure refrigerants

Theoretically a wide temperature range cooling power could be supplied by a suitable MRC with a very simple configuration as shown in Figure 2.3. However liquefying all the refrigerants directly requires a very high working pressure, making the system inefficient or even impractical. In a typical MRC, a self-cooling multi-stage configuration is employed as shown in Figure 2.7. The refrigerant stream, at approximately the ambient temperature and a low pressure, is compressed and partially condensed via air or cooling water in the condenser. The resulting vapor from Separator 1 is partially condensed in Heat Exchanger 1 by the returning refrigerants and the liquid is then expanded across a valve, reducing its temperature to supply cooling duty. Repeating this partial condensation and separation processes of the refrigerant stream leads to a multi-stage configuration. In such a self-cooling way the high pressure refrigerant is further cooled down and therefore can reach a lower temperature and/or a lower vapor fraction after the expansion.

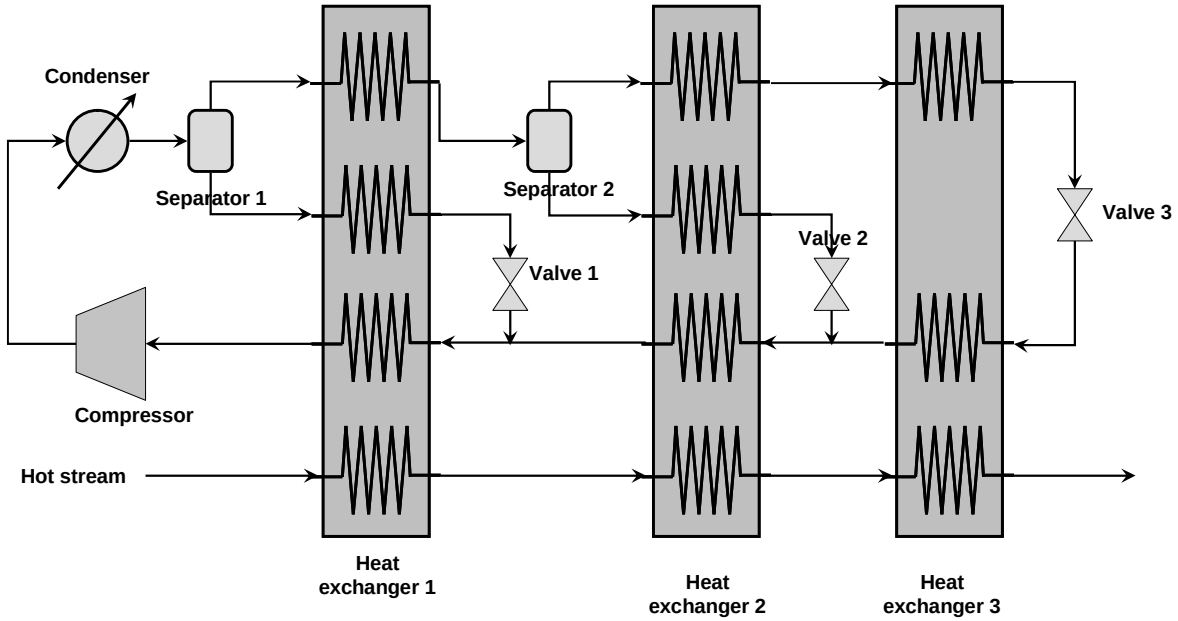

Figure 2.7 A self-cooling three-stage mixed refrigerants cycle

Comparing to the cascade refrigerant cycle, the MRC can operate at a smaller average temperature driving force, leading to a closer reversibility and a greater thermodynamic efficiency. Furthermore smaller machinery (mainly compression equipment) is required in MRCs and hence significantly lower capital costs are expected. Of course such a benefit is achieved at the expense of a higher heat transfer area (i.e. a larger heat exchanger).

The key to the MRC systems is to maintain a constant temperature difference through the cryogenic heat exchangers. However this requires a correct working pressure and a suitable refrigerant composition. In an attempt to design and optimise the MRC systems in a systematic manner, the thermodynamic accuracy of the multi-component mixture is often sacrificed by using some equations of state based on idea solution assumptions. In a cryogenic condition, a great error occurs due to this approximation, which makes the current exergy efficiency of MRC even a little smaller than that of the best cascade refrigerant cycle [49]. As a result, lots of attention has been drawn to the selection of the optimal mixed-refrigerant compositions using mathematical programming [51, 53-55].

New technologies emerge over the last decade or so for LNG production based on the combination or modification of the cascade cycle and MRCs. For example, the C3MR process consists of a MRC and a C3 (Propane) cycle in which natural gas is pre-cooled to about -35 °C through C3 cooler and than liquefied at -160 °C in the MR heat exchanger [44, 49, 56, 57]. The DMR (dual mixed refrigerants) cycle uses a separate mixed refrigerant rather than propane cycle to supply the initial chilling of the natural gas and pre-cooling of the first mixed refrigerant [49, 57]. In an MFC (mixed fluid cascade) process three mixed refrigerants are used to provide the cooling and liquefaction duty in a cascade manner [58]. The line up of APX (announced by Air Products and Chemicals International) combines a C3MR process with a closed N_2 cycle in series at the end to supply the high grade cooling power. These technologies dominate the current gas liquefaction market as shown in Figure 2.8 (the data between Year 2001 and 2012 is predicted by the installation and construction capacity in Year 2009) [56].

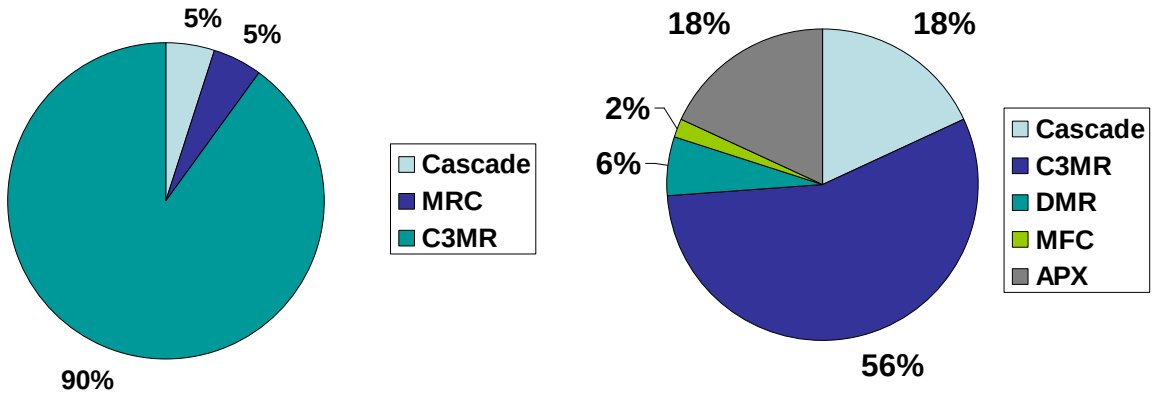

Liquefaction Capacity 1964 - 2000 Liquefaction Capacity 2001 - 2012

Figure 2.8 Evolution of LNG technologies

2.1.3 Expander Cycle

Different from the cascade cycle and MRC in which the refrigerants expand through an isenthalpic process in throttle devices, the expansion in expander cycles takes place following an isentropic process through power producing devices like turbines or expanders. Expander cycles attract more attention recently as they have several advantages over cascade cycle and MRC. The problem of distributing vapor and liquid phases into heat exchanger is eliminated because the cycle fluid maintains to be a gaseous phase. This enables a much wider working temperature and relatively

rapid and simple startups and shutdowns [49]. Reducing the startup time is economically a key factor for the intermittent operation of liquefaction plants [59].

Reversed-Brayton cycle is the simplest form of the expander cycle as shown in Figure 2.9. High pressure cycle gas is cooled in the ambient cooler and recuperative heat exchanger with returning gas. At an appropriate temperature, the cycle gas is then expanded in a near isentropic manner through an expansion turbine, reducing its temperature to a lower value than that of the expansion through a Joule-Thomson valve. Useful work is generated which is normally recovered through driving the compressor. A major disadvantage of the reversed-Brayton cycle is its relatively wide temperature differences in the heat exchangers which will lead to relatively high power consumption compared with cascade cycle and MRC. Many changes therefore have been made to increase the efficiency of the expander cycles.

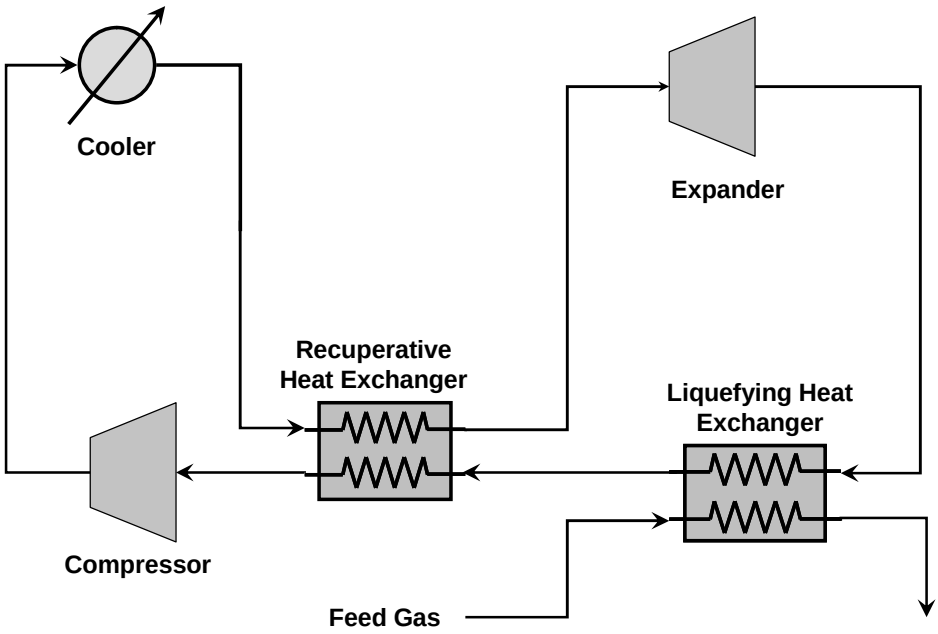

Figure 2.9 Flowsheet of a liquefaction system with reversed Brayton cycle

While multiple heat exchangers are employed with stream splitting prior to expansion, the system could be regarded as Collins cycle (normally consists of six heat exchangers and two reciprocating expanders [60]) or its modifications as shown in Figure 2.10. The refrigeration loop bypass turbines in such a cycle are organized in such a manner so that the inlet temperature of each expander is higher than the exit temperature of the preceding expander by an amount equal to the temperature

difference of the heat exchanger. Based on the fact that the cooling powers in different temperature range can be supplied by different expansion processes, a closer matching of the warming and cooling curves than Reversed-Brayton cycle could be attained, giving a reduced temperature driving force and a high thermodynamic efficiency. Low boiling point gases such as nitrogen, helium and hydrogen are normally working as the refrigerants in the Collins cycles to liquefy natural gas, air or even helium and hydrogen [44, 50, 60-63].

Valenti and Macchi [64] proposed a slightly different Collins cycle for hydrogen liquefaction with a helium based closed looped refrigeration cycle working at four different pressure levels. Such a system makes a greater topping pressure of refrigeration cycle up to 4.0MPa efficient to supply a lower temperature cooling power at about 18K. With a four-stream helium self-cooling cycle refrigeration unit the predicted exergy efficiency of the liquefaction system could attain as high as almost 48%.

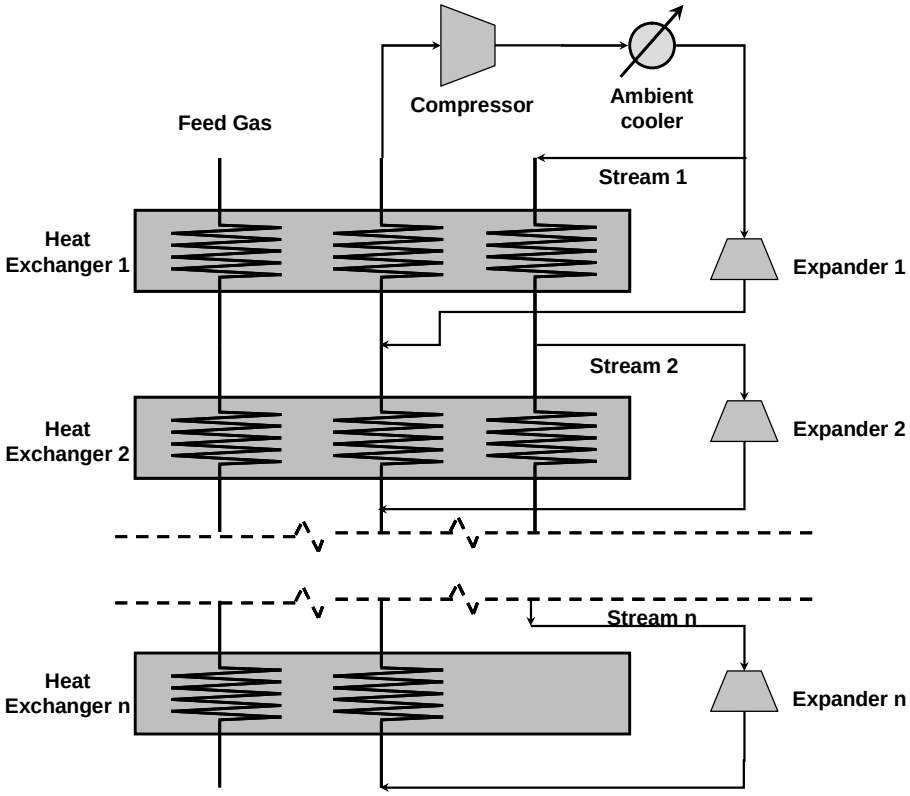

Figure 2.10 General configuration of Collins cycle

If the feed gas is used to replace the refrigerant in a Collins cycle, the system could be classified as a Claude cycle or its modification which is normally used to produce

liquid hydrogen [39, 65, 66]. In the Claude cycle part of the gases are expanded at different intermediate temperatures in expansion machines as illustrated in Figure 2.11 (For simplification only one stage expansion is depicted in the figure while in a specific design multiple expansion stages with inter-cooling may apply [39]). As the open loop refrigeration cycle could share the compression system with the feed gas stream, the capital cost of the components then could be reduced [42]. However as the lowest temperature of the cooling power generated by the refrigeration cycle is limited by the boiling point of the feed gas, the exergy efficiency of Claude cycle may be a little lower than that of the Collins cycle [61].

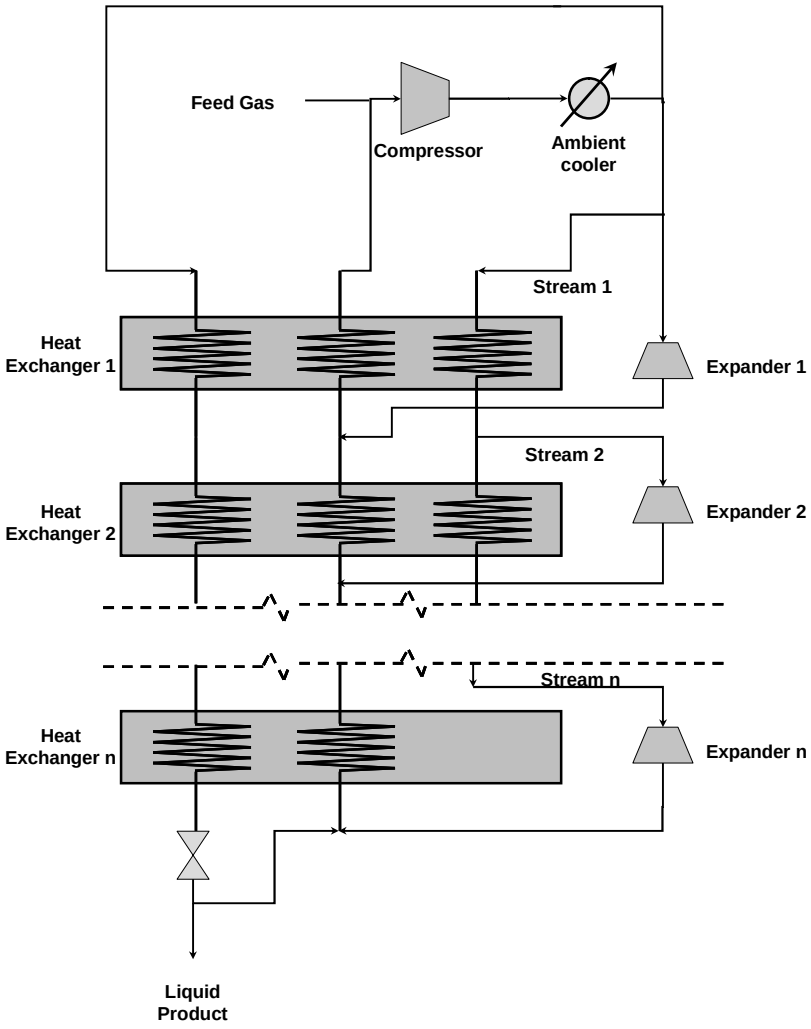

Figure 2.11 General configuration of Claude cycle

Another expander refrigeration method without stream splitting is also proposed which could be regarded as a modified Brayton cycle [43, 44, 62, 67]. In such a closed loop multiple compression and expansion processes occur with inter-heat

exchanging rather than stream splitting to achieve a better match between the warming curve and the cooling curve. A higher exergy efficiency up to 60% is reported based on such a system [62]. Of course this benefit is achieved at the expense of a more complicated heat transfer network and likely a higher capital cost.

2.1.4 Summary

Of the three methods for large scale liquefaction, the cascade refrigeration cycle and MRC are currently most widely used, especially in the LNG production. Most of the expander cycles are still on the conceptual design stage with few exceptions for hydrogen and helium liquefaction. Theoretically cooling power production in expander cycles taking place through power producing devices is more efficient than those in the cascade refrigeration cycles and the MRCs through throttling devices. The main limitation of the expander cycle in practical application is the less efficient compression processes. Refrigerants of expander cycles normally consist of small molecule gases such as hydrogen and helium which are less efficient for compression than large molecule hydrocarbons in the cascade refrigeration cycles and the MRCs. However with the development of multistage compression technologies with inter-cooling, the expander cycles are more promising to replace the other two technologies as the small molecule gases have better heat transfer properties [63]. This is more obvious especially for intermittent operations as the refrigerant in an expander cycle remains in a single phase and hence enables a rapid start-up and shutdown operation.

On contrast, the exergy efficiencies of the cascade cycles and the MRCs could be potentially improved by a more efficient expansion process. Using Joule-Thomson throttle valves for the expansion is an isenthalpic process. Liquid expanders or the so-called Cryoturbines could be used to attain an isentropic expansion where both temperature and enthalpy are decreased. If the cryoturbines are used in both refrigeration cycles and feed gas expansion processes, this technology could lead to an increase of 3-5% of the liquefaction efficiency compared with the use of throttle valves because these processes produce not only electrical power but also reduce the cold requirement [68, 69].

2.2 Cryogenic Energy Extraction Processes

Cryogenic energy recovery has been investigated theoretically using the second law of thermodynamics [28, 30, 70]. Four main methods have been proposed to extract the cold exergy from cryogen for power generation. The first one is the so-called direct expansion method. With such a method, cryogen is pumped to a high pressure and is then heated to the atmospheric temperature by the environmental heat or waste heat, followed by an expansion process to generate power. The second approach uses an indirect heating medium (working fluid) via a Rankine cycle in which the cryogen works as liquid condensate flowing through the condenser where the cryogenic exergy is transferred to the working fluid. The temperature difference between ambient and the cryogen drives the working fluid to generate power in the Rankine cycle. The third method uses a Brayton cycle in which the cryogen cools down the inlet gas of a compressor. The high-pressure working fluid after the compressor is then heated by the ambient and/or other heat sources and expands through an expander to generate power. Apparently, the lower the temperature of the inlet gas of a compressor, the less work required in the compression process, implying that the use of the cryogenic energy in the Brayton cycle can improve the cycle efficiency. The fourth method is the use of a combination of the above three methods. Among the four methods, the direct expansion is the simplest but is also the most inefficient method as it does not fully use the cold energy of the cryogen and a great deal of cold energy is discarded into the environment, leading to the loss of energy. As a consequence, in the following, attention is paid mainly to the other three methods.

2.2.1 Indirect Rankine Cycle Method

The Rankine cycle is a thermodynamic cycle which converts thermal energy, heat and/or cold to work. Figure 2.12 shows three schematic configurations of the Rankine cycle. The heat and cold sources are supplied externally to a closed loop, which usually uses a phase-change material as the working fluid. When used as a heat sink in the Rankine cycle, cryogen is vaporized at a pressure that is at or slightly higher than the ambient pressure. To recover both the latent cold and sensible cold released by the cryogen, a working fluid with a liquefaction/boiling point slightly higher than the cryogen would be an idea working fluid. Propane has a boiling point of -42^{o}C at the ambient pressure and has been used as the working medium in a simple Rankine cycle to extract the cryogenic exergy of liquefied nature gas (LNG) at industrial scales. Figure 2.12 (a) shows the schematic diagram of the

simple Rankine cycle, where propane is first pumped to a high pressure after liquefied by LNG. The high pressure propane is then heated up by seawater or other waste heat sources and expands in a turbine to generate electricity. Due to the large temperature difference of two fluids in the condenser and the lack of cold recovery in the evaporator, the overall efficiency is very low [29].

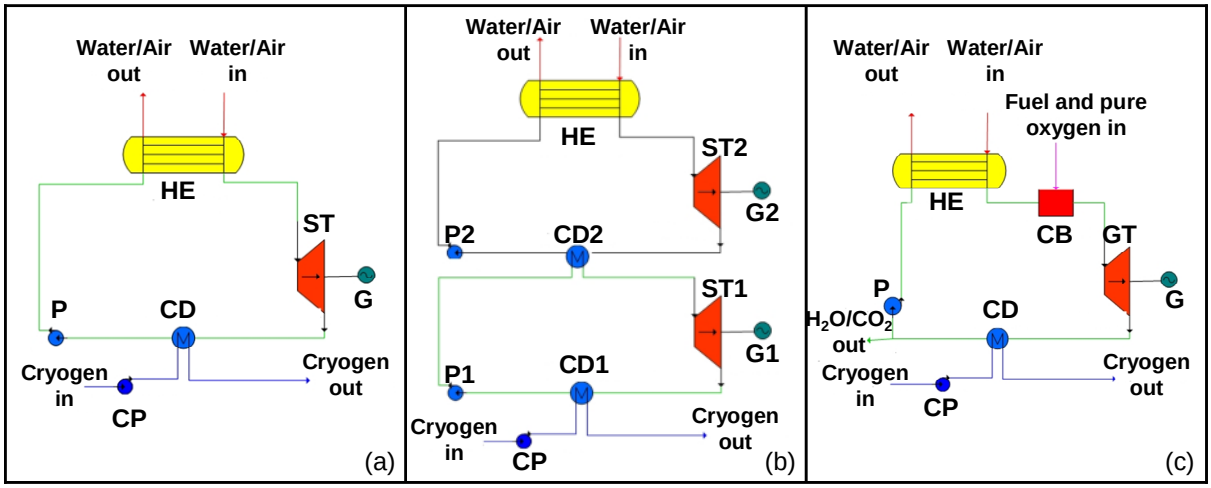

Figure 2.12 Schematic configurations of Rankine cycles

(a) simple Rankine cycle, (b) cascading Rankine cycle, and (c) CO_2 capture cycle (CB - Combustion, CD - Condenser, CP - Cryogenic Pump, G - Generator, GT - Gas Turbine, HE - Heat Exchanger, P - Pump, ST - Steam Turbine)

From the thermodynamic point of view, the use of a single fluid in a Rankine cycle is not the best approach to the use of cold exergy. In order to maximise the efficiency, the use of cascading cycles have been proposed [71, 72]; see Figure 2.12 (b). In these cycles lower boiling point materials such as methane and ethene are adopted as a working fluid in the first stage, while propane, water and ethane are used as the working media in the subsequent cycles. In the cascading configuration shown in Figure 2.12 (b), the cold energy is transferred in the form of latent heat thus the heat exchange occurs under the condition of constant and minimum temperature difference. In such a way, the overall efficiency is enhanced by minimising the exergy loss in the process of heat transfer. However, the cascading configuration greatly increases the system complexity, which can weaken the operation stability. Cryogenic energy can also contribute to carbon dioxide capture. For example, Deng et al. [73] proposed a cogeneration power system using LNG and the concept of oxy-fuel combustion. Figure 2.12 (c) shows the proposed process, where the cycle is essentially a recuperative Rankine cycle with carbon dioxide as the main working

fluid and natural gas is fired in the combustor with pure oxygen. Exhaust gas with a pressure higher than 0.5MPa from the turbine is cooled and condensed along with the vaporisation process of LNG. Such a cogeneration system is efficient and is regarded as commercially practicable. Table 2.2 gives a summary of the exergy recovery processes as discussed above.

Table 2.2 Summary of the cryogenic exergy recovery processes using the Rankine cycle

Thermal cycle type	Cryogen	Working medium	Heat source	Cryogenic exergy efficiency	System complexity	References
Simple Rankine cycle	LNG	Propane	Sea water/ air	< 20%	Simple	[29, 34, 74]
Cascading Rankine cycle	LNG	Propane, methane and water; Ethene and Ethane	Sea water and gas turbine exhaust heat	> 60%	Complex	[71, 72, 75]
CO_2 capture cycle	LNG	CO_2 and water	nature gas combustion heat	20 ~ 60%	Medium	[73, 76]

2.2.2 Indirect Brayton Cycle Method

The Brayton cycle is a thermodynamic cycle for gas turbines and engines. The main difference between the Brayton cycle and the Rankine cycles lies in that the working fluid in the Brayton cycle is pressurized by a compressor instead of the use of a pump in the Rankine cycle. The working fluid is in the gaseous state throughout the

Brayton cycle and the heat or cold transferred to the working fluid is in the form of sensible heat. Therefore the cryogenic energy could only be used to cool the inlet gas of the compressor. Figure 2.13 (a) shows schematically a direct way of using the cold energy to pre-cool the input working fluid in the gas cycle. The feasibility of the use of the cold energy of liquefied natural gas to cool the inlet air has been analysed by Kim and Ro [77] for gas/steam combined power plants during warm seasons. Air cooling capacity and power augmentation for a combined cycle system are demonstrated as a function of the ambient temperature and humidity in their research, while the corresponding increase in power is larger than 8% on average if the humidity is low enough for warm ambient air and water vapour in the air does not condense.

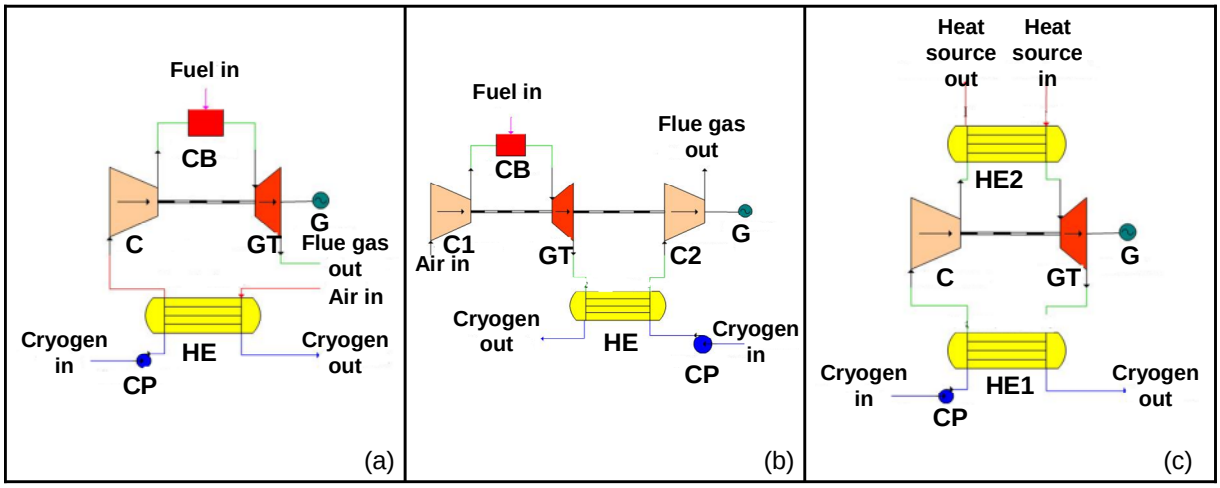

Figure 2.13 Schematic diagrams of Brayton cycles

(a) pre-cooling open cycle, (b) post-cooling open cycle, and (c) closed Brayton cycle (C - Compressor, CB - Combustion, CP - Cryogenic Pump, G - Generator, GT - Gas Turbine, HE - Heat Exchanger)

As a special Brayton cycle the mirror gas-turbine (MGT) method is introduced recently to recycle the cold exergy of LNG [78]; see Figure 2.13 (b) where the cold released from LNG is used to cool the exhaust gas from a turbine to increase the output work of the turbine and part of the cold exergy from LNG is transformed to decrease the compression work. This is different from the conventional way of cooling only the inlet gas of the compressor. It is reported that between seven and twenty percent of exhaust energy can be converted to useful work by introducing three-stage inter-cooling, and the thermal efficiency of the turbine can be improved by over 25% regardless the input of cryogenic exergy [76].

The two Brayton cycles discussed above are open cycles. Closed-loop Brayton cycles have also been investigated; see Figure 2.13 (c) for a schematic diagram. The closed Brayton cycles can be with or without a combustion process, and not only the air or nitrogen, but also hydrogen and helium can be used as the working fluids. As there is no water vapour in the closed cycle the working fluid can be cooled to a much lower temperature hence cryogenic energy recovery efficiency could be greatly improved. Table 2.3 gives a summary of the work on the cryogenic exergy recovery through Brayton cycles discussed above.

Table 2.3 Summary of the cryogenic exergy recovery processes using Brayton cycles

Thermal cycle type	Cryogen	Working medium	Heat source	Cryogenic exergy efficiency	System complexity	Reference
Open cycle	LNG	Air	Combustion heat	< 20%	Simple	[77, 78]
	LNG, LN_2	Nitrogen	Ambient air	< 20%	Simple	[31, 71, 72, 79]
	LNG	Hydrogen	Furnace waste heat	20 ~ 60%	Medium	[80]
Closed cycle	LH_2	Helium	Combustion heat	20 ~ 60%	Simple	[81]
	LNG	Helium	Combustion heat	20 ~ 60%	Simple	[82, 83]

It should be noted that the cryogenic exergy efficiency depends on not only the recovery cycle type but also the working pressure of the cryogen. At ambient pressure a great portion of the cryogenic energy is released in the form of latent heat at a very low temperature therefore the efficiency is not high. How ever in some circumstances the cryogenic energy is extracted at a much higher pressure (for example in Italian the natural gas enters the main pipelines of the transmission

system at a pressure rating up to more than 70 bar [82]) and then the cryogenic energy releases in the form of sensible heat leading to a much high efficiency. This is the reason the cryogenic exergy efficiency of the closed cycle ranges very large in Table 2.3.

2.2.3 Combined Method

A more efficient approach to the recovery of cryogenic exergy is the combined method, particularly by integrating a Rankine cycle or a Brayton cycle with a direct expansion method. In such a way, part of the thermal exergy is converted to high-pressure exergy. In a typical combined method, the cryogen is normally pumped first to a pressure above the critical point of the working fluid before vaporisation, which is followed by direct expansion to form a supercritical open cycle with only sensible heat discharged. Pilot-plant scale work based on the combined method was first established in Japan in 1970s, where closed-loop Rankine cycles were combined with direct expansion cycles in a LNG re-gasification process [84]; see Figure 2.14 (a) for the flow chart. The process shown in Figure 2.14 (a) uses propane as the working fluid for the Rankine cycles. Apart from propane, ammonia-water mixtures and Freon have also been used as the working fluids for the combined cycles [85-88]. However, liquefaction of these fluids involves phase change processes and the cold source is in the form of sensible heat, the cryogenic exergy could not be extracted efficiently.

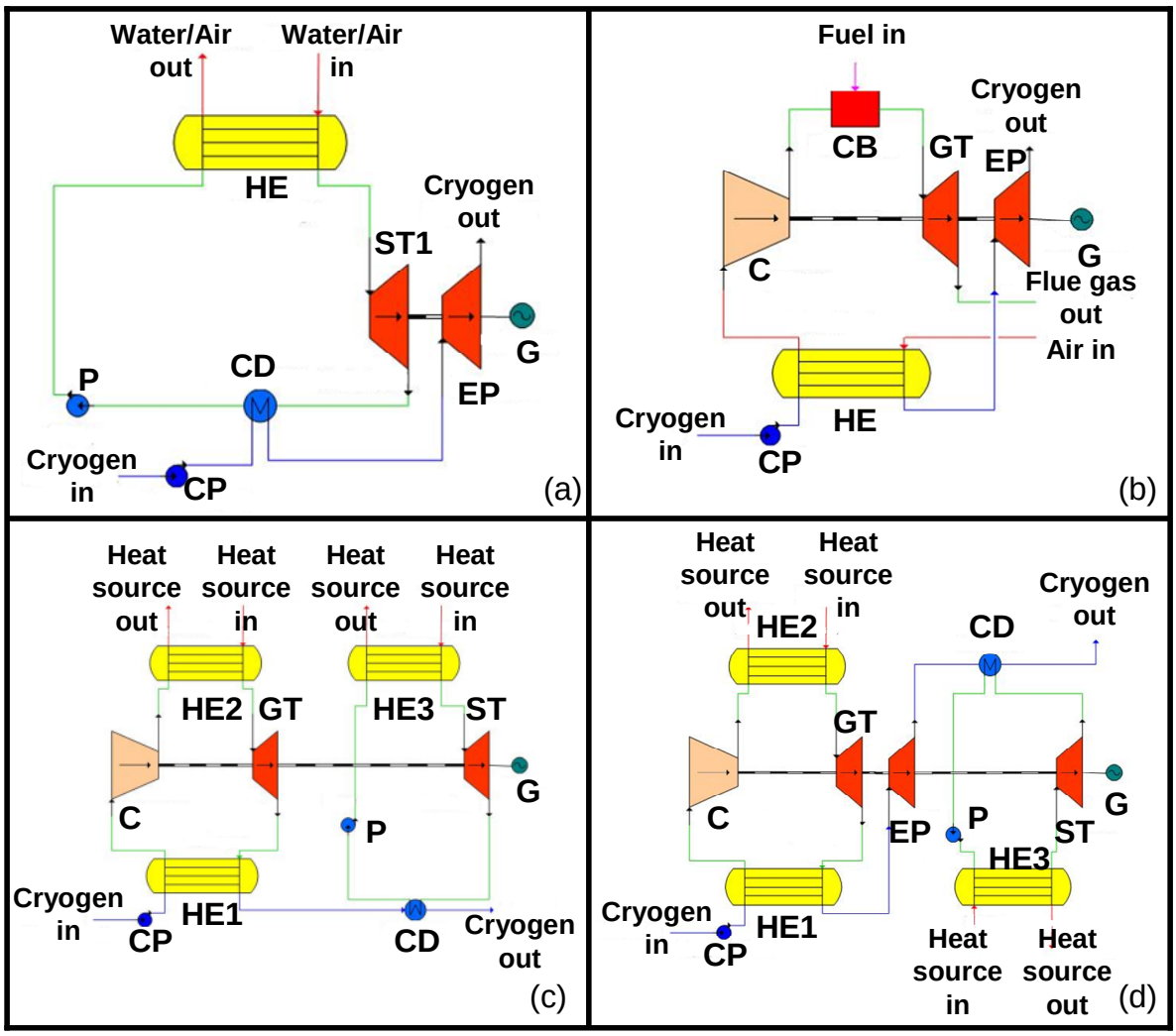

Figure 2.14 Schematic diagrams of combined cycles

(a) direct expansion-Rankine hybrid cycle, (b) direct expansion-Brayton hybrid cycle, (c) Rankine-Brayton hybrid cycle, and (d) direct expansion-Rankine-Brayton hybrid cycle (C - Compressor, CB - Combustion, CD - Condenser, CP - Cryogenic Pump, EP – Cryogenic Expander, G - Generator, GT - Gas Turbine, HE - Heat Exchanger, P - Pump, ST - Steam Turbine)

Figure 2.14 (b) shows a schematic diagram of combining the Brayton cycle with the direct expansion cycle, where the cooling of the working fluid occurs through a sensible heat discharging process, leading to a high performance of the cryogenic exergy recovery. Bisio and Tagliafico used nitrogen as the working fluid in their studies of a combined cycle involving a two-stage compression process with inter-cooling and showed that the system had an overall exergy efficiency of 46% [71, 72].

There have been reports on the cryogenic energy recovery process for both LNG and liquefied hydrogen [89-92], where the cold energy of the low pressure cryogens is discharged in two stages; see Figure 2.14 (c). The high grade cold is used to cool the low pressure working fluid before compression and the low grade cold is used to liquefy the working fluid in a Rankine cycle. Therefore this configuration can be regarded as a combination of the Rankine and the Brayton cycles. A particular example for this is the oxy-fuel combustion of LNG, where carbon dioxide could be separated in the condensation process for storage. This makes these technologies much more promising [90, 91, 93]. The combination of a closed Brayton cycle and a Rankine cycle with direct expansion has also been investigated by Bai and Mang and their aim was to maximise the efficiency [34]; see Figure 2.14 (d) for a schematic diagram. In their design, the Brayton cycle with nitrogen as the working fluid is employed to recover the high grade cold and the ammonia-water based Rankine cycle is used to recover the low grade cold. From the thermodynamic point of view, the combined cycle proposed by Bai and Mang [34] could also be regarded as a cascading system. Table 2.4 gives a summary of the work on cryogenic exergy recovery using combined cycles as discussed above.

Table 2.4 Summary of the cryogenic exergy recovery using combined cycles

Thermal cycle type	Cryogen	Working medium	Heat source	Cryogenic exergy efficiency	System complexity	Reference
D + R	LNG	Propane, Ammoina-water, freon	Combustion heat, low temperature waste heat	20 ~ 60%	Simple	[34, 74, 84-88, 94]
D + B	LNG	Combustion gas, nitrogen, air	Furnace waste heat	> 60%	Medium	[71, 72, 78]
R+ B	LH_2, LNG	CO_2/water mixture,	Combustion heat	20 ~ 60%	Complex	[89-92]

		water/air mixture				
D + R +B	LNG	Nitrogen and ammonia water	Low level waste heat	> 60%	complex	[34]

2.2.4 Further Discussion

Cryogens contain high grade thermal energy in the form of latent heat and sensible heat (low molecular kinetic energy and low enthalpy). Such a valuable energy could only be extracted effectively by selecting an effective thermodynamic method based on the thermodynamic properties and external conditions e.g. heat sources etc. Theoretically, Rankine cycle is an effective method to extract the cryogenic energy if a working medium with a slight higher boiling point than the corresponding cryogen can be found. In addition, the Rankine cycle uses pumps to compress the working fluid, which consumes very small amount of work, so the overall efficiency will not be affected much by the irreversible compression process. However the recovery of the cold released by the working fluid after compression has to be addressed in order to further enhance the efficiency. Although the cascading cycle can be a solution, process optimization is needed to find a balance between the cycle efficiency and the system complexity.

The Brayton cycle is not an effective method to directly recover the cryogenic energy as the cooling of a gas only requires sensible heat. A big loss of cold exergy is therefore inevitable during the heat transfer process involving high grade latent heat although the working fluid (gas) can be cooled to a very low temperature. A more effective way to extract the cryogenic exergy is the use of a method that combines a direct expansion cycle and other cycles.

Direct expansion converts part of the thermal energy into the pressure energy through pumping the cryogen to a high pressure. If one defines the pressure exergy, $E(P)$, as the maximum theoretical work obtainable by bringing the fluid to

equilibrium with the environmental pressure through an isothermal process at ambient temperature, then

$$E(P) = H(P,T_a) - H(P_a,T_a) - T_a \cdot [S(P,T_a) - S(P_a,T_a)] \tag{2.1}$$

H and S standing for the enthalpy and entropy respectively of the fluid are functions of the pressure P and temperature T . The values can be obtained from a commercial program named REFPROP. The proportion of the pressure energy in the cryogenic exergy can then be given as:

$$\eta = \frac{E(P) - W_P}{E_l(P_a) + W_P} \tag{2.2}$$

where $E_l(P)$ is the exergy of liquid cryogen at ambient pressure, and W_P is the pumping power which for an isentropic process can be given by:

$$W_P = [H(P, S_l(P_a, T_b)) - H_l(P_a, T_b)] / \eta_P \tag{2.3}$$

where η_P is the pump efficiency. In the above equations the subscripts a, b and l represent the ambient condition, boiling point and liquid phase of the fluid. The proportion of the pressure exergy is found to increase with increasing pressure, and the increase is very sharp at low pressures of up to ~ 10MPa. However, the increase tends to level off at higher pressures; see Figure 2.15 for three of the cryogens considered with the pump efficiency taken as 0.7. Considering the rapid increase in the pumping power consumption and the requirements for the turbine inlet pressure, the pumping pressure should be limited to a certain value which is higher than the critical pressure. From Figure 2.15 one can also see that the optimal working pressure for methane is about 20MPa, while these for nitrogen and hydrogen are a slightly higher. The pressure exergy could then be extracted through a direct expansion process. The remaining exergy exits in the form of sensible thermal cold, which has to be recovered in a thermal cycle, in which the pressure again plays an important role.

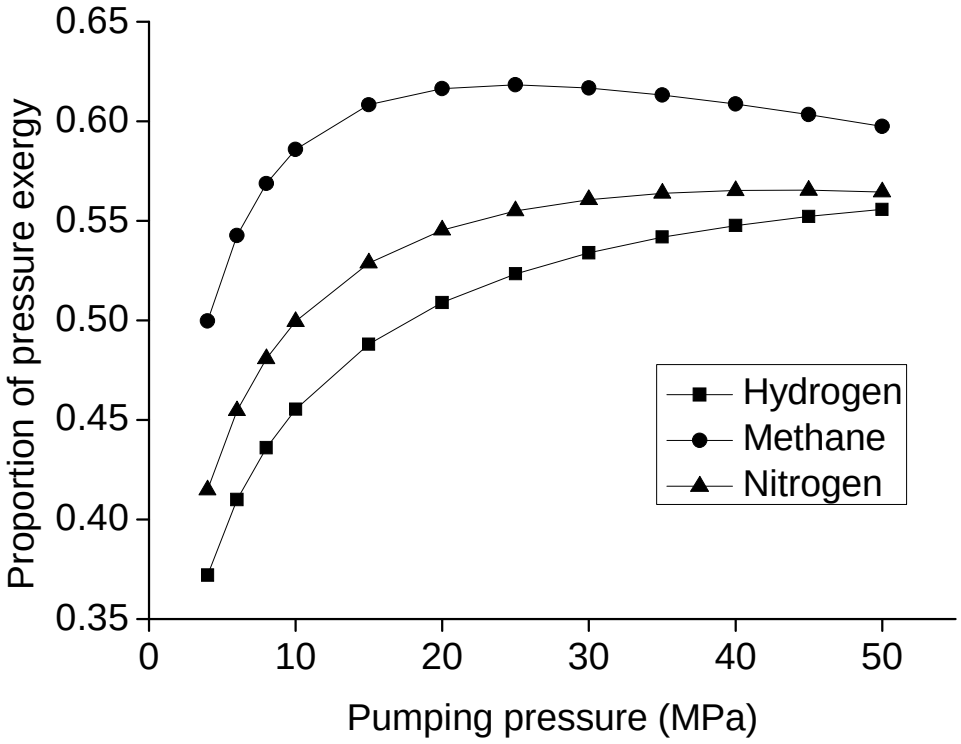

Figure 2.15 Exergy conversion of cryogen by pumping

Figure 2.16 plots the normalised temperature against the normalised heat at different pressures with the normalised temperature and heat defined respectively as:

$$\overline{T} = \frac{T - T_b}{T_a - T_b} \tag{2.4}$$

$$\overline{Q} = \frac{H(T) - H_l(T_b)}{H(T_a) - H_l(T_b)} \tag{2.5}$$

where $H_l(T_b)$ is the enthalpy of liquid cryogen at its boiling point. Note that the definition of $\overline{Q}$ in Equation (2.5) is similar to that in Equation (1.5). In Figure 2.16, the heat transfer processes are assumed to occur from the boiling point to the ambient temperature at different pressures. For methane and nitrogen, about half of the cold energy is released in the form of latent heat at low pressures. If the fluids are pumped to their supercritical states, the remaining cold will release in the form of sensible heat with approximately constant specific heat. This suggests that the combined direct expansion and Brayton cycle be the most efficient method for fully recovering the cryogenic energy of methane and nitrogen. This, however, does not seem to be held for hydrogen as the latent heat contributes to a very small portion of

the released cold. Therefore the simple Brayton cycle would be an efficient method to recover the cryogenic energy of liquid hydrogen, if a suitable working fluid could be found.

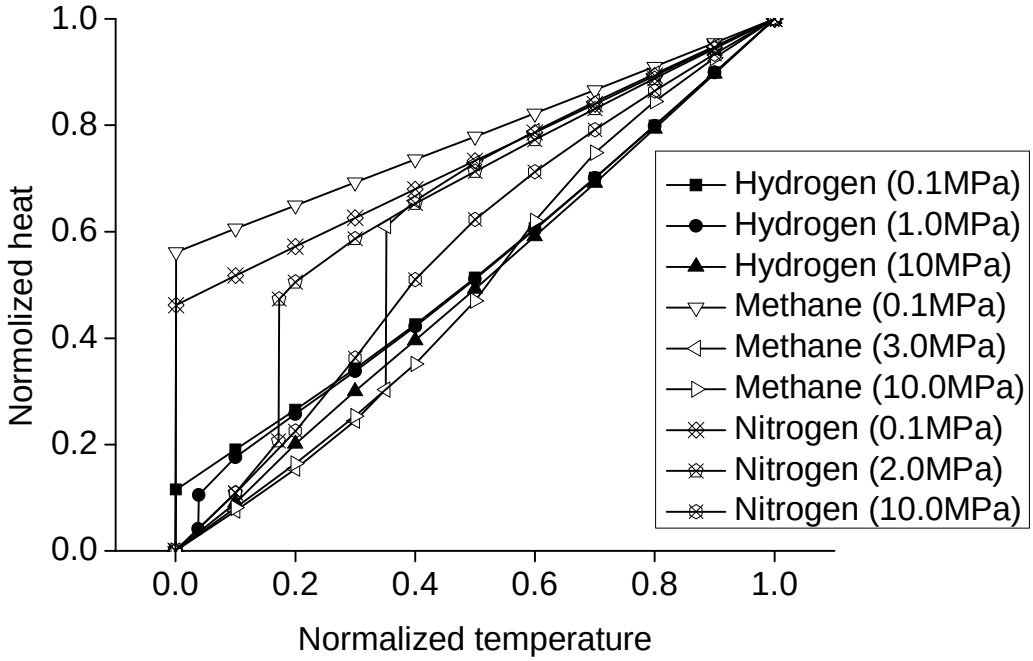

Figure 2.16 Normalised heat vs. normalised temperature diagram of cryogens at low temperature range

It should be noted that the heat source plays a very important role in the selection of the recovery method. If the environmental heat (seawater and air) and other low grade heat sources are available, the Rankine cycle is more suitable whereas the Brayton cycle is more suitable when medium and high grade heat sources are available.

2.2.5 Summary

This section reviews the work on energy extraction process of cryogen. It covers both the current status of technologies for cryogenic energy extraction and the associated thermodynamic aspects. The following observations are obtained:

- If a high grade heat source is available, the direct expansion - Brayton hybrid system is the most efficient method to extract the cryogenic exergy for most cryogens but not liquid hydrogen. This is because the latent heat of hydrogen

only contributes to a small part of the released cold and a simple Brayton cycle would be suitable for the exergy recovery.

- If there is only ambient and / or a low grade heat source, the combination of direct expansion and Rankine cycle is more attractive due to its low power consumption in the compression process.

2.3 Hydrogen and Liquid Air/Nitrogen as Energy Carriers

Besides cryogens such as liquid air/nitrogen, it is well-known that hydrogen has been regarded as a popular carrier of renewable energy in remote locations [95-97]. Using such a chemical energy carrier, renewable sources such as the ocean energy generates electricity first, which is then used to electrolyze water to produce hydrogen. Hydrogen is then transported to the end-users for transforming back to electricity or kinetic energy by a fuel cell or other devices. This process can be split into three sub-processes: hydrogen production for energy storage, hydrogen storage and/or transportation and chemical energy extraction.

The ocean energy is used as an example of the use of renewable energy sources in remote locations in this section as the world's oceans could emerge as an important source to provide an economically viable renewable energy source [98]. Ocean winds blow harder and are more consistent than the wind on lands. This offsets the greater cost of building offshore wind power facilities. Oceans tides also contribute massive amounts of renewable energy that is gravitationally derived through the interplay of the earth and the moon. The energy from ocean waves and tidal streams, along with ocean-based wind energy, make the world's oceans a source of renewable energy that may in the next few decades be an economical alternative of solar radiation.

Figure 2.17 illustrates schematically the use of ocean energy with hydrogen and liquid air/nitrogen as the energy carriers. This section aims to assess and compare the chemical energy carrier, hydrogen, with the physical energy carrier liquid air/nitrogen in terms of the overall efficiency, including production, storage and transportation, and energy extraction. The environmental impact, waste heat recovery and safety issues are also considered.

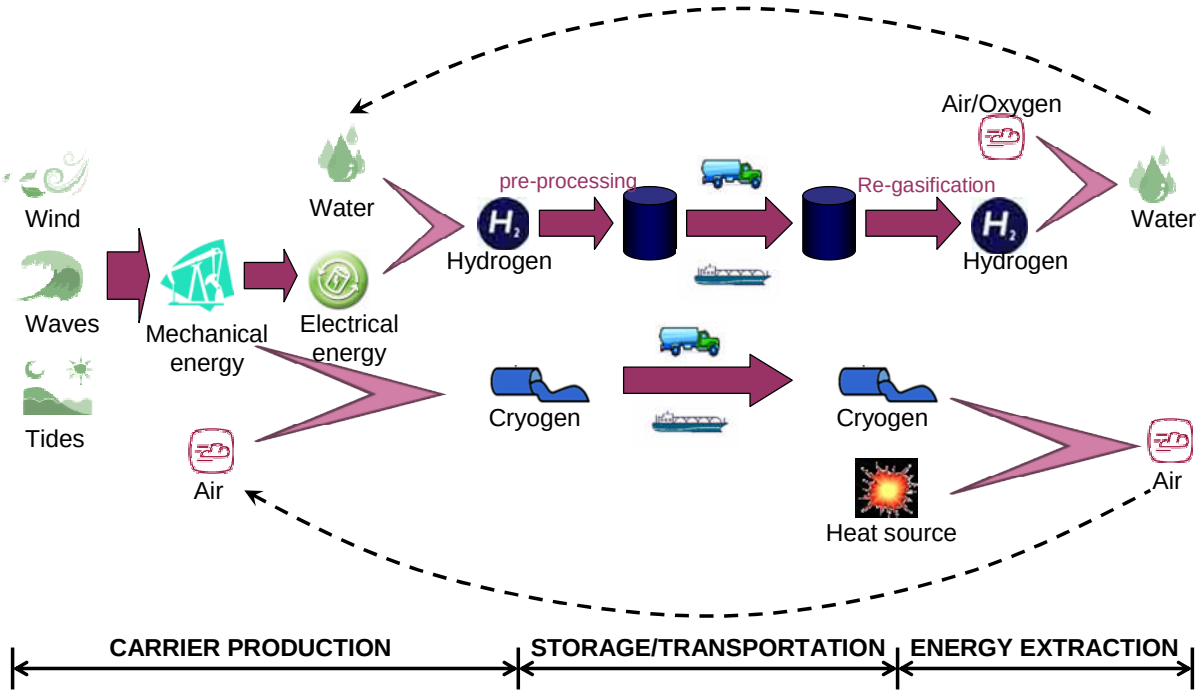

Figure 2.17 Diagram of ocean energy utilization

2.3.1 Carrier Production

Two main technologies used to produce hydrogen are considered in this section, reforming reaction and water splitting. The most common hydrogen production method in commercial use today is the former, which uses hydrocarbons or other chemical compounds such as coal and biomass as feed stocks. However, as the renewable resources considered here (wind, tides and waves) contain only the mechanical energy of moving masses of air or water, direct chemical path of hydrogen production is to split water using electrical energy generated by the kinetic energy of renewable resources. Therefore, hydrogen production using the ocean resources can be described as follows. The kinetic energy of moving masses (air/ seawater) is extracted first by mechanical machines to form the mechanical energy of the machines. The fraction of extractable power depends on the form of energy and extraction processes and devices, and is limited by a theoretical value determined by the thermodynamics. For example the upper bound of the wind energy extraction by an ideal horizontal axis machine is 0.593 (power coefficient) under some rather general assumptions [99]. Then the mechanical energy of the mechanical machines is converted to electricity with a conversion efficiency of about 75~95%. Finally, the electrical energy is employed to produce hydrogen by electrolysis. Table 2.5 summarizes the performance of electrolysis technologies,

along with their feed stock and efficiencies (defined as the low heating value of hydrogen produced divided by electrical energy consumed in the electrolysis cell) [100-105]. In the summary table, the high-temperature electrolysis efficiency is dependent on the temperature at which the electrolyzer operates and the efficiency of the thermal energy source. If everything is considered, the efficiency of converting mechanical energy to chemical energy (hydrogen) is within a range of 37.5~66.5%.

Table 2.5 Efficiencies of the different electrolysis technologies

Electrolysis Technology	Feed stock	Efficiency	Maturity
Alkaline Electrolyzer	water + electricity	50 ~ 63%	Commercial
PEM Electrolyzer	water + electricity	55 ~ 70%	Near term
Solid Oxide Electrolysis Cells	water + electricity + heat	40 ~ 65%	Med. Term

As mentioned before, the cryogen production is done by the air separation/liquefaction process in which cryogenic coolers liquefy the main components of air through the well-known Joule-Thomson effect. Although the process is energy-intensive, the compression and refrigeration processes could be directly powered by the mechanical work of the ocean energy. Therefore cryogen production could be more competitive than hydrogen production in terms of the overall efficiency and capital costs as the electricity conversion process is not essential at the cryogen production end.

2.3.2 Carrier Storage and/or Transportation

As the energy carriers are produced at the offshore power generation facility, they have to be stored and transported to an onshore location for distribution to the end-users. Hydrogen could be delivered to onshore facilities through one of the three forms: gas (compressed), liquid (liquefied), or solid (in a solid hydrogen carrier). In the gaseous form, hydrogen can be compressed and transported to onshore in pressurized containers. Because of its low molecular weight, hydrogen molecules are very small and leakage can be an issue particularly at high pressures. Because of this, the storage pressure of hydrogen is limited to ~35 MPa at present. Liquefaction of hydrogen and its transportation in containers are an established technology. However, the liquefaction process is energy-intensive and about 30~40% of the energy content is lost in the liquefaction process [106]. Because of its

added complexity and costs for both generation and transportation, the use of liquid hydrogen is not regarded as an attractive option.

Table 2.6 shows the volumetric capacity of hydrogen under different conditions. The energy density increases linearly with increasing storage pressure, and liquid hydrogen has a higher value. As mentioned above, high-pressure storage of hydrogen gas is limited by the possible leakage. This imposes potential safety issues [107]. A promising way to replace the conventional hydrogen fuel storage methods is to use a solid state hydrogen carrier, which refers to any substance that can store and transport hydrogen in either a chemical or a physical state. The advantages of using solid carriers are better safety and reliability in comparison with liquid or compressed gas storage methods. The carrier is charged with hydrogen at the offshore generation site and transported to onshore where hydrogen is stripped off. The carrier needs to be taken back for recharging (two-way carrier) or decomposed at the point of hydrogen use (one-way carrier). Examples of hydrogen carriers include ammonia (one-way) and liquid hydrocarbons and metal hydrides (two-way). It is reported that some of the hydrogen carriers could attain a volumetric capacity as high as liquid hydrogen [108, 109]. However the weight of current hydride substrates and their container is much greater than that of the stored hydrogen, so extra energy is required during both charging and discharging processes. While considerable effort has been made on the hydrogen carrier technology, no reports have been found so far on the commercial use of the carriers.

Table 2.6 Volumetric capacities of the energy carrier under different conditions

Energy Carrier	Liquid Air	Liquid Nitrogen	Compressed Hydrogen*				Liquid Hydrogen*
Pressure (bar)	1	1	50	150	250	350	1
Volumetric capacity (kWh/m^3)	177	171	133	377	593	785	2360

* The pressure potential energy of the compressed hydrogen and the cryogenic energy of liquid hydrogen are not considered as they are much lower than the chemical energy.

Compared to hydrogen, the delivery of cryogen is much easier. Once produced and stored in insulated containers, cryogen is ready to be delivered. No extra energy required except for the pumping power consumption which is negligible for a liquid. As shown in Table 2.6, the volumetric energy density of cryogen is much lower than that of liquid hydrogen but at the same order of magnitude as compressed hydrogen. It should be noted that the volume-based energy densities of both cryogen and compressed hydrogen gas (at practicable pressures) are significantly lower than that of traditional fossil fuels. In addition, cryogen is continuously vaporized and lost as boil-off gas (BOG) during storage and transportation. The amount of BOG depends on the design, the operating conditions of cryogenic tanks and the environment conditions. This is reported that the typical boil-off rate ranges between 0.05% and 0.15% per day for large scale storage [110, 111].

2.3.3 Energy Extraction of the Carriers

Upon delivered to end-users' side, the energy stored in the energy carriers is extracted. Current technologies converting the chemical energy of hydrogen to mechanical energy or electricity energy use one of the two methods, combustion and electrochemical conversion in e.g., a fuel cell.

For the combustion method, both hydrogen internal combustion engines and hydrogen fuelled gas turbines have been investigated [112-114]. Because of high burning temperatures, hydrogen internal combustion in a conventional engine produces a very high level of nitrogen oxides which cause environmental problems. Although a number of ways have been proposed to reduce nitrogen oxides emissions, efficiency decrease of the engine is inevitable. This is a serious issue as currently the low heating value (LHV) efficiency of internal combustion is only 20 ~ 35%. Another approach is the use of gas turbines in hydrogen fuelled combustion prior to which pure oxygen is generated from an air separation unit to avoid the production of nitrogen oxides. In such a process, water/steam is often added to reduce the turbine inlet temperature, see Figure 2.18(a). Here water is preheated by the exhaust gas from the gas turbine. Different from the internal combustion, the burning temperature of these cycles is limited by the turbine inlet temperature (TIT) which is currently about 1300 °C. In these cycles the exergy loss is mainly caused by preheating and mixing of the three inlet stream reactants in the combustor which accounts for about 40 ~ 50% of the overall exergy loss. This, plus energy consumption associated with oxygen production, the overall LHV efficiency of this

type of cycles is limited to about 50% using current technologies and may increase to about 60% if the turbine inlet temperature is increased to ~2000 °C with future developments in turbine and material technologies [115].

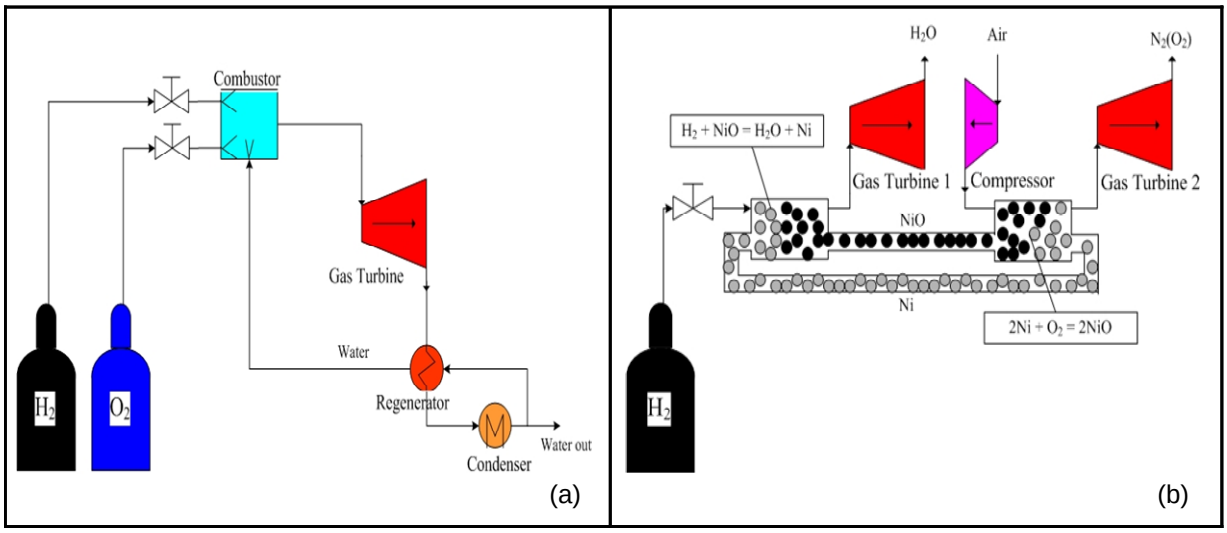

Figure 2.18 Diagrams for hydrogen fuelled gas turbine cycles

A different approach to the direct combustion of hydrogen is the so-called chemical-looping method for extracting chemical energy of hydrogen as shown in Figure 2.18(b). Such a method uses two successive reactions, metal oxide reduction with hydrogen, and subsequent oxidation of the metal by air, yielding the metal oxide and a high-temperature flue gas. The resulting high-temperature gas is then used to power turbines. By adding a chemical-looping process, the exergy loss in the combustion process decreases significantly [116, 117]. It is claimed that the LHV efficiency of hydrogen in such a cycle could be as high as 63% [115, 118].

Another approach for enhancing hydrogen energy extraction efficiency is the use of fuel cells, which could replace internal combustion engines and turbines as a primary way to convert chemical energy to kinetic or electrical energy. Fuel cells work via electrochemical principles, and hence are more efficient than heat engines. Table 2.7 [119-121] lists the technical information of three types of hydrogen fuelled fuel cells including typical efficiencies, operating temperatures, catalysts and other operating parameters, where the efficiency refers the cell efficiency and the system efficiency is generally 10% lower. However, there are still a number of barriers for the industrial take-up of the fuel cell technologies; these include requirements for

high purity of hydrogen, high manufacturing costs, low cell reliability and short service life. It is reported that the cost of fuel cell technologies is about 4~5 times more expensive than the combustion engines/turbines, while its service life 2~3 times shorter [122].

Table 2.7 Efficiency of hydrogen fuel cells

Fuel cell type	Operating temperature (°C)	Electrolyte	Catalyst, anode	Electrical efficiency (%)	Qualified power (kW)
Alkaline (AFC)	70 ~ 100	KOH (aqueous solution)	Ni	60 ~ 70	10 ~ 100
Proton exchange membrane (PEM)	50 ~ 100	polymer membrane	Pt	50 ~ 70	0.1 ~ 500
Phosphoric acid (PAFC)	150 ~ 220	Phosphoric acid (immobilized liquid)	Pt	40 ~ 55	5 ~ 10000

In contrast to hydrogen, energy extraction from cryogen is much more straightforward which is similar to a steam engine but expansion of cryogen does not emit pollutants such as NO_X and particulate matters etc. The methods for cryogenic energy extraction have been discussed in previous section and it has been concluded that the exergy efficiency could achieve to 60% or even higher. The exergy efficiency of cryogen expansion could be further enhanced if the working fluid is superheated by waste heat or heat from other renewable sources such as solar. At present, only high grade waste heat in gas turbine power cycles could be recovered efficiently by heat recovery steam generator (HRSG) technology while low grade heat is generally vented. The use of a cryogen expansion cycle can be a very

effective way to recover such low grade heat as the boiling point of air or nitrogen is much lower than the ambient temperature.

2.3.4 Summary

This section assesses and compares two energy carriers, hydrogen and cryogen, as examples for ocean energy sources exploitation. The assessment and comparison are based on the overall efficiency including production, storage and transportation, and energy extraction. The environmental impact, waste heat recovery and safety issues are also touched upon. The following observations are drawn:

- The production efficiencies of hydrogen and cryogen are similar at 40~65% based on the current technologies. However, cryogen may be more competitive than hydrogen as an energy carrier in terms of capital costs because electricity conversion may not be absolutely necessary at the cryogen production end.

- As an energy-intensive process which consumes up to ~40% of the chemical energy, pre-treatment is required for the storage and transportation of hydrogen regardless of the form of the carrier being compressed gas, liquefied hydrogen or solid hydrogen carrier. In addition, the transportation of hydrogen carrier may be two-way if the two-way carrier is adopted. In contrast, transportation of cryogen requires neither pre-treatment nor other carriers but insulated containers. However it should be noted that hydrogen has a higher volumetric energy density than cryogen regardless of storage forms.

- The energy extraction efficiency of hydrogen depends significantly on the conversion methods. Currently, gas turbine and fuel cell methods have better performances than conventional internal combustion engines though significant developments are needed in order for the fuel cell technologies to be competitive. Cryogen engines, if cold recovery technology is employed, may have an even higher efficiency than the fuel cell technologies.

- Waste heat especially low grade heat could be recovered efficiently by the use of cryogen engines.

- Although hydrogen is regarded as a clean fuel, nitrogen oxides can be produced if air is used as an oxidant. Cryogen is much more environmentally friendly as the processes of production (using the ocean energy) and

extraction are both physical involving no chemical transformation. Even the transportation of the cryogen can be cryogen-based.

Overall, hydrogen is viable as an ocean energy carrier only if a practical method to store and carry hydrogen is introduced and fuel cells become cheap with their service life much improved. Before these are achieved, cryogen appears to be a more attractive energy carrier as there are few technical difficulties to overcome. Moreover, the overall efficiency of the use of cryogen can be greatly increased if low grade heat is used in the process of cryogenic energy extraction. Low grade heat can be obtained easily from either traditional energy intensive industries like steel plants or directly from the abundant renewable solar energy. As mentioned before, the electricity conversion efficiency of solar energy is limited, it is much easier to use solar thermal energy in countries blessed with good sunshine (e.g., India with a mean daily solar radiation of 5~7 kW/m^2 [123]) via e.g., a cascading way. Solar energy, along with the thermal energy storage technology using e.g., phase change materials, has been extensively studied and used for heating, cooking and even electricity production [124-126]. Therefore, a solar-cryogen hybrid energy storage system appears to be a promising way for both transportation system and electricity production. This will be explored as part of this work.

2.4 Summary of the Literature Review

A wide variety of articles focusing on the gas liquefaction technology are presented in the literature. Cascade refrigerant cycle and MRC and their combinations are the dominant technologies for large scale liquefaction of natural gas. The exergy efficiency could attain up to 55% if multistage compression is adopted with inter-cooling. However such methods are not favorable for air liquefaction in CES as they require constant operation.

Gas liquefaction technologies based on expander cycle enables a rapid startup and shutdown. As a consequence it is likely to be more suitable for excessive electricity storage. The practical exergy efficiency of this technology is lower than 30%. And some conceptual designs are being developed which have been shown to achieve a potential exergy efficiency of 60% and higher. However both of the practical application and theoretical modelling focus on the liquefaction of hydrogen and

helium and they fail to address concerns that arise from air separation and liquefaction.

A significant amount of research work has been conducted in the cryogenic energy extraction as well in the literature which can be categorised into indirect Rankine cycle method, indirect Brayton cycle method and combined method. The work shows that for most cryogens (but not liquid hydrogen) the direct expansion – Brayton hybrid cycle is the most efficient method if a high grade heat source is available. On the other hand if only ambient and / or a low grade heat sources are available, the combination of direct expansion and Rankine cycle is more attractive due to its low power consumption in the compression process.

However the studies of both gas liquefaction and cryogenic energy extraction provide insight on the performance investigation of specific systems. Optimisations of the system configuration are not well documented in the literature. The present work aims to develop a systematic optimisation strategy which enables configuration selection and parametric optimisation at the same time. This strategy is used for the optimisation of the expander cycle based air liquefaction process in CES and other integrated systems related to CES technology.

A comparison of hydrogen and liquid air/nitrogen as energy carrier is also studied based on the literature in terms of production, storage and transportation, and energy extraction. The overall performances of the two carriers are similar if no external heat sources are available for cryogenic energy extraction. There are fewer technical difficulties to overcome for liquid air/nitrogen than that for hydrogen. More importantly, the exergy efficiency of cryogenic energy extraction could be significantly improved if a heat source is used to superheat the cryogen. Therefore liquid air/nitrogen is regarded as a more attractive energy carrier before conquering both technical and economic barriers related to hydrogen.

Chapter 3 Methodologies for Modelling and Optimisation

3.1 Thermodynamic Modelling

3.1.1 Component Modelling

Thermal energy system is made up of thermodynamic cycles, either closed-loop or open-loop. A thermodynamic cycle consists of a series of processes realised by power transfer units and heat transfer units; see Figure 3.1. In a single phase process the power transfer units include expanders (gas turbine, steam turbine and liquid expander or other expansion engine) and compressors (gas compressor and liquid pump).

Defining the isentropic efficiency of the expander as (see Figure 3.2 for an example of steam turbine):

$$\eta_{EP} = \frac{H_I - H_{O,r}}{H_I - H_{O,ie}} \tag{3.1}$$

The real power generated from the expander could be expressed as:

$$W = (H_I - H_{O,\text{ie}}) \cdot \eta_{EP} \tag{3.2}$$

In equation (3.1) and (3.2) H_I is the input enthalpy, $H_{O,\text{ie}}$ and $H_{O,\text{r}}$ are respectively the idea output enthalpy after an isentropic expansion and the real output enthalpy, W is the real specific power output of the expander.

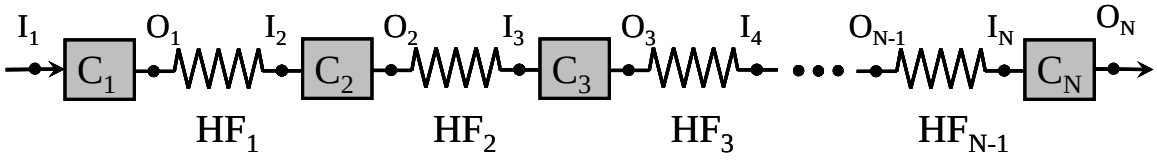

Figure 3.1 Diagram of a generalized thermodynamic cycle
(I – Inlet, O – Outlet, C – Power Component, HF – Heat Flux)

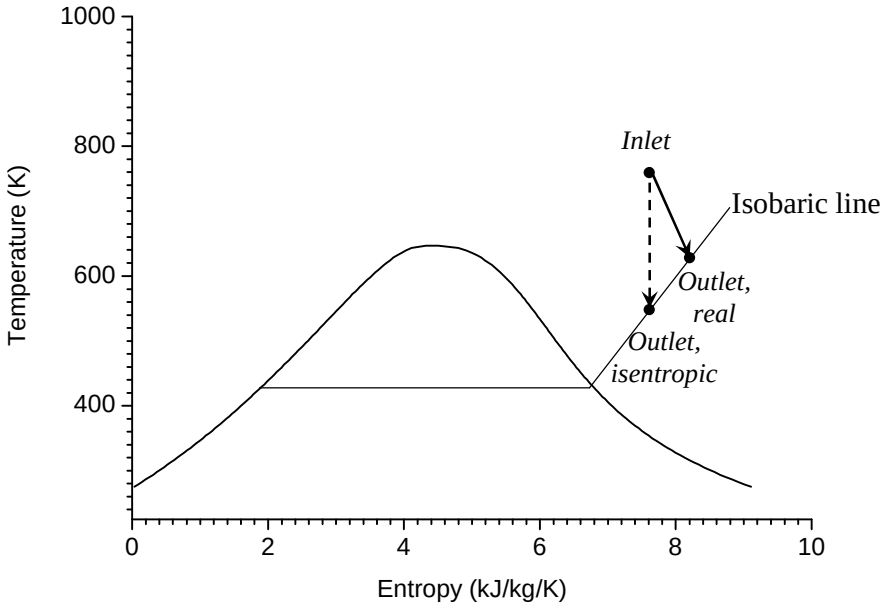

Figure 3.2 A Temperature-Entropy diagram showing an expansion process of a steam turbine

Practically the expansion could be regarded as an adiabatic process. The actual output enthalpy can be calculated as:

$$H_{O,r} = (H_{O,\text{ie}} - H_I) \cdot \eta_{EP} + H_I \tag{3.3}$$

In equations (3.3) $H_{O,r}$ is the actual output enthalpy.

There are two types of compression named adiabatic process and isothermal process. The compression processes without cooling could be regarded as adiabatic compression. In adiabatic compression the isentropic efficiency is defined similarly as the expansion process:

$$\eta_{AC} = \frac{H_{O,ie} - H_I}{H_{O,r} - H_I} \tag{3.4}$$

In equation (3.4) η_{AC} is the isentropic efficiency of the compressor. The real power consumption in the compression process is calculated as:

$$W = (H_I - H_{O,\text{ie}}) / \eta_{AC} \tag{3.5}$$

Again the actual output enthalpy of the adiabatic compressor is calculated as:

$$H_{O,r} = H_I - (H_I - H_{O,\text{ie}}) / \eta_{AC} \tag{3.6}$$

On the other hand if ambient thermal sources such as air or water are used for process cooling the compression is considered as an isothermal compression. The ideal power consumption in an isothermal compression is the exergy change. Considering the irreversibility the real power consumption is expressed as:

$$W = [(H_I - H_{O,\text{it}}) - T_a \cdot (S_I - S_{O,\text{it}})] / \eta_{IC} \tag{3.7}$$

And the output enthalpy of the isothermal compression is calculated as:

$$H_{O,r} = H_{O,\text{it}} \tag{3.8}$$

In equations (3.7) and (3.8) S_I is the input entropy, $H_{O,\text{it}}$ and $S_{O,\text{it}}$ are respectively the idea output enthalpy and entropy after an isothermal expansion, η_{IC} is the isothermal efficiency of the compressor.

In the present study the process is regarded as adiabatic compression while the working temperature is lower than the ambient temperature due to cooling technology is not applicable using the ambient thermal sources. Otherwise the isothermal model is applied to represent an ambient-temperature compression using water/air cooling technologies. Note that the power consumption of the compressor is negative for the convenience of the whole system design.

The throttle valve is neither a power transfer unit nor a heat transferring unit but could be regarded as a zero-output power transfer unit $W = 0$. As working fluid expands through an isenthalpic process the mass fraction of fluid that is liquefied can be calculated as:

$$x = \frac{H_I - H_{O,g}}{H_{O,l} - H_{O,g}} \tag{3.9}$$

In equation (3.9) x represents the liquid fraction, $H_{O,l}$ and $H_{O,g}$ represent respectively enthalpies of output liquid and gas. It is noted that in a throttling device the working fluid expands through an isenthalpic process and theoretically this can lead to either an increase (when the Joule-Thomson coefficient is negative) or a decrease (when the Joule-Thomson coefficient is positive) in temperature; see Figure 3.3 for an example using methane. From the figure one can see that the high-pressure fluid can be fully liquefied if it is cooled to a sufficient low temperature prior

to the throttle valve. In other words, the fluid could be fully liquefied with $x = 1$ when $H_I < H_{O,l}$.

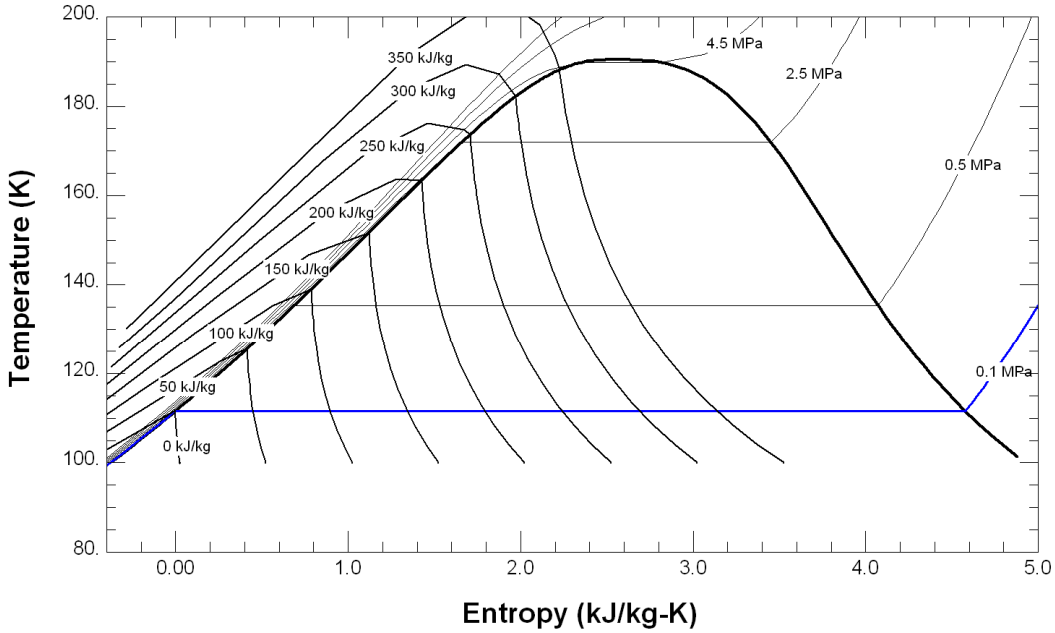

Figure 3.3 Isenthalpic process of methane in a Temperature-Entropy diagram

In the heat transfer unit the heat flux could be regarded as the enthalpy difference of the inlet and outlet flows:

$$q_i = H_{I,i+1} - H_{O,i} \tag{3.10}$$

In equation (3.10) q_i is the i^{th} heat flux, $H_{I,i+1}$ is the $(i+1)^{th}$ inlet enthalpy and $H_{O,i}$ is the i^{th} outlet enthalpy.

3.1.2 Thermodynamic Properties

Accurate data of thermodynamic properties are pre-requisite for a valid thermodynamic simulation. Numerically the thermodynamic properties could be predicted by the equations of state. One of the simplest equations of state for this purpose is the ideal gas law, which is roughly accurate for gases at low pressures and above moderate temperatures. However, this equation becomes increasingly less accurate at higher pressures and/or lower temperatures, and fails to predict condensation from a gas to a liquid. These cases occur in the current study. As a result, a valid prediction method for the thermodynamic properties is required.

A number of equations of state have been developed for gases and liquids since Van der Waals proposed his well-celebrated equation account for the real gas effects. Examples include Redlich and Kwong equations and Peng and Robinson equations [127]. These equations are empirical based and no one can accurately predict the properties of all substances under all conditions. In the present study a commercial program named REFPROP is used, which is able to provide the most accurate predictions for pure fluids and mixtures among all methods that are currently available.

REFPROP, developed by the US National Institute of Standards and Technology (NIST), provides tables and plots of the thermodynamic and transport properties of industrially important fluids and their mixtures with an emphasis on refrigerants and hydrocarbons, especially natural gas systems. This program includes three models to calculate the thermodynamic properties of pure fluids: equations of state (explicit in Helmholtz energy), the modified Benedict-Webb-Rubin equation of state, and an extended corresponding state (ECS) model. These models are implemented in a suite of FORTRAN subroutines. Written in a structured format, they are internally documented with extensive comments, and have been tested on a variety of compilers. Routines are provided to calculate thermodynamic and transport properties at a given (T,D,x) state, where T is temperature, D is density and x is mass fraction of the liquid. Iterative routines provide saturation properties for a specified (T,x) or (P,x) state, where P is pressure. Flash calculations describe single- or two-phase states given a wide range of input combinations (P,h,x), (P,T,x), etc, where h is enthalpy. The accuracy of REFPROP is obtained through the use of many coefficients in the equations, and thus the calculation speed is slower than other equations such as the Peng-Robinson cubic equations. The equations in the REFPROP are generally valid over the entire vapor and liquid regions of fluid, including the supercritical state [128].

It should be noted that the REFPROP "database" is actually a program and does not contain any experimental information, apart from the critical and triple points of the pure fluids. The program is friendly to self-developing users as it provides a dynamic link library (DLL) that allows interfacing with various softwares such as EXCEL, VISUAL BASIC & C, MATLAB, LABVIEW, etc.

3.2 The Pinch Technology

3.2.1 Introduction to the Pinch Technology

Most industrial processes involve transfer of heat either from one process stream to another (interchanging) or from a utility stream to a process stream. A target in an industrial process design is to maximize the process-to-process heat recovery and to minimize the utility (energy) requirements. Considering the fact that most processes involve a large number of processes and utility streams, it is a challenging task for process engineers to answer to the following questions [129]:

- Are the existing processes as energy efficient as they should be?
- How can new projects be evaluated with respect to their energy requirements?
- What changes can be made to increase the energy efficiency without incurring any cost?
- What investments can be made to improve energy efficiency?
- What is the most appropriate utility mix for the process?
- How to put energy efficiency and other targets like reducing emissions, increasing plant capacities, improving product qualities etc, into a coherent strategic plan for the overall site?

In late 1978, Bodo Linnhoff, a Ph.D student from the corporate laboratory, Imperial Chemical Industries Limited (ICI), under the supervision of Dr. John Flower, University of Leeds, devised a new approach to describe energy flows in process heat exchanger networks [130-133]. This was the first time to introduce the thermodynamic principles into heat-exchanger network design, and symbolize the establishment of a systematic methodology called Pinch Technology. Such a technology is based upon thermodynamic principles to achieve utility savings by better process heat integration, maximizing heat recovery and reducing the external utility loads [134]. All the above mentioned questions and more can be answered with full understanding of the Pinch Technology and awareness of the available tools for applying it in a practical way.

Pinch Technology is used to describe and analyze the heat exchanger network which is an important section of process design. The process design hierarchy can be represented by an "onion diagram" as shown in Figure 3.4 [135, 136]. The design of a process starts with the reactors (in the "core" of the onion). Once feeds, products, recycle concentrations and flowrates are known, the separators and power systems (the second and third layer of the onion) can be designed. The basic process heat and material balance can then be in place, and the heat exchanger network (the forth layer) can be designed. The remaining heating and cooling duties are handled by the utility system (the fifth layer). The process utility system may be regarded as a part of a centralised site-wide utility system. Using the Pinch Technology, it is possible to identify appropriate changes in the core process conditions that can have an impact on energy savings (onion layers one, two and three). After the heat and material balance is established, targets for energy saving can be set prior to the design of the heat exchanger network. The Pinch Technology ensures these targets achievable during the network design.

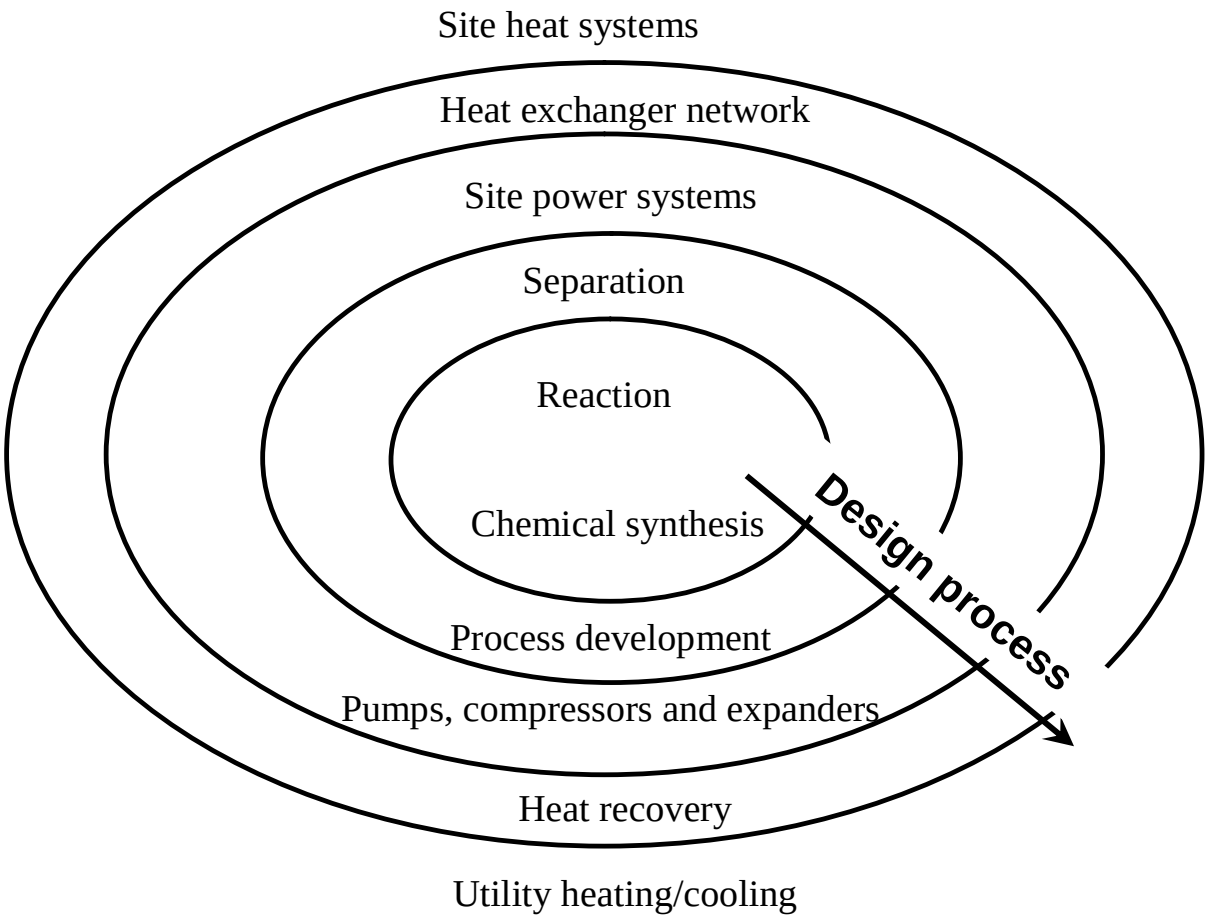

Figure 3.4 The onion diagram for process synthesis

The practical experience has shown that the Pinch Technology can bring benefits to a huge range of plants and processes, large and small, both within and outside traditional process industries [135]. Improvements come not only from heat recovery projects, but also from changing process conditions, improved operability and more effective interfacing with utility systems, all underpinned by better process understanding.

The Pinch Technology is now an integral part of the overall strategy for process development and design and the optimization of existing plants, often known as process synthesis or process integration. Furthermore, its application has broadened a long way beyond energy aspect including Mass Pinch [137-139], Water Pinch [140-142], Hydrogen Pinch [143, 144] and Oxygen Pinch [145, 146].

3.2.2 Principle of Pinch Technology

Pinch Technology is a simple methodology for systematically analyzing industrial processes and surrounding utility systems with the help of the first law and second law of thermodynamics. The first law provides the energy equation for calculating the enthalpy changes in the streams passing through a heat exchanger. The second law determines the direction of heat flow: in the absence of work input heat energy may only flow in the direction of hot to cold. In practice a minimum approach temperature (MAT) has to be maintained between the ‘hot’ process streams (which have to be cooled to specific temperatures) and ‘cold’ process streams (which have to be heated to specific temperatures).

The temperature-heat load diagram of a heat exchange process is plotted in Figure 3.5 which shows the opportunity for heat recovery as well as the minimum net heating and cooling requirements. In such a diagram the point of closest approach where available temperature driving forces between hot and cold streams are at a minimum is defined as the process pinch point where the temperature difference should be higher than MAT. The performance of the system is then limited by this constraint – the pinch point – just as the strength of a chain is determined by its weakest link. In other words if one needs a stronger chain the Pinch Technology teaches that the most cost-effective strategy is not to replace the chain with a new one but to increase the strength of the existing chain by selectively replacing the

weakest link. A simple way to increase the pinch temperature in Figure 3.5 is to shift the heating/cooling curves along the direction of heat load.

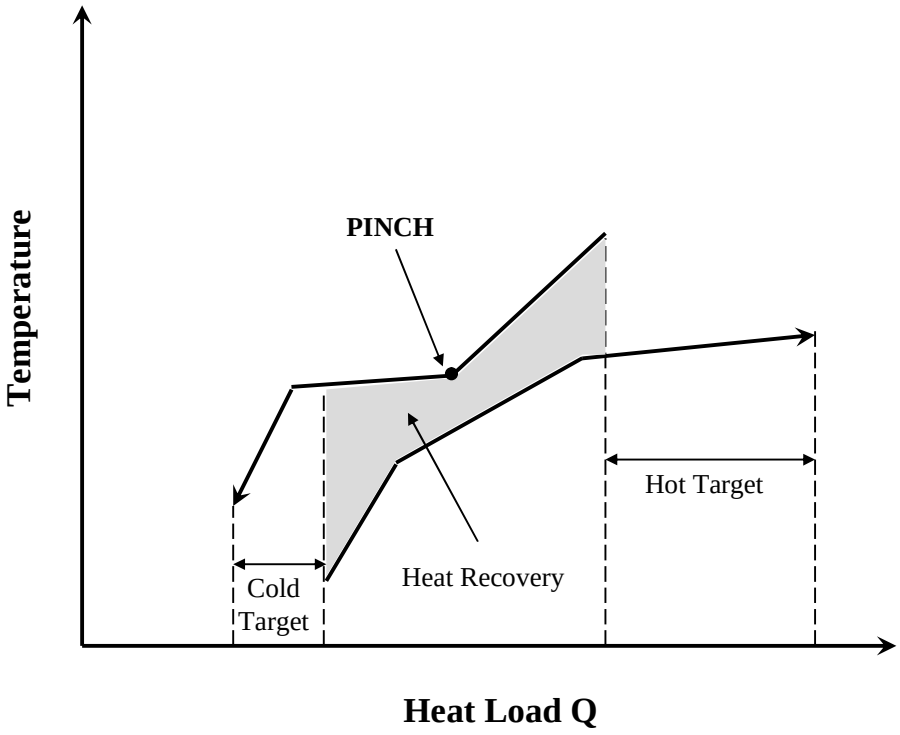

Figure 3.5 T-Q diagram of a heat recovery process

On the other hand, the change of pinch temperature will affect the heating and cooling requirements of the system. The heating power and cooling power are provided by external hot and cold utilities at unspecified temperatures sufficient to fulfill the duty. In practice, more than one utility may be available, and there are often price differentials between them. Therefore the selection and placement of the appropriate utilities is a key weapon for an efficient design.

In industrial practices hot utilities supplying heat to a process may include furnaces, steam heaters, flue gases, heat rejected from heat engines, thermal fluids or hot oil systems, exhaust heat from refrigeration systems and heat pump condensers and electrical heating systems. Likewise cold utilities removing heat from a process may include cooling water systems, air coolers, steam temperature rising up and boiler feed water heating, chilled water systems, refrigeration systems and heat pump evaporators [135]. These utilities can be further split into constant-temperature utilities (for example the condensing steam providing latent heat at a fixed

temperature), variable-temperature utilities (like the hot flue gas giving up sensible heat over a temperature range) and a mix-type utility (for example a furnace chamber gives out radiant heat at effectively a constant high temperature whereas the exhaust gases can release further heat as a variable-temperature utility). Often a wide range of hot and cold utilities can be used and some will be more convenient and effective than others. Taking the Figure 3.5 as an example, if two constant-temperature utilities are selected for the heat balance, two options are shown in Figure 3.6. If the temperature of hot utility is higher than the ambient temperature, it is obviously that the selection in option (b) is wiser as the low temperature heating may be cheaper than high temperature heating which may need to be supplied by dedicated devices. Likewise if the temperature of cold utility is lower than the ambient temperature, the selection and placement of the cold utility in option (b) is more efficient than that in option (a). This is because the biggest effect of temperature on unit cost of utilities occurs in refrigeration systems. Below ambient cooling needs heat pumping to the ambient temperature and the work requirement and cost increase steeply as the required temperature falls.

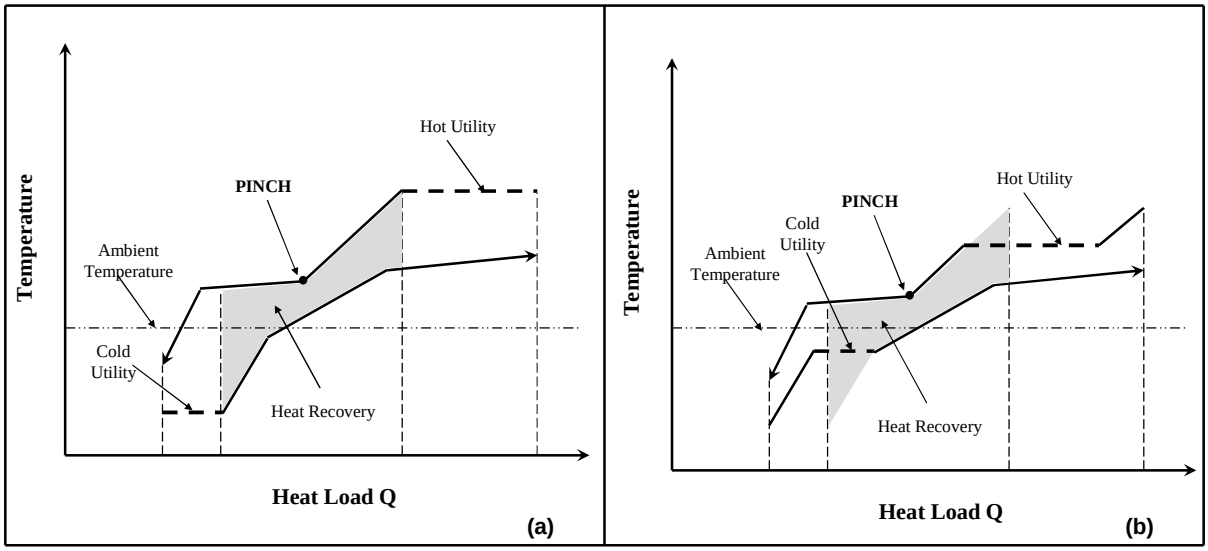

Figure 3.6 The selection and placement of utilities for energy balance

Although option (b) has a better performance than option (a), it might bring new pinch point. As a result the selection and placement of the utilities should be done very carefully. Furthermore the utilities themselves might be multi-stream systems with interactive heat exchange therefore should be integrated with the whole system to find the overall pinch. The indirect heat recovery through heat and power conversion should also be considered in this process. Using the process heat

sources to preheat the inlet working fluids of expansion machines could increase the power output while pre-cooling the inlet fluids of compression components by process cold sources could reduce the power consumption. All of these could impact on the heat distribution along with the temperature, which means that the temperature-heat load profile should be modified as well. Therefore Composite Curve and Balanced Composite Curves are introduced in Pinch Technology to deal with these multiple stream problems.

A Composite Curve is a graphical combination of all hot or cold process streams in a heat exchange process. While dividing all streams over any given temperature range into two groups named heat rejection and heat sink respectively, a single composite of all hot streams and a single composite of all cold streams can be produced in the Temperature-heat load diagram. In Figure 3.7 (a) three hot streams with constant heat capacity are plotted separately, where their supply and target temperatures define a series of temperatures T_1 to T_5. Between T_1 and T_2 only stream B exists and so the heat available in this interval is given by $B\cdot(T_1-T_2)$. However between T_2 and T_3 all three streams exist and so the heat available in this interval is $(A+B+C)\cdot(T_2-T_3)$. A series of values of heat can be obtained in this way and the results can be re-plotted against the heat load as shown in Figure 3.7 (b). The resulting temperature-heat load plot is a single curve representing all the hot streams, known as the hot composite curve. A similar procedure gives a cold composite curve of all the cold streams in a question.

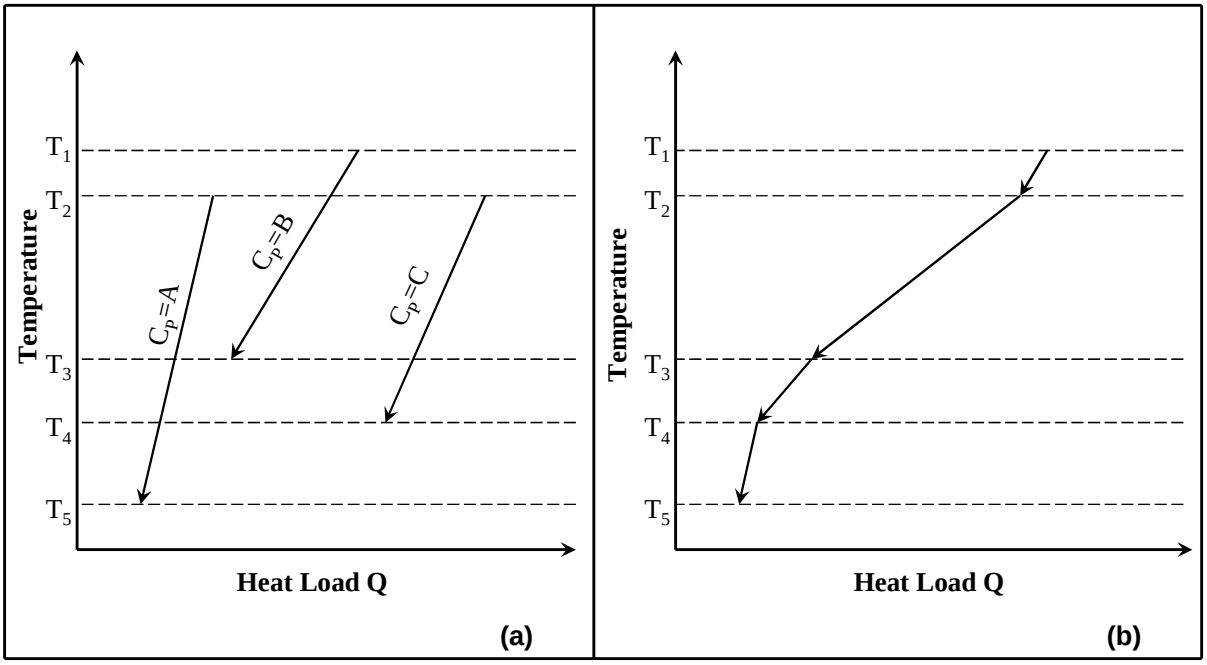

Figure 3.7 Formation of the hot composite curve

However this procedure is not suitable for practical simulation. As mentioned before the thermodynamic properties in this study are obtained from REFPROP "database" instead of a constant heat capacity model as some extreme working conditions may be involved. This makes the above staging treatment method inadequate. More importantly the above procedure cannot handle phase change processes which have effectively an infinite heat capacity. An alternative to the composite curve is to capture the exact temperature at a given heat load value. This is more applicable as the enthalpy increases monotonously with increasing heat load. The detailed program code used in this study for temperature capture in multiple flows can be found in Appendix A15.

While both the hot and cold Composite Curves plotted in the same diagram include all the utility streams at their target heat loads, the resulting curves should have no unbalanced overshoot at either ends. Therefore the so-called Balanced Composite Curves are particularly useful for showing the effect of multiple utilities, multiple pinches and variable-temperature utilities on temperature driving forces in the system and thus revealing more clearly constraints in the system design.

Based on the above discussion the stages of applying the Pinch Technology to a practical process plant or site design are as follows [135]:

(1) Obtain or produce a copy of the plant flowsheet including temperatures, flow rates, pressures and other thermal properties and produce consistent heat and mass balances.

(2) Extract the stream data from the heat and mass balances.

(3) Select an appropriate MAT and calculate energy targets and the pinch temperature.

(4) Examine opportunities for process change, modify the flowsheet and stream data accordingly and recalculate the targets.

(5) Once decided whether to implement process changes and what utility levels are used, design a heat exchanger network to recover heat within the process.

(6) Design the utility systems to supply the remaining heating and cooling requirements, modify the heat exchanger network as necessary.

(7) Reproduce the plant flowsheet based on the modifications of utilities and heat exchange network. Return to step (2) to study if further improvement is possible.

Although the above procedure is efficient and straightforward, the development of appropriate designs is less evident. Based on a specific configuration, the method here is to develop choices that are ‘close to the targets’, one then tries to eliminate rather than to determine choices. The modification of the specific configuration entails a great amount of manual developments that is particularly tedious for large industrial problem [147]. Furthermore, designs based on this procedure have been shown to be non-optimal in many cases, mainly due to its dependence on the initial structure, although some improvements have been noted [148]. An automatic design method therefore is desirable to overcome these drawbacks.

3.2.3 Systematic Optimisation Using Pinch Technology

Selection of an optimal configuration of a system is a difficult task. Commonly, the best configuration is obtained by parametric comparisons of different optimal structures, as shown in Figure 3.8. This task is highly time-consuming due to numerous design alternatives. In addition, an inherent uncertainty exists that a better alternative could be found [149]. For that reasons, an efficient and systematic

simultaneous optimisation procedure is of crucial importance for the selection of the best design alternative.

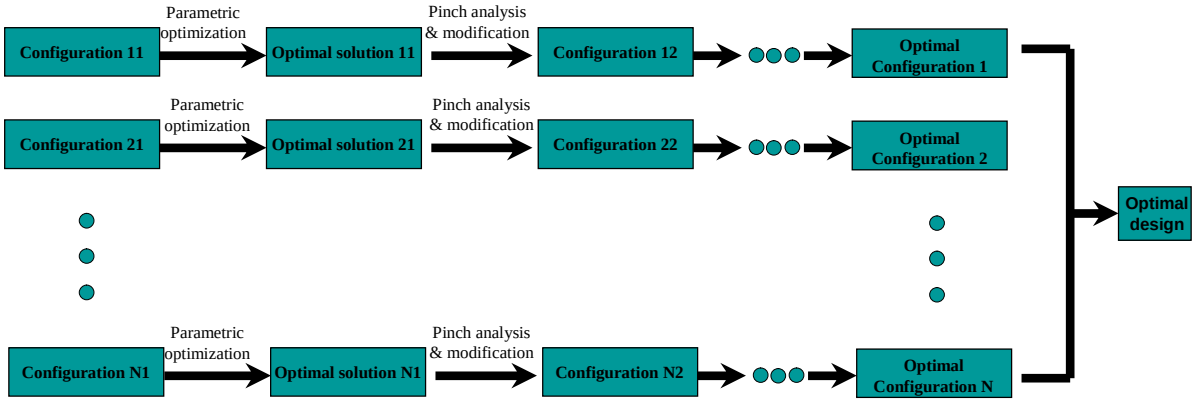

Figure 3.8 Common procedure of configuration optimisation

To simultaneously explore the benefits of both configuration and parameter, and to address complex trade-offs, the best approach appears to be the establishment a general superstructure including all possible options first, followed by optimisation to give an optimal design [150]. The superstructure concept of heat exchanger network has been widely used in the optimisation of energy recovery [151-155]. However such a concept is used to deal with the arrangement of give heat flows and power transfer components are not involved. In other words the method works with the forth layer of the ‘onion diagram’. Some researches has also extended the application of the superstructure to configuration selection [149, 156], but only few optional arrangements are given in their superstructure model. The present research extends the concept of superstructure and develops a generalized model for the systematic optimisation of complex thermal systems. In the proposed model not only the heat exchanger network but also the selection of power transfer components and the interactions between power transfer component and heat flow are considered. Different to the existing superstructure the generalized model includes all the possible options of system configurations and therefore enables optimisation at a systematic level.

A thermal cycle has two features. One is the alternative arrangement of power transfer units and heat transfer units as mentioned before. The other is the stream splitting and converging. As the stream converging does not affect the thermodynamic parameters of the fluids when they are regarded as different streams, only stream splitting is considered in the systematic optimisation. Despite of the specific heat exchanger network, the generalized superstructure of a thermal cycle

can be illustrated in Figure 3.9, which is a tree-like structure. This superstructure could be simplified by the upper limit of component stages, overall component numbers or the stream numbers of each splitting. For example if the streams numbers of each splitting is one, namely there is no stream splitting, the superstructure is simplified to the one as given in Figure 3.1.

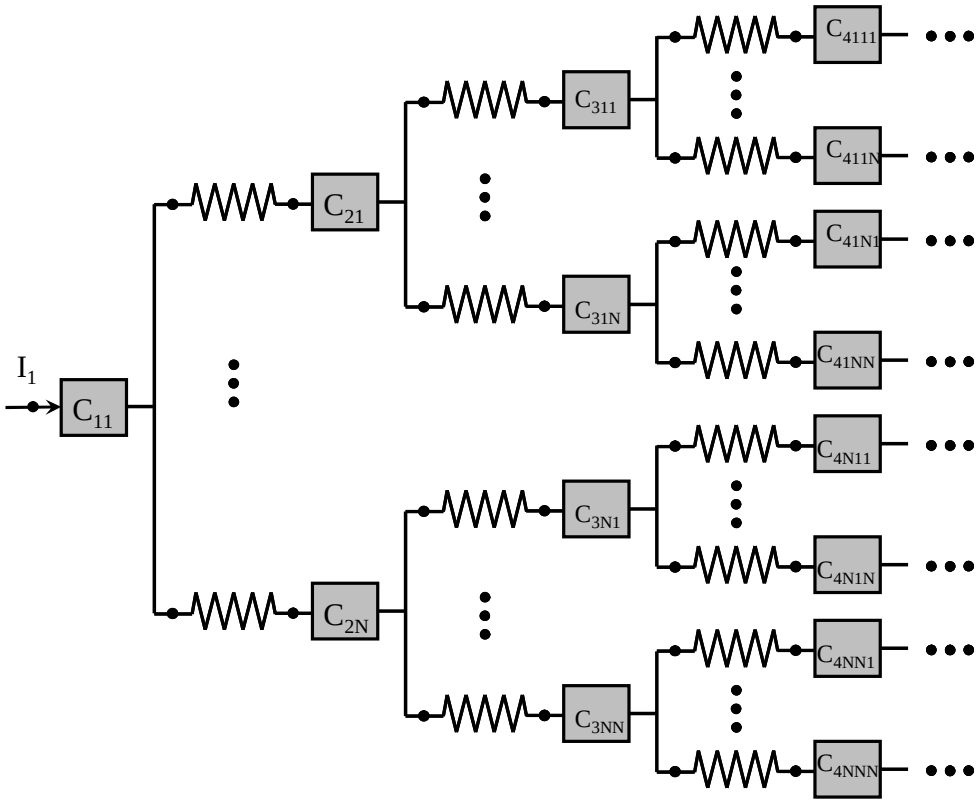

Figure 3.9 Generalized superstructure of a thermal cycle

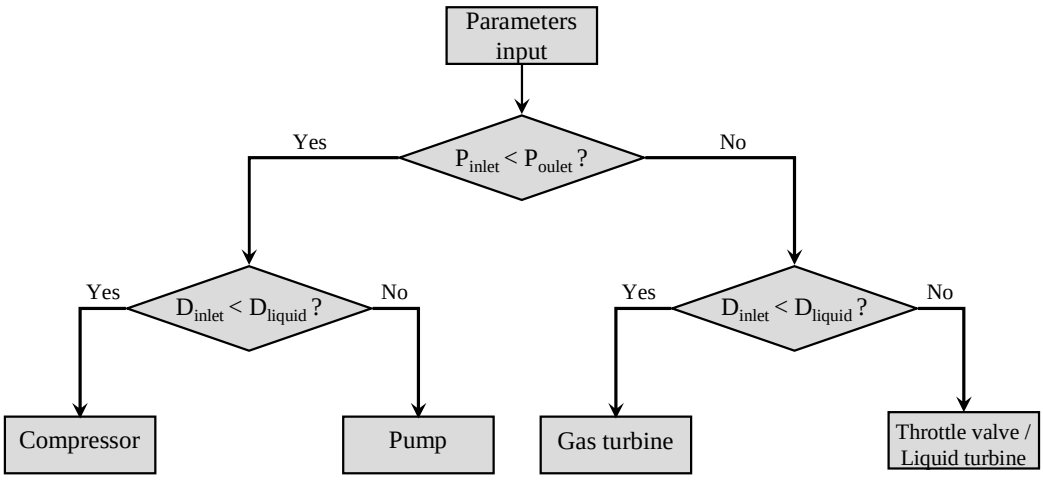

Figure 3.10 The selection procedure of component type

As can be seen from Figure 3.9, a general component model is used in the generalized superstructure which should be determined in a simulation process. In the present work the inlet and outlet pressure and inlet temperature is given for a specific flow and the selection procedure of the component type is shown in Figure 3.10 (in the figure ‘D’ represents density and the subscript ‘liquid’ represents the liquid state). One can see that decision is made first on the compression or expansion process. This is followed by the selection of the component based on the inlet state of the working fluid.

Any process flow diagrams can be expressed as a superstructure or a combination of superstructures. A systematic design and optimisation procedure can then be introduced as shown in Figure 3.11. A superstructure is first established based on the problem and specific requirements. The thermodynamic properties of the flows are then extracted to form a stream problem which could be optimised in both structure and parameter selections for a better performance. Pinch technology can be used in the optimisation process leading to an updated solution. After the optimisation the superstructure is transformed back into process flow diagram to check the feasibility prior to the final design.

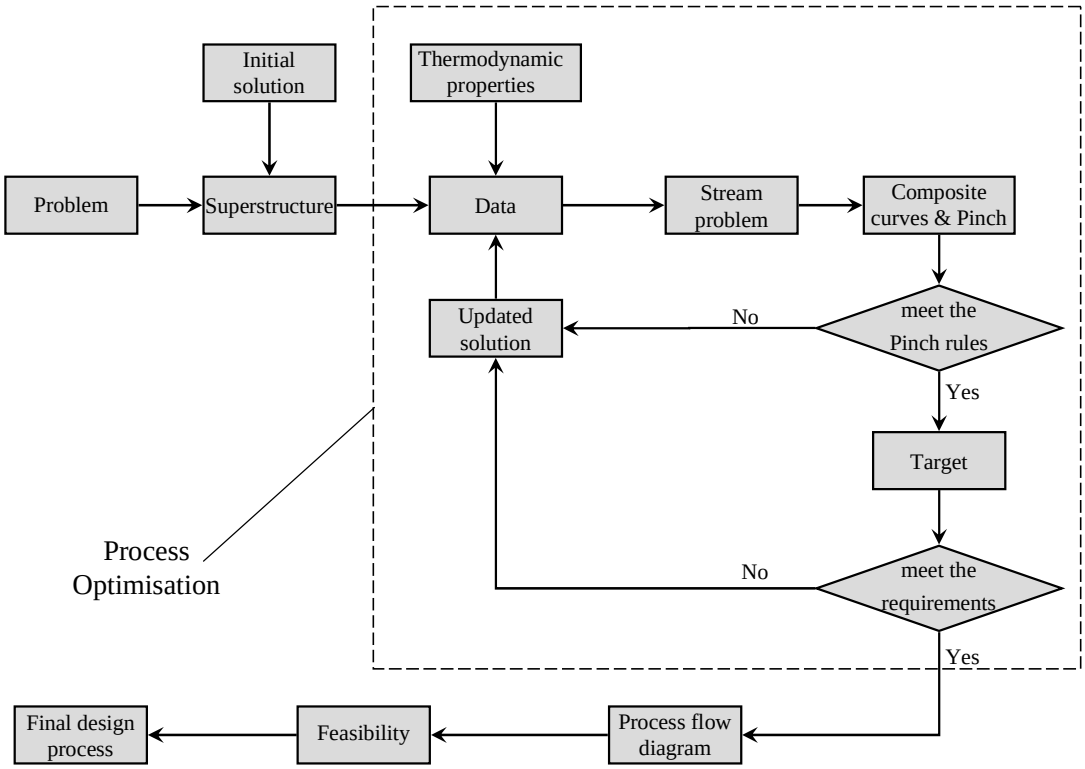

Figure 3.11 General procedures of a systematic design and optimisation

From the above one can see that the key to a systematic design is the optimisation process. As this is a complex problem including both structure selection and parameter analysis, an effective and efficient optimisation technique is required in order to obtain the best configuration and an optimal set of parameters.

3.3 Genetic Algorithm

3.3.1 Introduction to the Optimisation Algorithms

Superstructure based optimisation processes are in general formulated as mixed-integer non-linear programming (MINLP) models in a mathematical programming framework. According to the layout of the superstructure which includes all process structure variations, the MINLP problem can be expressed by an objective function $f(x,y)$, non-linear performance or balance equations $h(x,y)$ and non-linear constraints $g(x,y)$ together with the boundary conditions [156, 157]:

$$\begin{aligned} Z &= \min_{x,y} f(x,y) \\ \text{subject to } & h(x,y) = 0 \\ & g(x,y) < 0 \end{aligned} \tag{3.11}$$

In such a model the objective function, the balance equations and non-linear constraints correspond to the net power (or its transformation), the first law of thermodynamics and the second law of thermodynamics, respectively. The continuous variables x represent process parameters (e.g. heat exchanger duties, stream-split fractions) and integer variables y represent discrete decisions (e.g. the specific structure selection). Moreover, the thermodynamic properties themselves used in the simulation are obtained by solving a set of complex equations in REFPROP. This makes the nonlinear nature more significant.

Any application of MINLP to systematic optimisation must address two issues. The first involves resolving the integer decisions arising from the discretization of the problem into temperature or heat load intervals defined by the kinks in the composite curve. The second issue concerns continuous parametric optimisation [151, 152]. As there is in general more than one local optimum, it is often difficult to guarantee convergence to the global optimum for MINLP formulations, where a good starting point for a design problem is seldom available when applying many of the commonly used programming methods. An inappropriate initial guess could lead to a solution stuck at a local optimum.

A well-known technique for improving search and avoiding local optima is genetic algorithms (GA). Such a technique is based on the mechanics of natural selections. Motivated by the principle of evolution and heredity, GA is started with a set of random solutions called population instead of an initial guess. Whereas classical optimisation methods often rely on local gradient search, GA keeps track of a population of potential solutions. Thus GA is less sensitive to arbitrary initial guesses of the solution. The four significant differences between GA and the traditional search and optimization methods are [158]:

- GA searches a population of points in parallel, not a single point.
- GA does not require derivative information or other auxiliary knowledge; only the objective function and corresponding fitness levels influence the directions of search.
- GA uses probabilistic transition rules, not deterministic ones.
- GA works on an encoding of the parameter set rather than the parameter set itself (except in where real-valued individuals are used).

Lots of studies using GA to solve MINLP problem have been reported showing the successful engineering applications to process synthesis in general and heat exchanger network synthesis in particular [55, 154, 155, 159].

3.3.2 The principle of GA

The genetic algorithm (GA) was developed by John Holland and his colleague at the University of Michigan in 1960s. It is a search heuristic that mimics the process of natural evolution [159]. This heuristic is routinely used to generate useful solutions in large scale optimization problems.

GA starts with a set of random solutions called population. Individual solution is represented in encoded form called chromosome. Each chromosome comprises of individual structures called genes. Solutions from one population are used to form a new population. This is motivated by a hope that the new population will be better than an old population. In order to form a new population, GA uses genetic operators and selection process. Genetic operators are used to generate the new solutions

(offspring) from the current solutions (parents). Selection is the process of keeping and deleting some solutions from both parents and offspring for the same number of next population. Moreover, selection is the process of choosing some parents to generate offspring as well. In the selection process, the solutions are selected according to their values of objective function (fitness). The better fitness they have, the more chances of being selected. This process leads to the evolution of populations of individuals that are better suited to their environment than the individuals that they were created from, just as in natural adaptation. The algorithms will repeat until a termination condition is satisfied. The best solution is returned to represent the optimum solution.

The procedure of GA has the following steps [159]:

(1) Create a randomly generated population (feasible candidate solution).

(2) Scores each chromosome in the population by computing its fitness value.

(3) Scales the raw fitness scores to convert them into a more usable range of values.

(4) Select chromosomes called parents based on their fitness

(5) Some of the individual chromosomes in the current population that have better fitness are chosen as elite. These elite chromosomes are passed to the next population.

(6) Produces offspring from the parents. Offspring are produced either by making random changes to a single parent-mutation or by combining the vector entries of a pair of parents-crossover.

(7) Replaces the current population with the offspring to form the next generation.

(8) Checks termination conditions and stops when one of the stopping criteria is met. Else go to step (2) to create new populations.

From above one can see that GA creates three types of offspring for the next generation as shown in Figure 3.12:

- *Elite offspring* are the chromosomes in the current generation with the best fitness values. These individuals automatically survive to the next generation.

- *Crossover offspring* are created by combining the vectors of a pair of parents. At each coordinate of the offspring vector, the default crossover function randomly selects an entry or gene at the same coordinate from one of the two parents and assigns it to the offspring.

- *Mutation offspring* are created by introducing random changes or mutations to the genes of a single parent. By default, the algorithm adds a random vector from a Gaussian distribution to the parent.

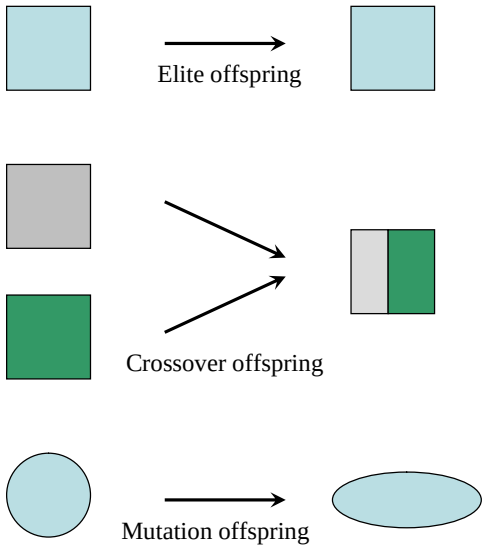

Figure 3.12 Schematic diagram of the offspring generation in GA

To sum up, GA does not use any information of derivative, and because of this, presents good chances of escaping from local solution. As a result, the application of GA to practical problems generally gives global optimal, or, at least, solutions more satisfactory than those obtained by other methods.

3.4 Summary of This Chapter

This chapter provides a systematic optimization strategy for thermodynamic designs of complex thermal/power systems. Unlike the traditional optimization methods, which treat the configuration selection and parametric optimization separately, the new technique performs the two simultaneously by extending the concept of superstructure. In the new model not only the heat exchanger network but also the selection of power transfer components and the interactions between power transfer component and heat flow are considered. As a result the new superstructure includes all the possible options of system configurations and therefore enables optimisation at a systematic level. In the new optimal procedure, the Pinch

Technology is adopted for the overall process analysis and Genetic Algorithm is used to solve the MINLP problems formulated from the optimization. Despite of the specific structure of the heat exchanger network, the proposed technique gives an automatic way avoiding tedious manual work for configuration selection.

Chapter 4 Integration of CES System with Liquefaction

4.1 Background

Electric utilities normally classify consumers into three broad groups: domestic, commercial and industrial. The industrial sector has long been the largest user in western countries although its contribution decreases recently, leading to a roughly even split with respect to two other sectors; see Figure 4.1 for the example of EU-27 [160]. On contrast, huge electricity demand in some developing countries makes the industrial sector a major consumer of electricity due to rapid industrialization. For example, the industrial sector in China contributes to over 70 % of the nation's total electricity generation since 1998 [161]. In the year of 2005 to 2007, the industrial electricity consumption share had increased to 79.4%, 77.7% and 78.4%, respectively [162]. As electricity generation capacity is lower than the demand, power cuts and erratic power supply often cause disruption of industrial production. Peak hour shortages are more severe in some developing countries, leading to huge discrepancies in production and operations management. Power thefts and low quality of power supply make the situation in the power sector even worse. With the demand far outstripping the electricity generation in these countries such as India and China, a lot of industries are now looking for alternatives.

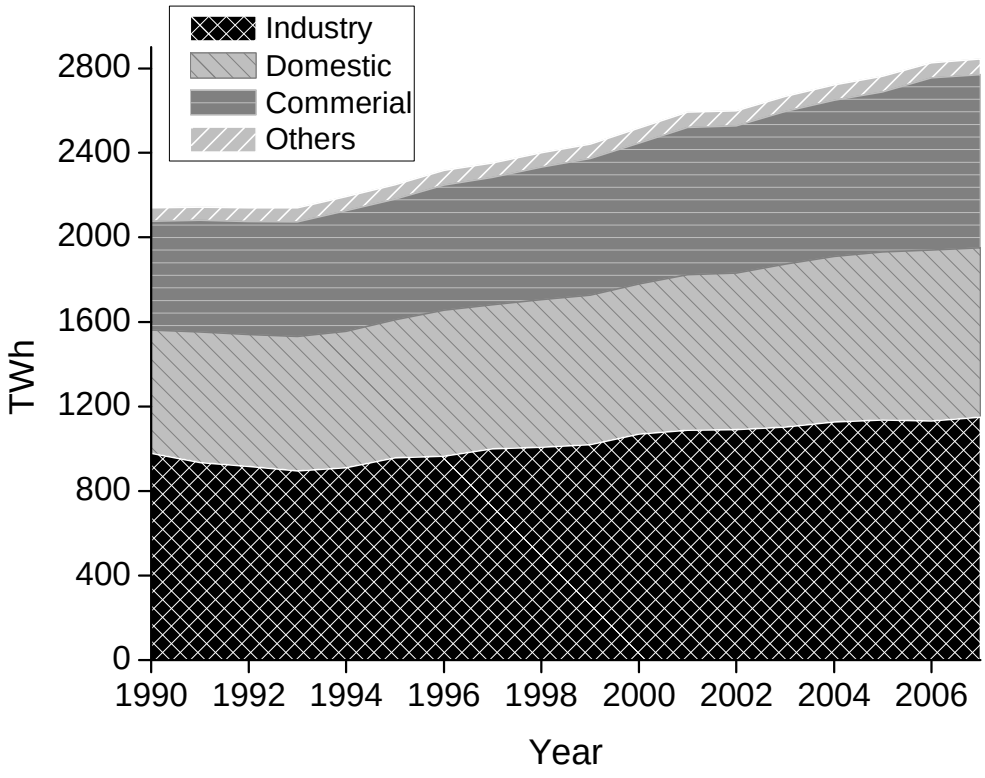

Figure 4.1 Final electricity consumption by sector, EU-27 (the 27 member countries of the European Union)

Comparing with the household and commercial sectors, individual industrial consumer requires much more electricity. In the US the industrial consumers comprise about 0.5% of total end-use consumers serviced by electric utilities but consume about 26.7% of the total electricity [163]. Particularly, the iron and steel making, chemical, construction material and non-ferrous metal production industries are the most electricity intensive sub-sectors among this sector. At present Chinese electricity consumption in the above sub-sectors accounts for 11%, 7%, 11% and 7% of the total national electricity consumption, respectively. The proportion of heavy industries as a whole has been on the rise from 58.9% in 1999 to 75.3% in 2003 [162]. Iron and steel making and chemical industries are good examples as shown in Figure 4.2 [164]. India is in a similar situation: the iron and steel sector consumes approximately one quarter of the total industrial electric consumption at present and this ratio is projected to increase as steel production through the arc-furnace route increases from the present share of 25%. For steel-making industries, the electricity consumption costs about 30% of the total production costs [165].

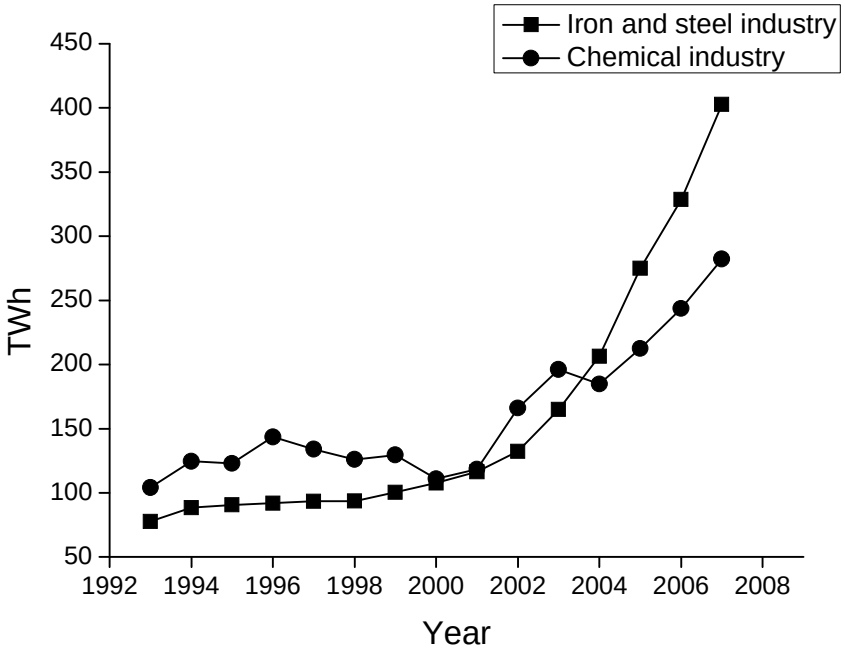

Figure 4.2 Electricity consumptions by iron and steel industry and chemical industry in China

Large industrial energy users who buy their electricity at spot rates (which tend to be higher when demand is high) are likely to be future consumers of bulky energy storage facilities. The use of electrical energy storage enables generation of own electricity at times of high demand when spot rates are high and switch back to the grid for industrial processes operation and electrical energy storage when demand and rates fall. Large scale energy storage technologies can store some excessive off-peak electricity and take some pressure off utility's peak energy demand, hence earn a name ‘load levelling’.

An issue associated with most heavy industrial processes is the cogeneration of significant amount of waste heat. Examples include hot gases from various types of furnaces in the steel industry and kilns in the cement industry, exhaust gases of internal combustion engines and gas turbines, hot liquids used to cool kilns or furnaces, etc [166]. Statistical investigations indicate that low-grade waste heat accounts for 50% or more of the total heat generated in industry [167]. The waste heat has considerable amount of available energy. Failure to recover the waste heat

leads to not only undesirable energy loss but also environmental pollution issues [168, 169].

A traditional Rankine cycle using water as the working fluid does not allow efficient recovery of such a waste heat below 370°C as the thermal efficiency becomes uneconomically low [167]. Organic Rankine Cycles (ORCs) have been investigated for power production using low grade waste heat. However, a wide range of applications has not been achieved because of concerns about economic feasibility and safety [170].

This chapter considers a potential application of CES for large scale heavy industries, not only for addressing their high demand of bulky energy storage, but also for efficient recovery of the cogenerated waste heat using a cryogen as the working fluid to increase the power output in the energy extraction process. Air liquefaction unit is integrated in the proposed systems. Based on the cooling power generation method in air liquefaction process, two types of system namely Linde-Hampson CES system and Expander CES system are studied in the following. In Linde-Hampson CES system the cooling power for air liquefaction is mainly generated by the expansion of the compressed air, while in Expander CES system an expander cycle is used to produce the cooling power.

4.2 Linde-Hampson CES System

Using liquid air as an energy carrier, the CES consists of three sub-processes: air liquefaction for energy storage, liquid air storage and cryogenic energy release. A state-of-art study shows the upper limits of both liquefaction efficiency and cryogenic energy extraction efficiency are about 60% as discussed in Chapter 2. That suggests that the overall efficiency of the CES be lower than 36% if the two processes are not integrated and no waste heat is available.

Detailed analysis indicates that a big share of exergy loss in liquefaction process is caused by the inefficient generation of high grade cold. On the other hand the exergy efficiency of cryogenic energy extraction could only be improved if the high grade cold could be efficiently recovered. In this study, it is proposed to integrate the two processes through cold storage to increase the overall exergy efficiency. The

schematic of such an integrated CES system is illustrated in Figure 4.3. The system works in the following manner. At off-peak hours the excessive (and also cheap) electricity as well as the stored cold are used to produce liquid air in an air liquefaction unit. In the peak hours liquid air powers an energy extraction unit to generate electricity and waste heat is added to increase the power output. The cold energy released in this process is stored and recovered in the air liquefaction process.

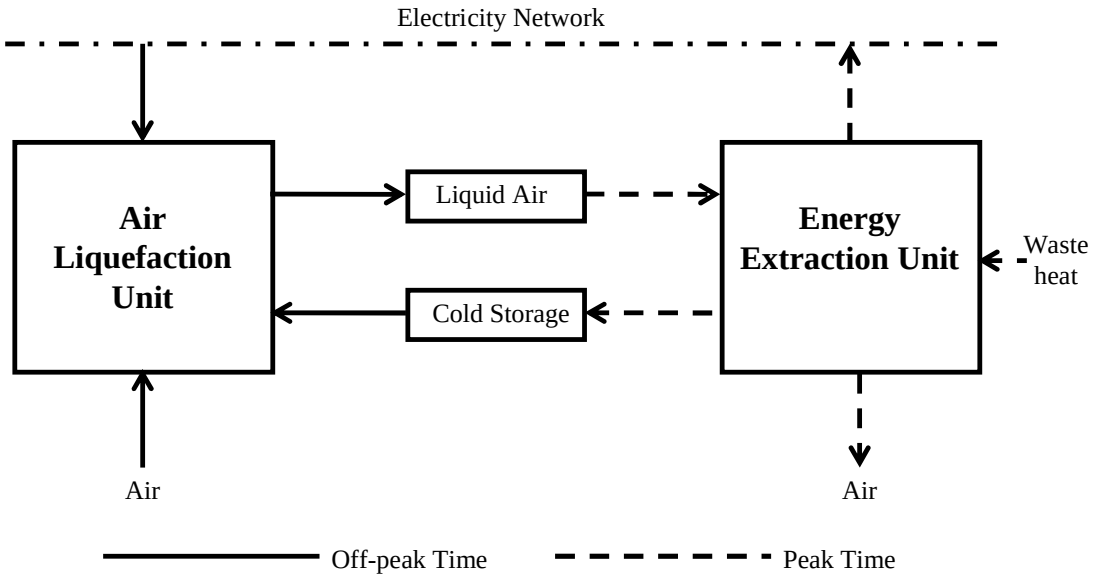

Figure 4.3 Principle diagram of the liquefaction integrated CES system

4.2.1 Cold Storage Medium

Cold storage aims to recover the cold energy released in liquid air preheating process. In this process air works as a supercritical fluid and as a result the cold is produced in the form of sensible thermal energy. From Figure 4.4 one can see that the isobaric heat capacity of air changes slightly in the heating process, especially while the pressure is very high. Like high temperature sensible heat storage, thermal fluids could be used to recover the cold energy very efficiently if the temperature gradients match well. In this process the thermal fluids will be used not only as working fluids but also cold storage media. As a result the following aspects associated with the fluids are expected:

- Ambient working pressure for the safety reasons and for reduction of the capital costs of associated facilities;
- Working in the liquid region to reduce the storage volume;

- Good heat capacity to reduce the storage volume;
- Good stability;
- Good safety performance (including flammability, toxicity etc);
- High thermal conductivity to reduce the surface area of the heat exchangers;
- Cheap and easy to obtain.

For the above reasons only common refrigerants are considered in this study and their thermodynamic properties are obtained from REFPROP. The isobaric heat capacity and thermal conductivity of the fluids are shown in Figure 4.5 and Figure 4.6 respectively and their freezing and boiling points are listed in Table 4.1 together with the main hazards. It is found that no fluid can fully cover the working temperature region of liquid air pre-heating process. As a result in this research the cold energy released by the liquid air will be recovered by several stages using different refrigerants.

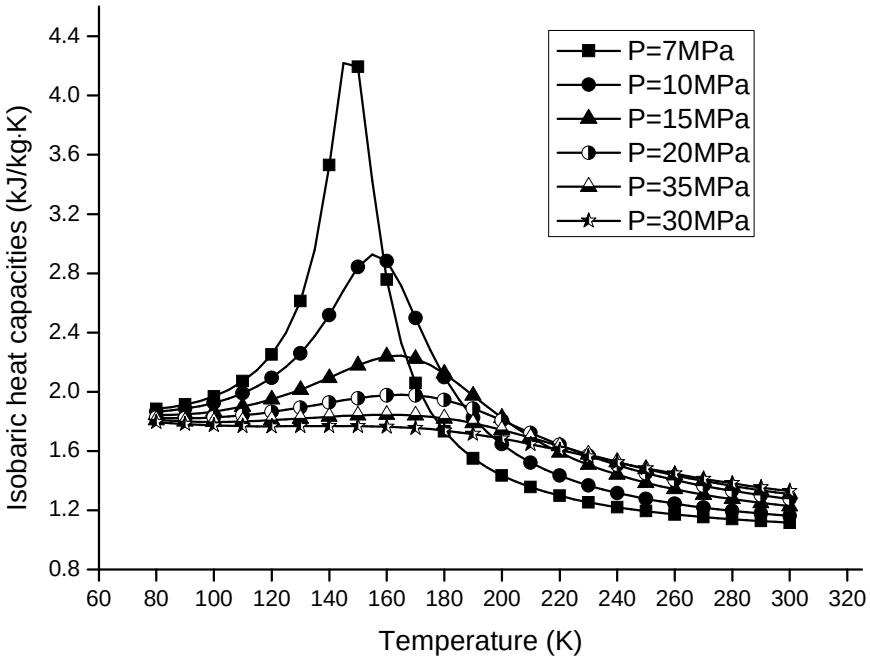

Figure 4.4 Isobaric heat capacities vs. Temperature diagram of air at different pressures

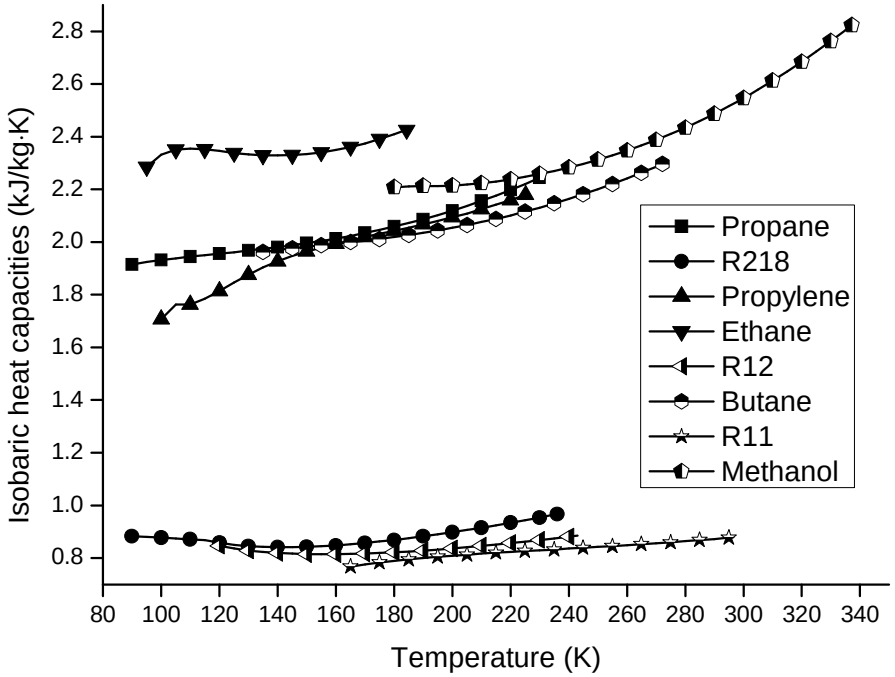

Figure 4.5 Isobaric heat capacities vs. Temperature diagram of some refrigerants at ambient pressure

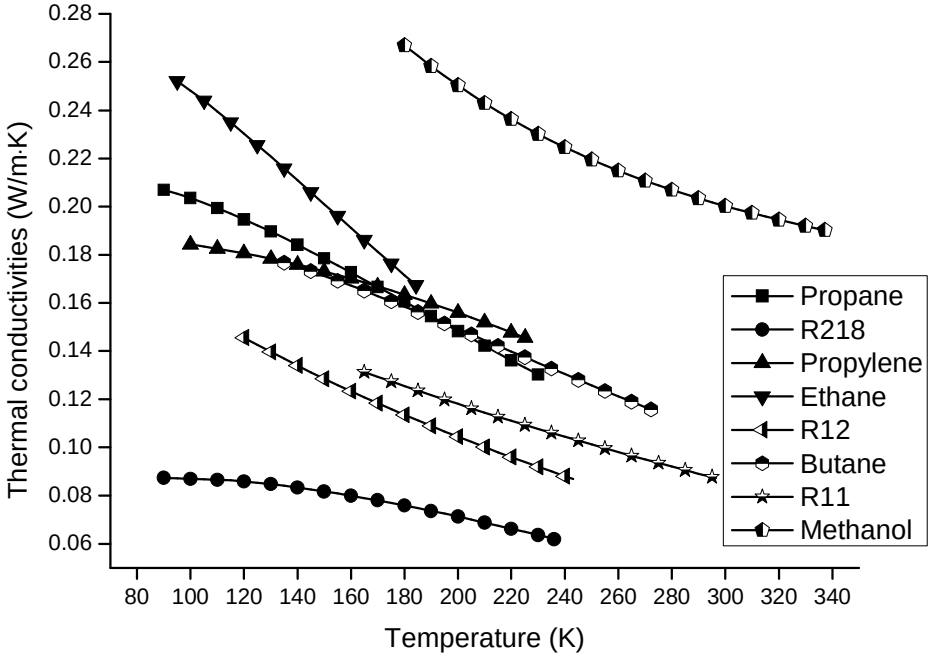

Figure 4.6 Thermal conductivities vs. Temperature diagram of some refrigerants at ambient pressure

Table 4.1 Freezing and boiling points and hazards of some common refrigerants

	Freezing Point (K)	Boiling Point (K)	Hazards
Propane	85	231	Extremely flammable
R218	90	235	Non-flammable, Non-toxic
Propylene	88	225	Extremely flammable
Ethane	90	184	Highly flammable
R12	116	243	Non-flammable
Butane	136	273	Highly flammable
R11	163	297	Non-flammable
Methanol	176	338	Highly Flammable, Toxic

From Figure 4.5 and Figure 4.6 one can see the propane and ethane are prior candidates for the recovery of high grade cold (lower temperature) as it has higher heat capacities and thermal conductivities while comparing with other two options R218 and Propylene. However as all these fluids become gas phases at ambient temperature, leakage of the refrigerants may cause explosions. For these reasons R218 is selected in this work which is non-flammable and non-toxic.

For the same reasons, R11 may be used for low grade cold recovery. It is worth to mention that R11 may evaporate at ambient temperature (warm tank). Methanol could be an alternative as it has a wider working temperature region. Although there are also safety issues with the use of methanol, it is not as serious as propane because it is in a liquid state at ambient condition.

4.2.2 System Configuration and Performance

By introducing the cold storage units, a base-case layout of the liquefaction integrated CES system is shown in Figure 4.7. Dry air 1 and return gas 9 are mixed and compressed to an elevated pressure 4 by a two stage compressor with inter-cooling 2-3. After rejecting heat in the main cold box in process 4-5 the high pressure air is cooled to the lowest temperature level, followed by an isentropic throttling process to produce liquid air. A fraction of the product is vaporized in the cryogenic

tank and introduced back to the main cold box and the inter-cooler to supply part of the cold energy. The remaining cold requirement of the main cold box is charged by the cold storage units.

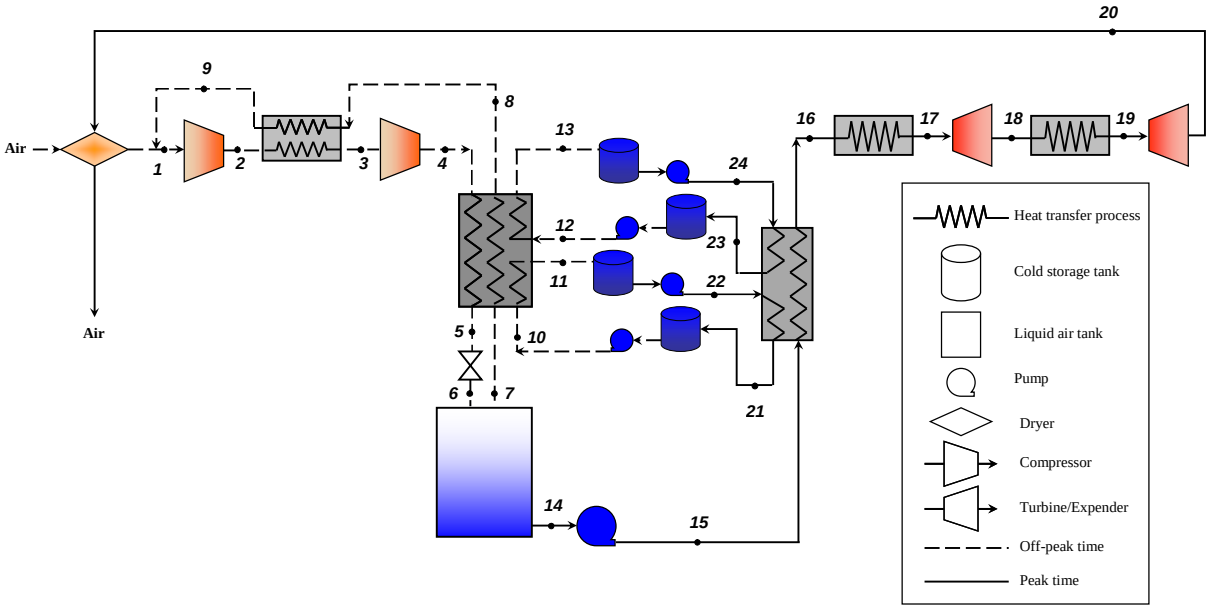

Figure 4.7 The flow sheet of the Linde-Hampson CES system

The liquefaction unit operates at off-peak time to store excessive electricity. At peak time the cryogenic energy is extracted by a direct expansion cycle to reproduce electricity. In this process, liquid air is pumped to a higher pressure level, releasing its cold energy to the cold storage media in process 15-16 via heat exchange. It is then superheated by waste heat before a two stage expansion with inter-heating. The flue gas of the expander can be used to regenerate the desiccant of the air dryer.

The cold storage unit in the proposed system consists of two dual-tank configurations in which the high temperature and low temperature fluids are stored separately in two tanks as shown in Figure 4.7. The thermal fluids are conveyed from high temperature tank to the low temperature tank during the energy release processes at peak hours, and are conveyed backwards during air liquefaction processes for cooling power supply. The use of the two thermal fluids R218 and R11 which can both transfer and store the cold energy simplifies the designs of the system. Moreover, the operation becomes easier in this way as the mass flowrate of the thermal fluids are easy to adjust.

In such a system, the air liquefaction unit process can be regarded as a modified Linde-Hampson cycle using external cold energy from power recovery process. As a result it is termed Linde-Hampson CES system in subsequent analysis.

A program based on Matlab 7.0 has been written for the simulation and parametric optimisation of the Linde-Hampson CES system. To simplify the computation, some assumptions are introduced (see also Table 4.2 for the performance of individual components):

- The flow is steady and the state of the working fluid at each specific location within the system does not change with the time [87].
- The power consumptions of the cold storage cycle during pumping are negligible.
- Pressure drop and heat losses in the heat exchangers and pipe lines are negligible [171].
- Before air enters the cold parts of the ASU the molecular sieves remove components from the air (H_2O, CO_2, hydrocarbons etc.) that would interfere with the cryogenic process. The power consumption of molecular sieves regeneration is negligible. Such an assumption is reasonable as the power consumption of ASU mainly consists of the power requirement for the compression of the feed air. Regenerating molecular sieves mainly consume thermal energy which can be supplied by the waste heat [172].

.

Table 4.2 Assumptions of individual components [69, 89-91]

Compressors	Isothermal efficiency (%)	87
Turbines/expanders	Isentropic efficiency (%)	88
Cryoturbine	Isentropic efficiency (%)	70
Cryogenic pump	Isentropic efficiency (%)	77
Heat exchanger network	Approach temperature (℃)	3

The round trip efficiency of the system is defined as the ratio of net power generation in energy extraction process and the power consumption in air liquefaction process:

$$\eta = \frac{\sum \dot{m} W_{EP} - \dot{m} W_P}{\sum \dot{m} W_{CP}} \tag{4.1}$$

The round trip efficiency is selected as the objective function of the parametric optimisation process while the inlet parameters of the power transfer component are used as the variables. Assuming there is no external heat sources to superheat the system the optimisation process is shown in Figure 4.8. The results show that the optimal round trip efficiency of the throttle valve based Linde-Hampson CES system is only about 22%. However while replacing the throttle value with cryoturbine the optimal round trip efficiency increases to about 37%. Based on the optimal solutions, the data in Table 4.3 and Table 4.4 are obtained respectively for throttle valve and cryoturbine based Linde-Hampson CES systems, which contain the values of temperature, pressure and flowrate at different positions as shown in Figure 4.7.

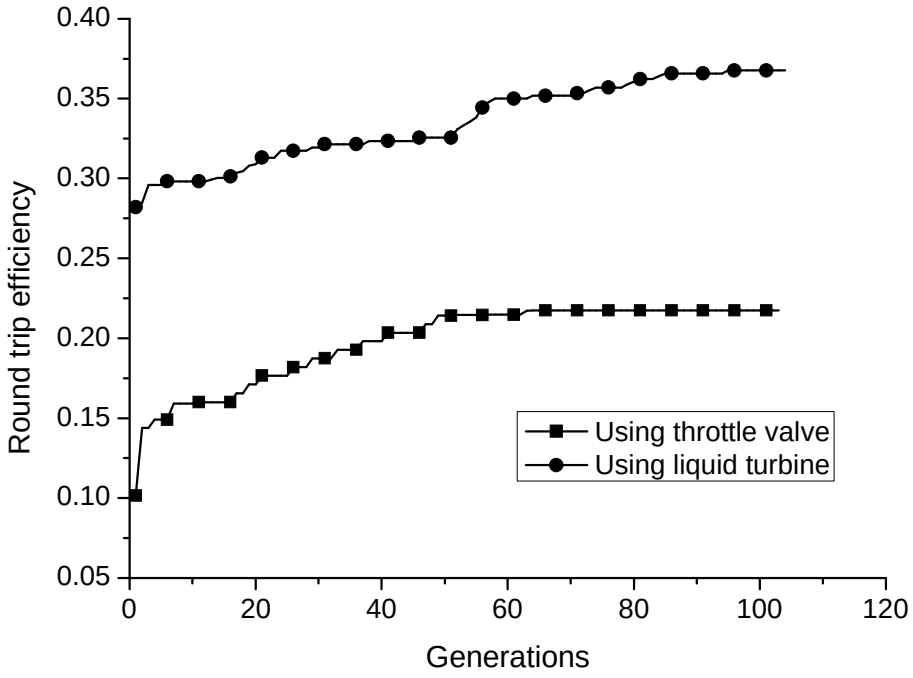

Figure 4.8 Round trip efficiency of Linde-Hampson CES system

Table 4.3 State parameters of the throltting valve based Linde-Hampson CES system – optimal conditions

State Number	Mass flow rate (kg/s)	Pressure (bar)	Temperature (K)

1	1.0	1.0	298.2
2	1.0	3.9	298.2
3	1.0	3.9	295.8
4	1.0	126.5	298.2
5	1.0	126.5	133.3
6	1.0	1.0	80.0
7	0.56	1.0	81.8
8	0.56	1.0	294.0
9	0.56	1.0	298.2
10	1.09	1.0	97.3
11	1.09	1.0	208.5
12	0.28	1.0	211.2
13	0.28	1.0	293.0
14	0.44	1.0	79.0
15	0.44	119.6	85.0
16	0.44	119.6	289.9
17	0.44	119.6	298.2
18	0.44	12.4	165.9
19	0.44	12.4	298.2
20	0.44	1.0	163.1
21	1.09	1.0	97.3
22	1.09	1.0	208.5
23	0.28	1.0	211.2
24	0.28	1.0	293.0

Table 4.4 State parameters of the cryoturbine based Linde-Hampson CES system – optimal conditions

State Number	Mass flow rate (kg/s)	Pressure (bar)	Temperature (K)
1	1.0	1.0	298.2
2	1.0	4.0	298.2
3	1.0	4.0	291.0
4	1.0	137.2	298.2
5	1.0	137.2	112.2
6	1.0	1.0	80.0
7	0.26	1.0	81.8
8	0.26	1.0	270.8
9	0.26	1.0	298.2
10	1.73	1.0	94.1
11	1.73	1.0	212.0
12	0.50	1.0	214.2
13	0.50	1.0	292.5
14	0.74	1.0	79.0
15	0.74	112.3	84.7
16	0.74	112.3	289.2
17	0.74	112.3	298.2
18	0.74	12.2	168.3
19	0.74	12.2	298.2
20	0.74	1.0	163.5
21	1.73	1.0	94.1
22	1.73	1.0	212.0
23	0.50	1.0	214.2

24	0.50	1.0	292.5

The data illustrate that supercritical liquefaction processes are required for a better overall performance of the Linde-Hampson CES systems. The topping liquefied pressures P_5 are very high for both of the systems, 127 bar and 137 bar, respectively, which are very close to the optimal topping pressure of Linde-Hampson liquefaction process [173]. In the decompression process 5-6 such a high pressure is released to the ambient value. As working fluid expands through an isenthalpic process in a throttle valve, a great part of energy is lost. This part of energy transfers into the form of heat and heats up the output products. On the other hand, part of the exergy could be transferred to power while using cryoturbine. This not only decreases the overall power consumption in liquefaction process but increase the output cold energy. As seen from the mass flowrate ratios in Table 4.3 and Table 4.4 about 74% of the feed air is liquefied in the cryoturbine based system comparing with only about 44% in the throttle valve based system.

The other reason that cryoturbine increases the round trip efficiency is that a more efficient heat exchange process is achieved than the throttle valve based system. Most of the cold energy in cold box is supplied by the returning gas 7-8 with a very low bottoming temperature of about 82K. Therefore the lower the feed gas 4-5 is cooled to, the higher efficiency the heat exchange process has. The above data shows that the feed air of the cryoturbine based system is cooled to about 112K while that of the throttle valve system is about 133K. As a result the cryoturbine should lead to a more effective heat exchange process than the throttle valve. This effectiveness of the heat exchange process could be identified by a dimensionless number named Effective Heat Transfer Factor.

4.2.3 Effective Heat Transfer Factor

No matter how complex a heat exchanger network is, the process can be plotted a temperature against heat load diagram called Balanced Composite Curves; see Figure 4.9. In the figure T_H and T_C are the temperature of hot fluid and cold fluid, respectively, and ΔT_{pi} is the pinch point temperature difference. In a reversibly infinitesimal heat transfer process the cold fluid attains a heat load of ΔQ ($\Delta Q > 0$). As a result the exergy change of the cold fluid could be calculated as:

$$dE_C = dH_C - T_a \cdot \frac{\Delta Q}{T_C} = \Delta Q \cdot \left(1 - \frac{T_a}{T_C}\right) \tag{4.2}$$

At the same time, as the hot fluid release a heat load of $-\Delta Q$, the exergy change of the hot fluid is expressed as:

$$dE_H = dH_H - T_a \cdot \frac{-\Delta Q}{T_H} = -\Delta Q \cdot \left(1 - \frac{T_a}{T_H}\right) \tag{4.3}$$

As all the heat transfer processes produce entropy (consume exergy, $dE_C + dE_H < 0$), the flow holds a high exergy change is regarded as exergy rejection. As a result if the hot fluid holds a higher exergy change ($dE_C < dE_H$), the idea heat transfer process can be regarded between the hot fluid and a third fluid with a temperature ΔT_{pi} lower than the hot fluid. On the other hand, if the cold fluid holds a higher exergy change ($dE_C > dE_H$), the idea heat transfer process can be regarded between the cold fluid and a third fluid with a temperature ΔT_{pi} higher than the cold fluid.

Therefore the third fluid temperatures T'_H and T'_C are defined as:

$$[T'_H \qquad T'_C] = \begin{cases} [T_H - \Delta T_{pi} \qquad T_C] & \frac{1}{T_H} + \frac{1}{T_C} \le \frac{2}{T_a} \\ [T_H \qquad T_C + \Delta T_{pi}] & \frac{1}{T_H} + \frac{1}{T_C} > \frac{2}{T_a} \end{cases} \tag{4.4}$$

Based on the definition of third fluid, a dimensionless number named Effective Heat Transfer Factor (EHTF) is defined in equation (4.5) to examine how effective the process is.

$$EHTF = \frac{\int_{Q_1}^{Q_2} \left(\frac{1}{T'_H} - \frac{1}{T_H} + \frac{1}{T_C} - \frac{1}{T'_C}\right) dQ}{\int_{Q_1}^{Q_2} \left(\frac{1}{T_C} - \frac{1}{T_H}\right) dQ} \tag{4.5}$$

In equation (4.5) Q_1 and Q_2 are the initial and terminated heat load values of the heat transfer process and T_H , T_C , T'_H and T'_C are all the functions of heat load Q.

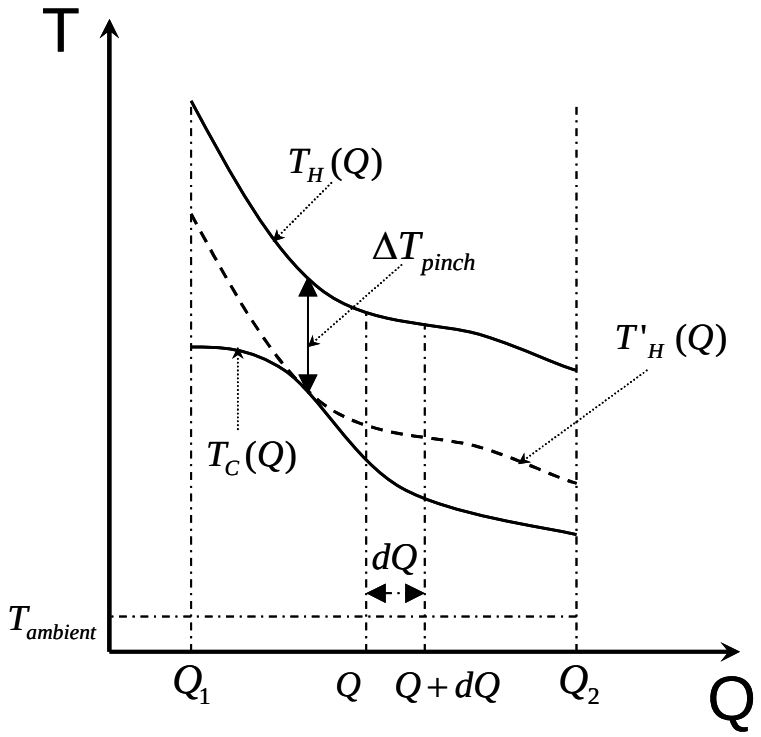

Figure 4.9 Balanced composite curves of heat transfer processes

EHTF ranges between 0 and 1, representing exergy loss ratio of idea heat transfer process and actual heat transfer process. The idea heat transfer process cannot be achieved in a practical heat exchanger network, especially where phase-change occurs. Therefore EHTF is a parameter that indicates how close a real process approaches to an idea heat transfer process.

Figure 4.10 shows how the EHTF value changes. It can be seen that the dependence roughly agrees with the dependence of the round trip efficiency. One of the important reasons for the increased round trip efficiency is due to a more efficient heat transfer process achieved through optimisation. Note that, for the cryoturbine, after 60 generations of optimisation, the EHTF valve still increases (Figure 4.10). However the round trip efficiency is unchanged (Figure 4.8). This reveals the arrangement of power transfer components could be another important factor affecting the overall performance of the system.

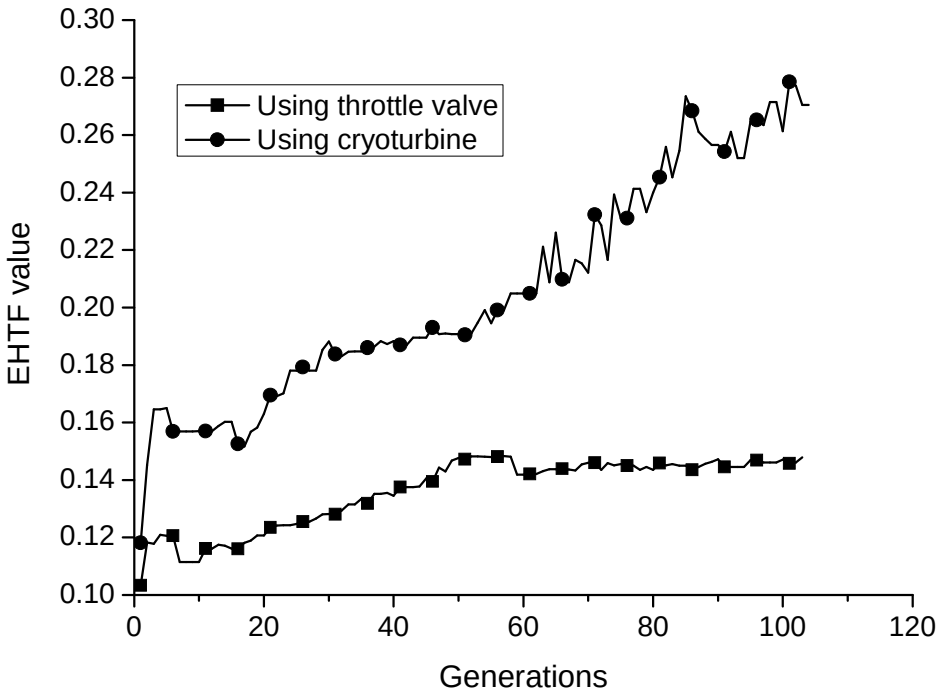

Figure 4.10 Corresponding EHTF values versus number of generations

Figure 4.10 also indicates that the optimal EHTF values are about 0.14 and 0.28 respectively for the throttle valve and cryoturbine based Linde-Hampson CES systems. This implies the exergy loss of the throttle valve system in the main cold box is as about twice as that of the cryoturbine based system. As both of the values are much lower than 1.0, a further decrease in the exergy loss in the heat exchange processes is still possible. This is demonstrated in next section.

4.2.4 Effect of Individual Component Performance

The influence of individual component performance on the round trip efficiency is investigated. These include waste heat temperature, efficiencies of compressors, turbines, pumps, cryoturbine and stages of turbines. Figure 4.11 shows the effect of waste heat temperature while other parameters are kept constant. The round trip efficiencies increase linearly and significantly with increasing waste heat temperature. At a waste heat temperature of 600K which is uneconomical for power generation using a traditional steam turbine system, the round trip efficiency reaches a value of

about 0.48 and 0.82 respectively for the throttle valve and cryoturbine. Therefore the availability of waste heat is a key to the practical uptake of the CES systems.

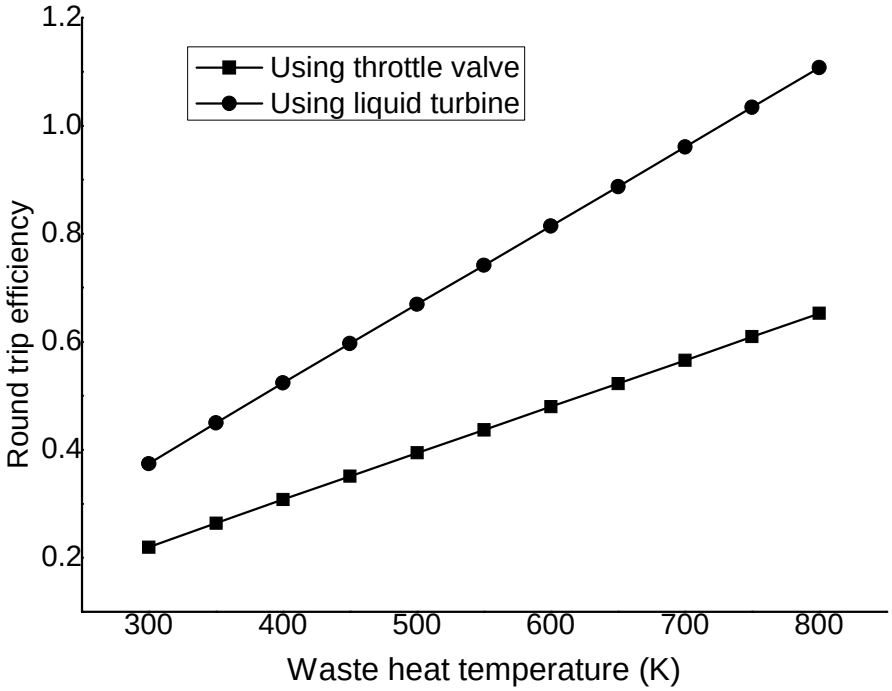

Figure 4.11 Effect of waste heat temperature on the round trip efficiency

The influence of compressor and turbine efficiencies on the round trip efficiency are shown in Figure 4.12 and Figure 4.13 respectively. One can observe that the performance of compressors exerts a similar effect on the round trip efficiency as that of turbines. Quantitatively the round trip efficiencies increase by about 1% and 2% respectively for the throttle valve and cryoturbine based Linde-Hampson CES systems for every 4% increase in the compressor and turbine efficiencies. This suggests that compressors and turbines be the key components that affect the overall performance of the system. On contrast, the influences of cryogenic pumps are negligible as shown in Figure 4.14.

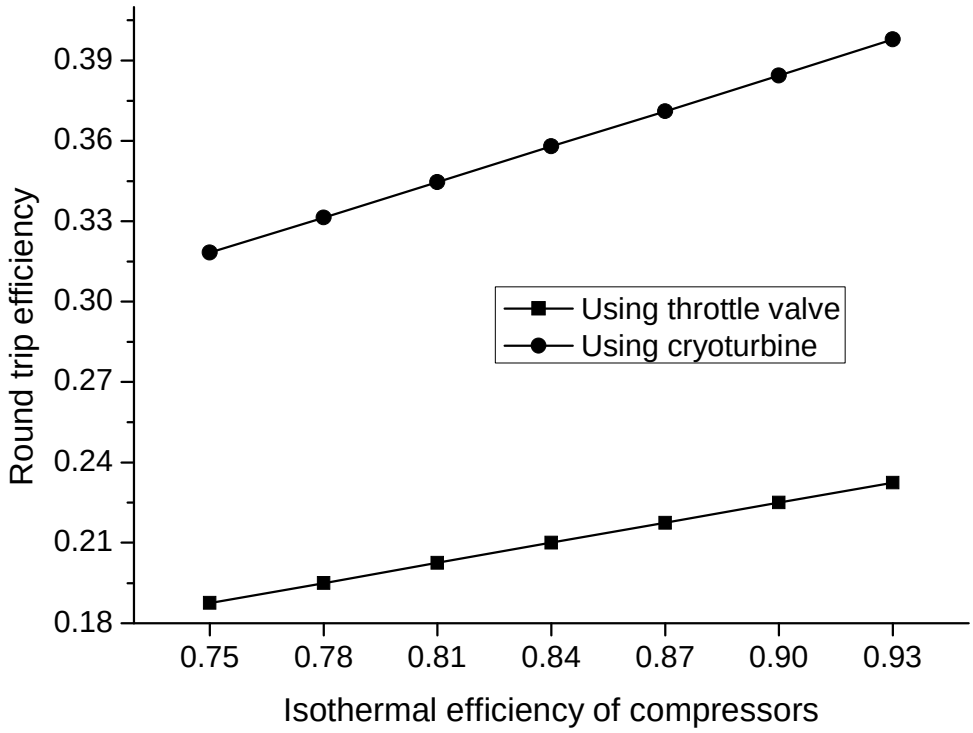

Figure 4.12 Effect of compressor efficiency on the round trip efficiency

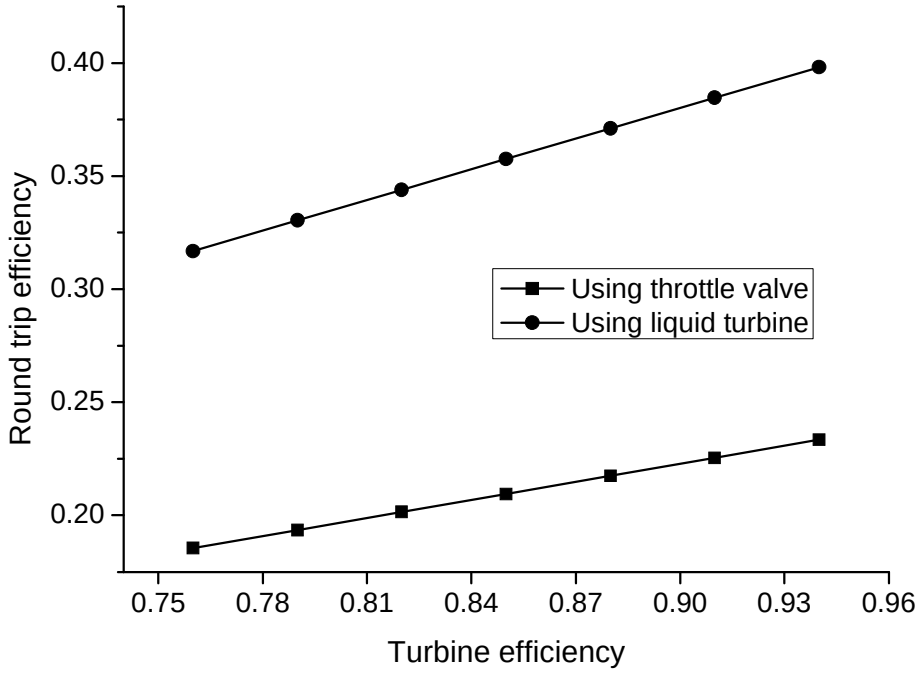

Figure 4.13 Effect of turbine efficiency on the round trip efficiency

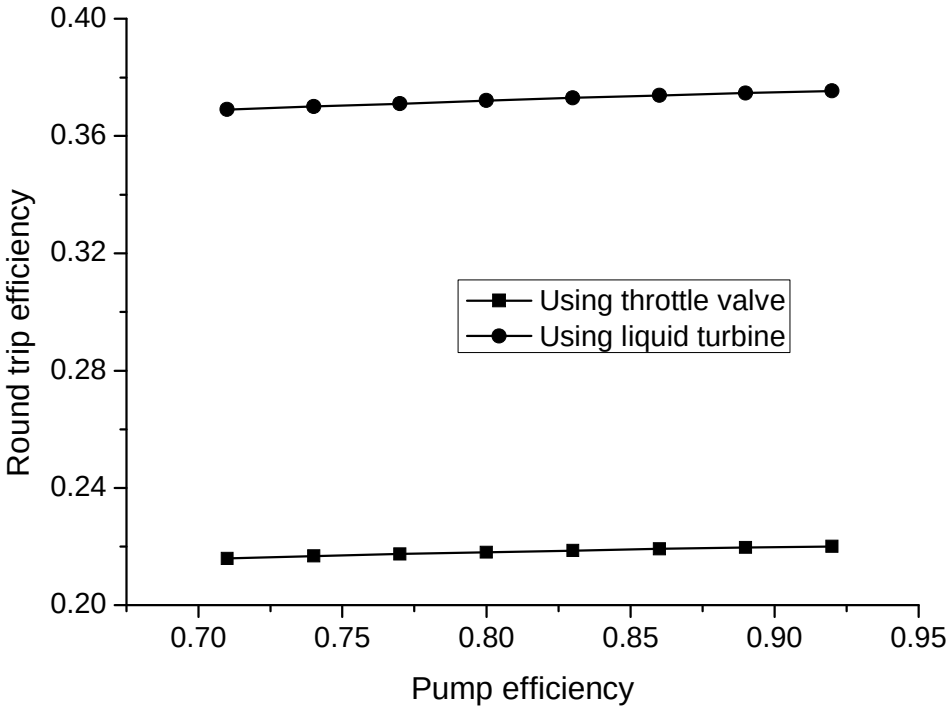

Figure 4.14 Effect of cryogenic pump efficiency on the round trip efficiency

As a baseline study, it is assumed liquid air expands in a two-stage turbine in the cryogenic energy extraction process. As the topping pressure P_{15} is very high (>100bar), more stages might needed with inter-heating to increase the output power (refer to Figure 4.7). Figure 4.15 shows the effects of number of stages of the turbine in energy release process. The round trip efficiency increases with increasing stages of expansion particularly at small stage numbers. One can also see that to attain a good overall performance at least a four stage expansion process should be used. It is worth to mention that a four stage turbine is currently used in a demonstration plant by *Highview Power Storage Ltd*.

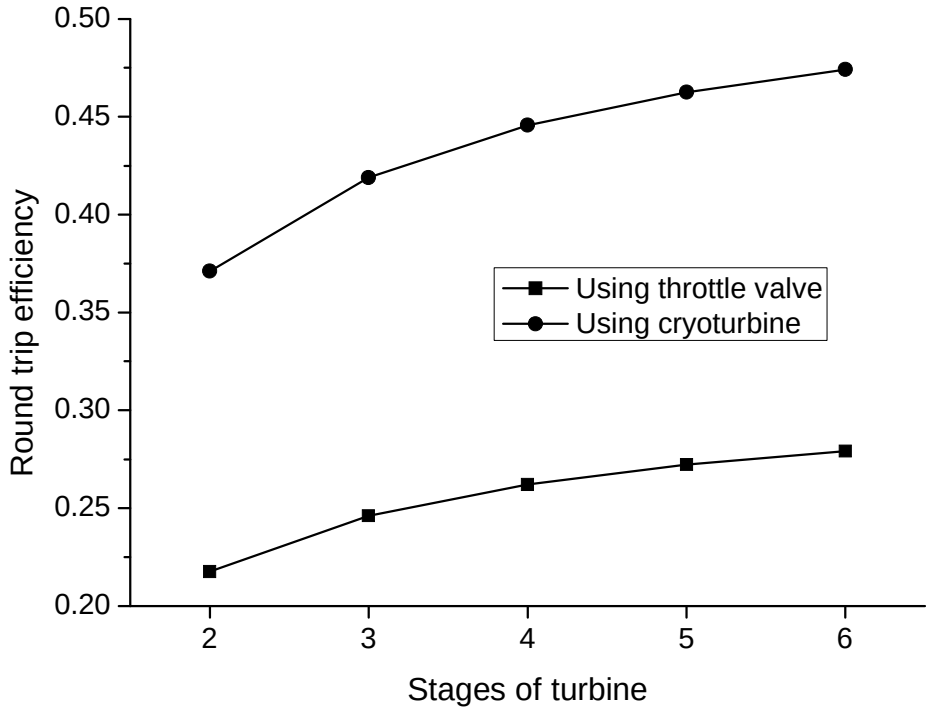

Figure 4.15 Effect of turbine stages on the round trip efficiency

The influence of the cryoturbine performance is also examined and the results are shown in Figure 4.16. An increase of the cryoturbine efficiency gives a great increase in the round trip efficiency while the cryoturbine efficiency is lower than 0.75, beyond which, the increase tends to level off.

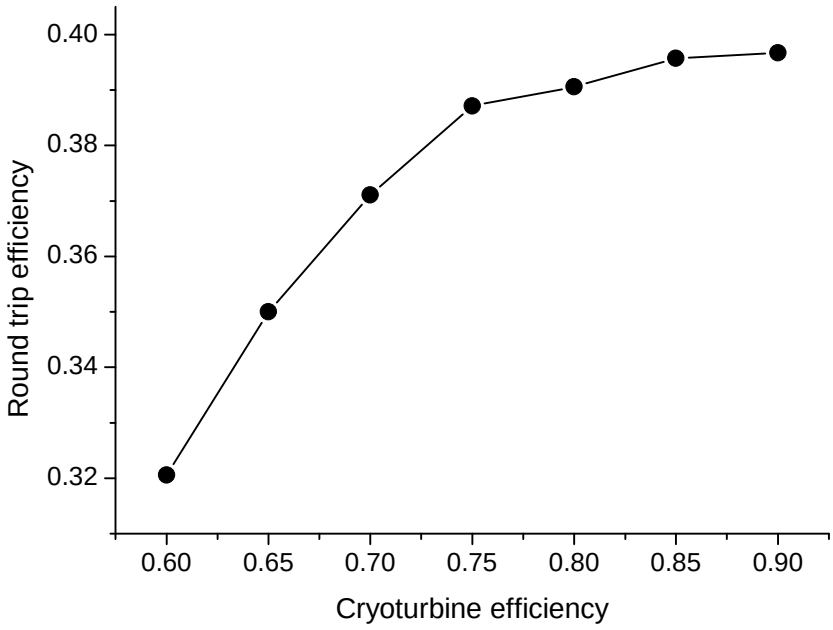

Figure 4.16 Effect of cryoturbine efficiency on the round trip efficiency

4.3 Expander CES System

4.3.1 Expander Cycle

As no moving parts at the cold end Linde-Hampson CES system has a very simple configuration. However there are two main drawbacks restricting its applications:

First is the low round trip efficiency, especially for the throttle valve based system which has an optimal efficiency of only about 22% if there is no waste heat. Such a low efficiency is not competitive with other energy storage technologies, even waste heat is available.

Secondly, even such a low efficiency is only achievable with a very high liquefied pressure. The optimal results in the previous section show the topping liquefied pressures are 127 bar and 137 bar respectively for the two systems, leading an ultra-supercritical process for the working air. Such a high pressure is required not only to supply sufficient cold energy but also to attain a better match between the heat sink and heat source. As will be discussed in the following section on the economic

analysis, operating the liquefaction unit at such a high pressure will dramatically increase the capital cost of the system, especially the compressors.

Similarly, for large scale liquefaction, an effective way to overcome the above challenges is to add a refrigerant cycle. The refrigerant cycle can supply cold energy or transfer low grade cold energy into high grade cold energy. In this way a better match can be obtained between the heat sink and heat source and the topping liquefied pressure can be reduced by decreasing the cold load requirement of the feed air. As reviewed in Chapter 2 there are three types of refrigerant cycles, namely Cascade Refrigerant Cycle, Mixed Refrigerant Cycle and Expander Cycle. Expander cycles are suitable for energy storage systems due to possible rapid startup and shutdown operation. In this work the Expander Cycle is added to the Linde-Hampson CES system to give the so called Expander CES system; see Figure 4.17.

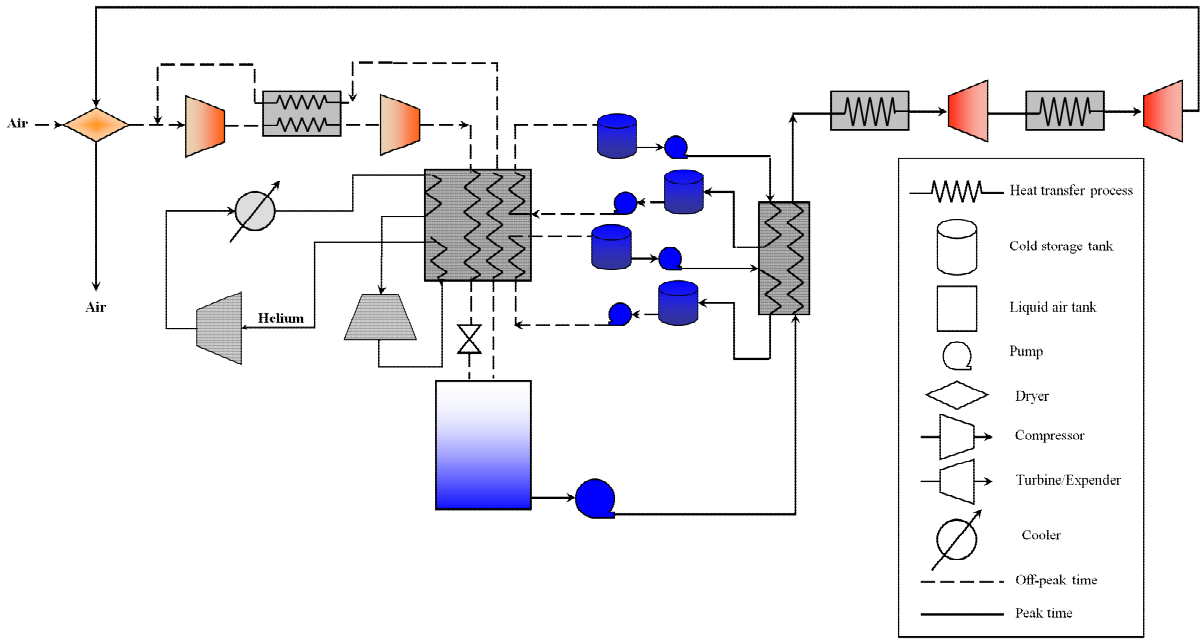

Figure 4.17 The flow sheet of the expander CES system

In the expander cycle, the cold energy is produced by working fluid expansion. Three working fluids, nitrogen, helium and hydrogen are often used for the expander cycles. However, hydrogen is excluded for the safety reasons in the proposed Expander CES system. Figure 4.18 shows a comparison of the isentropic expansion properties between nitrogen and helium. Assuming the compressed gases are at ambient temperature, it is illustrated that the required pressure ratio of helium is much lower

than that of nitrogen if they are used to generate the cold energy at the same target temperature. The difference becomes more dramatic when the target temperature gets lower. Therefore, the use of helium as the working fluid can lead to a much lower topping pressure than that of nitrogen and hence a reduced capital cost.

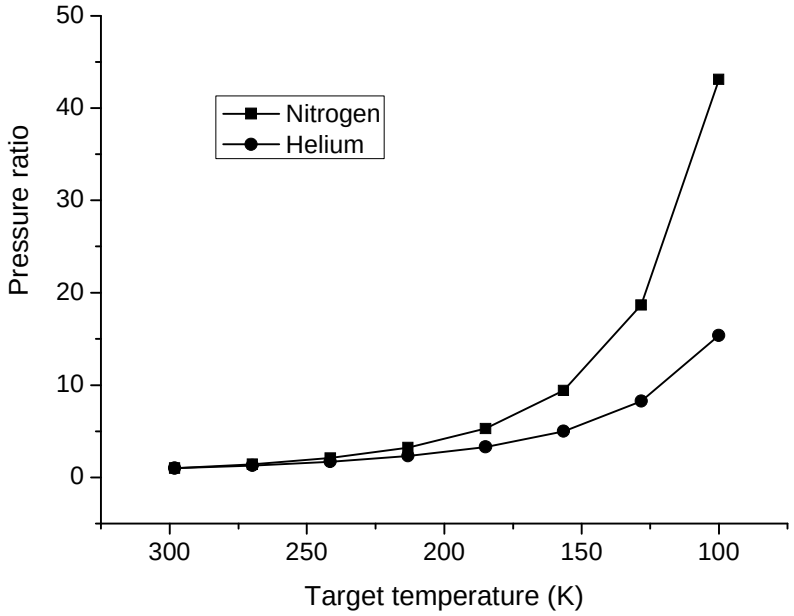

Figure 4.18 The isentropic expansion properties of nitrogen and helium

4.3.2 Optimisation Strategy

Compared with the Linda-Hampson CES systems, the expander CES system has a far more complicated configuration. As the expander cycle aims to generate effective cold energy or to transfer the low grade heat to the high grade heat, a highly efficient heat exchanger network is crucial to the overall performance of the system. Therefore in the optimisation process the system is divided into four thermal flows as shown in Figure 4.19 for a better approach of the heat exchanger network where air liquefaction is considered:

(1) Air expansion flow: The liquid air is pumped to a high elevated pressure and super-heated, followed by a two-stage expansion process in turbines/expanders with inter-heating. The output gas exchanges the heat to about ambient temperature and is then sent to dryers to regenerate the desiccant.

(2) Cold storage flow: Similarly to the cold storage in the Linda-Hampson CES system the cold storage aims to store the cold energy released from the air

expansion flow and use the stored energy to supply the cold in the air liquefaction process. To examine the performance enhancement of the cold storage, three flows are considered. One uses R218 and the other two use methanol as the storage medium.

(3) Air liquefaction flow: This flow is similar to that used in the Linda-Hampson CES system. Dry air and return air are mixed and compressed to the elevated pressure by a two stage compressor with inter-cooling. After rejecting heat the high pressure air is cooled to a low temperature level, followed by an isentropic throttling process to produce liquid air. A fraction of the product is vaporized in the cryogenic tank and introduced back to supply part of the cold energy.

(4) Refrigerant flow: A four stage refrigerant cycle is considered to supply external cold for air liquefaction. At each outlet of the power transfer component the heat flow may be split into two flows. By introducing the stream splitting more system configuration could be formed and only the one has the best performance will be selected for the optimisation.

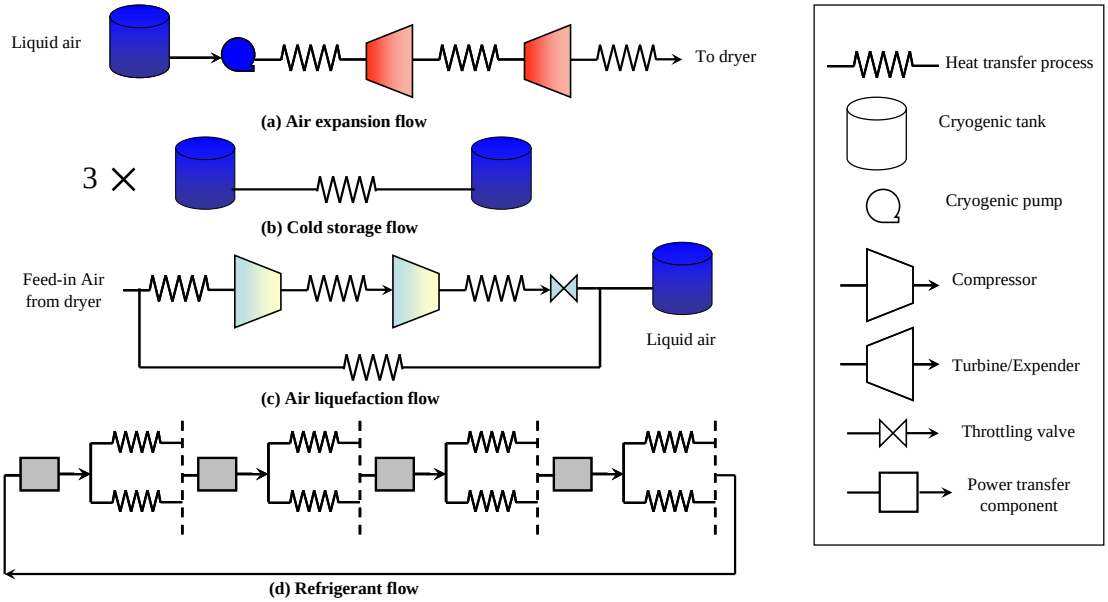

Figure 4.19 Sub-flows of the expander CES system

One can see that the four flows are all made up of a series of power transfer components and heat transfer processes placed alternatively. Given the inlet parameters (including flow rate, temperature and pressure), some outlet parameters (e.g. outlet pressure) and configuration control parameter (whether split or not) the system configuration could be identified and other state parameters as well as the

heat loads and power could be calculated. Therefore the global design method mentioned in Chapter 3 can be used for a systematic optimisation.

4.3.3 Results and Discussion

To simplify the simulation the system are divided into two sub-systems. They are described and discussed in the following:

The first is an energy release unit made of flow (a) and flow (b) in Figure 4.19 with the outputs of power and cold energy stored in the cold medium. Exergy efficiency is set as the objective function which is defined as the ratio of output exergy and input exergy. Figure 4.20 shows the exergy efficiency and the EHTF value as a function of the optimisation process. It is seen that an exergy efficiency as high as about 85% could be achieved. This is because the exergy loss in the heat exchange process decreases with increasing EHTF value as a result of systematic optimisation. The EHTF value corresponding to the 85% exergy efficiency is about 47%. Figure 4.21 compares the temperature distributions before and after the optimisation. It reveals that the optimisation enables a smaller temperature difference.

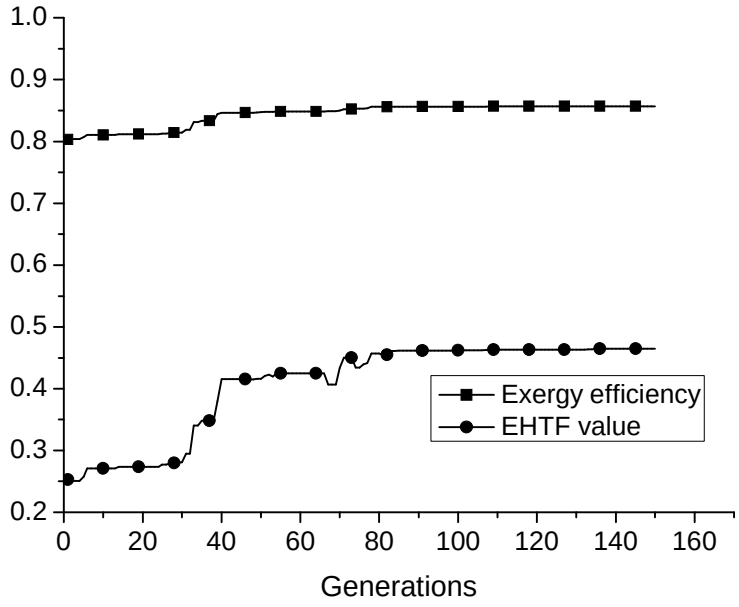

Figure 4.20 Changes of the exergy efficiency and EHTF value of the energy release unit during process optimisation

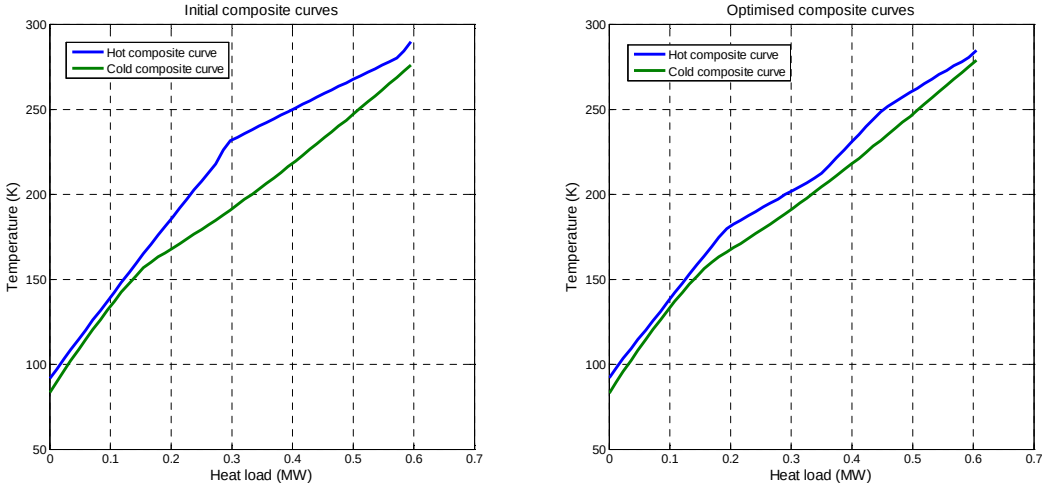

Figure 4.21 A comparison between the composite curves before and after optimisation

The second unit is the air liquefaction system made of flow (b), flow (c) and flow (d) in Figure 4.19. Such a unit consumes off-peak electricity and stores the cold energy to produce liquid air. The round trip efficiency is selected as the objective function for the optimisation and the output power and cold energy data are supplied from the energy release unit. Figure 4.22 shows the round trip efficiency trend during optimisation. Compared with the Linda-Hampson CES system, the expander CES system has a much higher efficiency, about 40% for the throttle valve based system and about 46% for the cryoturbine based system. Figure 4.23 shows the corresponding EHTF values which are about 30% and 34% for the throttle valve and cryoturbine systems, respectively. These values are much higher than those of the corresponding Linda-Hampson CES systems, leading to a significant improvement of the overall performance.

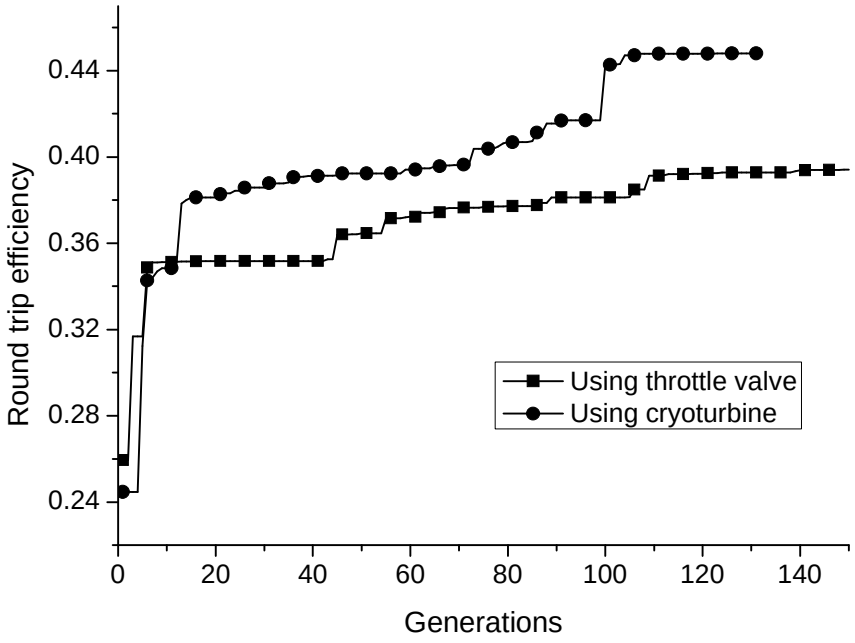

Figure 4.22 Round trip efficiency of expander CES system

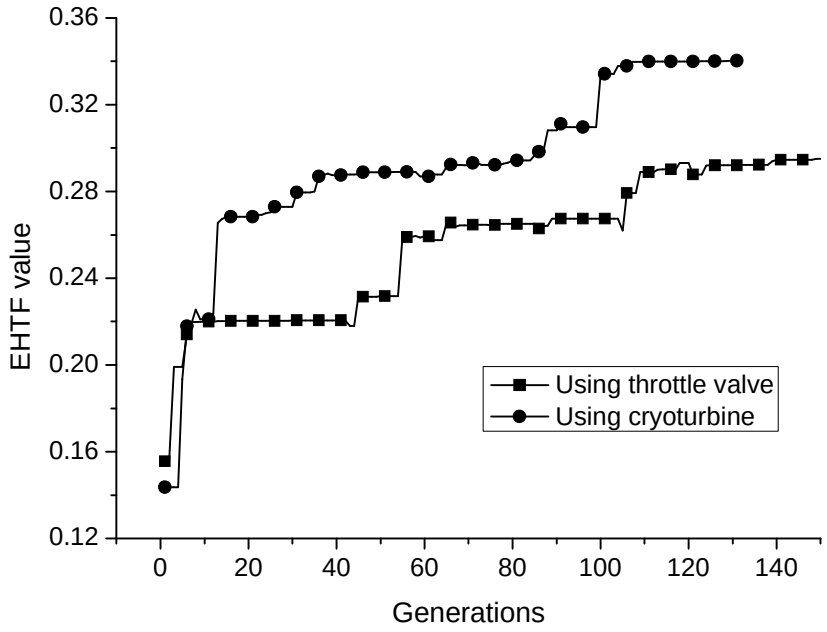

Figure 4.23 EHTF values of expander CES system

From the above simulation results, the following conclusions can be drawn:

- Liquefaction unit is the key part of the CES system as the energy release unit has a very simple configuration and a very high efficiency. Further

improvement on the performance of the liquefaction unit is possible as the EHTF values are still very low.

- Cryoturbine is a very important component of the CES system. Using cryoturbine to replace throttle valve could bring at least an improvement of about 6% on the round trip efficiency.

- The availability of waste heat or heat from renewable energy sources plays a crucial role to the application of the CES system. Without the use of waste heat, the best optimised CES system only has a round trip efficiency of about 45%. This is less competitive with other energy storage technologies. The round trip efficiency increases linearly with increasing waste heat temperature. At a waste heat of above 300°C, the round trip efficiency is nearly doubled to about 90%, making the technology highly competitive.

4.4 Economic Analysis

As the proposed technology is novel, it is necessary to estimate the capital cost associated with the system. Detailed expressions for estimating the costs are presented in Appendix B, which are widely used [174-177]. Note that these expressions also take into account the cost of installation, electrical equipment, control system, piping and local assembly.

A CES system with the net peak power of 60 MW is used as a case study for the economic analyses. Such a scale is typical for the power requirement of heavy industries. Further assumptions for the calculations include:

- The CES system is for load levelling with air liquefaction unit to store excessive electricity and energy release unit to generate peak load. Both the energy release unit and air liquefaction unit can start up and shut down instantaneously.

- Waste heat is available in the heavy industries, which is sufficient to super-heat the energy release unit of the CES system and the waste heat is considered to be a free heat source.

- The CES system operates at an optimal performance based on the optimisation results presented in Section 4.2 and Section 4.3.

Other baseline assumptions for the simulation are listed in Table 4.5. In the table, γ represents the operation period ratio defined as:

$$\gamma = \frac{O_{ASU}}{O_{pk}} \tag{4.6}$$

Where O_{ASU} and O_{pk} correspond the operation hours of air liquefaction unit and energy release unit, respectively. φ is the maintenance factor; in is the interest rate; ri is the rate of inflation; CP is the construction period; k is the amortization period ; CE_{opk} is the off-peak electricity price ; h is the heat transfer coefficient of the heat exchangers; T_{wh} is the waste heat temperature.

Table 4.5 Baseline parameters for the economic analysis of the CES system

φ	1.06	O_{pk} (hours)	4
in (%)	6.00	γ	2
ri (%)	5.00	CE_{opk} (US$/kWh)	0.045
CP (years)	1	h (W/(m^{2}K))	300.0
k (years)	30	T_{wh} (K)	600

Two parameters are considered based on the above assumptions. The first is the capital cost of the CES system, which can be expressed as [176]:

$$C_{CES} = \frac{I_{CES}}{W_{CES}} \tag{4.7}$$

Where I_{CES} is the total cost for components purchasing of the CES system and W_{CES} is the output power of the energy release unit.

The second is the peak electricity production cost of the CES system given by [176]:

$$CE_{CES} = \frac{1}{W_{CES}}\left[CE_{opk} w_{ASU} \gamma + \frac{WfI_{CES}}{365 O_{pk}}\right] \tag{4.8}$$

Figure 4.24 shows the main component purchase costs of four optimised cases of the CES system. One can see that turbines and compressors take the major share of the costs. Due to high topping pressure and large mass flowrate, the cost of compressors in the throttle valve based Linde-Hampson CES system is very high. Replacing the throttle valve with cryoturbine, the cost of compressors is reduced by over half as the flowrate of the input mass is reduced. In the expander CES systems

the cost of compressors is further reduced due to reduction in both the mass flowrate and the topping pressure of the input air. The capital costs of other components of the four cases are more or less the same and play an insignificant role. Figure 4.25 reveals the capital cost of the baseline condition is about 1200 US$/kW for the throttle valve based Linde-Hampson CES system, whereas the costs for the other three cases are much smaller between 600 and 800 US$/kW. These costs are much cheaper than other technologies for large scale energy storage such as PHS, CAES and Batteries [1, 17].

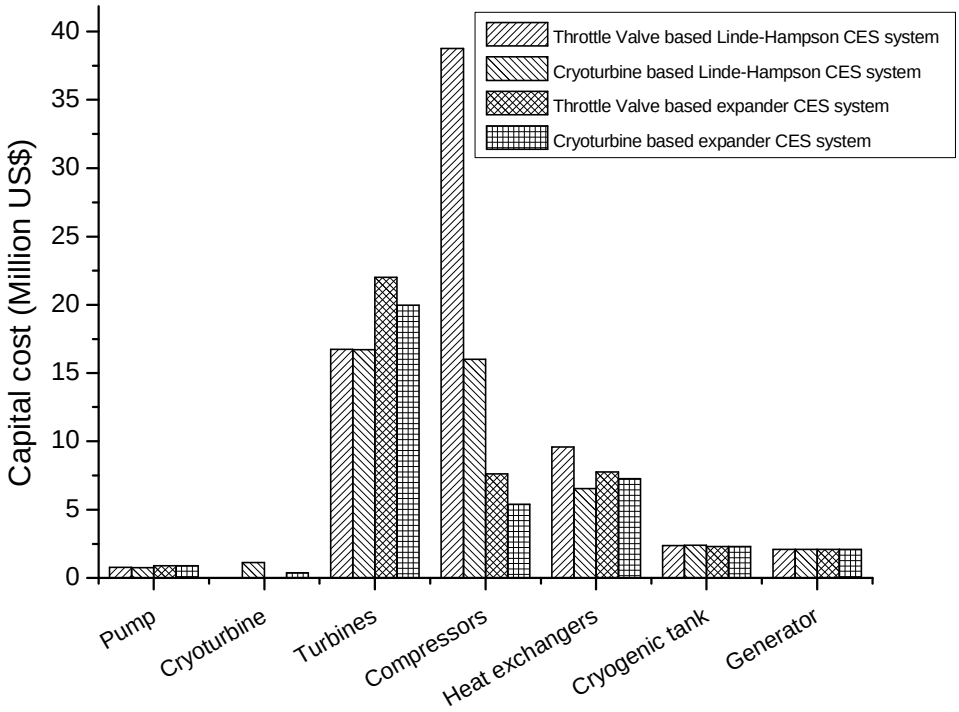

Figure 4.24 Breakdown of component cost of CES systems

Having examined the baseline cases, the influences of waste heat temperature, energy release unit operation period and operation ratio are investigated and the results are shown in Figure 4.25, Figure 4.26 and Figure 4.27, respectively. One can see that the waste heat temperature and the operation ratio are the key parameters that affect the capital cost of the systems. An increase in the waste heat temperature decreases the mass flowrate of the input air, whereas the capital costs of the CES system decreases with increasing operation period ratio. On the other hand, the capital costs is only slightly affected by the change of the operation period of the

energy release unit because this change only affect the size of the cryogenic tank for liquid air storage. The above three figures also show that the capital cost of the cryoturbine based system is much cheaper than the throttle valve based system, especially for the Linde-Hampson CES system. This is because the efficiency of throttle based system is much lower. As a result in order to give the same power output larger scale components are required which leads higher capital costs.

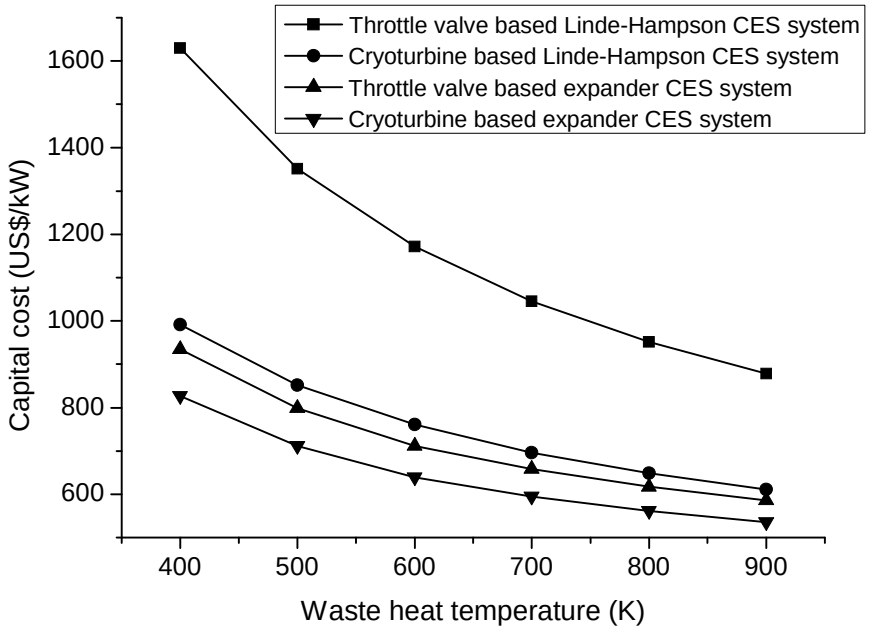

Figure 4.25 Effect of waste heat temperature on capital cost of CES systems

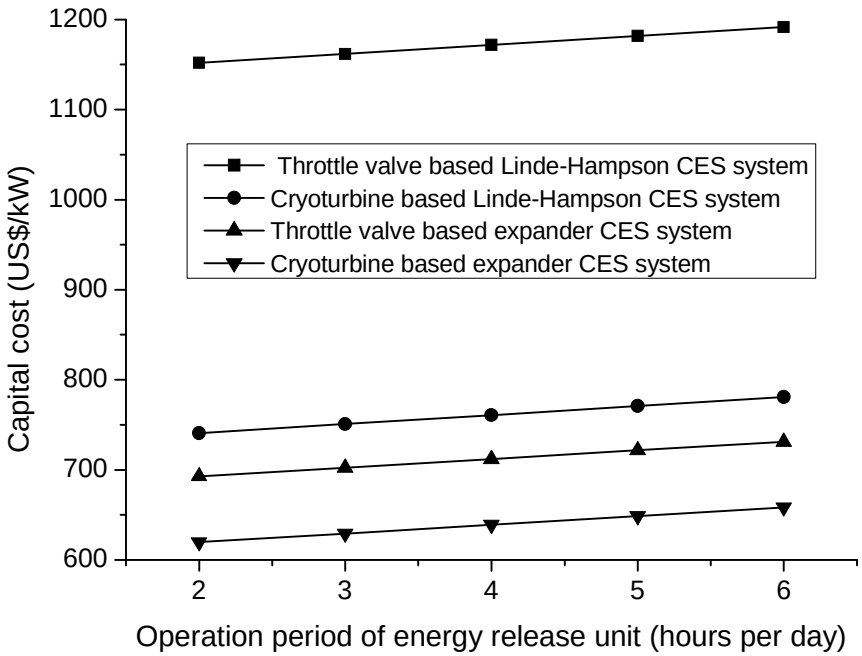

Figure 4.26 Effect of operation period of energy release unit on capital cost of CES systems

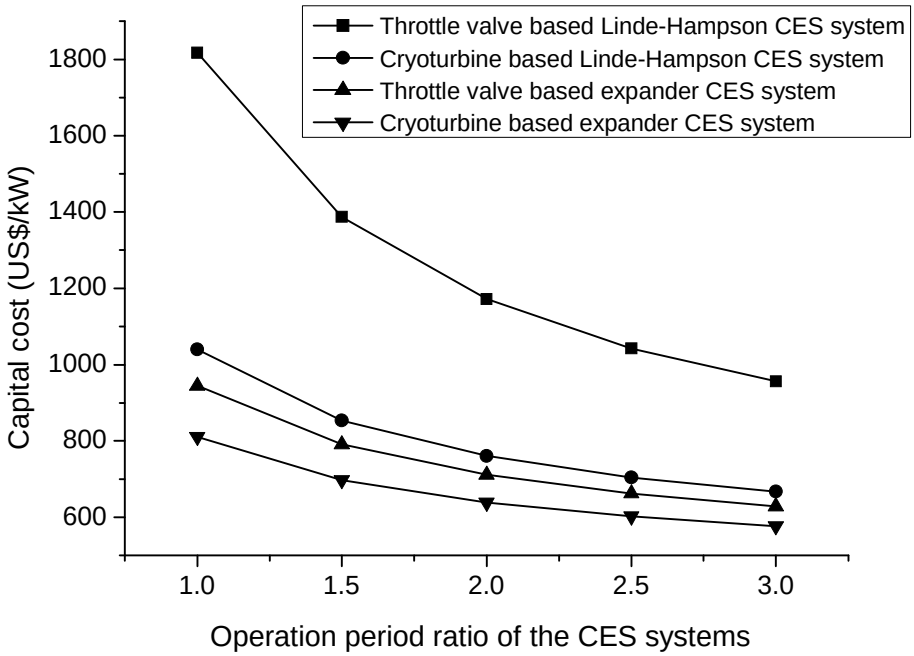

Figure 4.27 Effect of operation period ratio on capital cost of CES systems

Figure 4.28 shows the cost breakdown of the peak electricity into the capital and off-peak electricity costs. The operation and maintenance costs are not considered in this breakdown. It can be seen that the capital charges and off-peak electricity costs under the baseline condition have nearly the same share for all the CES systems. Except for the throttle valve based Linde-Hampson CES system, the peak electricity costs are 2 to 3 times that of the off-peak electricity. Note that the market price ratio of peak to off-peak electricity is about 3 to 4 or even higher [59], the cryoturbine based systems and throttle valve based expander CES system are expected to be very competitive in the market.

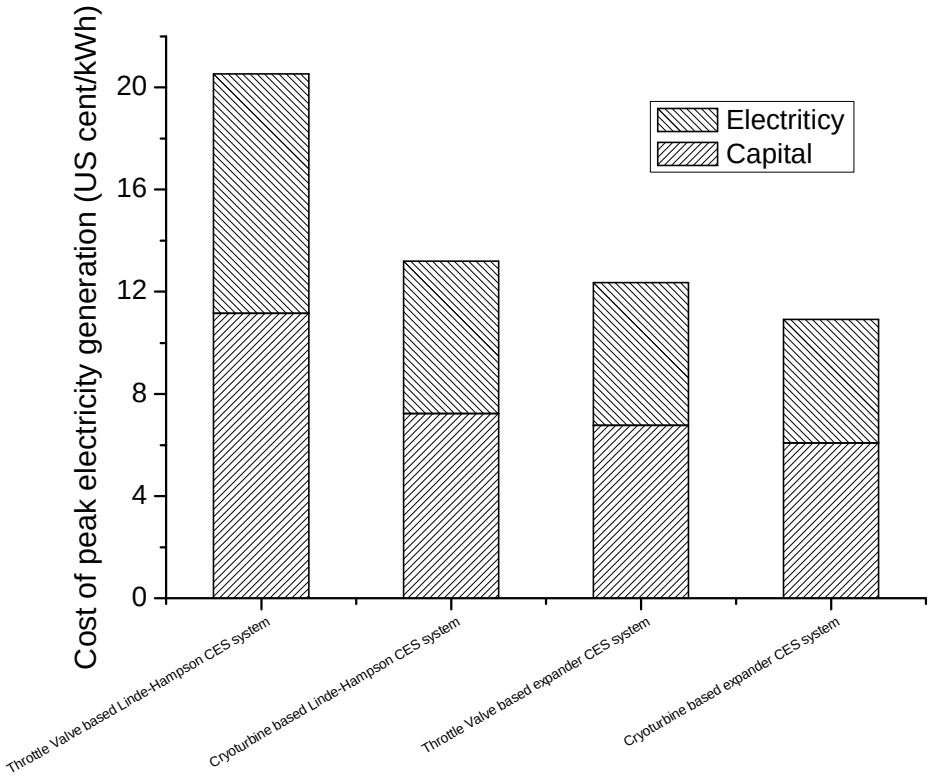

Figure 4.28 Breakdown of peak electricity cost

A comparison of the influences of waste heat temperature, energy release unit operation period and operation ratio on the peak electricity cost are respectively given in Figure 4.29, Figure 4.30 and Figure 4.31. The three parameters are seen to affect the peak electricity cost in a similar manner: an increase in any of the three parameters leads to a decrease in the electricity cost particularly at the low value of the parameters. Similarly to the results for the capital cost, the throttle valve based Linde-Hampson CES system gives a much higher peak electricity cost than the other

three systems and the cryoturbine based expander CES system has the lowest peak electricity generation cost.

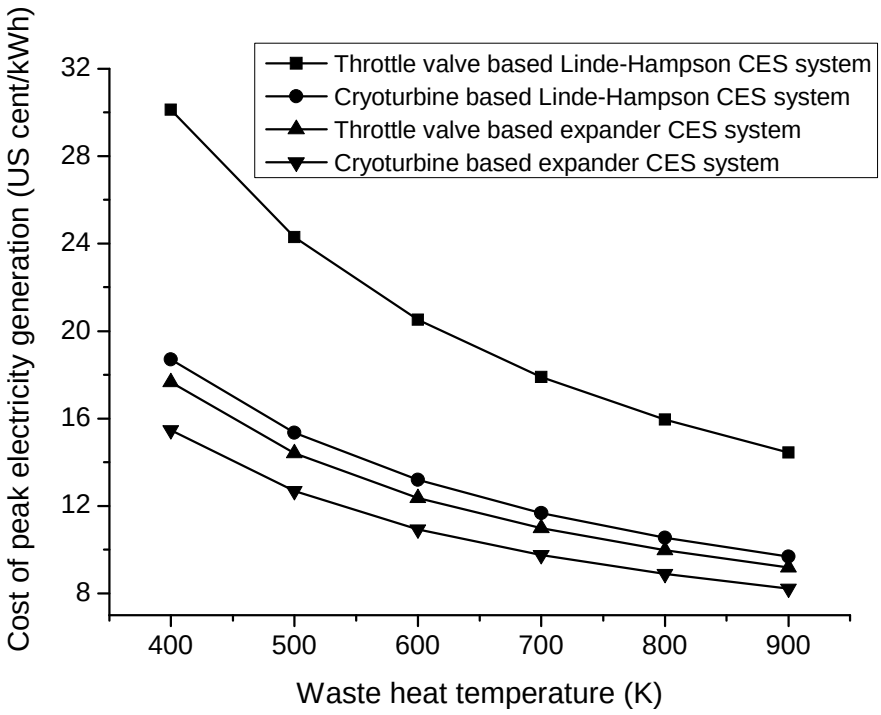

Figure 4.29 Effect of waste heat temperature on peak electricity cost

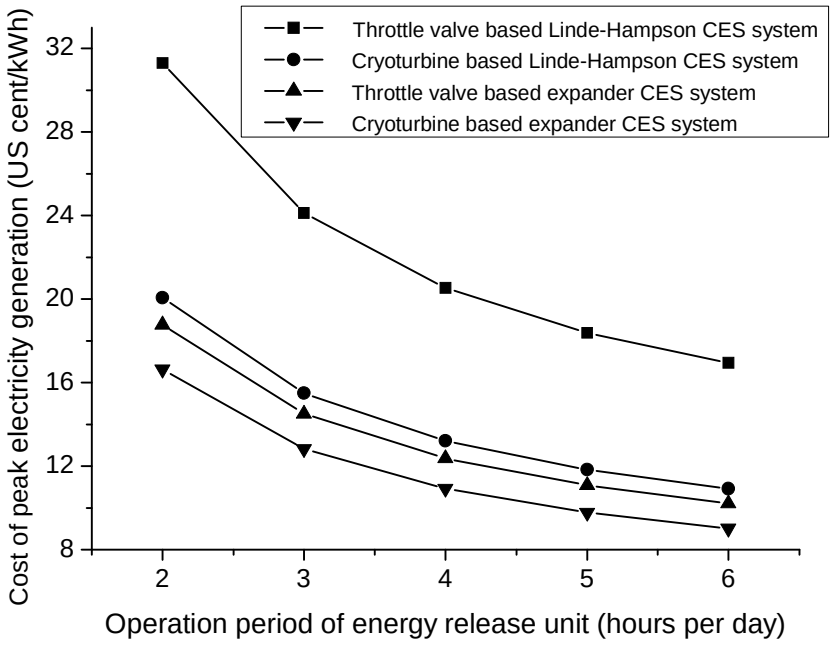

Figure 4.30 Effect of operation period of energy release unit on peak electricity cost

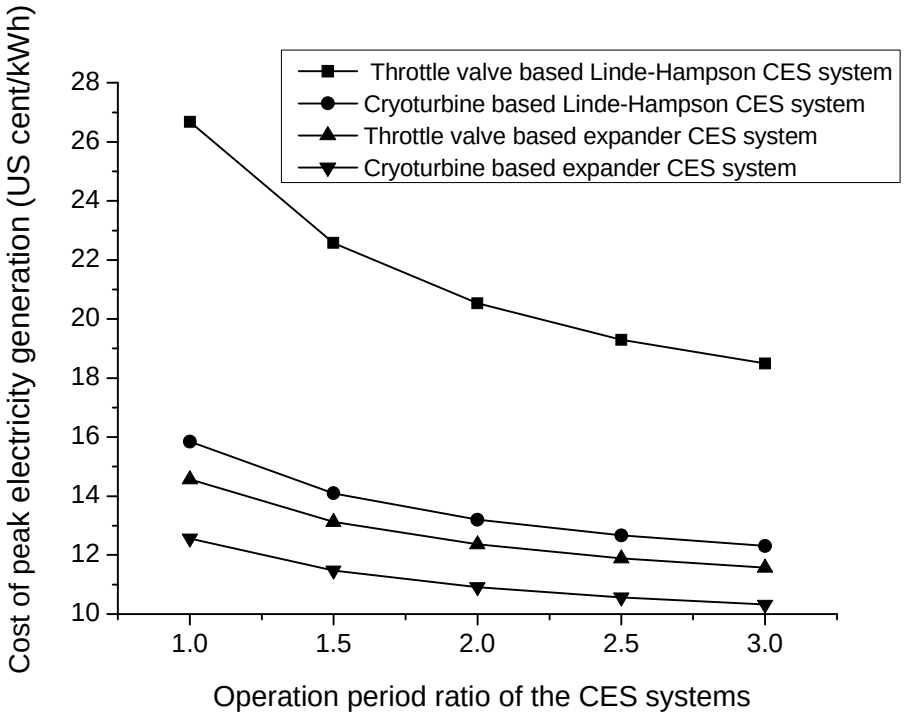

Figure 4.31 Effect of operation period ratio on peak electricity cost

The peak electricity cost is also affected by the price of the off-peak electricity as shown in Figure 4.32. One can see that the peak electricity cost increases linearly with increasing off-peak electricity. For the throttle valve based Linde-Hampson CES

system the peak electricity cost increases by about 2 US cents while the off-peak electricity price increases by about 1 US cent. For the other systems the corresponding price increases are all about 1.5 US cents.

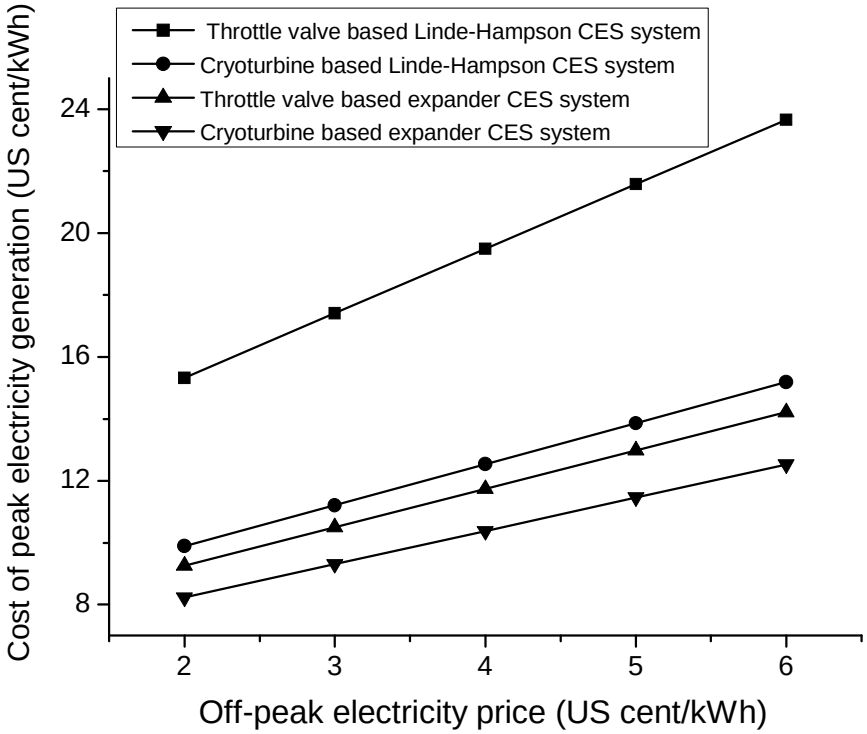

Figure 4.32 Effect of off-peak electricity price on peak electricity cost

From above discussions and comparisons one can see that the throttle valve based Linde-Hampson CES system is not suitable for practical applications due to the low exergy efficiency and relatively high cost. The key parameters for the CES technology are the waste heat temperature and operation period of energy release unit. In general, if the waste heat temperature is higher than 600 K and the operation period of energy release unit is higher than 4 hours per day, the rest three CES systems show a great potential for load levelling for heavy industries.

4.5 Summary of This Chapter

This chapter discusses the Cryogen based Energy Storage technology for load levelling for heavy industries. Four configurations are considered, which are grouped into Linde-Hampson CES and expander CES according to the methods of air liquefaction. Optimisation is done in terms of the use of a throttle valve and a

cryoturbine as the expansion component in the liquid formation process. Thermodynamic studies show that the expander CES can give higher round trip efficiency although its configuration is much complicated. The results also suggest the use of cryoturbine instead of a throttle valve lead to a significant improvement on the round trip efficiency from about 22% to 37% for the Linde-Hampson CES and from about 40% to 45% for the expander CES under the baseline conditions.

A dimensionless parameter named Effective Heat Transfer Factor is introduced for assessing the performance of the heat exchanger network. The treads of such a parameter roughly agree with those of the round trip efficiency in the optimisation process, from about 0.12 to 0.28 for the cryoturbine based Linde-Hampson CES and from about 0.14 to 0.34 for the cryoturbine based expander CES under the baseline conditions. This indicates that the efficient heat exchanger network is an important factor to improve the round trip efficiency.

Economic analyses have been carried out for the optimised CES systems. It reveals that the throttle valve based Linde-Hampson CES system is not suitable for practical applications. The other three systems are very competitive for load levelling for heavy industries if the waste heat temperature and the operation period of the energy release unit are adequately set (e.g. the waste heat temperature is higher than 600K; the operation period is longer than 4 hours per day for peak electricity generation).

Chapter 5 Cryogen based Peak-shaving Technology

5.1 Introduction

It is well known that utility companies ramp power plants up and down very frequently to follow the end-use load demand, which changes significantly in a day. It is also understood that the peak demand only lasts for a few hours in a day, which often occurs at the end of the daytime when there is superposition of commercial, industrial, public lighting and residential uses [178, 179]. As the difference between the peak and off-peak loads is significant, it is very expensive and technically challenging for the power companies to deal with the demand-supply mismatch. As a consequence, electrical industry must develop new technologies to meet the highest peak demand of the year at any given moment and operate within a *just-in-time* framework that follows the variable end-use demands. Currently two Supply Side Management (SSM) technologies are often used to address the issue:

- Peaking power plants or 'Peakers' are the power stations provide power to electrical grids for peak demands. Natural gas fuelled power stations and hydropower have a rapid startup and are therefore often utilized at peak demand times.

- Grid energy storage (also called large-scale energy storage) refers to the methods used to store electricity in large-scale within an electrical power grid. As mentioned before Pumped Hydroelectric Storage (PHS) and Compressed Air Energy Storage (CAES) are capable to provide very large energy storage deliverability (above 100 MW with single unit).

However building peaking power plants has a big issue in terms of costs because of their short operating time and high fuel costs [180, 181]. On the other hand most grid energy storage technologies are still under the developing stage except for PHS and CAES systems. However, as mentioned before the major barrier for the implementations of PHS and CAES is their dependence on favourable geo-conditions which are not always available. Recently the integration technology of CES and natural gas fuelled power generation had been proposed by Hitachi Ltd (Japan) [182] and Expansion Energy LLC (USA) [183]. However their systems are the extension of compressed air energy storage technology and liquid air is only used to produce compressed air for the combustion process. As liquid air carries

much more exergy than compressed air the excessive cryogenic energy will be lost in the energy extraction process, leading to an inefficient process.

In this paper, a new peak-shaving technology with CES and CO_2 capture is proposed. Such a technology uses cryogen (liquid nitrogen and oxygen) as the energy carrier and natural gas (or alternative gaseous fuels, e.g. from gasification of coal) as the fuel for peak power generation. The working principle is schematically shown in Figure 5.1. Off-peak electricity is used to produce liquid nitrogen and oxygen in an air separation and liquefaction unit (ASU). At peak hours, natural gas or alternative gas is burned by oxygen from the ASU (oxy-fuel combustion) to generate electricity in gas turbine power plant. CO_2 produced is then captured from the flue gas in the form of dry ice. The remaining gas mixture is then sent back to the combustor in gas turbine power plant after recompressed to the combustion pressure. Liquid nitrogen produced in the ASU not only serves as an energy storage medium but also supplies the high grade cold energy for CO_2 separation. In addition, waste heat from the tail gas can be used to superheat nitrogen in the expansion process during power recovery to further increase the system efficiency. The nitrogen after expansion could be used to purge the sorbent bed of the ASU dryer.

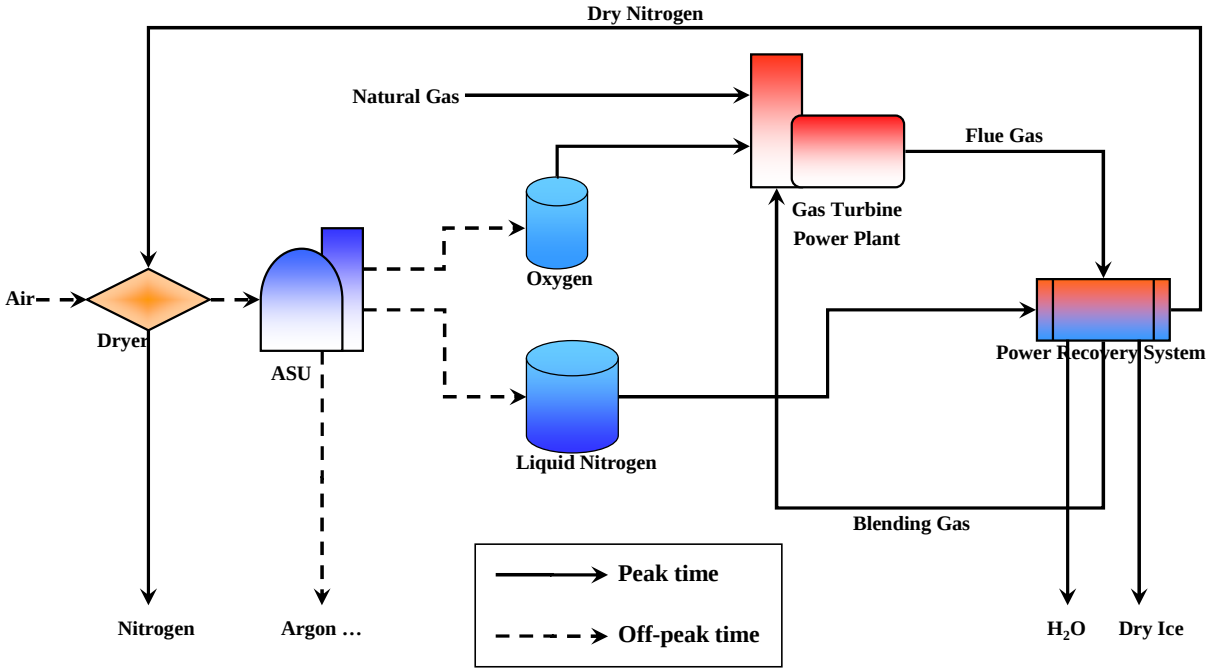

Figure 5.1 Principle diagram of the cryogen based peak-shaving technology

This cryogen based peak-shaving technology is far better positioned if CO_2 capture is taken into account. CO_2 is one of the main greenhouse gases. Global fossil-fuelled power generation sector generates the largest amount of CO_2 emission, accounting for about 33–40 percent of the total [184, 185]. As fossil fuelled power plants are at fixed locations, they are much more easily to manage than other major sources of CO_2 emission including transportation, space heating and industrial processing sectors. Should CO_2 reduction be deemed necessary, it is likely that the electricity generation sector would be required to make significant contributions [186]. For fossil fuel powered electricity generation, oxy-fuel combustion approach appears to be very promising for CO_2 capture [187]. This requires oxygen production, which can be done by air separation and liquefaction process. Furthermore the energy extraction process of CES produces lot of relatively low grade cold which could be used for condensing CO_2. These arguments form the basis for the work reported in this chapter.

This chapter is organized in the following manner. Section 5.2 gives the details of the newly proposed process where thermodynamic analyses are also carried out. Systematic optimisation is carried out in Section 5.3, followed by an economic analysis in Section 5.4. Finally, a summary is given in Section 5.5.

5.2 Thermodynamic Analysis

5.2.1 Cycle Configuration

Figure 5.2 shows the process flow sheet for the newly proposed cycle, whereas the corresponding *t-s* (temperature – entropy) diagram is given in Figure 5.3. The cycle works in the following way. At off-peak hours, excessive electricity generated by the base-load units is used to power the air separation and liquefaction (ASU) plant to produce oxygen and liquid nitrogen while the rest of the system is powered off. The produced oxygen and liquid nitrogen are stored in pressurized vessels and cryogenic tanks, respectively, for generating power via a high pressure turbine (HT) and a low pressure turbine (LT) through nitrogen expansion, and assisting combustion through an oxy-fuel combustor (B) at peak hours.

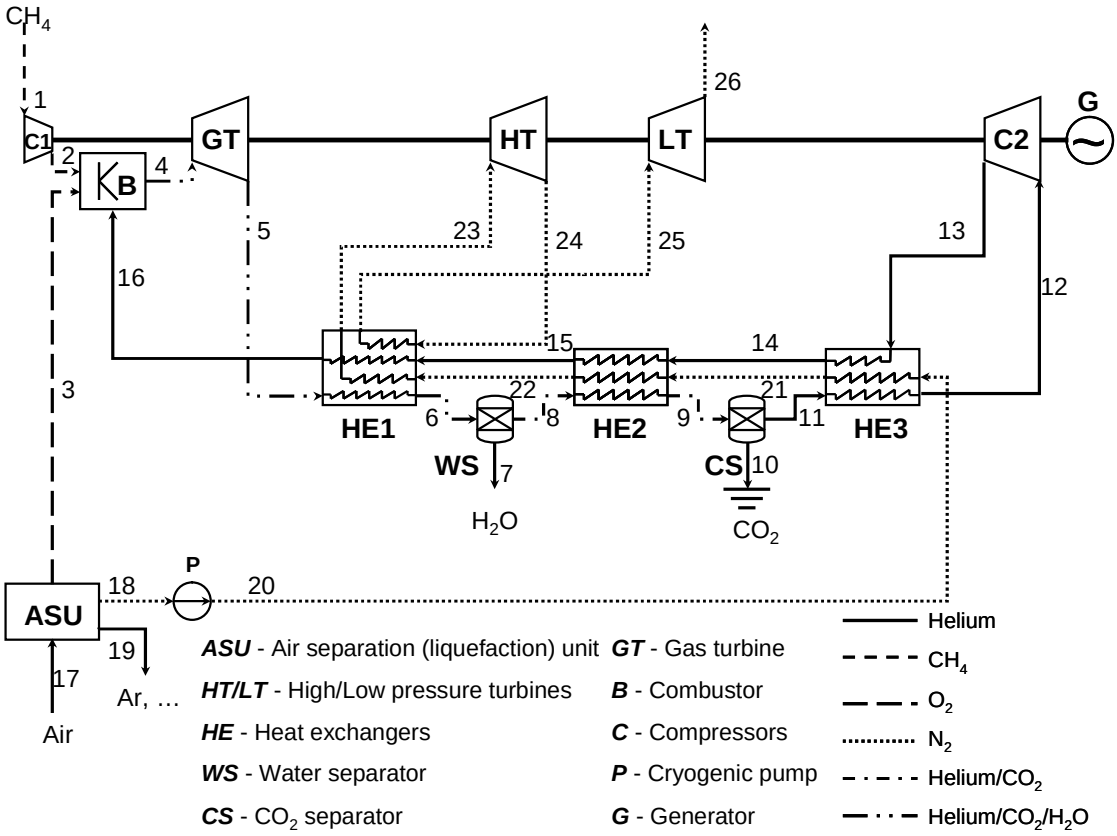

Figure 5.2 The flow sheet of the proposed cycle

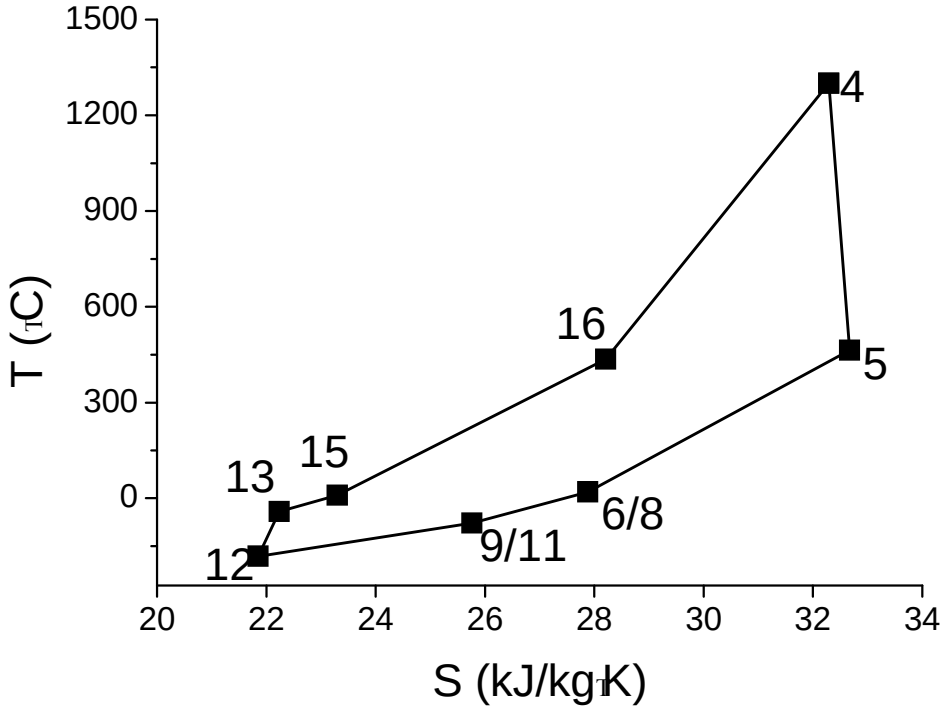

Figure 5.3 *T-S* diagram for helium cycle

At peak hours, natural gas is compressed in the compressor C1 to the working pressure. The working fluid then mixes with the oxygen in the combustor (B) where combustion takes place to give high temperature and high pressure flue gas consisting of CO_2 and H_2O. Combustion of the natural gas in an oxygen environment can produce a temperature that is too high for the gas turbine (GT). To control such a temperature, an appropriate amount of blending gas is required. Helium is selected as the blending gas first which is mixed with the flue gas before entering the GT for power generation through a generator (G). Note that the helium gas is not consumed but circulates in the system; see below for details. The flue gas containing helium from the GT then goes through a series of heat exchange processes via heat exchangers 1 (HE1), 2 (HE2) and 3 (HE3) to recover the waste heat by passing the heat to a nitrogen stream from the ASU; see below for details. During the heat recovery processes, steam in the flue gas is removed via a condenser (WS), whereas CO_2 is removed in the form of dry ice through a solidification process in CS (the triple point of CO_2 is 5.718 bar and 56.6^{o}C). As a result, the flue gas stream after CO_2 removal contains only helium. The helium stream is then cooled down further in HE3 and compressed in compressor C2 to the working pressure, and finally goes through further heat exchange in HE2 and HE1 before flows back to the combustor. Note that there may be a very small amount of CO_2 in the separated water stream (WS) due to thermodynamic equilibrium, for simplification of the calculations it is assumed that water, CO_2 and helium are fully separable.

Come back to the nitrogen stream starting from the cryogenic storage tank where liquid nitrogen is pumped to the working pressure by a cryogenic pump (P). The high pressure liquid nitrogen is then heated in heat exchangers (HE3, HE2 and HE1 in series) and expands in two stages via respectively a high pressure turbine (HT) and a low pressure turbine (LT) to generate electricity. Heat exchanger 1 (HE1) serves as an inter-heater between the two stage expansion. After expansion, the pure nitrogen can be used to purge the sorbent bed of the ASU air dryer.

From the above, one can see that the newly proposed cycle consists of a closed-loop topping Brayton cycle with He/CO_2/H_2O as the working fluid and a open-loop bottoming nitrogen direct expansion cycle. The topping Brayton cycle can be identified as 4 → 5 → 6 → 8 → 9 → 11 → 12 → 13 → 14 → 15 → 16 → 4, whereas the bottoming cycle goes through 18 → 20 →21 → 22 → 23 → 24 → 25 → 26. It is the combination of the two cycles that produce electricity at the peak hours. The

Brayton cycle uses a smaller amount of natural gas (then it would use without the cryogen based system), which is burned in the pure oxygen produced by the ASU during off-peak hours. Helium is only used to control the turbine inlet temperature (TIT) and is circulating. The working fluid of the open cycle, nitrogen, is the actual energy carrier of the off-peak electricity. As CO_2 is captured, only water and nitrogen are given out from the process.

5.2.2 Performance Analysis

To simplify the computation, the whole system is assumed to be in the steady state. Further assumptions for the calculations include (see also Table 5.1 for details):

- HE1 is a four-pass heat exchanger as one hot stream and three cold streams go through it. It is used to preheat the helium stream, superheat the nitrogen stream prior to HT and reheat the nitrogen stream between HT and LT.

- HE2 and HE3 are three-pass or two-pass heat exchangers depending on the combustion pressure for cryogenic exergy recovery. This is because after compression the temperature of stream 13 may not low enough for CO_2 and/or water separation.

- The positions of the heat exchangers in the cycle and temperatures at the inlets/outlets are selected on the basis of reducing the heat transfer irreversibility and for separating water and CO_2. This is achievable by adjusting the flow rate ratio of natural gas and liquid nitrogen.

- Natural gas contains pure methane, and the combustion is stochiometric with CO_2 and H_2O as the combustion products (practically an oxygen-rich environment is required for a complete combustion process. In this case the additional oxygen can be used as part of blending gas). The separated water from WS does not contain CO_2.

- No turbine blade cooling takes place. Oxygen from the ASU is pure and the storage vessel is at the working pressure of the combustion.

- The temperatures between HE1 and HE2 are set to be at the ambient temperature (or with an approach temperature difference for heat transfer). Such an assumption is realistic as the outlet flow from the Brayton cycle can be cooled by ambient water and the cryogen can be heated by the ambient

water if needed. Also, the direct expansion nitrogen turbines can be heated by water while its working temperature is lower than ambient value.

Table 5.1 Main assumptions for the calculation

ASU	Power consumption for liquid nitrogen production (kJ/kg)	1297 [188, 189]
Fuel compressor (C1)	Isothermal efficiency (%)	88
Combustor (B)	Efficiency (%)	100
	Pressure loss (%)	3
Gas turbine (GT)	Inlet temperature (℃)	1300
	Isentropic efficiency (%)	88
Recuperation system	Water separator working temperature (℃)	20
	CO_2 separator working temperature (℃)	−78
	Heat exchangers pressure loss (%)	2
	Approach temperature (℃)	10
Helium compressor (C2)	Isentropic efficiency (%)	88
Cryogenic pump (P)	Efficiency (%)	77
High pressure turbine (HT)	Isentropic efficiency (%)	88
Low pressure turbine (LT)	Isentropic efficiency (%)	88
Fuel	Methane LHV (kJ/kg)	50,010
Conventional oxy-fuel combined cycle	Net LHV efficiency (%)	47 [184]

Two efficiencies are employed to assess the performance of the newly proposed cycle. One is the exergy efficiency defined as the ratio of the exergy obtained to that consumed:

$$\eta_e = (W + \dot{m}_c E_c) / (\dot{m}_f E_f + \dot{m}_n E_n + \dot{m}_o E_o) \tag{5.1}$$

where W is the overall power output from turbines less the power consumed by the compressors and cryogenic pump. $\dot{m}_c$, $\dot{m}_f$, $\dot{m}_n$ and $\dot{m}_o$ are respectively the mass flow rates of carbon dioxide, fuel (natural gas), cryogen (nitrogen) and oxygen, E_f denotes the fuel exergy, which is approximately equal to its lower heating value, and E_c, E_n and E_o are respectively the differences between the exergies of carbon dioxide, cryogen and oxygen at their initial states and that at the ambient state defined by:

$$E_c = (H_{10} - H_{a,c}) - T_a(S_{10} - S_{a,c}) \tag{5.2}$$

$$E_n = (H_{18} - H_{a,n}) - T_a(S_{18} - S_{a,n}) \tag{5.3}$$

$$E_o = (H_3 - H_{a,o}) - T_a(S_3 - S_{a,o}) \tag{5.4}$$

where h_i and s_i (i=3, 10 and 18) are respectively enthalpy and entropy at point *i* (see Figure 5.2), T_a, H_a and S_a refer respectively to the ambient temperature, the enthalpy and the entropy under the ambient conditions, and the second subscripts *c*, *n* and *o* represent carbon dioxide, cryogen (liquid nitrogen) and oxygen, respectively.

The other efficiency is the so-called electricity storage efficiency and is defined as the ratio of increased power output of the system to the energy consumed for cryogen production:

$$\eta_s = (W - \dot{m}_f E_f \eta_f) / (\dot{m}_c W_c + \dot{m}_o E_o) \tag{5.5}$$

where η_f is electricity generation efficiency using a conventional oxy-fuel combined cycle and W_c refers to the specific work consumption for cryogen production. In the denominator, $\dot{m}_o E_o$ accounts for the compression work needed to bring oxygen from the ASU to the working pressure in the combustor. Here the increased power output is in comparison with the case where no cryogen is used; see late for details.

From the above, one can see that, if the mass flow rate of natural gas, the pressure in the combustor and the pressure of the cryogen at the inlet of HE3 are given, then the mass flow rates of helium, water, carbon dioxide and oxygen can be determined. In this work, calculations are based on a flowrate of 1kg/s methane entering the combustor operated at 8 bar and a cryogen pressure of 100bar at the inlet to HE3. Under such conditions, the data in Table 5.2 are obtained, which contains the values of temperature, pressure, flowrate and composition at different positions as shown in

Figure 5.2. Table 5.3 summarises the performance data of the cycle. One can see that the total power output of the proposed system is 46.12 MW. This is approximately twice of the power output of an oxy-fuel combined cycle based on the LHV efficiency (23.50 MW for a natural gas flowrate of 1.0kg/s). As a consequence, the power capacity installation of peak-load units could be halved if the newly proposed cycle is adopted. In addition, the newly proposed cycle produces dry ice and the exergy stored in the solids CO_2 is about 0.79MW. This implies a net exergy output of the newly proposed system at 46.91 MW, leading to an exergy efficiency of 63.29%. The calculations based on the net LHV efficiency of oxy-fuel combined cycle show a value of the recovered power for the newly proposed cycle of 22.62 MW. This gives an electricity storage efficiency of 54.04%.

Table 5.2 Working fluid parameters of the proposed cycle

No.	T (℃)	P (bar)	G (kg/s)	Mass composition					
				He	CO_2	H_2O	CH_4	O_2	N_2
1	20.0	1.0	1.0	0	0	0	1.0	0	0
2	20.0	8.2	1.0	0	0	0	0	0	0
3	20.0	8.2	4.0	0	0	0	0	1.0	0
4	1300.0	8.0	14.2	0.65	0.19	0.16	0	0	0
5	463.5	1.0	14.2	0.65	0.19	0.16	0	0	0
6	20	1.0	14.2	0.65	0.19	0.16	0	0	0
7	20	1.0	2.3	0	0	1.0	0	0	0
8	20	1.0	11.9	0.77	0.23	0	0	0	0
9	-78.2	1.0	11.9	0.77	0.23	0	0	0	0
10	-78.2	1.0	2.8	0	1.0	0	0	0	0
11	-78.2	1.0	9.2	1.0	0	0	0	0	0
12	-181.4	1.0	9.2	1.0	0	0	0	0	0
13	-41.1	8.4	9.2	1.0	0	0	0	0	0
14	-	8.4	9.2	1.0	0	0	0	0	0
15	10.0	8.3	9.2	1.0	0	0	0	0	0

16	453.5	8.2	9.2	1.0	0	0	0	0	0
18	-195.8	1.0	31.7	0	0	0	0	0	1.0
20	-191.4	102.0	31.7	0	0	0	0	0	1.0
21	-88.2	101.5	31.7	0	0	0	0	0	1.0
22	10	101.5	31.7	0	0	0	0	0	1.0
23	126.2	100.0	31.7	0	0	0	0	0	1.0
24	20.0	10.0	31.7	0	0	0	0	0	1.0
25	149.5	10.0	31.7	0	0	0	0	0	1.0
26	20.0	1.0	31.7	0	0	0	0	0	1.0

Table 5.3 Proposed cycle performance summary

CH_4 compressor work (MW)	0.36
He compressor work (MW)	6.70
Gas turbine work (MW)	41.57
HT turbine work (MW)	5.96
LT turbine work (MW)	6.16
Cryogenic pump work (MW)	0.51
Exergy stored in solid CO_2 (MW)	0.79
Exergy stored in high pressure O_2 (MW)	0.72
Exergy efficiency (%)	63.29
Electricity storage efficiency (%)	54.04

Figure 5.4 shows the t-Q diagram for the heat recuperation processes in the cycle, where Q is the normalized heat duty of heat exchangers. One can observe that the heat load distributions are uneven across the three sets of heat exchangers and the minimal temperature differences occur in all of the heat exchangers. The pinch points in HE1 occur at the inlet and outlet and a position where steam starts to condense. The pinch point in HE2 takes place at a position where CO_2 starts to freeze and the pinch point in HE3 appears at the cold inlet. An inspection of Figure

5.4 also indicates that heat exchange processes with large temperature differences occur mainly at regions close to the ambient temperature. As the exergy of the working fluid in such a condition is relatively low, its effect on the overall system performance is expected to be small. Figure 5.5 shows a pie chart of exergy loss distribution of the components. It can be seen that HE3 loses the highest proportion of exergy among all the heat exchangers although it has the lowest heat load (see Figure 5.4). This is mainly because the high grade cold exergy is used to freeze carbon dioxide at a relative high temperature. A possible way to reduce the high exergy loss is to use a multi-stage compression process with inter-cooling by cryogen. Furthermore, nearly half of the exergy loss occurs in the combustion process due to mixing of low temperature helium with high temperature combustion products. Therefore, increasing the turbine inlet temperature would be the most effective way to enhance the exergy efficiency of the system. In addition, Figure 5.5 also indicates that increasing the isentropic efficiency of the gas turbine will be very effective in improving the overall performance of the system. This, however, represents a big challenge in the field of gas turbine and is out of the scope of this work.

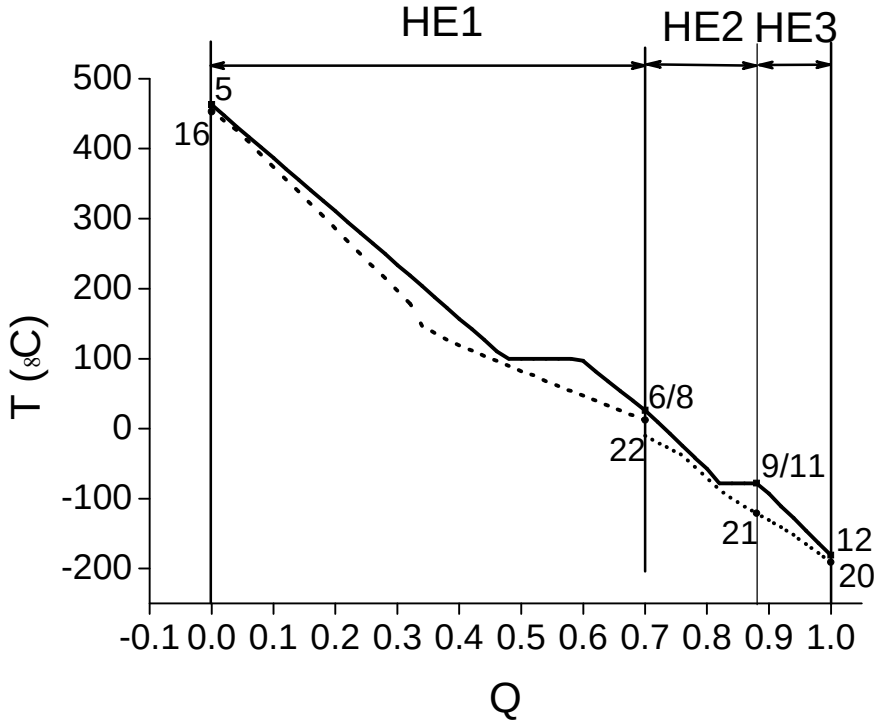

Figure 5.4 T-Q diagram for the heat exchange processes

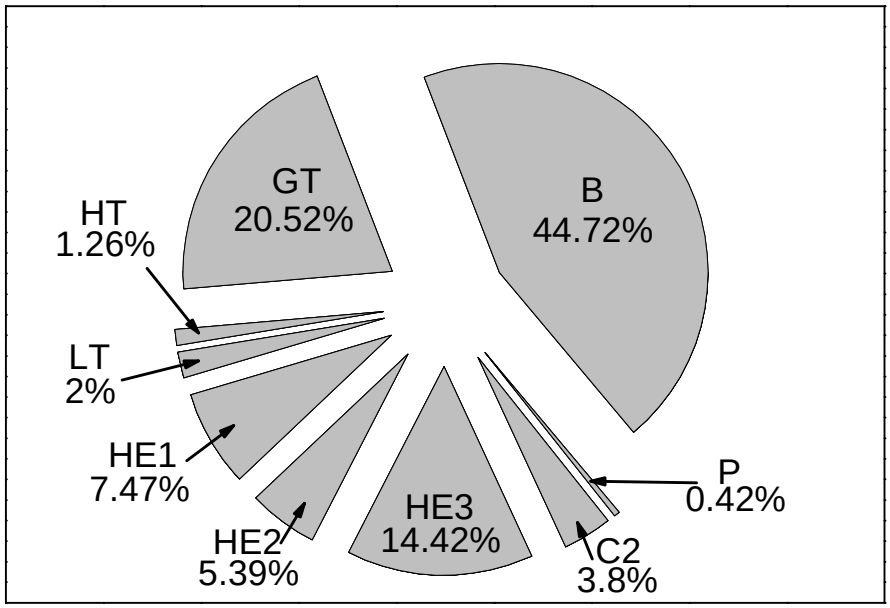

Figure 5.5 Pie chart of exergy loss distribution
(GT-Gas Turbine; B-Combustor; P-Cryogenic Pump; C-Compressors; HE-Heat Exchangers; HT/LT-High/Low Pressure Turbines)

5.2.3 Parameter Sensitivity Analysis and Discussion

The sensitivity of four parameters are investigated, including the combustor working pressure, the turbine inlet temperature, the cryogenic cycle topping pressure and the approach temperature of recuperation (heat exchange) processes. The effects of these parameters on the exergy efficiency and electricity storage efficiency are analysed. In addition, the effects of these parameters on the net output power of the cycle and the mass flow rate of cryogen are also investigated.

Figure 5.6 shows the effect of combustor working pressure while other parameters are kept constant. Overall the working pressure of the combustor has a very small effect on the exergy efficiency. An increase in the working pressure gives a small increase in both the exergy and electricity storage efficiencies first. Both the efficiencies reach a maximum at a pressure of ~ 7 bars, followed by a decrease in the efficiencies with a further increase in the combustion pressure. This is mainly because that, at pressures lower than ~ 7 bars, the mass flow rate of helium decreases significantly with increasing combustor pressure as a result of an

decreased inlet temperature, leading to a decrease in the flow rate of cryogen. At pressures above ~7 bars, the rate of decrease in the helium flowrate becomes small and the exergy loss due to mixing of the flue gas with helium becomes more considerable, thus leading to a gentle decrease in both the exergy and electricity storage efficiencies. Note that the optimal combustion working pressure in the newly proposed cycle is much lower than the conventional cycles. As is known, manufacturing of high inlet temperature gas turbines for high pressure applications currently represents a great challenge. It is however possible to make high inlet temperature turbines for lower pressure applications with currently available technologies. As a consequence, the use of the newly proposed cycle indirectly appears to address the manufacturing challenges of gas turbines in both technical and economic aspects as will be discussed later. It is also noted that the output power decreases slightly with increasing the combustion working pressure. This is because the increase of the combustion working pressure decreases the outlet temperature of gas turbine and the amount of waste heat. As a result of thermal balance the mass flow rate of cryogen decreases accordingly as well as the power generated by cryogen expansion.

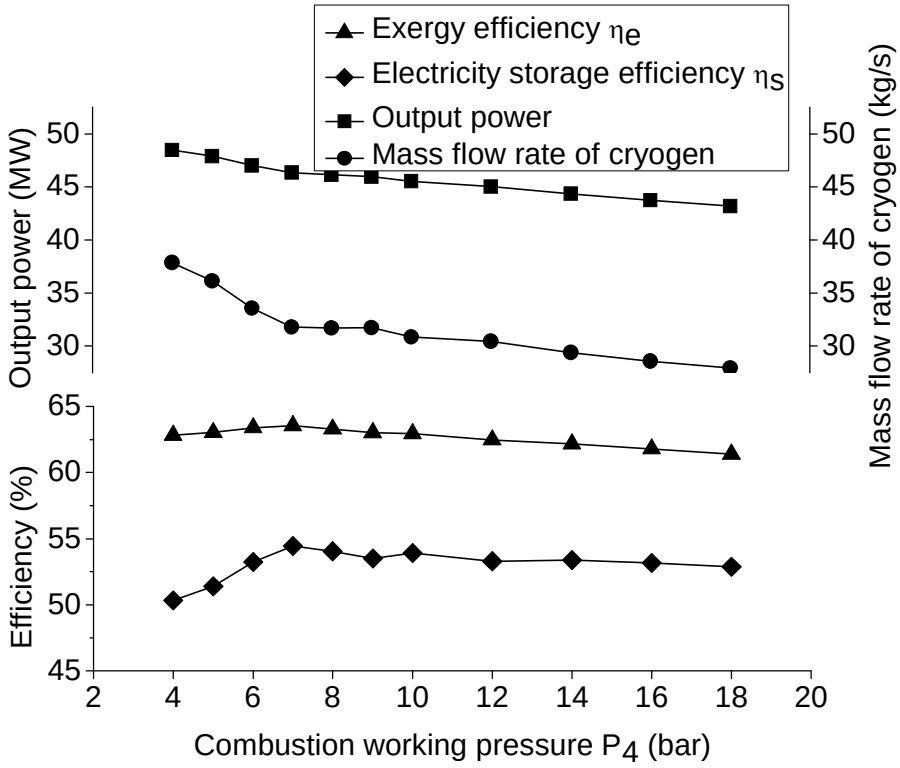

Figure 5.6 The influence of combustion working pressure P_4

The influence of turbine inlet temperature is illustrated in Figure 5.7, which shows that a significant increase in both the exergy and electricity storage efficiencies and a considerable decrease in the cryogen mass flow rate with increasing turbine inlet temperature (TIT). However, the net power output only decreases slightly with an increase of TIT from 1000 to 1350^{o}C. Quantitatively, for every 100^{o}C increase in the TIT, the exergy efficiency increases by ~ 1%, while the electricity storage efficiency increases by about 3%. This, again, shows that increasing the turbine inlet temperature is a very effective way to enhance the performance of the newly proposed system.

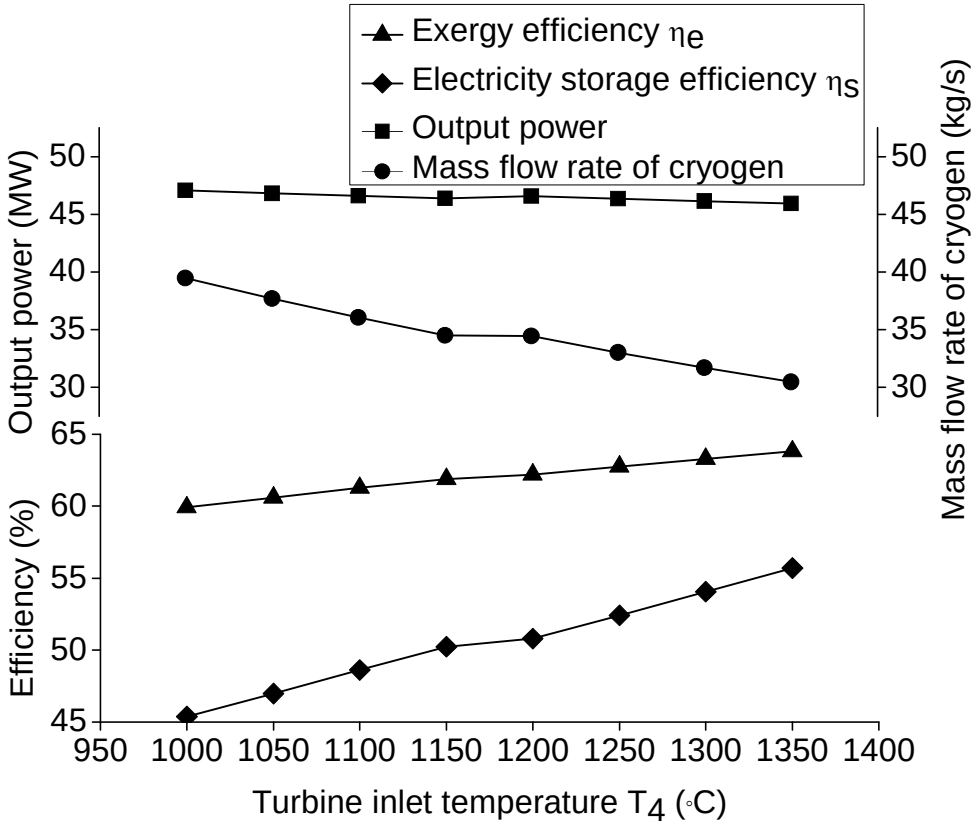

Figure 5.7 The influence of turbine inlet temperature *T_4*

Figure 5.8 shows the effect of pressure of the cryogen on the performance of the newly proposed cycle for the range of 30 and 300bar. One can see that the exergy efficiency is approximately constant at pressures above 100 bar whereas an optimal pressure of ~ 90 bar appears to exist at which the electricity storage efficiency is the

highest. Such a pressure level is easily achievable with current available technologies.

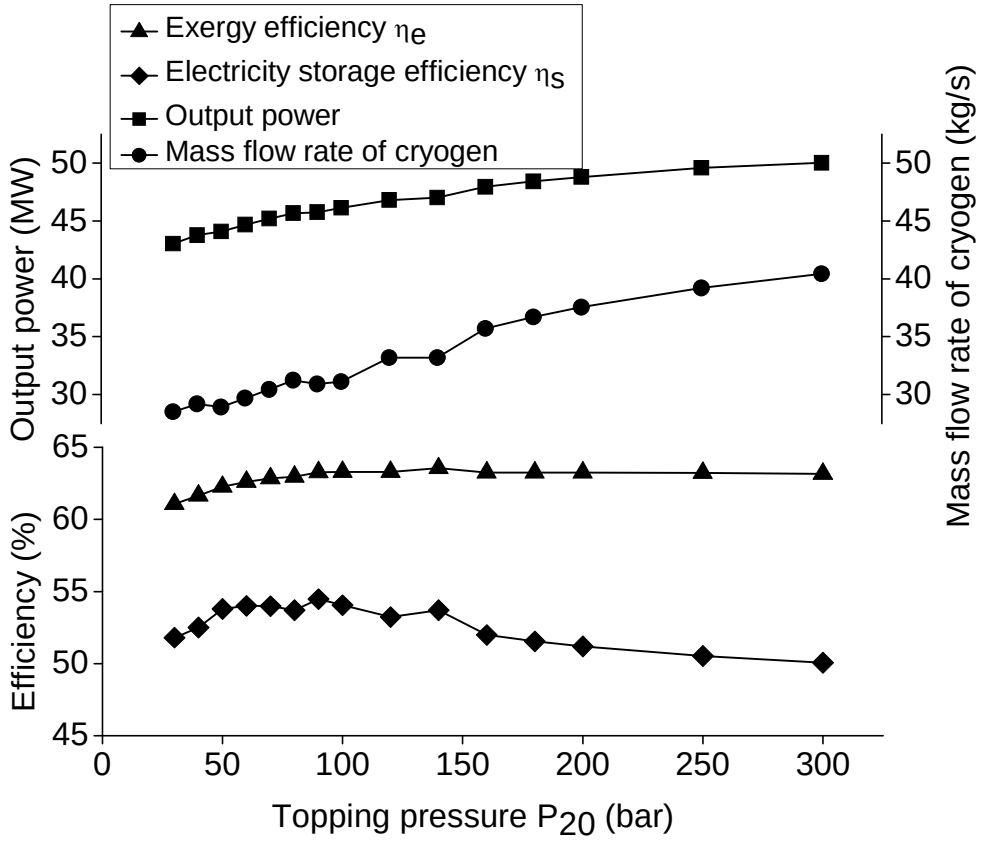

Figure 5.8 The influence of cryogenic cycle topping pressure P_{20}

The effect of the approach temperature of the heat exchangers on the cycle performance is illustrated in Figure 5.9. One can observe that the exergy and electricity storage efficiencies decrease by about 1.5% and 3%, respectively, for every 10^{o}C increment in the approach temperature. As a consequence, a low approach temperature should be adopted for the newly proposed cycle, which should also increase the thermal efficiency of the system. However, a low approach temperature implies an increase in the heat transfer surface area and hence a higher pressure drop, which is not considered in the current study. In addition, the increase in the heat transfer surface area also implies an increase of the costs.

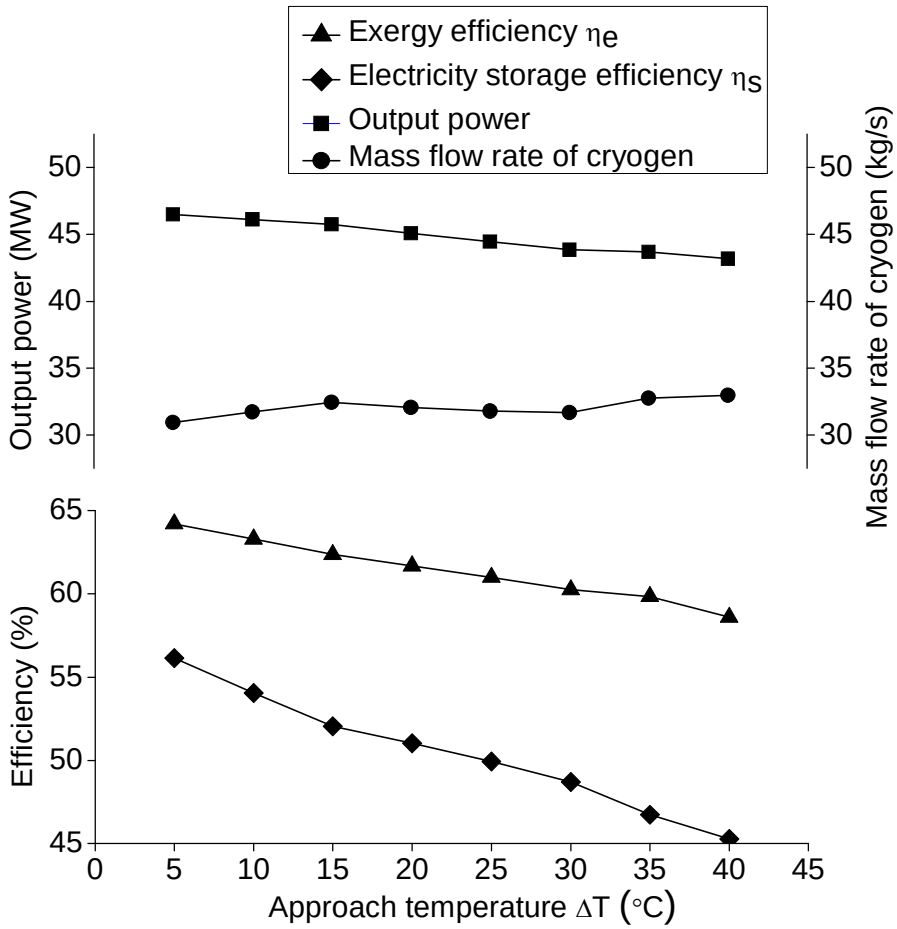

Figure 5.9 The influence of approach temperature ΔT of the recuperation system

The above sensitivity analyses show that the newly proposed cycle is likely to give an optimal performance at a relatively low combustor working pressure (~7bar) and medium cryogenic cycle topping pressure (~ 90bar). These pressure levels are much lower than those currently used in the conventional cycles. The analyses also show that an increase in the turbine inlet temperature and a decrease in the approach temperature of the heat exchanging processes are very effective to enhance the overall performance. From the practical point of view, the above operating conditions are relatively easily to achieve as high temperature gas turbines are available for low to medium pressures operations. Furthermore it is also found that the mass flowrate of liquid nitrogen consumed by the system is about seven times as that of required oxygen. This indicates there will be excess oxygen if the air is fully separated in the ASU unit.

The above analysis is based on the given baseline conditions and the effects of the parameters are investigated independently. However as the system contains complicated heat-power conversion and heat transfer processes, a systematic approach is required to further enhance the system's performance. This is to be discussed in the following section.

5.3 Systematic Optimisation

5.3.1 Optimisation Strategy

Apart from the combustion process, the peak-shaving system (the electricity generation part) could be sub-divided into four stream flows as shown in Figure 5.10 if a more effective heat exchanger network is considered.

(1) Natural gas flow: The feed-in natural gas is pre-cooled to reduce the compression power prior to the compressor. The compressed gas is then sent to the combustor after a super-heating process.

(2) Oxygen flow: Assuming the oxygen produced by off-peak electricity is stored in the liquid form and the power consumption of oxygen liquefaction is 1071 kJ/kg (Such a value is calculated by comparing with the power consumption of liquid nitrogen production as it cannot be found in public resources). At peak times the liquid oxygen is firstly pumped to a high elevated pressure. After super-heating the high pressure oxygen drives a high pressure turbine (HT2) to generate electricity while its pressure drops down to the combustion pressure. The pure oxygen is then sent to combustor after a re-heating process.

(3) Flue gas flow: The flue gas from the combustor drives a gas turbine (GT) to produce electricity. The output gas is super-cooled gradually during which the steam and CO_2 could be separated in the form of liquid water and dry ice, whereas the remaining blending gas is compressed in two compressors (C2 and C3) with inter-cooling and sent back to the combustor after a pre-heating process (in the case of CO_2 being used as blending gas only a suitable fraction is removed in the form of dry ice).

(4) Nitrogen flow: The liquid nitrogen is pumped to an elevated pressure and super-heated, followed by a two-stage expansion process in turbines (HT1 and LT) with inter-heating. The output gas releases its thermal energy through a heat exchange process to about ambient temperature and is sent to ASU dryers to regenerate the desiccant.

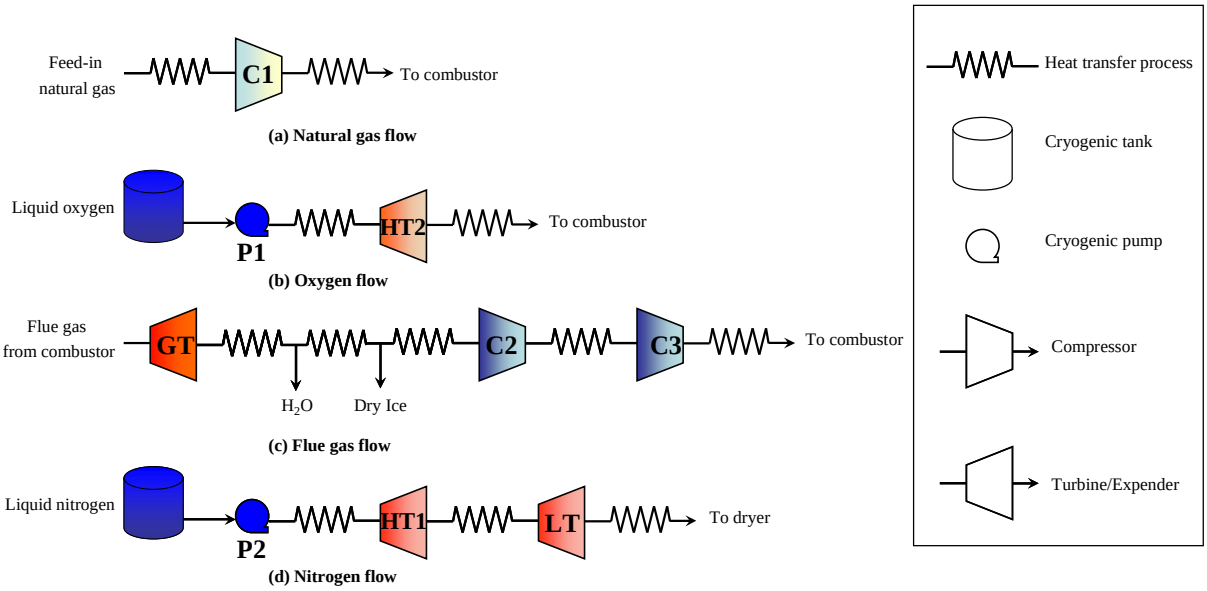

Figure 5.10 Sub-flows of the peak-shaving system

For these sub-flows again the global design method discussed in Chapter 3 is used for the systematic optimisation. Apart from the use of helium as the cooling gas for the control of TIT, CO_2 and oxygen are also considered as options for comparison in terms of thermodynamic performance and capital costs of peak electricity production.

5.3.2 Results and Discussions

To simplify the computation, again the whole system is assumed to be run in the steady state and the pressure and heat loss in heat transfer process are not considered. Other assumptions for the calculations are the same as that stated in last section.

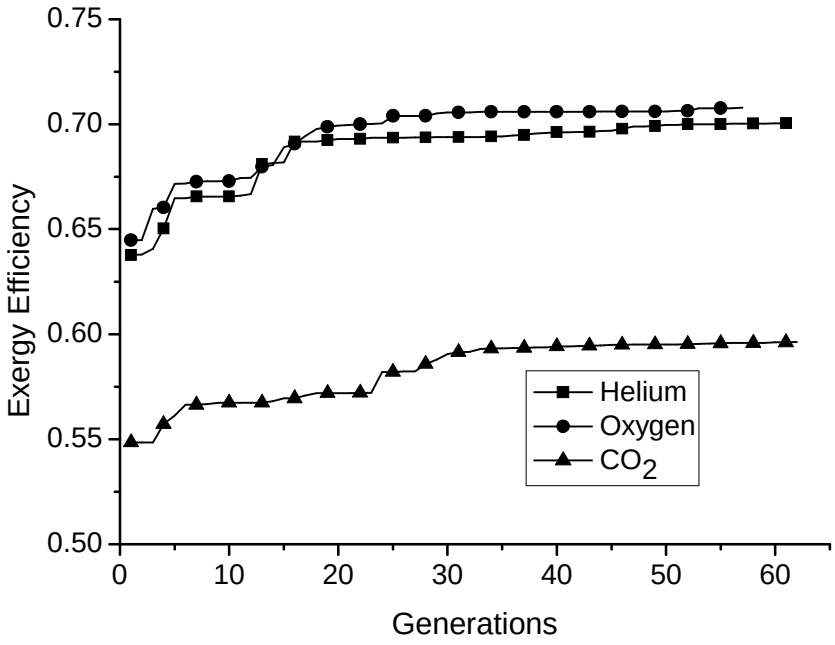

Figure 5.11 Exergy efficiencies versus number of generations using different blending gases

The exergy efficiency for the different blending gases as a function of the optimisation process is shown in Figure 5.11. It can be seen that the exergy efficiency with helium increases from 64% to around 70%, whereas the use of oxygen gives a very similar but a slight higher efficiency. This is easily to explain because the two gases work completely in the gas phase region, unlike the use of steam which involves phase change. Figure 5.12 shows the heat capacities of helium and oxygen during the heat exchange process. One can see that the heat capacity of helium is almost constant whereas that oxygen decreases slightly. This means that the use of oxygen as the blending gas is able to recover more high-grade cold and therefore make the heat transfer process more efficient. The very different heat capacities of helium and oxygen give two different sets of optimised operating parameters and the data are listed in Table 5.4.

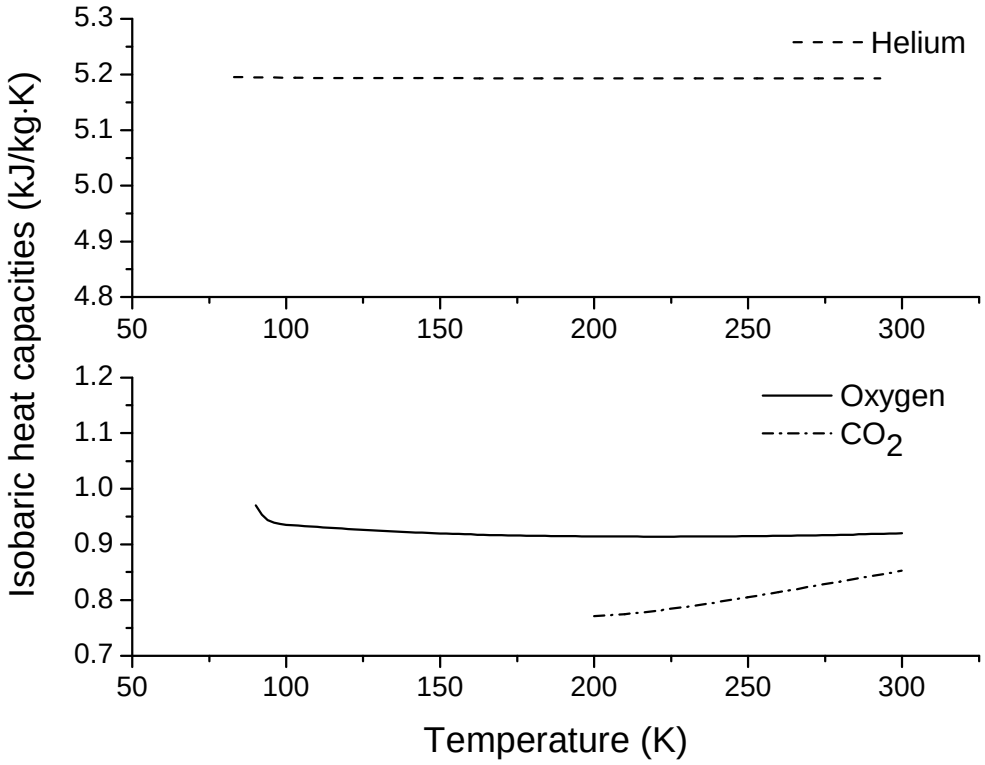

Figure 5.12 Isobaric heat capacities vs. Temperature diagram of blending gases at ambient pressure

On contrast, the optimised exergy efficiency using CO_2 as the blending gas is about 10% lower than the use of helium and oxygen. This is mainly because the lowest working temperature of CO_2 has to be higher than its freezing point to avoid solidification. As a result the cryogenic energy from the liquid nitrogen could not be extracted efficiently due to the large temperature difference in the heat transfer processes.

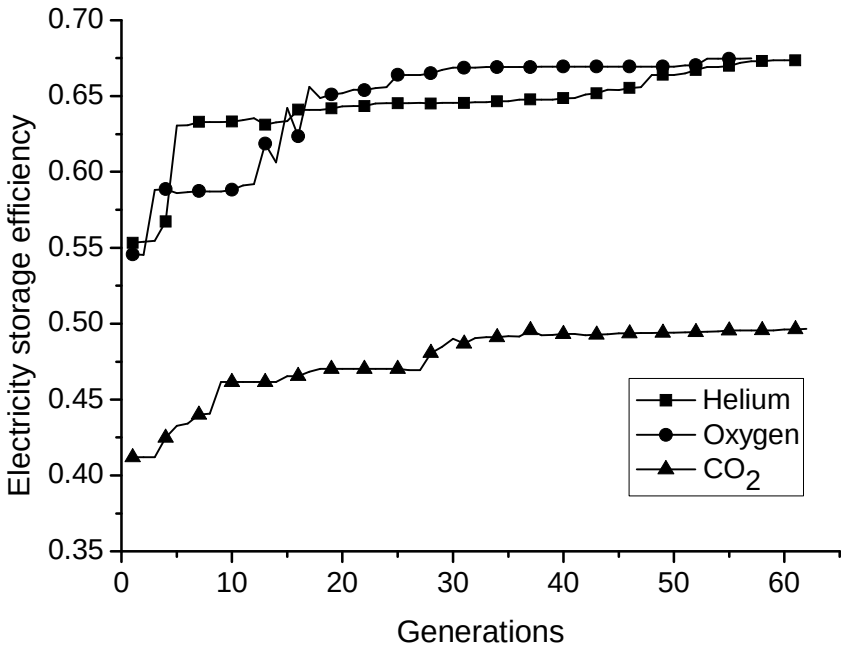

Figure 5.13 Electricity storage efficiencies versus number of generations using different blending gases

Apart from the exergy efficiency, the calculated electricity storage efficiency is shown in Figure 5.13 as a function of optimisation process. One can see the performance for the use of helium and oxygen which is similar, with an efficiency of about 67%. Such a value is much higher than other TES technologies and hydrogen storage and is even competitive with PHS and CAES [1]. While the use of CO_2 as the blending gas only gives an electricity storage efficiency of about 50%.

Comparison of the performance of CO_2 with that of helium and oxygen shows inefficient heat transfer processes being the reason for low efficiency. As a result, the Effective Heat Transfer Factor is used to investigate the performance of the heat transfer processes.

Table 5.4 Key parameters of the optimized peak-shaving system using different blending gases

Blending gas	Helium	Oxygen	CO_2
Combustion pressure (bar)	6.4	16.9	13.8

Flowrate of blending gas (kg/s)	11.2	56.9	44.6
Flowrate of nitrogen (kg/s)	29.3	28.5	27.9
Output power (MW)	50.8	51.6	41.9

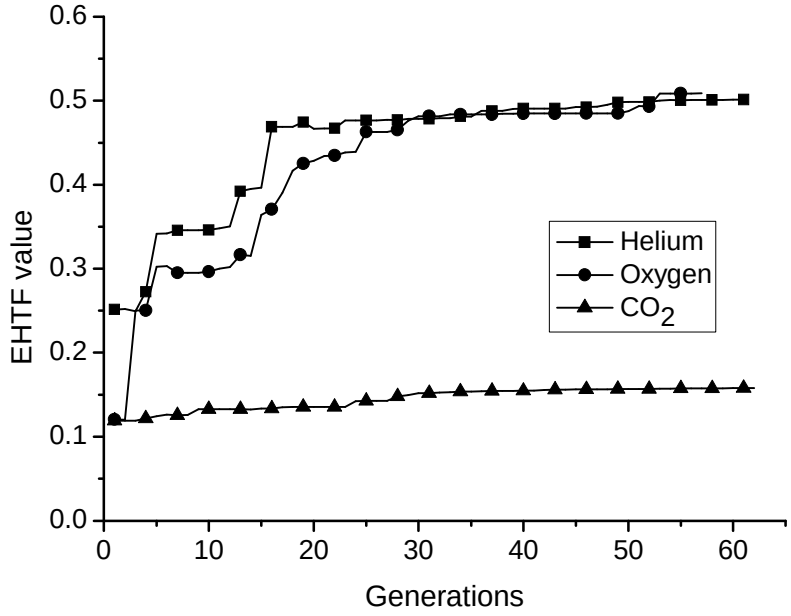

Figure 5.14 Corresponding EHTF values versus number of generations

Figure 5.14 shows the EHTF value as a function of optimisation generations for the three blending gases. One can see that the EHTF has a similar trend to that of the exergy efficiency shown in Figure 5.11. This indicates an important reason that the exergy efficiency can be improved because a more efficient heat exchanger network can be achieved through the optimization process. Figure 5.14 shows that the optimal EHTF values are nearly 0.5 when helium and oxygen are used as the blending gases. Such a value indicates a good performance as phase change occurs in the steam and CO_2 separation processes. The EHTF value of CO_2 is only about 0.15 therefore thermodynamically CO_2 is not the best option as a blending gas.

Form the above simulation it can also be concluded that all the blending gases should have similar thermodynamic performance as long as it works completely in

their gaseous region. Therefore not only helium, but also other inert gases can be the candidates of blending gas.

5.4 Economic Analysis

5.4.1 Economic Modelling

Estimation of the capital costs as well as costs associated with owning and operating the system at the component level is a key step to assess the competitiveness and viability of the technology. The methodology for estimating the main components costs and amortization factor are the same as those used in Chapter 4 and presented in Appendix B.

It is difficult to estimate the capital cost of ASU facility from published information. However it is reported that the cost ratio of capital charges to recover the investment and provide a return on investment and power charges is between 0.43 and 1.0 while the operating labour costs only form a small fraction[59, 189, 190]. Personal communication with liquefaction facility suppliers shows the capital cost is about 30,000 US$/(ton/day) (for a 500 ton/day system) which corresponds a cost ratio of about 0.86. Therefore such a value is adopted in the following calculations.

Based on the above definition, the capital cost of peak-shaving system is expressed as:

$$C_{PS} = \frac{I_{PS}}{W_{PS}} \tag{5.6}$$

The electricity production cost of the peak-shaving system could be expressed as:

$$CE_{PS} = \frac{1}{W_{PS}}\left[CF_{CH_4}\dot{m}_{CH_4} + CE_{opk}W_{ASU}\frac{24-O}{O} + \frac{\varphi f I_{PS}}{365O}\right] \tag{5.7}$$

Ideally the air separation and liquefaction unit should operate only at off-peak times. Such a scenario is impracticable as it typically takes several hours for the oxygen and nitrogen product streams to reach the desired product purities [59]. Recent flexibility studies of cryogenic air separation technology show that a turn-down of 50% of the nominal ASU (semi base load) is achievable with the load change velocity of 1-2% per minute [191]. However such a technology is still under development and not fully demonstrated. Therefore in the following economic

analyses it is assumed the air separation and liquefaction unit operates continuously at a constant load.

5.4.2 Results and Discussions

A peak-shaving plant with a net output power (generated power subtracts the power consumed by ASU) of 600 MW is used as a case study for the economic analyses. Other baseline assumptions are listed in Table 5.5.

Three peak-shaving systems using different blending gases are calculated. The purchase prices of main components are shown in Figure 5.15. One can see that the ASU, gas turbine and expenders (including high pressure turbines HT and low pressure turbine LT) take the major shares of the costs for all the three systems. Comparison of the three systems indicates that the costs of compressors and gas turbine of the helium system is much lower than that of the other two systems. This is because helium has a much higher heat capacity leading to a smaller mass flowrate and combustion pressure and hence a lower capital cost. It is also seen that the ASU and the expander costs of CO_2 system is much higher than the other two systems. This is because the exergy efficiency of CO_2 system is much lower than the other systems, which requires a higher mass flowrate of liquid nitrogen to give the same amount of net output power.

The above discussion is based on a scenario of 2 hours peak shaving operation per day. Increasing the operation duration will require more capacity of liquefaction unit and hence the costs. Figure 5.16 shows the results. One can see that the capital costs of the peak-shaving systems increase dramatically with increasing operation hours. Even so they are much cheaper than oxy-NGCC based technology for peak shaving when the operation time is less than 8 hours per day (see Figure 5.16). Of particular interest is that if the operation period is lower than 2 hours, the capital cost of the three peak-shaving systems could be lower than traditional NGCC technology (see Figure 5.16) [184]. Again among the three peak-shaving systems the capital cost of helium based is the lowest.

Table 5.5 Baseline parameters for the economic analysis

φ	1.06	O (hours)	2
in (%)	6.00	CE_{opk} (US$/kWh)	0.045
ri (%)	5.00	CF_{CH_4} (US$/kg)	0.150
CP (years)	1	h (W/(m^{2}K))	300.0
k (years)	30		

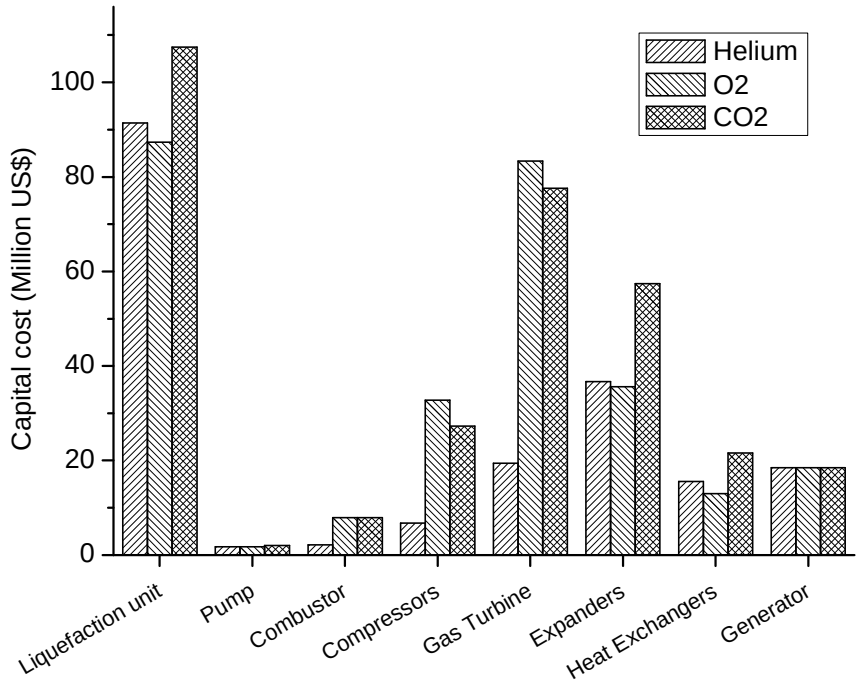

Figure 5.15 Breakdown of component cost of peak-shaving system using different blending gases

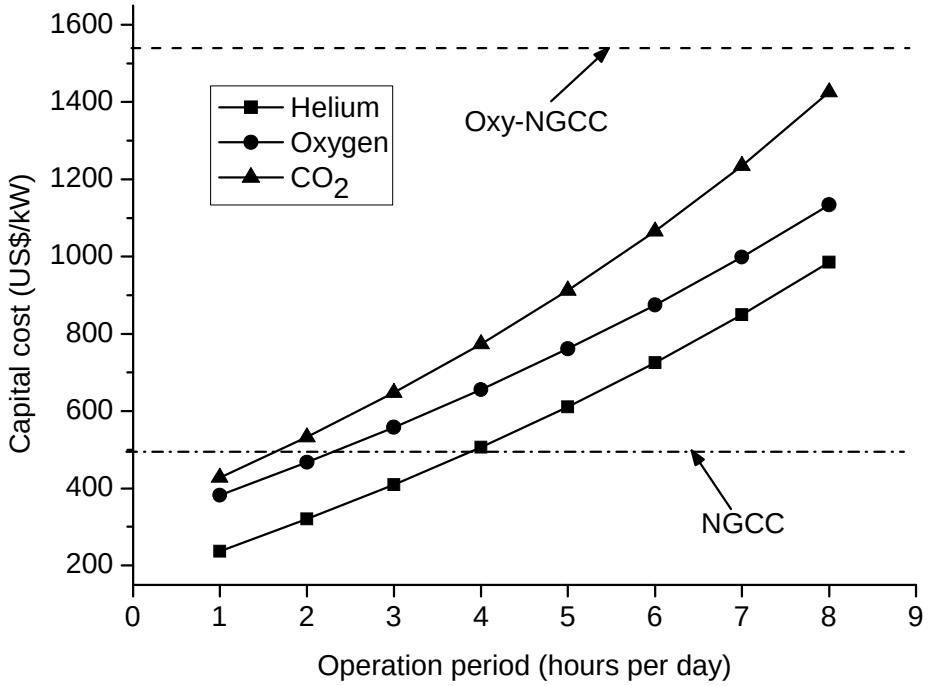

Figure 5.16 Effect of operation period on capital cost of peak-shaving systems

The cost of peak electricity production consists of capital cost, fuel cost and off-peak electricity cost for the peak-shaving systems. Figure 5.17 shows the baseline costs of peak electricity production using the three different systems, together with the NGCC and oxy-NGCC. For all the three peak-shaving systems the capital cost is the dominant factor, followed by the cost of off-peak electricity. The fuel only takes a small fraction. The peak electricity costs of the three peak-shaving systems considered in this work are more or less the same as that of the NGCC system, but they are much lower than that of the oxy-NGCC system.

Similarly to the capital costs, the peak electricity costs are affected by the operation period. Figure 5.18 shows the results. One can see that the costs of peak-shaving systems decrease first with increasing of operation hours, but then levels off once the operation period is longer than 4 hours a day. This is mainly because of the capital costs of liquefaction unit as discussed before. On the other hand the peak electricity costs of NGCC and oxy-NGCC decrease monotonously with the increase of operation hours. The comparison indicates that the peak-shaving systems are

economically competitive only when the operation period is shorter than ~ 4 hours per day.

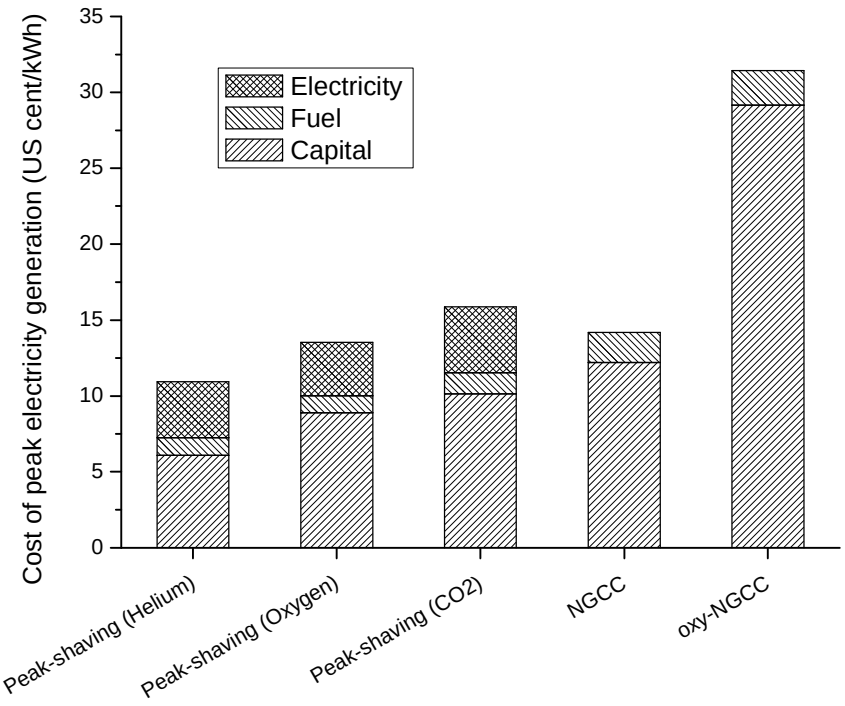

Figure 5.17 Breakdown of peak electricity cost

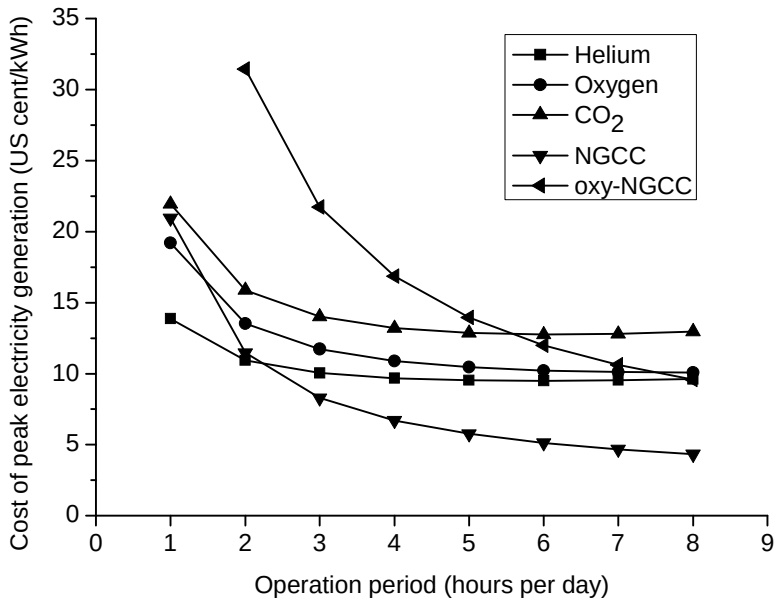

Figure 5.18 Effect of operation period on peak electricity cost

The effects of off-peak electricity and fuel costs on the peak electricity cost are compared and are shown in Figure 5.19 and Figure 5.20, respectively. A linear relationship is seen before the peak and off-peak electricity costs, the rate (slope) of the increase is much smaller than that of the dependence on the operation period. Figure 5.20 also shows that costs of the NGCC and oxy-NGCC technologies are more sensitive to the fuel costs than the three systems considered in this work.

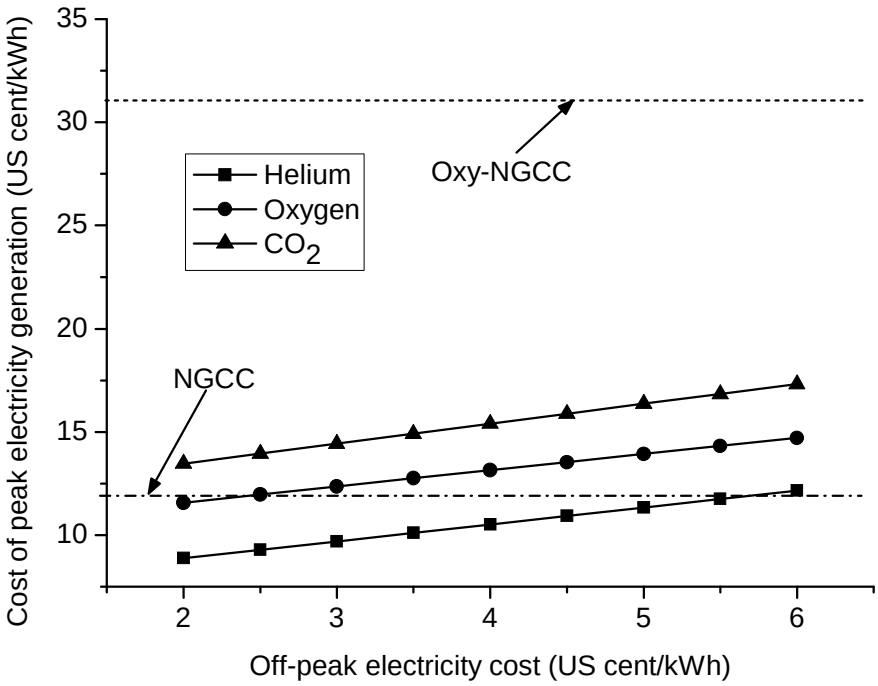

Figure 5.19 Effect of off-peak electricity cost on peak electricity cost

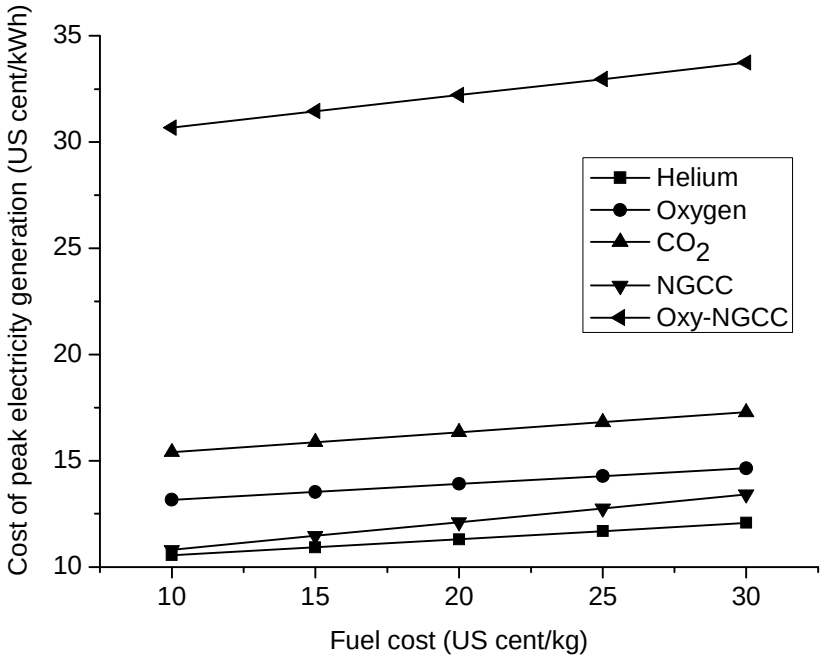

Figure 5.20 Effect of fuel cost on peak electricity cost

From the above discussion, one can see that the cryogen based peak-shaving technology is very competitive especially for short peak durations. If the operation time is less than 3 hours a day, both the capital and the peak electricity costs are comparable with the NGCC, but are much lower than the oxy-NGCC. Particularly if helium is used as the blending gas the costs of the peak-shaving system is even lower than that of NGCC even with CO_2 captured from the flue gas.

It should be noted that there are two challenges associated with the use of helium as the blending gas. The first is the unavoidable leakage in the water and CO_2 separation processes, which requires helium makeup and hence the increase in the operation cost as helium is expansive. The second is that it requires a new gas turbine for the working fluid consisting of a mixture of helium, CO_2 and steam. Using oxygen as the blending gas the makeup cost for leakage is not considered as a main challenge as oxygen is produced in the air separation and liquefaction system and the cost is low. As oxygen has similar thermodynamic properties as air it is expected that the traditional gas turbine could be used directly. Of course, a disadvantage of using oxygen is associated safety related issue. But this should be manageable using today's technologies.

Selecting CO_2 as the blending gas the safety and leakage issues are greatly decreased. However the capital cost for peak electricity production will increase as discussed above. Further work is needed to evaluate the leakage and safety issues, particularly during the heat recovery and CO_2 separation processes.

5.5 Summary of This Chapter

A new peak-shaving system integrating peak electricity generation, electrical energy storage and CO_2 capture is proposed. Such a system combines a direct open nitrogen expansion cycle with a natural gas-fuelled closed Brayton cycle. Thermodynamic analyses are carried out on the system under the baseline conditions of 1 kg/s natural gas, combustor operating pressure of 8 bar and cryogen topping pressure of 100 bar. It is found that the exergy efficiency is as high as 64% under the baseline conditions, whereas the corresponding electricity storage efficiency is about 54%. The sensitivity analyses indicate that the above baseline performance can be enhanced by increasing the gas turbine inlet temperature,

decreasing the approach temperature of the heat exchange process, operating the combustor at an optimal pressure (~7 bar) and operating the cryogen topping pressure at ~ 90 bar. Further enhancement can be achieved by increasing the isentropic efficiency of the gas turbine and the liquefaction processes. The results also suggest that the fuel consumption could be reduced by half by using the newly proposed system.

A global thermodynamic optimisation is carried out for the new proposed system. Helium, oxygen and CO_2 are used as the blending gas for the system. Helium and oxygen are found to have nearly the same thermodynamic performance with exergy efficiency increasing from 64% to about 70% and the corresponding electricity storage efficiency increasing from 54% to about 67%. On contrast the optimal efficiency of CO_2 system is much lower due to the limitation of the lowest working temperature of CO_2 for avoiding solidification.

Economic analyses show that both the capital and peak electricity costs of the peak-shaving systems are comparable with the NGCC which are much lower than the oxy-NGCC if the operation period is relatively short. Among the three peak-shaving systems, the use of helium as the blending gas has the lowest costs due to the lowest combustion pressure and mass flowrate.

Capital costs are found to be the dominant factor for all the peak systems considered and the ASU takes a large share. Therefore the costs of the peak-shaving systems could be reduced by taking the following measures:

- Decreasing the cost of the ASU. The data used for costing in this work is based on a liquefaction system with a capacity of 500 ton per day. Reduction is possible by increasing the capacity.

- Variable load operation of air liquefaction unit. As the air liquefaction unit operates continuously it consume part of the power generated by the peak-shaving system. If the liquefaction unit could run at a variable load (e.g. semi base load at peak time) the capital cost of other components could be decreased. Furthermore variable load operations could follow the real price change of off-peak electricity and save the operating cost.

- Excess oxygen. It is found that the ratio of liquid oxygen and nitrogen consumed by the peak-shaving system is about 1:7. For fully separated air by the ASU, there will be excess oxygen. This part of oxygen can be used as process gas if the system is installed close to a process plants such as chemical and iron and steel-making plants. The excess oxygen can also be sold as products.

Chapter 6 Solar-Cryogen Hybrid Power System

6.1 Background

Energy and environment are two of the most concerning issues in the current world. For over a century cheap, plentiful fossil energy has been supporting the industrialization and the increasingly higher living standards. However, increasing energy demand particularly in developing countries implies depletion of the fossil fuel resources at a rapid rate. In the meantime, the use of fossil fuels continues to cause environmental degradation. All these call for the use of new and renewable energy resources. Currently, renewable energy contributes to only 11% of the world primary energy and this is expected to increase to 60% by 2070 [192]. Solar energy is one of the most promising clean and non-depleting sources that is able to fulfill the increasing energy demands. Apart from direct heating applications, solar energy can be converted to electrical energy in two main ways. One is through solar cells (photovoltaic technology), which convert solar radiation to electrical energy directly. The other is via an indirect solar thermal route, which converts the solar radiation to thermal energy by means of solar collectors or concentrators followed by electricity generation through a conventional thermal process. Solar cells are most suitable for small scale low-power applications, while solar thermal power plants are often the best option for large-scale and grid-connected systems [193, 194].

The work reported in this chapter is concerned about improving the indirect power generation via the solar thermal route in a Solar Thermal Power Plant (STPP). The STPP is a conventional power station that obtains all or parts of its thermal energy load by concentrating solar radiation, producing high temperature solar heat to activate a Rankine power cycle. In this process the concentrated solar radiation does not heat the working fluid of the power cycle directly but uses a solar energy carrier, which transport the solar radiation to a storage vessel and also transfer the heat to the working fluid. The use of heat carrier has an advantage of more precise control of quality and quantity of vapour of the working fluid according to needs. In addition, the use of storage and a heat carrier also enables the mass flow rate of the working fluid to be optimized independent of the fluctuations either or both of the load and solar radiation [22, 195]. The stored thermal energy can be used to either pre-heat water/steam in steam cycle power plants [196] or super-heat the steam in combined cycle power plants [25, 197] or even produce steam directly in Direct Steam

Generation (DSG) [22, 23]. Generally in these cycles water/steam or other organic liquids are selected as the working fluid and the solar energy is stored in the form of high temperature sensible heat. It is therefore less efficient when taking the behavior of the solar thermal energy carrier into account due to temperature glide mismatching between the solar thermal energy carrier and the working fluid.

This part of work is also concerned with efficient extraction of cold energy from cryogens which has been one of the main objectives of this work. Cryogenic energy extraction is of importance not only for CES but also for the fast developing liquefied natural gas (LNG) industry. For example it is estimated that the amount of LNG imported to China is 20 million tons by end of 2010 [171]. However, efficient recovery of the cryogenic energy is a challenge during the evaporation process without providing some heat to increase the temperature difference. This constitutes the primary motivation of working on integrating the solar thermal and cryogen power systems. This integration, as will be seen later, is able to give a higher overall energy efficiency and in the meantime alleviate the environmental impact of the re-gasification processes of cryogens.

For achieving the above objective, an integrated solar-cryogen hybrid power system is proposed and analyzed. A solar thermal power system and a cryogen fuelled power system are used as the benchmarks to evaluate the performance of the newly proposed integrated system.

6.2 Thermodynamic Consideration and Modelling Methodologies

In this section, analyses will be carried out on the three power systems of (i) Solar thermal power system, (ii) Cryogen fuelled power system and (iii) Solar-cryogen hybrid power system, where (i) and (ii) are used as the benchmarks for evaluating third system - the integrated power system proposed in this work.

6.2.1 Solar Thermal Power System

A solar thermal power system usually involves focusing sunlight on a small area to create a high-temperature heat source. A thermal energy carrier is often used to transport the heat and pass the heat to the working fluid via a heat exchange system. Table 6.1 shows a list of frequently-used high temperature thermal energy carriers [25, 198], which are either pure or mixtures of different thermal fluids. Figure 6.1

shows a schematic diagram of the solar thermal power system. The system uses water as the working fluid running on a Rankine cycle and there have been practical applications of the system [23]. The system works in the following way: first solar radiation is concentrated by the parabolic trough or other types of collectors to heat the thermal energy carrier. The high temperature energy carrier superheats high pressure water in heat exchanger 1 (HX1) before entering the high pressure steam turbine (HT). Part of the steam extracted from the HT at an intermediate pressure is reheated by the high temperature energy carrier in heater exchanger (HX2) and then sent to the low pressure steam turbine (LT) for further expansion. The exhaust steam is condensed in the condenser (CD) and then pumped to the regenerator (RG) where it mixes with the outlet steam of the HT. Finally, the condensed steam is pumped to high pressure to complete the closed power cycle. In such a manner the solar thermal energy is used in two levels and the cooled energy carrier is stored in MC and LC respectively.

Table 6.1 Frequently-used liquid materials for the storage of high temperature sensible heat

Material	Temperature range (K)	Density* (kg/m^3)	Specific heat (J/kg·K)	Volumetric heat capacity ($kJ/m^3 \cdot K$)
Draw salt (50% KNO_3+50% $NaNO_3$ by weight)	493 – 813	1733	1550	2686
Molten salt (53% KNO_3+40% $NaNO_2$+ 7% $NaNO_3$ by weight)	419 – 813	1680	1560	2620
Liquid sodium	373 – 1033	750	1260	945
Thermal-oil 66	263 – 616	750	2100	1575

*Average density and specific heat in the temperature range given.

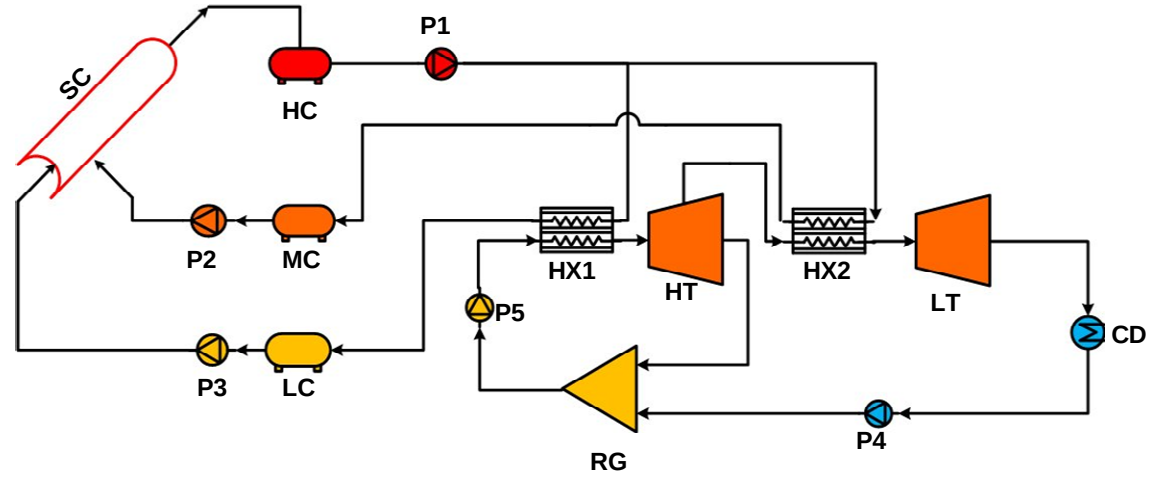

Figure 6.1 Configuration of a solar thermal power system

The thermal efficiency of a solar collector is given as [199]:

$$\eta_{1,SC}\{T\}=\frac{dQ}{dIR}=(\alpha\tau)F_{SC}+(\alpha\varepsilon)F_{SC}\frac{\sigma T_{CSC}^4}{C_{SC}{}^{S}E_b}-(\varepsilon\overline{\rho})F_{SC}\frac{\sigma T^4}{C_{SC}{}^{S}E_b}-UF_{SC}\frac{T-T_a}{C_{SC}{}^{S}E_b} \tag{6.1}$$

where Q is usable process heat and IR is the total irradiance of the collector. $(\alpha\tau)F_{SC}$, $(\alpha\varepsilon)F_{SC}$ and $(\varepsilon\overline{\rho})F_{SC}$ are respectively the absorption term coefficient, the emission term coefficient and the absorber loss term coefficient of solar collector. σ is the Stefan–Boltzmann constant, equals to 5.67×10^{-8}W/(m^2·K^4), UF_{SC} is the convection heat loss coefficient of solar collector, T is the fluid temperature, T_{CSC} is the cover temperature, T_a is the ambient temperature, C_{SC} is the concentration ratio, ${}^{S}E_b$ is the direct radiation, ${}^{S}E_b={}^{S}E-{}^{S}E_d$ with ${}^{S}E_d$ the diffusion radiation and ${}^{S}E$ the global irradiance, ${}^{S}E=f_S\sigma T_s^4$ with f_S being the dilution factor which can be assumed to be wavelength independent. In case of concentrated radiation the diffuse solar part in the incident global radiation can be omitted, one has ${}^{S}E_b={}^{S}E$. Integrating Equation (6.1) from State 1 to State 2, the total irradiance of the collector can be obtained as:

$$IR=\int_{T_1}^{T_2}\frac{1}{\eta_{1,SC}\{T\}}dQ \tag{6.2}$$

The exergy released by the solar irradiance [199]:

$$E_{si} \approx IR\left(1-\frac{4}{3}\frac{T_a}{T_S}\left(1-0.28\ln f_S\right)\right) \tag{6.3}$$

For a constant specific heat thermal fluid $dQ = d(c_p \dot{m} T) = c_p \dot{m} dT$, then

$$Q = \int_{T_1}^{T_2} dQ = c_p \dot{m}(T_2 - T_1) \tag{6.4}$$

The exergy transferred to the solar heat carrier is then given as [23]:

$$E_Q = Q\left\{1-\frac{T_0}{T_2-T_1}\ln\left[\frac{T_2}{T_1}\right]\right\} \tag{6.5}$$

As a consequence, one has the exergetic efficiency of the collector as follows:

$$\eta_{\mathrm{II},SC} = \frac{E_Q}{E_{si}} = \frac{1-\frac{T_a}{T_2-T_1}\ln\left[\frac{T_2}{T_1}\right]}{\frac{1}{T_2-T_1}\int_{T_1}^{T_2}\frac{1}{\eta_{\mathrm{I},SC}\{T\}}dT\left(1-\frac{4}{3}\frac{T_a}{T_S}\left(1-0.28\ln f_S\right)\right)} \tag{6.6}$$

The thermodynamic performances of other components of the systems are calculated in the same way as detailed in Chapter 3.

6.2.2 Cryogen Fuelled Power System

If ambient heat is the only source available, as shown in literature review, a combination of direct expansion and Rankine cycle is the most practical and efficient way to extract the cryogenic energy in a cryogen fuelled power system due to its low power consumption in the compression process [200]. Figure 6.2 shows such a system with a two-stage direct expansion. The cryogen stored in the storage tank (CT) is first pumped to a high pressure by a cryogenic pump (CP) and then heated gradually in the heat exchanger (HX) and the room heater (RH1: using the ambient heat sources like air or seawater to heat the working fluid; the same to RH2 and RH3) before subject the two-stage expansion process in the high pressure turbine (HT) and low pressure turbine (LP) with inter-heating (RH2). The high grade cold discharged in HX is recovered by liquefying a refrigerant in a Rankine cycle. The liquid refrigerant is pumped and heated in room heater (RH3) to drive the refrigerant

turbine (RT) to produce more power. The commonly used refrigerant, propane, is selected as the working fluid for the Rankine cycle in this section. Again the mathematical formulae detailed in Chapter 3 are used to evaluate the thermodynamic performance of the components in this system.

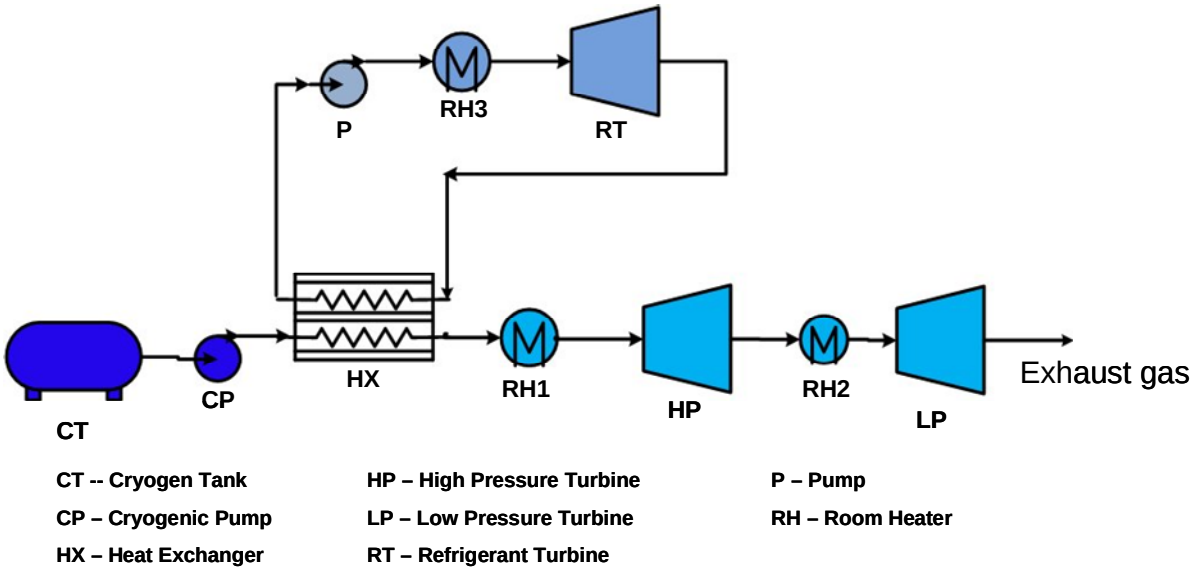

Figure 6.2 Configuration of cryogen fueled power system

6.2.3 Solar-Cryogen Hybrid Power System

The hybrid system proposed in this chapter integrates the solar thermal power cycle and the cryogen fuelled power cycle and the cryogen itself is used as the common working fluid. Figure 6.3 illustrates such a system. One can see that the hybrid system consists of three parts: an open cycle of cryogen direct expansion, a closed Brayton cycle for full extraction of cryogenic energy and a solar energy collection and storage unit to capture the solar energy and provide the heating source for both the cycles. In this system the closed Brayton cycle shares the intermediate pressure turbine (IT) and low pressure turbine (LT) with the direct expansion cycle to simplify the configuration while the cryogen is also used as the working fluid of the Brayton cycle. The cold energy released by the cryogen direct expansion is recycled by the Brayton cycle through a heat transfer process in HX1. Similarly to the solar thermal power system, the solar thermal energy (the heat source) is extracted at two levels: the superheating process between State 14 and State 16 corresponding respectively to the high temperature and low temperature carriers and the inter-heating process between State 14 and State 15 corresponding respectively to the high temperature

and intermediate temperature carriers. Comparing with the solar thermal power system, an additional compressor is used in the hybrid system.

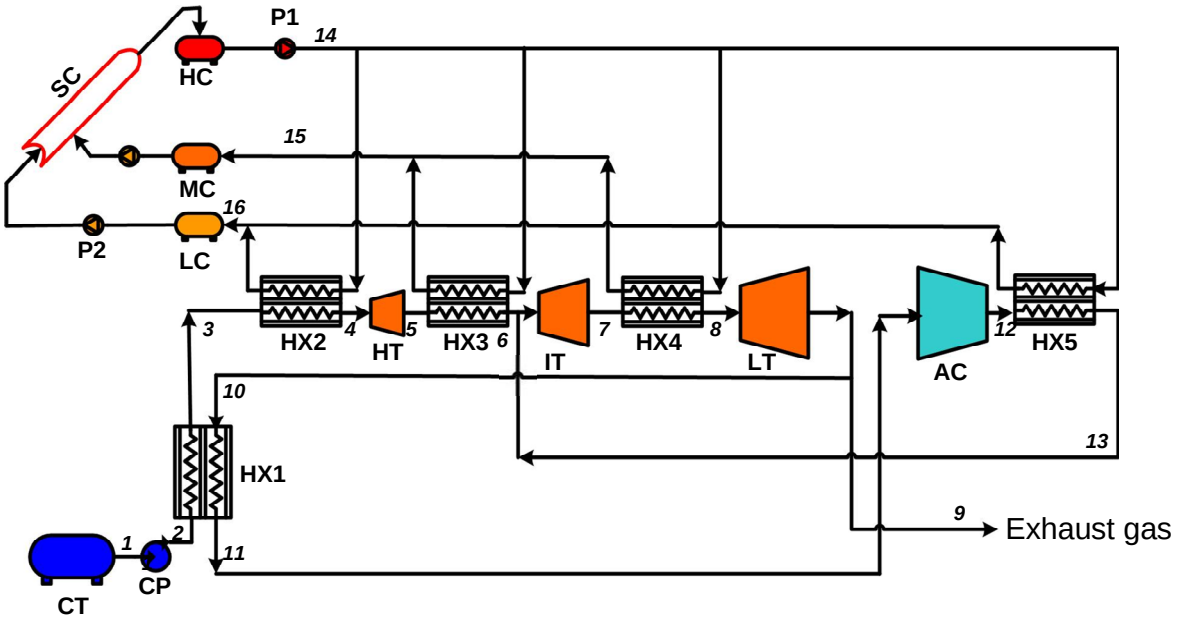

CT -- Cryogen Tank	IT – Intermediate Pressure Turbine	P – Pump
CP – Cryogenic Pump	LT – Low Pressure Turbine	HC – High Temperature Carrier Tank
HX – Heat Exchanger	AC – Adiabatic Compressor	MP – Intermediate Temperature Carrier Tank
HT – High Pressure Turbine	SC – Solar Collector	LC – Low Temperature Carrier Tank

Figure 6.3 Configuration of a cryogen-solar hybrid power system

6.3 Parametric Optimisation and System Analysis

Based on the power systems detailed above, parametric optimisation is carried out. The following exergy efficiencies are selected as the objective functions for the optimisation:

$$\eta_{SP} = \frac{W_{net}}{E_{si}} \tag{6.7}$$

$$\eta_{CF} = \frac{W_{net}}{W_{ASU}} \tag{6.8}$$

$$\eta_{SCH} = \frac{W_{net}}{E_{si} + W_{ASU}} \tag{6.9}$$

where η_{SP}, η_{CF} and η_{SCH} are respectively the exergy efficiencies of the solar thermal power system, the cryogen fuelled power system and the solar-cryogen hybrid power system, W_{net} is the net power output (equal to the turbine output power subtracting the power consumed by compression and pumping processes) and W_{ASU} is the power consumed by the cryogen production process.

Liquid nitrogen is taken as an example of the working cryogen in the parametric optimization and the solar energy carrier is assumed to have a constant specific heat. Other data used in the simulations are summarized in Table 6.2 [23, 92, 199, 201] (here the assumption of turbine isentropic efficiency is slightly higher than the previous assumptions as the inlet temperature in this system is more closer to the ambient as a result the thermal loss should be lower than traditional gas turbines or cryogenic turbines). The overall optimal performance of the three systems is given in Table 6.3. From the table, one can see that the exergy efficiency of the hybrid power system is much higher than the solar thermal and cryogen fuelled only power systems. Given the same energy source, the net output power of the hybrid power system is 1.0118 MW, which is almost 31% higher than that the summation of output power of both solar thermal and cryogen fuelled power systems.

Table 6.2 Main assumptions for the parametric optimisation

Solar collector	Absorption term coefficient $(\alpha\tau)F_{SC}$	0.8
	Emission term coefficient $(\alpha\varepsilon)F_{SC}$	0.8
	Absorber loss term coefficient $(\varepsilon\overline{\rho})F_{SC}$	0.8
	Convection heat loss coefficient UF_{SC} /Wm^{-2}K^{-1}	20
	Cover temperature T_{CSC} /K	300
	The concentration ratio C_{SC}	40
Cryogenic pump isentropic efficiency η_P		0.75
Turbine isentropic efficiency η_{EP}		0.90
Compressor isentropic efficiency η_{CP}		0.87

Approach temperature of heat exchanger system ΔT_{MAT} /K	10
The wet vapour quality of steam turbine	>0.9
The effective solar temperature T_s /K	5,777
The dilution factor f_S	1.3×10^{-5}
Ambient temperature T_a /K	298.15
Ambient pressure P_a / bar	1.0
Power consumption of liquid nitrogen production W_{ASU} / (kWh/kg)	0.5
The mass flow of liquid nitrogen $\dot{m}_n$ / (kg/s)	1.0

Table 6.3 Overall optimal performances of the three systems

		Solar thermal power system	Cryogen fueled power system	Solar-cryogen hybrid power system
Exergy efficiency (%)		23.89	18.10	27.55
Energy Source	Solar radiation (MW)	2.628	0	2.628
	Liquid nitrogen (kg/s)	0	1.0	1.0
Net output power (MW)		0.4485	0.3259	1.0118

The performance improvement of the hybrid power system comes from more efficient heat transfer processes. This can be demonstrated by the exergy analysis of the energy conservation processes using a graphical representation method named energy utilization diagram (EUD). In the EUD method an intensive parameter called availability factor or energy level (AL) is introduced as an indicator of the potential of the energy donated and accepted by the processes [202]:

$$AL = \frac{\Delta E}{\Delta H} \tag{6.10}$$

Defining a process that releases energy as an ‘energy donor (ED)’ and a process that receives energy as an ‘energy acceptor (EA)’, the exergy loss of the processes can then be given by:

$$EXL = -\sum \Delta E_i = \sum \Delta H_i (AL_{ed,i} - AL_{ea,i}) = \int (AL_{ed} - AL_{ea}) dH \tag{6.11}$$

By plotting the availability factor of the energy donating and accepting processes against the transferred energy, the amount of exergy loss in the system can be obtained as the area between the two curves.

Figure 6.4 and Figure 6.5 show the EUD representations of the optimised cryogen fuelled and hybrid power systems, respectively. One can see the exergy loss in the heat exchangers and room heaters of the hybrid power system is significantly lower than that in the cryogen fuelled power system. There are two reasons for this. First, the use of the Brayton cycle in the hybrid system enables a much more efficient heat transfer to recover the high grade cold energy due to better temperature glide matching between heat addition and heat rejection. Second, the outlet temperature of the expanded gas is increased as the compressed gas is superheated by the solar thermal energy prior to entering the turbines. Therefore the exergy loss in the exhaust gas is reduced. Meanwhile, the use of cryogen as the working fluid is beneficial for the solar thermal energy utilization. This can be understood from Table 6.4, which shows that the critical temperatures and pressures of nitrogen are much lower than that of the steam. As a consequence, supercritical cycles are much easily to achieve using the cryogen. Listed in Table 6.4 also includes the critical properties of methane, which, as will be discussed in the following section in terms of applications, also gives much better performance than the use of steam as the working fluid.

Table 6.4 Critical temperature and pressure for water, nitrogen and methane

	Water/Steam	Nitrogen	Methane
Critical temperature (K)	647	126	190

Critical pressure (MPa)	22.06	3.39	4.60

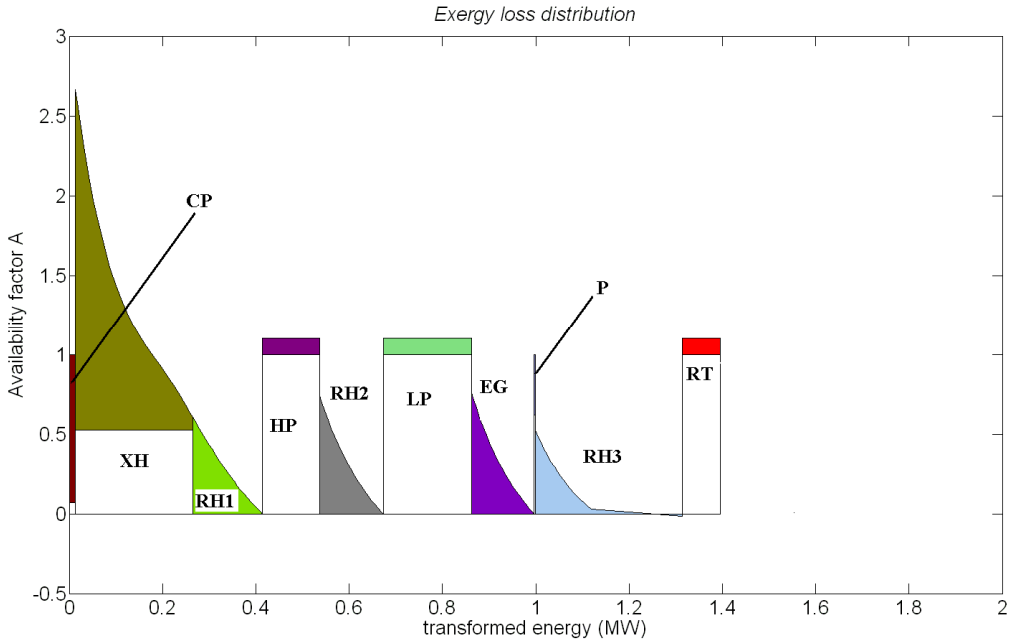

Figure 6.4 EUD representation of the optimised cryogen fuelled power system

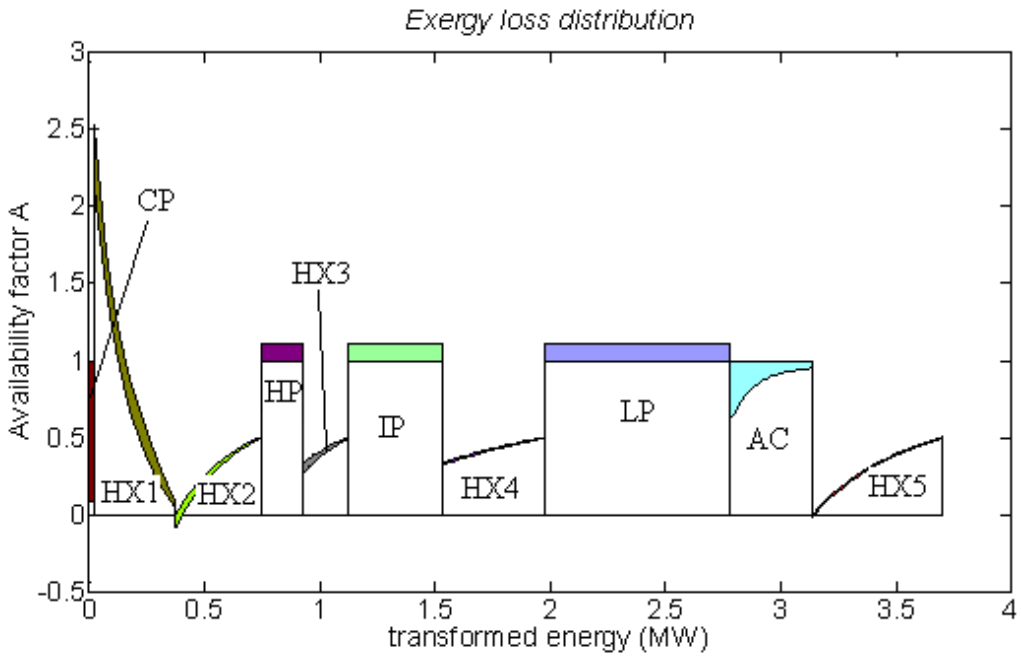

Figure 6.5 EUD representation of the optimised hybrid power system

6.4 Further Discussion on the Hybrid System

In this section, further discussion will be on (i) selection of thermal energy carrier, (ii) optimal thermal carrier temperature provided by solar heat, (iii) possible commercial position of the hybrid system.

Selection of thermal energy carrier The state parameters of the optimised hybrid system are listed in Table 6.5, which shows the highest working temperature is above 600K. This, according to Table 6.1, suggests Thermal-oil 66 could be used as heat carrier fluid and the mass flowrate data in Table 6.5 are produced according to the properties of this fluid. The data in Table 6.5 also shows that the mass flow rate of heat carrier is 3.6 times that of liquid nitrogen, which should be practically possible. In addition, under the conditions of the hybrid power system, the Thermal-oil 66 has an energy density of about 447kJ/kg, which is even higher than most high temperature phase change materials [200]. These make the Thermal oil-66 a competitive thermal energy storage medium for this type of applications (though it is recognised that low thermal conductivity is potentially an issue).

Table 6.5 State parameters of the optimal hybrid system

State Number	Mass flow rate (kg/s)	Pressure (bar)	Temperature (K)
1	1.0	1.0	77.4
2	1.0	150.0	84.0
3	1.0	150.0	275.7
4	1.0	150.0	593.9
5	1.0	39.0	406.8
6	1.0	39.0	593.9
7	2.8	13.0	441.1
8	2.8	13.0	593.9
9	1.0	1.0	298.2
10	1.8	1.0	298.2

11	1.8	1.0	94.0
12	1.8	39.0	294.4
13	1.8	39.0	593.9
14	3.6	-	603.9
15	2.1	-	451.1
16	1.5	-	304.4

Optimal thermal carrier temperature provided by solar heat The optimisation also indicates that the optimal temperature of the heat carrier heated by the solar collectors for the hybrid system is about 600K. This requirement is easily achievable as most of the concentrated solar power plants give a temperature up to 600~700K [203].

Potential commercial aspects of the hybrid power system The proposed hybrid system is best suited to locations with (i) cryogen such as LNG and (ii) sunshine. There are a number of places satisfy these criteria, including for example, large scale LNG importing ports in Japan and Southeast coast of China. However, the new system requires a high pressure gas turbine with 15MPa inlet pressure according to the optimisation analyses, which, to the knowledge of the author, is not available in commercial market. This is not necessarily a technological challenge in my view as this working pressure is lower than currently available steam turbines and the working temperature is much lower than that of combustion based gas turbines. Another key factor that affects commercial uptake of the hybrid system is the economic aspects. Although this is beyond the scope of this work, it is expected that capital and running costs for the hybrid power system should be significantly lower than that needed for the summation of a solar thermal power system and a cryogen fuelled power system. It is also noted that the hybrid system provides ~30% more power that the summation of the two systems. It is therefore reasonably optimistic about the commercial future of the proposed hybrid system.

6.5 Summary of This Chapter

A new solar-cryogen hybrid power system is proposed and is compared with a solar thermal power system and a cryogen fuelled power system. Thermodynamic analyses and optimisation are performed on these systems. The results show that the hybrid system provides over 30% more power than the summation of the power outputs of the other two systems. The results also suggest that the optimal hot end temperature of the heat carrier heated by the solar collectors be about 600K for the hybrid system.

Chapter 7 Program Developments on Thermal System Design

The methodology discussed in Chapter 3 is a general approach for the global design of thermal systems. It is applicable not only for the thermodynamic optimisation of CES technologies but also for other systems. A general programming package named TSOD (Thermal System Optimal Designer) is therefore developed for both thermodynamic and economic analyses. In this chapter the structure of the package is introduced and a specific example is given on the use of the program.

7.1 The Structure of the Program

7.1.1 Overview

TSOD (Thermal System Optimal Designer) is a systematic simulator of the thermal systems. It is developed based on Matlab and contains 17 Matlab files as shown in Figure 7.1(Each Matlab file may contain several functions, as seen from Appendix A). The key feature of TSOD is that it processes the configuration selection and parameter optimisation simultaneously in the unit of thermal cycle. In terms of functions,

- to evaluate both the thermodynamic and economic performances of existing thermal systems (evaluation mode).
- to optimally design new thermal systems based on the end-users' requirements (optimisation mode).

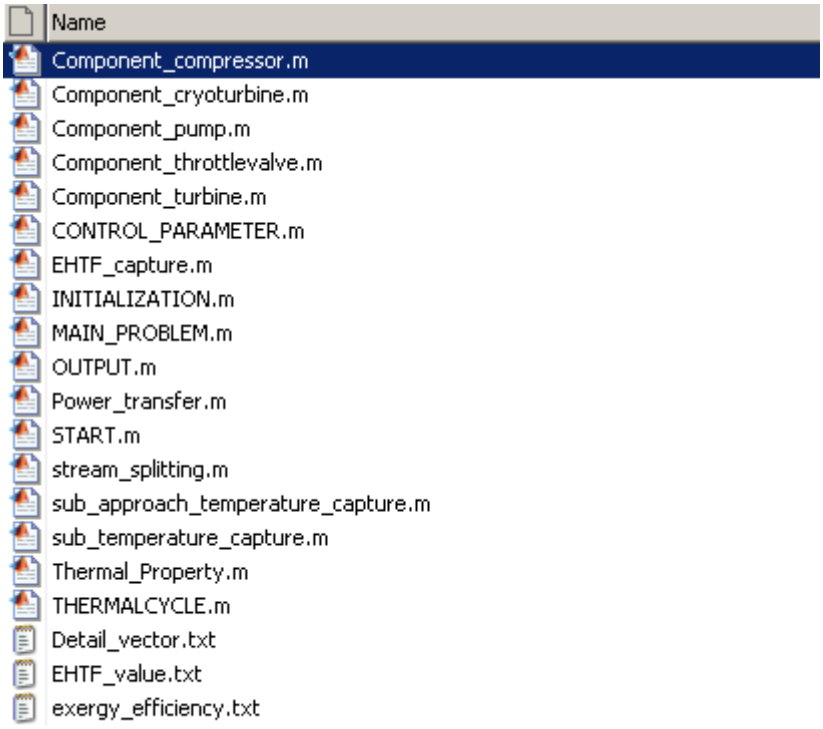

Figure 7.1 Matlab files of TSOD

Taking the optimisation mode as an example, the flow chart of TSOD is shown in Figure 7.2. TSOD begins with the two user-defined subroutines: *Main Problem* and *Control Parameter*. The *Main Problem* containing the *Objective Function* is transformed into the state parameters which are identifiable for *thermal cycle* by the subroutine *Initialization*. The state function calculations are done in *thermal cycle* and two groups of calculation results are obtained: performance data and heat flow. Performance data includes power consumption or generation, capital cost of components and product of thermal cycle. The heat flow contains the inlet and outlet information of the heat exchange processes. This information is then sent to *Pinch Analysis* for process simulation. The Pinch Temperature ΔT_{pi} is obtained and compared with Minimum Approach Temperature (MAT). If ΔT_{pi} is smaller than MAT, the input state parameter is invalid and new solution will be generated in *Initialization* to repeat the process. Otherwise the process data along with the performance data are used to calculate the objective value. The objective value is compared with the previous iterations to determine whether it is a better solution. Such processes repeat for a better objective target until meeting the stopping criteria and then output files are generated in *Output*.

The evaluation mode runs similarly but without determination section of stopping criteria. The information in two user-defined subroutines is sent to *thermal cycle* for *Initialization.* The performance data and heat flows results obtained from the *thermal cycle* and the *Initialization* are used to calculate both the Pinch Temperature ΔT_{pi} and the objective value. The calculation results are all given to the file *Output*. From above one can see the evaluation mode is a single-cycle operation.

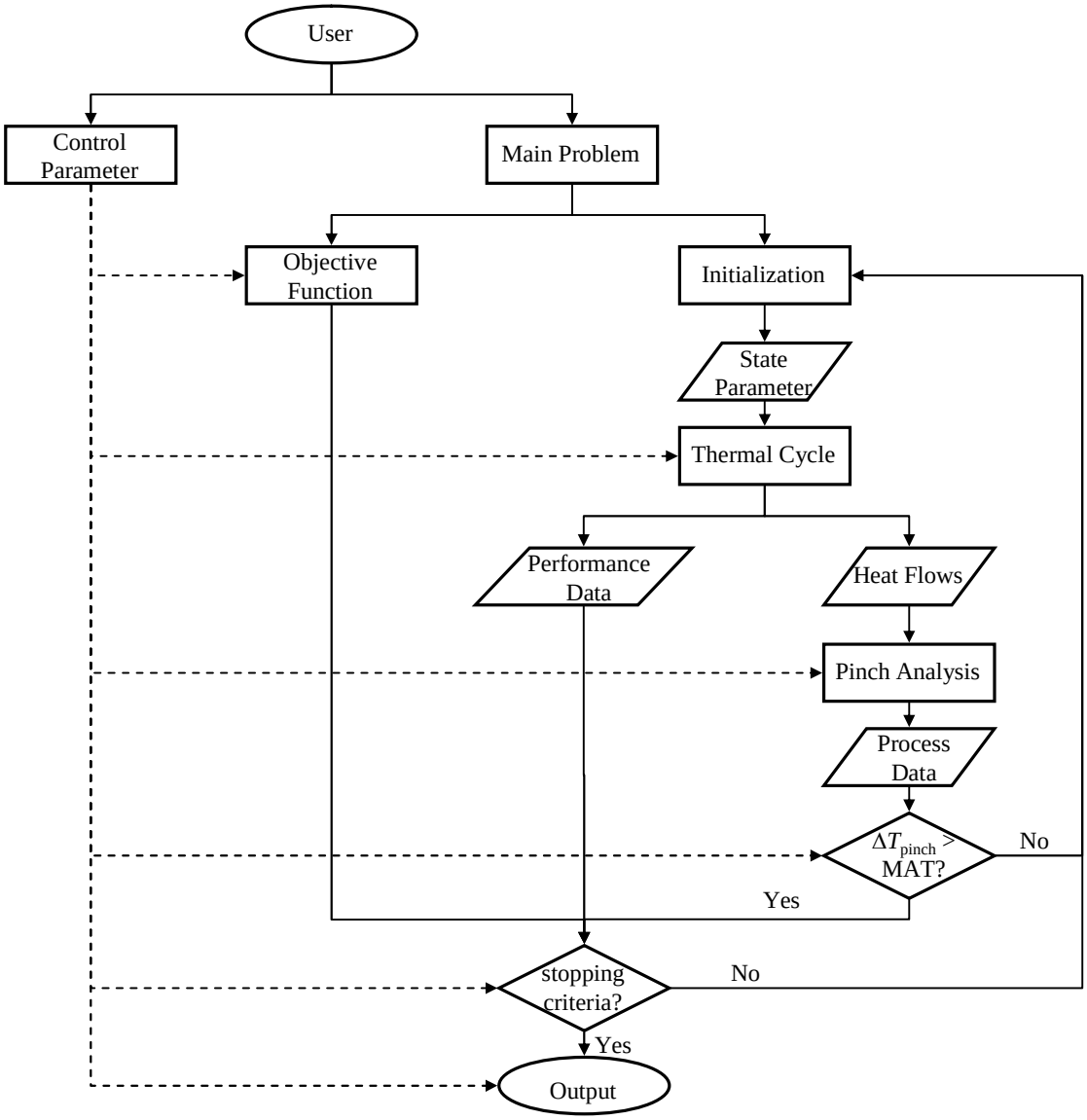

Figure 7.2 Main program flow-chart of TSOD

7.1.2 Subroutine Description

Figure 7.2 shows there are mainly five subroutines in TSOD: Main Problem, Control Parameter, Initialization, Thermal Cycle and Pinch Analysis (Objective Function is

defined by users in Main Problem). In this section the functions of these subroutines are explained in details to enable users to have a better understanding.

- *Main Problem*

Main Problem is the one of two user editing subroutines. It contains only a single file named *MAIN_PROBLEM.m*. In this file the user has to:

(1) Describe the thermodynamic model in the form of thermal cycle (If there is combustion process in the thermal cycle, the user has to either split the process into two thermal cycles like the example shown in Chapter 5 or take the combustion heat as a special heat flow).

(2) Define the optimisation variables. The optimisation variables of TSOD could be the state parameters (In *MAIN_PROBLEM.m* mass flowrate, pressure and temperature are used to define the state of the flow), configuration parameters or even the performance of the components. It should be noted that all these parameters could be given in this subroutine or *Control Parameter* either as constant or as variables. Otherwise the program will fail during the operation.

(3) Define the objective function. As will be discussed later the outputs of subroutines *Thermal Cycle* and *Pinch Analysis* include power consumption/generation, capital costs and final product (for example a liquid product or a heat flow). The objective function could be either of these variables or their combination. Therefore TSOD can be used not only for thermodynamic optimisation but also economic optimisation.

- *Control Parameter*

Control Parameter is another user editing subroutine of TSOD. It is a single file as well named *CONTROL_PARAMETER.m* and dominates the operation process by pre-defined global parameters. These parameters include environmental conditions, the performances of the components, the coefficients of the economic model, the precision of the calculations, boundary conditions, stopping criteria etc.

- *Initialization*

The function of *Initialization* is to transform the parameters in *Main Problem* into the form that is identifiable to *Thermal Cycle*. It is worth to mention that the state parameter in *Main Problem* is in the form of (m,P,T) which is familiar with the user. However (m,P,T) cannot be used to describe a two-phase flow. Therefore in the core

subroutines *Thermal Cycle* and *Pinch Analysis* the state parameters are in the form of (m,P,H).

- *Thermal Cycle*

Thermal cycle is one of the core subroutines of TSOD. It contains eight matlab files: *THERMALCYCLE.m, Stream_splitting.m, Power_transfer.m, Component_compressor.m, Component_turbine, Component_pump.m, Component_cryoturbine.m and Component_throttlevalve.m*. The input parameters of Thermal Cycle are the node variables of the cycle, including the inlet flow properties (m,P,H), the outlet pressure and the configuration parameter (if the stream is split). Based on these input information three functions are established in this subroutine:

(1) The configuration of the system is established by *Stream_splitting.m*.

(2) The power transfer component is identified by *Power_transfer.m*. The identification is based on the inlet density, pressure and outlet pressure. Note that the selection of throttle valve or cryoturbine is determined by setting in *Control Parameter*.

(3) Performance data and heat flow are calculated. The performance data include the net power of the thermal cycle, the final product and the capital cost of the power transfer components.

It should be noted that in Thermal Cycle only state parameters (inlet and outlet) are calculated. The temperature distribution in the heat exchange processes are considered in *Pinch Analysis*.

- *Pinch Analysis*

Pinch Analysis is made up of three matlab files: sub_*approach_temperature_capture.m*, *sub_temperature_capture.m* and *EHTF_capture.m*. The subroutine is used to check the heat balance and calculate the temperature distribution and the pinch temperature. The EHTF value of the heat exchange process is also calculated by the *EHTF_capture.m.*

Besides the subroutines explained above there are three additional functions:

- *START*

The function of this subroutine is to start TSOD. It contains the information of GA settings and operation mode.

- *OUTPUT*

This subroutine is used to generate the output files. The simulation results include the trend of the objective function and EHTF value, the optimal solutions and Composite curves (temperature distributions), the capital cost, the product, the heat flows and the state parameters. Of course the output file is optional and can be controlled by the settings in *Control_Parameter*.

- *Thermal_Property*

The thermal properties of the working fluids in TSOD are obtained from REFPROP. However sometimes REFPROP fails to converge while calculating the thermal property, especially in the region near the critical point, as shown in Figure 7.3. If this occurs in the operation process of TSOD the program will stop. Therefore in TSOD the thermal properties is not attained directly from REFPROP but from a subroutine named *Thermal_Property*. In such a function if the working condition is close to the critical point the specific value is obtained by the approximation of linear interpolation.

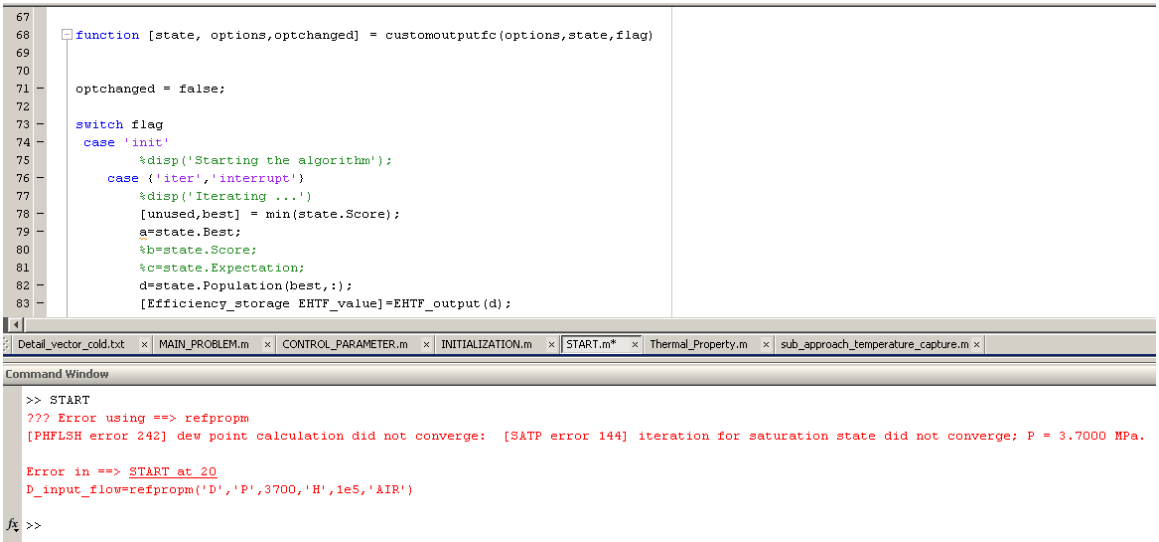

Figure 7.3 Error information of REFPROP

From the above, one can see that once the *Main_Problem* and *Control_Parameter* are set or edited the TSOD is ready to run. In the following section an operation example is given to show how to use the program.

7.2 A Case Study

7.2.1 Sample Problem Description

Liquid hydrogen is considered as a preferred option for bulk transport with the growing prospect of hydrogen as a significant component in the future energy portfolio [204]. Although it is an established technology the hydrogen liquefaction is an energy-intensive process and about 30 ~ 40% of the energy content is lost in the liquefaction process. As a result it is vital for the overall energy chain performance that more efficient liquefaction processes are developed.

In this section TSOD is used for the design of large scale hydrogen liquefaction system. The Collins cycles is selected as the thermodynamic model of the system. More specifically the system is made up of two thermal cycles: hydrogen based flow to produce liquid hydrogen and helium based expander cycle as the refrigerant cycle to supply the cold energy for the feed gas. Based on these assumptions, the simulation can be done in the TSOD environment.

7.2.2 User Setting Procedure

- Settings of the *Main_Problem*

(1) Open the file *Main_Problem.m*.

(2) Set the properties of the thermal cycles. As shown in Figure 7.4, the user has to edit the corresponding information according to the instruction messages. Based on the above assumptions, there are two thermal cycle in the hydrogen liquefaction system: Hydrogen flow and helium based refrigerant cycle. In this example we set the hydrogen flow to have three power transfer components without stream splitting (exclude the gas-liquid separation). The pressure levels (stages) of the helium cycle are set as four which agrees with the Collins cycle system proposed by Valenti and Macchi [64]. The mass flowrates of the two thermal cycles are also given. However the values of the closed-loop cycle may be renewed in the simulation process if the given values cannot achieve the heat balance (The program can distinguish if the thermal cycle is a closed-loop cycle by the inlet and outlet conditions).

```
% 1. Please set the Number of the thermal cycle in the form of
%'Number_THERMALCYCLE=2;'.
Number_THERMALCYCLE=2;

% 2. Please set the working fluid for each thermal cycle in the form of
% 'FLuid(i)='FLUID';'.
Fluid(1)='HYDROGEN';
Fluid(2)='HELIUM';

% 3. Please set if the thermal cycle produce liquid product in the form of
% 'If_product(i)=1;' for producing liquid and 'If_product(i)=0;'for no liquid product.

If_product(1)=1;
If_product(2)=0;

% 4. Please set if the stream split in the thermal cycle in the form of
% 'If_split(i)=1;' for yes and 'If_split(i)=0;'for no.

If_split(1)=0;
If_split(2)=1;

% 5. Please set the stages of each thermal cycle in the form of
% 'Number_stage(i)=2;'.
Number_stage(1)=3;
Number_stage(2)=4;

% 6. Please set the mass flow rate of each thermal cycle in the form of
% 'Mass_flow(i)=1;'.
Mass_flow(1)=1;
Mass_flow(2)=1;
```

Figure 7.4 The user settings of the thermal cycles

(3) Set the optimisation variables. The program deal with the problem in the unit of thermal cycle. All the state parameter should be stated either as constant or variables. As seen from Figure 7.5 in this example we set the inlet and outlet of the hydrogen flow to be the ambient conditions (the outlet temperature is a little bit lower than the ambient temperature as it is heated by the inlet flow). And the inlet pressure of the helium flow equals to the ambient pressure. The remaining parameters including pressures, temperatures and the coefficients (the fraction) of stream splitting are set as the optimisation variables.

```
% 7. %Please edit the state pressure and temperautreof each thermal cycle
% in the below forms
%%%%%%%%%%%%%%%%%%%%%%%%%%%%%%%%%%%%%%%%%%%%%%%%%%%%%%%%%%%%%%%%%%%%%%%%%%%
%%%             for i=1:Number_THERMALCYCLE                              %%%
%%%                 Number_code{i}=1+2^(Number_stage{i}-1);              %%%
%%%                 for j=1:Number_code{i}                               %%%
%%%                     P{j}=[];                                         %%%
%%%                     T{j}=[];                                         %%%
%%%                 end                                                  %%%
%%%                 Pressure{i}=P;                                       %%%
%%%                 Temperature{i}=T;                                    %%%
%%%             end                                                      %%%
%%%%%%%%%%%%%%%%%%%%%%%%%%%%%%%%%%%%%%%%%%%%%%%%%%%%%%%%%%%%%%%%%%%%%%%%%%%
            k=1;
            for i=1:Number_THERMALCYCLE
                Number_code=1+2^(Number_stage{i}-1);
                for j=1:Number_code
                    if j==1
                        if i==1
                            P{j}=P_ambient;
                            T{j}=T_ambient;
                        elseif i==2
                            P{j}=P_ambient;
                            T{j}=x(1);
                        end
                    elseif j==Number_code
                        if i==1
                            P{j}=P_ambient;
                            T{j}=T_ambient-Approach_temperature;
                        elseif i==2
                            P{j}=P_ambient;
                            T{j}=x(1);
                        end
                    else
                        k=k+1;
                        P{j}=x(k);
                        k=k+1;
                        T{j}=x(k);
                    end
                end
                Pressure{i}=P;
                Temperature{i}=T;
            end
```

```
% 8. %Please edit the state pressure and temperautreof each thermal cycle
% in the below forms
%%%%%%%%%%%%%%%%%%%%%%%%%%%%%%%%%%%%%%%%%%%%%%%%%%%%%%%%%%%%%%%%%%%%%%%%%%%
%%%             for i=1:Number_THERMALCYCLE                              %%%
%%%                 Number_code{i}=2^(Number_stage{i}-1)-1;              %%%
%%%                 for j=1:Number_code{i}                               %%%
%%%                     T_split{j}=[];                                   %%%
%%%                     Q{j}=[];                                         %%%
%%%                 end                                                  %%%
%%%                 Temperature_splitting{i}=T;                          %%%
%%%                 Coefficient_splitting{i}=Q;                          %%%
%%%             end                                                      %%%
%%%%%%%%%%%%%%%%%%%%%%%%%%%%%%%%%%%%%%%%%%%%%%%%%%%%%%%%%%%%%%%%%%%%%%%%%%%
            for i=1:Number_THERMALCYCLE
                Number_code=2^(Number_stage{i}-1)-1;
                if If_split{i}==1
                    for j=1:Number_code
                        k=k+1;
                        T_split{j}=x(k);
                        k=k+1;
                        Q{j}=x(k);
                    end
                    Temperature_splitting{i}=T_split;
                    Coefficient_splitting{i}=Q;
                end
            end
```

Figure 7.5 The user settings of optimisation variables

(4) Set the objective function. This example aims to thermodynamically design a high efficiency hydrogen liquefaction system. The exergy efficiency defined as the ratio of product exergy and consumed power is set as the objective function, as shown in Figure 7.6. As the optimisation algorithm GA is written as a minimization tool, in this example the maximization problem has to be converted to the minimization problem by setting the exergy efficiency as a negative number (the net power *W_net* is a negative number as hydrogen liquefaction is a power consumption process).

```
% 9. %Please edit the objective function
% in the below forms 'Objective=[];'.

Exergy_Product=0;
for i=1:a
    Liquid_product=Product{i};
    if ~isempty(Liquid_product)
        Exergy_Product=Exergy_Product+Exergy_liquid(Liquid_product);
    end
end

if approach_temperature<MAT
    Objective=Exergy_Product/W_net;
end
```

Figure 7.6 The user settings of the objective function

- Settings of the *Control_Parameter*

(5) Open the file *Control_Parameter.m.*

(6) Set the component performance as shown in Figure 7.7.

```
%%%%%%%%%%%%%%%%%%%%%%%%%%%%%%%%%%%%%%%%%%%%%%%%%%%%%%%%%%%%%%%%%%%%%%%%%%%%
%%%%%%%%%%%%%%%%%%%%  Component performance %%%%%%%%%%%%%%%%%%%%%%%%%%%%%%%%
%%%%%%%%%%%%%%%%%%%%%%%%%%%%%%%%%%%%%%%%%%%%%%%%%%%%%%%%%%%%%%%%%%%%%%%%%%%%
global pump_efficiency
global turbine_isentropic_efficiency
global compressor_isothermal_efficiency
global liquid_turbine_efficiency
global MAT

turbine_isentropic_efficiency=0.88;
compressor_isothermal_efficiency=0.87;
liquid_turbine_efficiency=0.7;
pump_efficiency=0.77;
MAT=3;
```

Figure 7.7 The user settings of the component performance

(7) Set the boundary conditions as shown in Figure 7.8. It should be noted that the setting of the boundary conditions should agree with the corresponding settings of the optimisation variables.

(8) Set the initial variables. In this example the initial solution is given in Figure 7.9. It represents the simplest four pressure level hydrogen liquefaction system without stream splitting. The settings of the initial variables are optional. If the user does not supply the initial conditions the program can generate a first solution based on the given boundary conditions. However the practical application indicates valid initial conditions could significantly reduce the calculating time. Moreover, changing the initial settings and running the program for several times are also the validation criteria of a global optimisation.

(9) Set the output options. This example aims at a thermodynamic optimisation of the hydrogen liquefaction system. Therefore only the thermodynamic properties including the exergy efficiency, the EHTF, the composite curve and the heat flows are set as the output options as shown in Figure 7.10.

(10)Other settings. The remaining settings include the control parameters of GA, the selection of the liquid expansion component (default setting is cryoturbine), the precision of the calculation etc. In this example all these settings keep their default values.

```
%Please edit the boundary conditions in the below forms
%%%%%%%%%%%%%%%%%%%%%%%%%%%%%%%%%%%%%%%%%%%%%%%%%%%%%%%%%%%%%%%%%%%%%%%%%%%%
%%%                          Lower_Boundary(i)=a;                          %%%
%%%                          Upper_Boundary(i)=b;                          %%%
%%%%%%%%%%%%%%%%%%%%%%%%%%%%%%%%%%%%%%%%%%%%%%%%%%%%%%%%%%%%%%%%%%%%%%%%%%%%
            k=1;
            for i=1:Number_THERMALCYCLE
                Number_code=1+2^(Number_stage(i)-1);
                for j=1:Number_code
                    if j==1
                        if i==1
                        elseif i==2
                            Lower_Boundary(1)=50;
                            Upper_Boundary(1)=280;
                        end
                    else
                        k=k+1;
                        Lower_Boundary(k)=P_ambient;
                        Upper_Boundary(k)=40*P_ambient;
                        Lower_Boundary(k)=30;
                        Upper_Boundary(k)=T_ambient;
                    end
                end
            end

            for i=1:Number_THERMALCYCLE
                Number_code=2^(Number_stage(i)-1)-1;
                if If_split(i)==1
                    for j=1:Number_code
                        k=k+1;
                        Lower_Boundary(k)=30;
                        Upper_Boundary(k)=T_ambient;
                        k=k+1;
                        Lower_Boundary(k)=0.1;
                        Upper_Boundary(k)=1.7;
                    end
                end
            end
```

Figure 7.8 The user settings of boundary conditions

```
% Please set the initial variables in the form of 'Initial=[];'
Initial=[250          10*P_ambient        273        30*P_ambient     40      35*P_ambient     40 ...
                      30*P_ambient        100        10*P_ambient     50       4*P_ambient     50 ...
                    1.5*P_ambient          50         1*P_ambient     24      30*P_ambient    373 ...
                      30*P_ambient        273                250      1               114      1 ...
                               114          1                114      1               114      1 ...
                               273          1                273      1];
```

Figure 7.9 The user settings of the initial variables

```
%%%%%%%%%%%%%%%%%%%%%%%%%%%%%%%%%%%%%%%%%%%%%%%%%%%%%%%%%%%%%%%%%%%%%%%%%%%%
%%%%%%%%%%%%%%%%%%%%%%%%    Output setting    %%%%%%%%%%%%%%%%%%%%%%%%%%%%%
%%%%%%%%%%%%%%%%%%%%%%%%%%%%%%%%%%%%%%%%%%%%%%%%%%%%%%%%%%%%%%%%%%%%%%%%%%%%
global Output_Objective_trend
global Output_Objective_data
global Output_EHTF_trend
global Output_EHTF_data
global Output_Optimal_vector
global Output_Composite_curves
global Output_Captial_cost
global Output_Liquid_product
global Output_Heat_flow
global Output_State_parameter

Output_Objective_trend=1;
Output_Objective_data=0;
Output_EHTF_trend=1;
Output_EHTF_data=0;
Output_Optimal_vector=0;
Output_Composite_curves=1;
Output_Captial_cost=0;
Output_Liquid_product=0;
Output_Heat_flow=1;
Output_State_parameter=0;
```

Figure 7.10 The user settings of output control

7.2.3 Simulation Results

Once the settings of *Main_Problem.m* and *Control_Parameter.m* are completed the program is ready to run. As the first step of the operation it is essential to examine if the given initial conditions are the valid ones. Open the *Control_Parameter.m* file and set the parameter *optimisation_mode = 0* (Corresponds to the evaluation mode) and then run *START* in Command Window, the output is shown in Figure 7.11. The result shows the initial settings give valid solutions although the corresponding efficiency is very low. The poor performance of the initial solution is caused by the inefficient heat exchange process. As illustrated in Figure 7.12 the average temperature difference of the heat transfer is about 50K. This leads to a great exergy loss as the heat transfer occurs at a very low temperature region. A systematic optimisation on the other hand is able to decrease the exergy loss and therefore enhance the overall performance of the system.

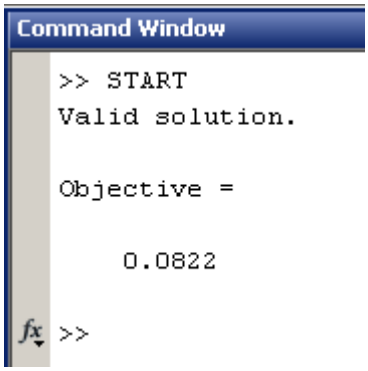

Figure 7.11The output of initial solution examination

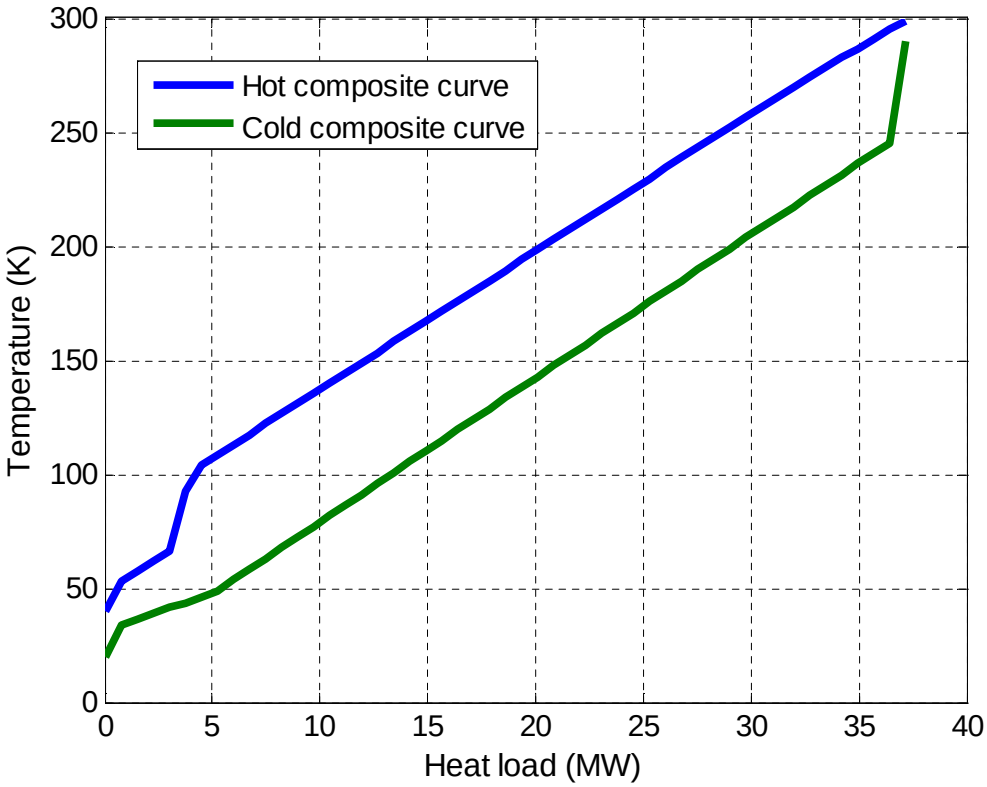

Figure 7.12 The composite curves of the initial solution

Changing the parameter setting *optimisation_mode = 1* in the *Control_Parameter.m* file and then rerunning *START* in Command Window, the program will operate in the optimisation model. After running on a personal computer (Processor: 2.40 GHz; RAM: 1.96 GB) for about 90 hours the program stop and below results are attained.

Figure 7.13 shows the trends of exergy efficiency and EHTF value in the optimisation process. It is found the exergy efficiency increases from 8% to about 55% which is much higher than the Collins cycle system proposed by Valenti and Macchi (with the

exergy efficiency of about 48%). One important reason for the much improved exergy efficiency is that a more efficient heat exchanger network is established by the optimisation process. The evolution of EHTF is shown in Figure 7.13. One can see that the value is increased from about 0.09 to 0.45. This indicates that the exergy loss in the heat exchange process is decreased to a fifth of the initial solution. The composite curves of the optimised system are drawn in Figure 7.14. Compared with the initial composite curves shown in Figure 7.12, the temperature difference is greatly decreased especially at temperatures lower than 200K.

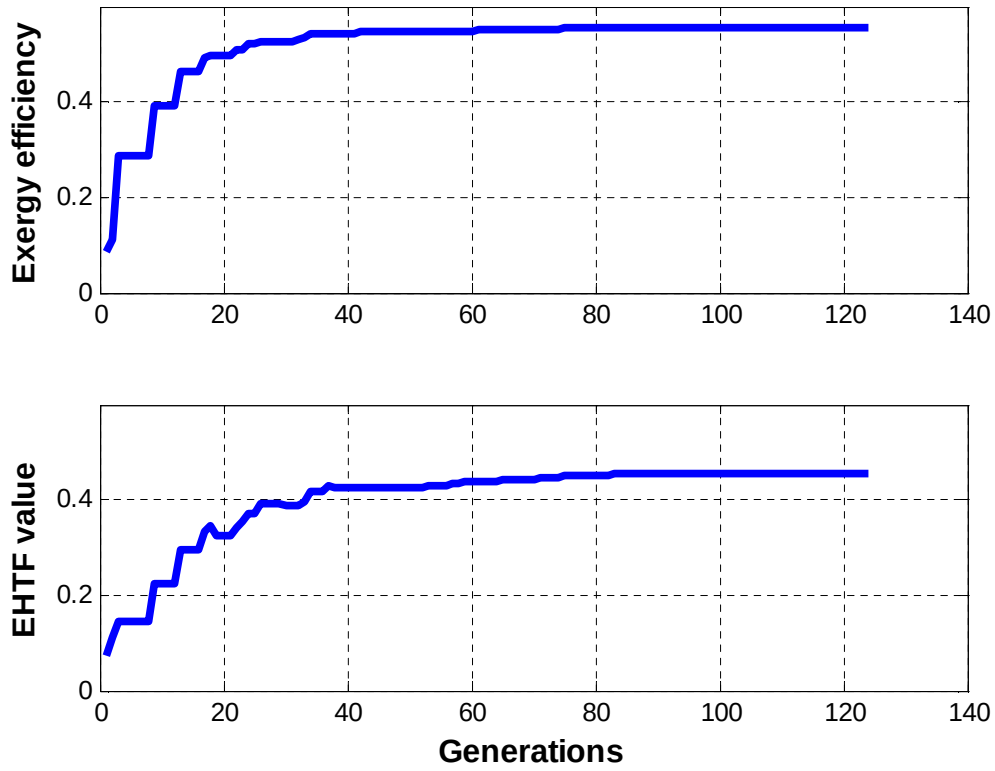

Figure 7.13 The trends of exergy efficiency and EHTF value in the optimisation process

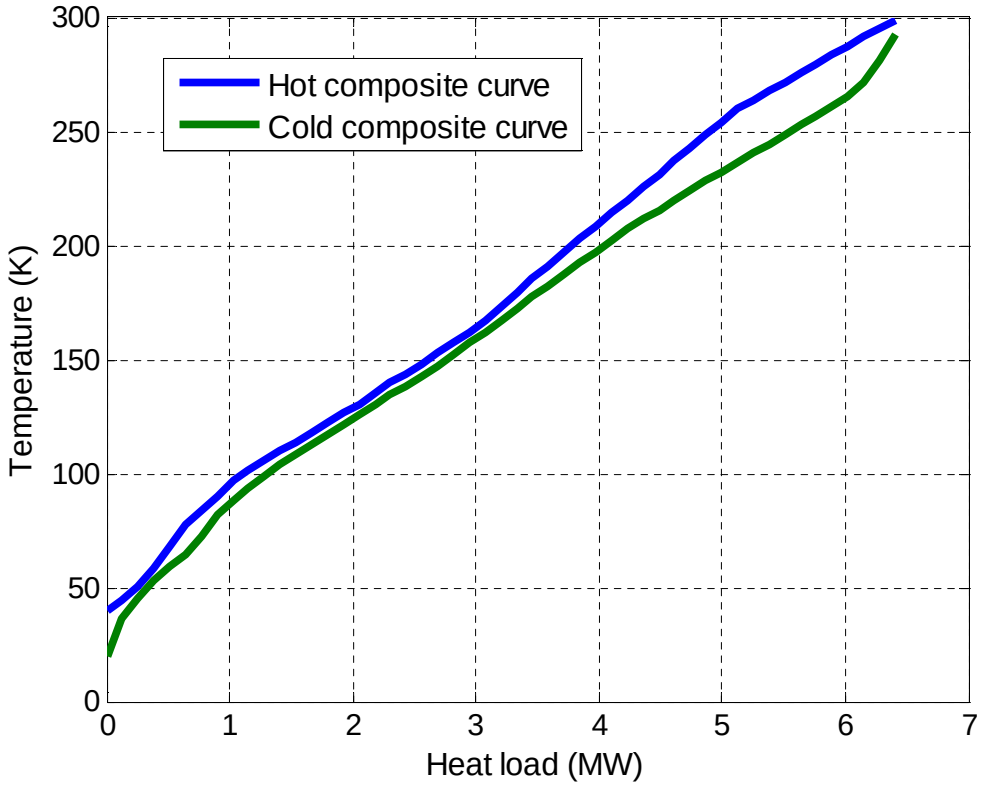

Figure 7.14 The composite curves of the optimised solution

Having reviewed the liquefaction process, the attention is now paid to the specific configuration of the system. The information of the heat flows is listed in the form of txt file as shown in Figure 7.15. This gives a detailed data sheet for the optimised system including the state parameters. Based on the information the flowchart of the system can be drawn as shown in Figure 7.16. The heat exchanger network of the system is complicated and made up of six hot streams and seven cold streams. As one hot stream may exchange heat with more than one cold stream, the splitting of streams into parallel branches or multi-stream heat exchanger may be therefore required. This will increase the capital cost which should be considered in practical applications.

No.	Mass flow (kg/s)	Pressure (kPa)	Inlet Temp (K)	Outlet Temp (K)	Fluid
1	1.000000E+000	1.945389E+003	2.991500E+002	1.375774E+002	HYDROGEN
2	1.000000E+000	3.064605E+003	1.630944E+002	3.999999E+001	HYDROGEN
3	5.460652E-001	1.013250E+002	2.136890E+001	2.921500E+002	HYDROGEN
4	1.615735E+000	3.001079E+003	2.991500E+002	1.607309E+002	Helium
5	1.908738E+000	3.001079E+003	2.991500E+002	2.595082E+002	Helium
6	1.615735E+000	2.309782E+003	1.467524E+002	7.799106E+001	Helium
7	1.908738E+000	4.001835E+002	1.334199E+002	9.869523E+001	Helium
8	1.615735E+000	7.670186E+002	5.364027E+001	6.875001E+001	Helium
9	9.946499E-001	2.682687E+002	8.587017E+001	2.944831E+002	Helium
10	9.140882E-001	2.682687E+002	8.587017E+001	1.497449E+002	Helium
11	1.615735E+000	1.013250E+002	3.520683E+001	2.699302E+002	Helium
12	9.946499E-001	1.013250E+002	2.109076E+002	2.699302E+002	Helium
13	9.140882E-001	1.013250E+002	1.072560E+002	2.699302E+002	Helium

Figure 7.15 The optimised heat flows

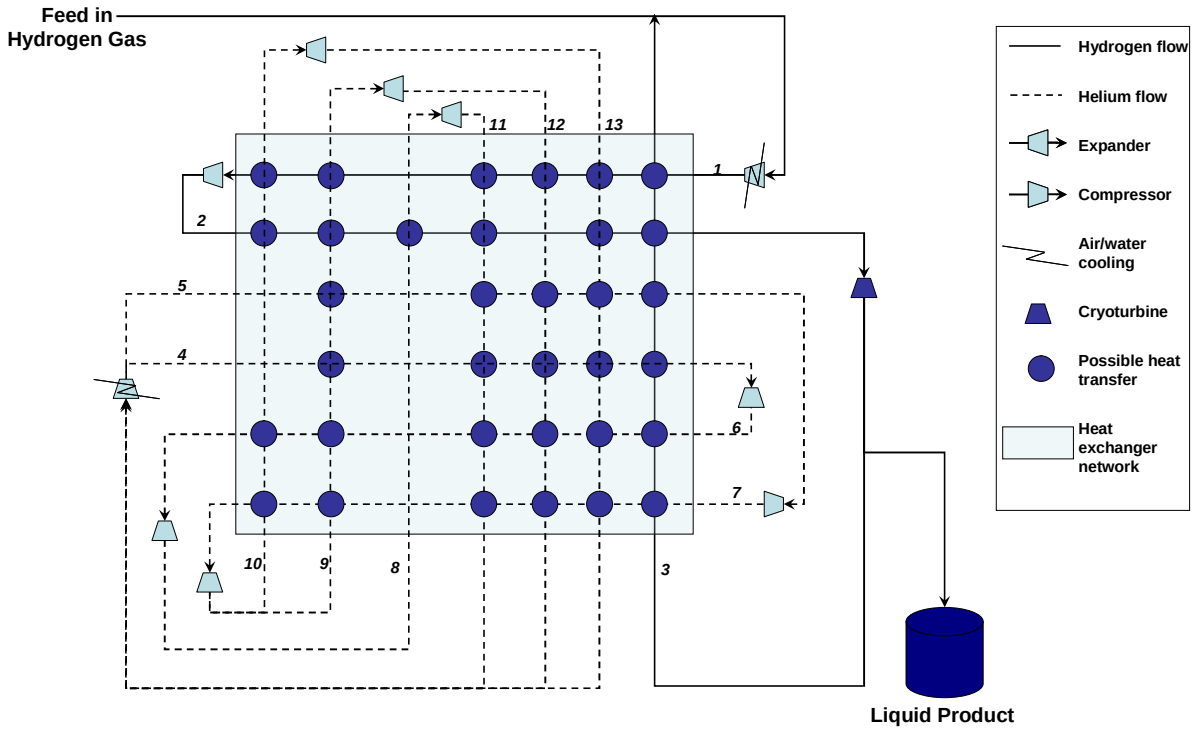

Figure 7.16 The configuration of the optimised hydrogen liquefaction system

7.3 Summary of This Chapter

This chapter introduces the program developed for the systematic design of thermal systems. Such a program processes the configuration selection and parameter optimisation simultaneously in the unit of thermal cycle. It can be used to evaluate or optimise both the thermodynamic and economic performances of thermal systems. Thermodynamic design of a hydrogen liquefaction system is used as an example to illustrate how the program works. The simulation results indicate the exergy

efficiency of the optimal system could be as high as 55% which is much higher than the results repeated in the literature. The output also shows that the program is able to give detailed information for the configuration description.

Chapter 8 Conclusions and Suggestions for Further Research

This chapter gives a summary of main conclusions obtained in this work. Recommendations for the future are also given based on this work.

8.1 Summary of Main Conclusions

This work focuses on three aspects associated with the Cryogen based Energy Storage technology: i) to gain a fundamental understanding of the use of cryogen as an energy carrier, ii) to develop technical routes and strategies for the use of Cryogen based Energy Storage for load levelling, peak-shaving and renewable energy utilisation, and iii) to develop methodologies for systematic optimisation of the proposed technical routes. The following are the main conclusions:

(A) Cryogens have a relatively high energy density in comparison with other thermal energy storage media. They can be efficient working media for recovering low grade heat due to their low critical temperature. The overall efficiency of the use of cryogen for energy storage can be greatly increased if low grade heat is used in the process of cryogenic energy extraction. On the other hand the main constraint for the practical use of cryogen as energy carrier is the low efficiency in the cryogen production process (gas liquefaction).

(B) The integration of air liquefaction and energy releasing process for load levelling gives a remarkable improvement of the round trip efficiency. If the expander cycle is used to supply cold energy and the waste heat with a temperature higher than 600K is available, the round trip efficiency attains to 80 - 90% under rather reasonable conditions. The system efficiency can be further enhanced if cryoturbine is used to replace throttle valve in the air liquefaction process. From the economic aspect, the key parameters to reduce the capital cost of such a system are the waste heat temperature and the operation period of the energy release unit. If the waste heat with a temperature higher than 600K is available and the operation period of the energy releasing unit is longer than 4 hours a day, such a CES system is very competitive with the current energy storage technologies.

(C) If CES is integrated with Natural Gas Combined Cycle (NGCC) for peak-shaving, a oxy-fuel combustion is formed and CO_2 in the flue gas can be captured in the form of dry ice. The optimisation of such a peak-shaving system gives an exergy efficiency of 70% and electricity storage efficiency of 67% while using helium or oxygen as the blending gas. On contrast the use of CO_2 as the blending gas only gives an exergy efficiency of 60% and an electricity storage efficiency of 50%. This is due to the limitation of the lowest working temperature of CO_2 for avoiding solidification.

Capital costs are the dominant factor for the peak systems and the ASU takes a large share. Both the capital and peak electricity costs of the peak-shaving systems are comparable with the NGCC which are much lower than the oxy-NGCC if the operation period is relatively short. And the use of helium as the blending gas gives the lowest costs due to the lowest combustion pressure and mass flowrate. And costs of the peak-shaving systems could be further reduced by decreasing the cost of the air liquefaction unit, operating the air liquefaction unit at variable loads and making use of the excess oxygen in the air liquefaction process.

(D) Solar thermal energy can be used in cryogenic energy extraction process to form a solar-cryogen hybrid power system. Comparison of such a hybrid system with a solar thermal power system and a cryogen fuelled power system show that the hybrid system provides over 30% more power than the summation of the power outputs of the other two systems. This is because in the hybrid system the exergy loss in the heat transfer processes is very low. The optimal hot end temperature of the heat carrier heated by the solar collectors is about 600K for the hybrid system.

(E) A systematic optimisation strategy is established by extending the concept of ‘superstructure’ and combining with Pinch Technology and Genetic Algorithm. In this strategy not only the heat exchanger network but also the selection of power transfer components and the interactions between power transfer component and heat flow are considered in the optimisation process. As a result the new technique processes the configuration selection and parametric optimisation simultaneously at a systematic level. Based on this strategy a program named Thermal System Optimal Designer (TSOD) is developed to evaluate or optimise both the thermodynamic and economic performances of thermal systems. Design of a hydrogen liquefaction

system is used as an operation example and the simulation results indicate the exergy efficiency of the optimal system could attain as high as 55% which is much higher than the value proposed in the literature.

8.2 Suggestions for the Future Work

Although interesting and promising results have been obtained in this study, practical applications of CES technology requires a number of challenges to be addressed. They are summarised in the following.

(A) The work reported in this dissertation is restricted to steady state operation of the energy storage systems. However the cost of electric energy can vary drastically with time during a day as industrial and domestic demands change with ambient temperature and the activities. The availability of renewable energy is also intermittent and unpredictable. Therefore a possible approach to improve the performance of the energy storage system is dynamic operation. For example, the energy release unit can be shut down while keeping the air liquefaction unit running at a high throughput when power is cheap or renewable electricity is available; and the air liquefaction unit can be shut down while the energy release unit is running at a high throughput at peak hours.

(B) Only sensitivity analyses are carried out on the economic aspects of the systems. Theoretically optimisation can be done on the economic aspects based on the economic models discussed in this research. However in practice the costs can vary significantly at different locations and the cost relativities can also change in the future. As a result the standardised economic models may be inaccurate or even misleading under some conditions. For a specific application the uncertainties can be reduced and some of the economic data may be obtained from the industrial companies. In this case, better economic benefits may be obtained through economic optimisation.

(C) The work reported in this thesis focuses on numerical simulation of the CES technology. Although most of the components and technologies used in this study are developed and commonly used in other thermal systems, experimental study is also needed. This is particularly important for some components such as high pressure turbines (using air or mixture of helium, steam and CO_2 as the working fluid)

and cryoturbine, which are not commercially available and may need new design and more research and development. Experimental study should also be done on high pressure heat exchangers in which the working fluids may in be supercritical state. A large scale demonstration is also needed to investigate the system integration.

(D) This work also leads to the development of a program named TSOD for the design of thermal systems. Such a program is based on the Matlab environment. Users must have code skill for running it. Graphical interface should be developed to give a friendly end-user operation platform. The software is recommended to be programmed in C++ environment so that it can operate independently. As the program uses the thermal properties of the working fluid from REFPROP, authorisation should be obtained from NIST before the program is to be used by third parties.

Appendix A Program Code for TSDO

A1. Code for compressor

```
function [W work_unit_output_flow]=Component_compressor(input_flow,output_pressure)

global T_ambient
global compressor_isentropic_efficiency
global compressor_isothermal_efficiency
%%% The elements of the input flow contains: (1)mass flow rate (2)pressure (KPa) (3)enthalpy
(4)fluid name
M_in=input_flow{1};
P_in=input_flow{2};
H_in=input_flow{3};
fluid=input_flow{4};
P_out=output_pressure;
T_max=T_ambient;

S_in=Thermal_Property('S','P',P_in,'H',H_in,fluid);
S_in=Thermal_Property('S','P',P_in,'H',H_in,fluid);

T_in=Thermal_Property('T','P',P_in,'H',H_in,fluid);
T_in=Thermal_Property('T','P',P_in,'H',H_in,fluid);

if T_in>T_max
    [T_tem H_tem]=PStoTH(P_out,S_in,fluid);
    W_unit=-(H_in-H_tem)*compressor_isentropic_efficiency;
    Hout=H_tem;
    W=M_in*W_unit;

    work_unit_output_flow{1}=input_flow{1};
    work_unit_output_flow{2}=output_pressure;
    work_unit_output_flow{3}=Hout;
    work_unit_output_flow{4}=input_flow{4};
else
    [T_tem H_tem]=PStoTH(P_out,S_in,fluid);

    H_tem_out=H_in+(H_tem-H_in)/compressor_isentropic_efficiency;

    [T_tem_out S_tem_out]=PHtoTS(P_out,H_tem_out,fluid);

    if T_tem_out<T_max
        H_out=H_tem_out;
        W_unit=(H_tem_out-H_in);
        W=M_in*W_unit;

        work_unit_output_flow{1}=input_flow{1};
        work_unit_output_flow{2}=output_pressure;
        work_unit_output_flow{3}=H_out;
        work_unit_output_flow{4}=input_flow{4};
    else
        T_out=T_max;

        P_min = P_in;
        P_max = P_out;

        while P_max-P_min > 1
            x = (P_max+P_min)/2;

            [Tout_temp_temp Hout_temp_temp]=PStoTH(x,S_in,fluid);
            W_consuming_adiabatic_unit_temp=-(H_in-
Hout_temp_temp)/compressor_isentropic_efficiency;
            Hout=H_in+W_consuming_adiabatic_unit_temp;

            [Tout Sout]=PHtoTS(x,Hout,fluid);

            if Tout<T_max
                P_min = x;
            else
                P_max = x;
```

```
            end

        end

            P_adiabatic=P_min;
            [Tout_temp Hout_temp]=PStoTH(P_adiabatic,S_in,fluid);
            W_consuming_adiabatic_unit=-(H_in-Hout_temp)/compressor_isentropic_efficiency;

            P_compressor_inlet=P_adiabatic;
            T_compressor_inlet=T_max;
            P_compressor_outlet=P_out;
            T_compressor_outlet=T_max;

H_compressor_inlet=Thermal_Property('H','T',T_compressor_inlet,'P',P_compressor_inlet,fluid);

H_compressor_inlet=Thermal_Property('H','T',T_compressor_inlet,'P',P_compressor_inlet,fluid);

S_compressor_inlet=Thermal_Property('S','T',T_compressor_inlet,'P',P_compressor_inlet,fluid);

S_compressor_inlet=Thermal_Property('S','T',T_compressor_inlet,'P',P_compressor_inlet,fluid);

H_compressor_outlet=Thermal_Property('H','T',T_compressor_outlet,'P',P_compressor_outlet,fluid
);

H_compressor_outlet=Thermal_Property('H','T',T_compressor_outlet,'P',P_compressor_outlet,fluid
);

S_compressor_outlet=Thermal_Property('S','T',T_compressor_outlet,'P',P_compressor_outlet,fluid
);

S_compressor_outlet=Thermal_Property('S','T',T_compressor_outlet,'P',P_compressor_outlet,fluid
);
            W_compressor_isothermal_unit=((H_compressor_outlet-H_compressor_inlet)-
T_max*(S_compressor_outlet-S_compressor_inlet))/compressor_isothermal_efficiency;

            W_unit=(W_consuming_adiabatic_unit+W_compressor_isothermal_unit);
            W=M_in*W_unit;

            work_unit_output_flow{1}=input_flow{1};
            work_unit_output_flow{2}=output_pressure;
            work_unit_output_flow{3}=H_compressor_outlet;
            work_unit_output_flow{4}=input_flow{4};
    end
end

W=-W;

function [T_in H_in]=PStoTH(P_in,S_in,fluid)

length_fluid=length(fluid);
IFFLUID=0;
if length_fluid==5
    if fluid=='WATER'
        T_limit=1250;
        IFFLUID=1;
    else
        T_limit=100000;
    end
elseif length_fluid==6
    if fluid=='HELIUM'
        T_limit=1450;
        IFFLUID=1;
    elseif fluid=='OXYGEN'
        T_limit=950;
        IFFLUID=1;
    else
        T_limit=10000;
    end
elseif length_fluid==3
    if fluid=='CO2'
        T_limit=1050;
        IFFLUID=1;
    else
        T_limit=100000;
```

```
    end
elseif length_fluid==7
    if fluid=='METHANE'
        T_limit=600;
        IFFLUID=1;
    else
        T_limit=100000;
    end
else
    T_limit=100000;
end

if IFFLUID
    S_limit=Thermal_Property('S','T',T_limit,'P',P_in,fluid);
    S_limit=Thermal_Property('S','T',T_limit,'P',P_in,fluid);
else
    S_limit=100000;
end
%%%%%%%%%%%%%%%%%%%%%%%%%%%%%%%%%%%%%%%%%%%%%%%%%%%%%%%%%%%%%%%%%%%%%%%%%%%%%%%

if S_in<S_limit
    T_in=Thermal_Property('T','P',P_in,'S',S_in,fluid);
    T_in=Thermal_Property('T','P',P_in,'S',S_in,fluid);

    H_in=Thermal_Property('H','P',P_in,'S',S_in,fluid);
    H_in=Thermal_Property('H','P',P_in,'S',S_in,fluid);
else
    Cp=Thermal_Property('C','T',T_limit,'P',P_in,fluid);
    Cp=Thermal_Property('C','T',T_limit,'P',P_in,fluid);

    H_limit=Thermal_Property('H','T',T_limit,'P',P_in,fluid);
    H_limit=Thermal_Property('H','T',T_limit,'P',P_in,fluid);

    T_in=T_limit*exp((S_in-S_limit)/Cp);
    H_in=H_limit+Cp*(T_in-T_limit);
end

%%%%%%%%%%%%%%%%%%%%%%%%%%%%%%%%%%%%%%%%%%%%%%%%%%%%%%%%%%%%%%%%%%%%%%%%%%%%%%%
function [T_in S_in]=PHtoTS(P_in,H_in,fluid)

length_fluid=length(fluid);
IFFLUID=0;
if length_fluid==5
    if fluid=='WATER'
        T_limit=1250;
        IFFLUID=1;
    else
        T_limit=100000;
    end
elseif length_fluid==6
    if fluid=='HELIUM'
        T_limit=1450;
        IFFLUID=1;
    elseif fluid=='OXYGEN'
        T_limit=950;
        IFFLUID=1;
    else
        T_limit=10000;
    end
elseif length_fluid==3
    if fluid=='CO2'
        T_limit=1050;
        IFFLUID=1;
    else
        T_limit=100000;
    end
elseif length_fluid==7
    if fluid=='METHANE'
        T_limit=600;
        IFFLUID=1;
    else
        T_limit=100000;
    end
else
```

```
    T_limit=100000;
end

if IFFLUID
    H_limit=Thermal_Property('H','T',T_limit,'P',P_in,fluid);
    H_limit=Thermal_Property('H','T',T_limit,'P',P_in,fluid);
else
    H_limit=1e15;
end
%%%%%%%%%%%%%%%%%%%%%%%%%%%%%%%%%%%%%%%%%%%%%%%%%%%%%%%%%%%%%%%%%%%%%%%%%%%%%%%

if H_in<H_limit
    T_in=Thermal_Property('T','P',P_in,'H',H_in,fluid);
    T_in=Thermal_Property('T','P',P_in,'H',H_in,fluid);

    S_in=Thermal_Property('S','P',P_in,'H',H_in,fluid);
    S_in=Thermal_Property('S','P',P_in,'H',H_in,fluid);
else
    Cp=Thermal_Property('C','T',T_limit,'P',P_in,fluid);
    Cp=Thermal_Property('C','T',T_limit,'P',P_in,fluid);

    S_limit=Thermal_Property('S','T',T_limit,'P',P_in,fluid);
    S_limit=Thermal_Property('S','T',T_limit,'P',P_in,fluid);

    T_in=T_limit+(H_in-H_limit)/Cp;
    S_in=S_limit+Cp*log(T_in/T_limit);
end
```

A2. Code for cryoturbine

```
function [W work_unit_output_flow_2
work_unit_output_flow_1]=Component_cryoturbine(input_flow,output_pressure)

global liquid_turbine_efficiency
%%% The elements of the input flow contains: (1)mass flow rate (2)pressure (KPa) (3)enthalpy
(4)fluid name
M_in=input_flow{1};
P_in=input_flow{2};
H_in=input_flow{3};
fluid=input_flow{4};
P_out=output_pressure;

S_in=Thermal_Property('S','P',P_in,'H',H_in,fluid);
S_in=Thermal_Property('S','P',P_in,'H',H_in,fluid);

H_tem=Thermal_Property('H','P',P_out,'S',S_in,fluid);
H_tem=Thermal_Property('H','P',P_out,'S',S_in,fluid);
W_unit=(H_in-H_tem)*liquid_turbine_efficiency;
H_out=H_in-W_unit;

Q_gas=Thermal_Property('Q','P',output_pressure,'H',H_out,fluid);
Q_gas=Thermal_Property('Q','P',output_pressure,'H',H_out,fluid);

if Q_gas>1
    work_unit_output_flow_2{1}=input_flow{1};
    work_unit_output_flow_2{2}=output_pressure;
    work_unit_output_flow_2{3}=H_out;
    work_unit_output_flow_2{4}=input_flow{4};
    work_unit_output_flow_1=[];
else if Q_gas<0
        work_unit_output_flow_1{1}=input_flow{1};
        work_unit_output_flow_1{2}=output_pressure;
        work_unit_output_flow_1{3}=H_out;
        work_unit_output_flow_1{4}=input_flow{4};
        work_unit_output_flow_2=[];
    else
        work_unit_output_flow_1{1}=(1-Q_gas)*input_flow{1};
        work_unit_output_flow_1{2}=output_pressure;
        work_unit_output_flow_1{3}=Thermal_Property('H','P',output_pressure,'Q',0,fluid);
        work_unit_output_flow_1{3}=Thermal_Property('H','P',output_pressure,'Q',0,fluid);
        work_unit_output_flow_1{4}=input_flow{4};

        work_unit_output_flow_2{1}=Q_gas*input_flow{1};
```

```
        work_unit_output_flow_2{2}=output_pressure;
        T_tem=Thermal_Property('T','P',output_pressure,'Q',1,fluid)+1;
        T_tem=Thermal_Property('T','P',output_pressure,'Q',1,fluid)+1;
        work_unit_output_flow_2{3}=Thermal_Property('H','T',T_tem,'P',output_pressure,fluid);
        work_unit_output_flow_2{3}=Thermal_Property('H','T',T_tem,'P',output_pressure,fluid);
        work_unit_output_flow_2{4}=input_flow{4};
    end
end

W=W_unit*M_in;
```

A3. Code for pump

```
function [W work_unit_output_flow]=Component_pump(input_flow,output_pressure)

global pump_efficiency

%%% The elements of the input flow contains: (1)mass flow rate (2)pressure (KPa) (3)enthalpy
(4)fluid name
Hin=input_flow{3};
Sin=Thermal_Property('S','P',input_flow{2},'H',input_flow{3},input_flow{4});
Sin=Thermal_Property('S','P',input_flow{2},'H',input_flow{3},input_flow{4});
Hout_temp=Thermal_Property('H','P',output_pressure,'S',Sin,input_flow{4});
Hout_temp=Thermal_Property('H','P',output_pressure,'S',Sin,input_flow{4});
W_consuming_unit=(Hin-Hout_temp)/pump_efficiency;
Hout=Hin-W_consuming_unit;
W=input_flow{1}*W_consuming_unit;

work_unit_output_flow{1}=input_flow{1};
work_unit_output_flow{2}=output_pressure;
work_unit_output_flow{3}=Hout;
work_unit_output_flow{4}=input_flow{4};
```

A4. Code for throttle valve

```
function [W work_unit_output_flow_2
work_unit_output_flow_1]=Component_throttlevalve(input_flow,output_pressure)


%%% The elements of the input flow contains: (1)mass flow rate (2)pressure (KPa) (3)enthalpy
(4)fluid name
M_in=input_flow{1};
P_in=input_flow{2};
H_in=input_flow{3};
fluid=input_flow{4};
P_out=output_pressure;

W=0;

Q_gas=Thermal_Property('Q','P',output_pressure,'H',H_in,fluid);
Q_gas=Thermal_Property('Q','P',output_pressure,'H',H_in,fluid);

if Q_gas>1
    work_unit_output_flow_2{1}=input_flow{1};
    work_unit_output_flow_2{2}=output_pressure;
    work_unit_output_flow_2{3}=H_in;
    work_unit_output_flow_2{4}=input_flow{4};
    work_unit_output_flow_1=[];
else if Q_gas<0
        work_unit_output_flow_1{1}=input_flow{1};
        work_unit_output_flow_1{2}=output_pressure;
        work_unit_output_flow_1{3}=Thermal_Property('H','P',output_pressure,'Q',0,fluid);
        work_unit_output_flow_1{3}=Thermal_Property('H','P',output_pressure,'Q',0,fluid);
        work_unit_output_flow_1{4}=input_flow{4};
        work_unit_output_flow_2=[];
    else
        work_unit_output_flow_1{1}=(1-Q_gas)*input_flow{1};
        work_unit_output_flow_1{2}=output_pressure;
        T_tem=Thermal_Property('T','P',output_pressure,'Q',1,fluid)+1;
        T_tem=Thermal_Property('T','P',output_pressure,'Q',1,fluid)+1;
```

```
        work_unit_output_flow_2{3}=Thermal_Property('H','T',T_tem,'P',output_pressure,fluid);
        work_unit_output_flow_2{3}=Thermal_Property('H','T',T_tem,'P',output_pressure,fluid);
        work_unit_output_flow_1{4}=input_flow{4};

        work_unit_output_flow_2{1}=Q_gas*input_flow{1};
        work_unit_output_flow_2{2}=output_pressure;
        work_unit_output_flow_2{3}=Thermal_Property('H','P',output_pressure,'Q',1,fluid);
        work_unit_output_flow_2{3}=Thermal_Property('H','P',output_pressure,'Q',1,fluid);
        work_unit_output_flow_2{4}=input_flow{4};
    end
end
```

A5. Code for turbine

```
function [W work_unit_output_flow]=Component_turbine(input_flow,output_pressure)

global T_ambient
global turbine_isentropic_efficiency
calcualtion=0;
%%% The elements of the input flow contains: (1)mass flow rate (2)pressure (KPa) (3)enthalpy
(4)fluid name
M_in=input_flow{1};
P_in=input_flow{2};
H_in=input_flow{3};
fluid=input_flow{4};
P_out=output_pressure;


T_min=T_ambient;

S_in=Thermal_Property('S','P',P_in,'H',H_in,fluid);
S_in=Thermal_Property('S','P',P_in,'H',H_in,fluid);

T_in=Thermal_Property('T','P',P_in,'H',H_in,fluid);
T_in=Thermal_Property('T','P',P_in,'H',H_in,fluid);


    H_tem=Thermal_Property('H','P',P_out,'S',S_in,fluid);
    H_tem=Thermal_Property('H','P',P_out,'S',S_in,fluid);
    W_unit=(H_in-H_tem)*turbine_isentropic_efficiency;
    Hout=H_in-W_unit;
    W=M_in*W_unit;

    work_unit_output_flow{1}=input_flow{1};
    work_unit_output_flow{2}=output_pressure;
    if T_in<T_min
        work_unit_output_flow{3}=Hout;
    else
        work_unit_output_flow{3}=H_tem;
    end
    work_unit_output_flow{4}=input_flow{4};
if calcualtion
        T_tem_out=Thermal_Property('T','P',P_out,'S',S_in,fluid);
        T_tem_out=Thermal_Property('T','P',P_out,'S',S_in,fluid);
        H_tem_out=Thermal_Property('H','P',P_out,'S',S_in,fluid);
        H_tem_out=Thermal_Property('H','P',P_out,'S',S_in,fluid);

        if T_tem_out>T_min
            T_out=T_tem_out;
            W=M_in*(H_in-H_tem_out)*turbine_isentropic_efficiency;
            H_out=H_tem_out;
            work_unit_output_flow{1}=input_flow{1};
            work_unit_output_flow{2}=output_pressure;
            work_unit_output_flow{3}=H_out;
            work_unit_output_flow{4}=input_flow{4};
        else
            T_out=T_min;
            P_min = P_out;
            P_max = P_in;

        while P_max-P_min > 1
            x = (P_max+P_min)/2;
```

```
            Tout=Thermal_Property('T','P',x,'S',S_in,fluid);
            Tout=Thermal_Property('T','P',x,'S',S_in,fluid);

            if Tout<T_min
                P_min = x;
            else
                P_max = x;
            end

        end

            P_adiabatic=P_min;
            Hout_temp=Thermal_Property('H','P',P_adiabatic,'S',S_in,fluid);
            Hout_temp=Thermal_Property('H','P',P_adiabatic,'S',S_in,fluid);
            W_consuming_adiabatic_unit=(H_in-Hout_temp)*turbine_isentropic_efficiency;

            P_compressor_inlet=P_adiabatic;
            T_compressor_inlet=T_min;
            P_compressor_outlet=P_out;
            T_compressor_outlet=T_min;

H_compressor_inlet=Thermal_Property('H','T',T_compressor_inlet,'P',P_compressor_inlet,fluid);

H_compressor_inlet=Thermal_Property('H','T',T_compressor_inlet,'P',P_compressor_inlet,fluid);

S_compressor_inlet=Thermal_Property('S','T',T_compressor_inlet,'P',P_compressor_inlet,fluid);

S_compressor_inlet=Thermal_Property('S','T',T_compressor_inlet,'P',P_compressor_inlet,fluid);

H_compressor_outlet=Thermal_Property('H','T',T_compressor_outlet,'P',P_compressor_outlet,fluid
);

H_compressor_outlet=Thermal_Property('H','T',T_compressor_outlet,'P',P_compressor_outlet,fluid
);

S_compressor_outlet=Thermal_Property('S','T',T_compressor_outlet,'P',P_compressor_outlet,fluid
);

S_compressor_outlet=Thermal_Property('S','T',T_compressor_outlet,'P',P_compressor_outlet,fluid
);
            W_compressor_isothermal_unit=-((H_compressor_outlet-H_compressor_inlet)-
T_min*(S_compressor_outlet-S_compressor_inlet))*turbine_isothermal_efficiency;

            W=(W_consuming_adiabatic_unit+W_compressor_isothermal_unit)*M_in;
            work_unit_output_flow{1}=input_flow{1};
            work_unit_output_flow{2}=output_pressure;
            work_unit_output_flow{3}=H_compressor_outlet;
            work_unit_output_flow{4}=input_flow{4};
        end
end
```

A6. Code for control parameters

```
function CONTROL_PARAMETER

%%%%%%%%%%%%%%%%%%%%%%%%%%%%%%%%%%%%%%%%%%%%%%%%%%%%%%%%%%%%%%%%%%%%%%%%%%%%%%%%
%%%%%%%%%%%%%%%%%%%%%%  Mode setting  %%%%%%%%%%%%%%%%%%%%%%%%%%%%%%%%%%%%%%%%
%%%%%%%%%%%%%%%%%%%%%%%%%%%%%%%%%%%%%%%%%%%%%%%%%%%%%%%%%%%%%%%%%%%%%%%%%%%%%%%%
global optimisation_mode
optimisation_mode=0;

%%%%%%%%%%%%%%%%%%%%%%%%%%%%%%%%%%%%%%%%%%%%%%%%%%%%%%%%%%%%%%%%%%%%%%%%%%%%%%%%
%%%%%%%%%%%%%%%%%%%%%%  Ambient condition  %%%%%%%%%%%%%%%%%%%%%%%%%%%%%%%%%%%%%
%%%%%%%%%%%%%%%%%%%%%%%%%%%%%%%%%%%%%%%%%%%%%%%%%%%%%%%%%%%%%%%%%%%%%%%%%%%%%%%%
global P_ambient
global T_ambient
P_ambient=1.01325e2;
T_ambient=298.15;
%%%%%%%%%%%%%%%%%%%%%%%%%%%%%%%%%%%%%%%%%%%%%%%%%%%%%%%%%%%%%%%%%%%%%%%%%%%%%%%%
%%%%%%%%%%%%%%%%%%%%%%  stream splitting %%%%%%%%%%%%%%%%%%%%%%%%%%%%%%%%%%%%%%
%%%%%%%%%%%%%%%%%%%%%%%%%%%%%%%%%%%%%%%%%%%%%%%%%%%%%%%%%%%%%%%%%%%%%%%%%%%%%%%%
```

```
global min_splitting_coefficieny
global max_splitting_coefficieny

min_splitting_coefficieny=0.1;
max_splitting_coefficieny=0.9; %%if the flow splitting coefficient is too high or too low than
the splitting should not be taken place.
%%ifproduct=1;%%%%%%%set if the liquid is the product
%%%%%%%%%%%%%%%%%%%%%%%%%%%%%%%%%%%%%%%%%%%%%%%%%%%%%%%%%%%%%%%%%%%%%%%%%%%%
%%%%%%%%%%%%%%%%%%  Component efficiency %%%%%%%%%%%%%%%%%%%%%%%%%%%%%%%%%%
%%%%%%%%%%%%%%%%%%%%%%%%%%%%%%%%%%%%%%%%%%%%%%%%%%%%%%%%%%%%%%%%%%%%%%%%%%%%
global pump_efficiency
global turbine_isentropic_efficiency
global turbine_isothermal_efficiency
global compressor_isentropic_efficiency
global compressor_isothermal_efficiency
global liquid_turbine_efficiency

turbine_isentropic_efficiency=0.88;
turbine_isothermal_efficiency=0.88;
compressor_isentropic_efficiency=0.87;
compressor_isothermal_efficiency=0.87;
liquid_turbine_efficiency=0.7;
pump_efficiency=0.77;
%%%%%%%%%%%%%%%%%%%%%%%%%%%%%%%%%%%%%%%%%%%%%%%%%%%%%%%%%%%%%%%%%%%%%%%%%%%%
%%%%%%%%%%%%%% minimum temperature converge for temperature capture %%%%%%%
%%%%%%%%%%%%%%%%%%%%%%%%%%%%%%%%%%%%%%%%%%%%%%%%%%%%%%%%%%%%%%%%%%%%%%%%%%%%
global minimum_temperature_grid

minimum_temperature_grid=0.1;
%%%%%%%%%%%%%%%%%%%%%%%%%%%%%%%%%%%%%%%%%%%%%%%%%%%%%%%%%%%%%%%%%%%%%%%%%%%%
%%%%%%%%%%%%%%%%% Fluid conditions setting %%%%%%%%%%%%%%%%%%%%%%%%%%%%%%%%
%%%%%%%%%%%%%%%%%%%%%%%%%%%%%%%%%%%%%%%%%%%%%%%%%%%%%%%%%%%%%%%%%%%%%%%%%%%%
global Main_fluid
global Refrigerant
Main_fluid='NITROGEN';
Refrigerant='HELIUM';

global Stage_main_flow
global ifproducr_main_flow
global Stage_refrigeration


Stage_main_flow=4;
ifproducr_main_flow=1;
Stage_refrigeration=5;
%%%%%%%%%%%%%%%%%%%%%%%%%%%%%%%%%%%%%%%%%%%%%%%%%%%%%%%%%%%%%%%%%%%%%%%%%%%%
%%%%%%%%%%%%%%%%% Approach temperature %%%%%%%%%%%%%%%%%%%%%%%%%%%%%%%%%%%%
%%%%%%%%%%%%%%%%%%%%%%%%%%%%%%%%%%%%%%%%%%%%%%%%%%%%%%%%%%%%%%%%%%%%%%%%%%%%
global Approach_temperature
global min_approach_temperature
Approach_temperature=3;
min_approach_temperature=Approach_temperature;
%%%%%%%%%%%%%%%%%%%%%%%%%%%%%%%%%%%%%%%%%%%%%%%%%%%%%%%%%%%%%%%%%%%%%%%%%%%%
%%%%%%%%%%%%%%%%% Initial solution setting %%%%%%%%%%%%%%%%%%%%%%%%%%%%%%%%
%%%%%%%%%%%%%%%%%%%%%%%%%%%%%%%%%%%%%%%%%%%%%%%%%%%%%%%%%%%%%%%%%%%%%%%%%%%%
global Initial_solution
Initial_solution=[253/300 ...
    1000/100 273/300 1500/100 273/300 2000/100 90/300 ...
    2000/100 90/300  2000/100  90/300 2000/100 90/300 ...
    3000/100 227.5/300 247.5/300 1.0 ...
    1000/100 84/300 114/300 1.0 ...
    400/100 84.3/300 114.3/300 1.0 ...
    150/100 74.4/300 114.4/300 1.0 ...
    100/100 74/300 95/300 1.0 ...
    3000/100 273/300 273/300 1.0 ...
    3000/100 273/300 273/300 1.0 ...
    3000/100 273/300 273/300 1.0 ...
    3000/100 273/300 273/300 1.0 ...
    3000/100 273/300 273/300 1.0 ...
    3000/100 273/300 273/300 1.0 ...
    3000/100 273/300 273/300 1.0 ...
    3000/100 273/300 273/300 1.0 ...
    3000/100 273/300 273/300 1.0 ...
    3000/100 273/300 273/300 1.0 ...
```

```
    ];
%%%%%%%%%%%%%%%%%%%%%%%%%%%%%%%%%%%%%%%%%%%%%%%%%%%%%%%%%%%%%%%%%%%%%%%%%%%%
%%%%%%%%%%%%%%%%% Boundary conditions %%%%%%%%%%%%%%%%%%%%%%%%%%%%%%%%%%%%%%%
%%%%%%%%%%%%%%%%%%%%%%%%%%%%%%%%%%%%%%%%%%%%%%%%%%%%%%%%%%%%%%%%%%%%%%%%%%%%
global Number_of_variables
global Number_of_variables_mail_flow
global Number_of_variables_refrigeration
global Lower_condition
global Upper_condition
Number_of_variables_mail_flow=2*(Stage_main_flow-1);
Number_of_variables_refrigeration=2^(Stage_refrigeration-1)-1;
Number_of_variables=2*Number_of_variables_mail_flow+4*Number_of_variables_refrigeration+1;
%%%% Lower condition
Lower_condition(1)=150/300;
if Number_of_variables_mail_flow>1
    for i=1:(Number_of_variables_mail_flow-1)
        Lower_condition(2*i)=P_ambient/100;
        Lower_condition(2*i+1)=90/300;
    end
end
Lower_condition(2*Number_of_variables_mail_flow)=500/100;
Lower_condition(2*Number_of_variables_mail_flow+1)=80/300;
if Number_of_variables_refrigeration>0
    for i=1:Number_of_variables_refrigeration
        Lower_condition(4*i-3+2*Number_of_variables_mail_flow+1)=P_ambient/100;
        Lower_condition(4*i-2+2*Number_of_variables_mail_flow+1)=60/300;
        Lower_condition(4*i-1+2*Number_of_variables_mail_flow+1)=60/300;
        Lower_condition(4*i+2*Number_of_variables_mail_flow+1)=0.1;
    end
end
%%%%%%%%%%%%%%%%%%%%%%%%%%%%%%%%%%%%%%%%%%%%%%%%%%%%%%%%%%%%%%%%%%%%%%%%%%%%
%%%% Upper condition
Upper_condition(1)=280/300;
if Number_of_variables_mail_flow>1
    for i=1:(Number_of_variables_mail_flow-1)
        Upper_condition(2*i)=4000/100;
        Upper_condition(2*i+1)=T_ambient/300;
    end
end
Upper_condition(2*Number_of_variables_mail_flow)=8000/100;
Upper_condition(2*Number_of_variables_mail_flow+1)=120/300;
if Number_of_variables_refrigeration>0
    for i=1:Number_of_variables_refrigeration
        Upper_condition(4*i-3+2*Number_of_variables_mail_flow+1)=3000/100;
        Upper_condition(4*i-2+2*Number_of_variables_mail_flow+1)=T_ambient/300;
        Upper_condition(4*i-1+2*Number_of_variables_mail_flow+1)=T_ambient/300;
        Upper_condition(4*i+2*Number_of_variables_mail_flow+1)=1.7;
    end
end

%c=(Lower_condition+Upper_condition)/2;
%%%%%%%%%%%%%%%%%%%%%%%%%%%%%%%%%%%%%%%%%%%%%%%%%%%%%%%%%%%%%%%%%%%%%%%%%%%%
%%%%%%%%%%%%%%%%%%%% Output setting %%%%%%%%%%%%%%%%%%%%%%%%%%%%%%%%%%%%%%%%
%%%%%%%%%%%%%%%%%%%%%%%%%%%%%%%%%%%%%%%%%%%%%%%%%%%%%%%%%%%%%%%%%%%%%%%%%%%%

global Output_Objective_trend
global Output_Objective_data
global Output_EHTF_trend
global Output_EHTF_data
global Output_Optimal_vector
global Output_Composite_curves
global Output_Captial_cost
global Output_Liuqid_product
global Output_Heat_flow
global Output_State_parameter

Output_Objective_trend=1;
Output_Objective_data=0;
Output_EHTF_trend=1;
Output_EHTF_data=0;
Output_Optimal_vector=0;
Output_Composite_curves=1;
Output_Captial_cost=0;
Output_Liuqid_product=0;
```

```
Output_Heat_flow=1;
Output_State_parameter=0;
```

A7. Code for EHTF calcualtion

```
function EHTF=EHTF_capture(Z1,Z2)

N_plot=0;
N_EHTF=0;

EHTF=0;
global ifplot
global T_ambient
global min_approach_temperature

if ifplot
    N=200;
else
    N=50;
end

approach_temperature=100;
A1=length(Z1);
A2=length(Z2);
A=A1+A2;
for i=1:A1
    y{i}=Z1{i};
    a=Z1{i};
    T_in_1=ST(a{2},a{3},a{5});
    T_in_2=ST(a{2},a{4},a{5});
    b={a{1},a{2},T_in_1,T_in_2,a{5}};
end

for i=(A1+1):A
    y{i}=Z2{i-A1};
    a=Z2{i-A1};
    T_in_1=ST(a{2},a{3},a{5});
    T_in_2=ST(a{2},a{4},a{5});
    b={a{1},a{2},T_in_1,T_in_2,a{5}};
end

for i=1:A
    Tempy=y{i};
    [Q_(i) y_update]= temperature_ordering(y{i});
    y_update_{i}=y_update;
end

Q_all_HR=0;
Q_all_HA=0;

k1=0;
k2=0;
for i=1:A
[Q_all_HR Q_all_HA y_HR y_HA]=heat_source_grouping(Q_all_HR,Q_all_HA,Q_(i),y_update_{i});

if ~isempty(y_HR)
    k1=k1+1;
    y_HR_{k1}= y_HR;
end

if ~isempty(y_HA)
    k2=k2+1;
    y_HA_{k2}= y_HA;
end
end

aaaaa=y_HR_;
bbbbb=y_HA_;

if abs((Q_all_HR+Q_all_HA)/Q_all_HR)>0.01
    approach_temperature=-5;
```

```
    return;
else
    for i=1:A
        approach_temperature=mass_sign(y{i});
        if approach_temperature<0
            return
        end
    end

    for Q=0:Q_all_HR/N:Q_all_HR
        if ifplot
            N_plot=N_plot+1;
            Heat_all(N_plot)=Q;
            Temp_temperature_High(N_plot)=sub_temperature_capture(Q,y_HR_)-273.15;
            Temp_temperature_Low(N_plot)=sub_temperature_capture(Q,y_HA_)-273.15;
        end
        N_EHTF=N_EHTF+1;
        Temp_temperature_HR=sub_temperature_capture(Q,y_HR_);
        Temp_temperature_HA=sub_temperature_capture(Q,y_HA_);
        Temp_temperature_HR_EHTF(N_EHTF)=sub_temperature_capture(Q,y_HR_);
        Temp_temperature_HA_EHTF(N_EHTF)=sub_temperature_capture(Q,y_HA_);
        Approach_temperature_temp=Temp_temperature_HR-Temp_temperature_HA;
        if Approach_temperature_temp<approach_temperature
            approach_temperature=Approach_temperature_temp;
            if approach_temperature<0
                T_high=Temp_temperature_HR;
                T_low=Temp_temperature_HA;
            return
            end
        end
    end
end

approach_temperature=approach_temperature;

 for i=1:N_EHTF
         if (1/Temp_temperature_HR_EHTF(i)+1/Temp_temperature_HA_EHTF(i))<2/T_ambient
             Temp_temperature_High_temp(i)=Temp_temperature_HR_EHTF(i)-
min_approach_temperature;
             Temp_temperature_Low_temp(i)=Temp_temperature_HA_EHTF(i);
         else
             Temp_temperature_High_temp(i)=Temp_temperature_HR_EHTF(i);
             Temp_temperature_Low_temp(i)=Temp_temperature_HA_EHTF(i)+min_approach_temperature;
         end
 end
     DD_1=0;
     DD_2=0;
     for i=1:(N_EHTF-1)
         D_2=1/(Temp_temperature_HA_EHTF(i)+Temp_temperature_HA_EHTF(i+1))-
1/(Temp_temperature_HR_EHTF(i)+Temp_temperature_HR_EHTF(i+1));
         D_1=1/(Temp_temperature_HA_EHTF(i)+Temp_temperature_HA_EHTF(i+1))-
1/(Temp_temperature_HR_EHTF(i)+Temp_temperature_HR_EHTF(i+1))+...
             (1/(Temp_temperature_High_temp(i)+Temp_temperature_High_temp(i+1))-
1/(Temp_temperature_Low_temp(i)+Temp_temperature_Low_temp(i+1)));
         DD_1=DD_1+D_1;
         DD_2=DD_2+D_2;
     end

     EHTF=DD_1/DD_2;

function [Q y_update]=temperature_ordering(y2)

    if ~isempty(y2)
            M_1=y2{1};
            P_1=y2{2};
            H_1_in=y2{3};
            H_1_out=y2{4};
            fluid_1=y2{5};

            T_1_in=ST(P_1,H_1_in,fluid_1);
            T_1_out=ST(P_1,H_1_out,fluid_1);

            Q=M_1*(H_1_in-H_1_out);
```

```
            if T_1_in<T_1_out
                y_update{1}=M_1;
                y_update{2}=T_1_in;
                y_update{3}=T_1_out;
                y_update{4}=P_1;
                y_update{5}=P_1;
                y_update{6}=fluid_1;
            else
                y_update{1}=M_1;
                y_update{2}=T_1_out;
                y_update{3}=T_1_in;
                y_update{4}=P_1;
                y_update{5}=P_1;
                y_update{6}=fluid_1;
            end

    else
        Q=[];
        y_update=y2;
    end

function [Q_all_HR Q_all_HA y_HR y_HA]=heat_source_grouping(Q_all_HR,Q_all_HA,Q,y)

if ~isempty(Q)
    if Q>0
        Q_all_HR=Q_all_HR+Q;
        y_HR=y;
        y_HA=[];
    else
        Q_all_HA=Q_all_HA+Q;
        y_HR=[];
        y_HA=y;
    end
else
    y_HR=[];
    y_HA=[];
end


function T_out=mass_sign(y)

T_out=100;

if ~isempty(y)
    if y{1}<0
        T_out=-5;
    end
end

%%%%%%%%%%%%%%%%%%%%%%%%%%%%%%%%%%%%%%%%%%%%%%%%%%%%%%%%%%%%%%%%%%%%%%%%%%%%
%%%%%%%%%%%%%%%%%%%%%%%%%%%%%%%%%%%%%%%%%%%%%%%%%%%%%%%%%%%%%%%%%%%%%%%%%%%%
function T_in=ST(P_in,H_in,fluid)

length_fluid=length(fluid);
if length_fluid==3
    if fluid=='CO2'
        IFCO2=1;
    else
        IFCO2=0;
    end
else
    IFCO2=0;
end
%%%%%%%%%%%%%%%%%%%%%%%%%%%%%%%%%%%%%%%%%%%%%%%%%%%%%%%%%%%%%%%%%%%%%%%%%%%%

if IFCO2
    if P_in>100 && P_in<102
        if  H_in>1.3278e+006
            Cp=Thermal_Property('C','P',P_in,'H',1.3278e+006,fluid);
            Cp=Thermal_Property('C','P',P_in,'H',1.3278e+006,fluid);
            T_in=1050+(H_in-1.3278e+006)/Cp;
        elseif H_in>4.3987e+005
            T_in=Thermal_Property('T','P',P_in,'H',H_in,fluid);
            T_in=Thermal_Property('T','P',P_in,'H',H_in,fluid);
```

```
        elseif H_in>4.2285e+005
            Cp=Thermal_Property('C','P',P_in,'H',4.3987e+005,fluid);
            Cp=Thermal_Property('C','P',P_in,'H',4.3987e+005,fluid);
            T_in=217+(H_in-4.3987e+005)/Cp;
        elseif H_in>-1.5059e+005
            T_in=195;
        else
            T_in=195+(H_in+1.5059e+005)/1240;
        end
    else
        T_in=Thermal_Property('T','P',P_in,'H',H_in,fluid);
        T_in=Thermal_Property('T','P',P_in,'H',H_in,fluid);
    end

else
        T_in=Thermal_Property('T','P',P_in,'H',H_in,fluid);
        T_in=Thermal_Property('T','P',P_in,'H',H_in,fluid);
end
```

A8. Code for initialization

```
function INITIALIZATION(x)

%%%%%%%%%%%%%%%%%%%%%%%%%%%%%%%%%%%%%%%%%%%%%%%%%%%%%%%%%%%%%%%%%%%%%%%%%%%%%%%
%%%%%%%%%%%%%%%% Fluid conditions setting %%%%%%%%%%%%%%%%%%%%%%%%%%%%%%%%%%%%
%%%%%%%%%%%%%%%%%%%%%%%%%%%%%%%%%%%%%%%%%%%%%%%%%%%%%%%%%%%%%%%%%%%%%%%%%%%%%%%
global Main_fluid
global Refrigerant
global P_ambient
global T_ambient

global Start_point_main_flow
global End_point_main_flow
global Start_point_refrigeration
global End_point_refrigeration


global Approach_temperature


global Number_of_variables_mail_flow
global Number_of_variables_refrigeration

H_ambient_main_fluid=Thermal_Property('H','T',T_ambient,'P',P_ambient,Main_fluid);
H_ambient_main_fluid=Thermal_Property('H','T',T_ambient,'P',P_ambient,Main_fluid);
H_ambient_main_fluid_outlet=Thermal_Property('H','T',T_ambient-
2*Approach_temperature,'P',P_ambient,Main_fluid);
H_ambient_main_fluid_outlet=Thermal_Property('H','T',T_ambient-
2*Approach_temperature,'P',P_ambient,Main_fluid);
H_ambient_refrigeration=Thermal_Property('H','T',x(1)*300,'P',P_ambient,Refrigerant);
H_ambient_refrigeration=Thermal_Property('H','T',x(1)*300,'P',P_ambient,Refrigerant);
Start_point_main_flow={1.0,P_ambient,H_ambient_main_fluid,Main_fluid};
End_point_main_flow={P_ambient,H_ambient_main_fluid_outlet,H_ambient_main_fluid_outlet,1};


H_ambient_main_fluid=Thermal_Property('H','T',273,'P',P_ambient,Main_fluid);
H_ambient_refrigerant=Thermal_Property('H','T',273,'P',P_ambient,Refrigerant);
H_ambient_refrigerant=Thermal_Property('H','T',273,'P',P_ambient,Refrigerant);

Start_point_refrigeration={1.0,P_ambient,H_ambient_refrigeration,Refrigerant};
End_point_refrigeration={P_ambient,H_ambient_refrigeration,H_ambient_refrigeration,1};


global outlet_parameter_main_flow
global outlet_parameter_refrigeration

if Number_of_variables_mail_flow>1
    for i=1:Number_of_variables_mail_flow
        P_tem=x(2*i)*100;
        H_tem=Thermal_Property('H','T',x(2*i+1)*300,'P',P_tem,Main_fluid);
        H_tem=Thermal_Property('H','T',x(2*i+1)*300,'P',P_tem,Main_fluid);
        outlet_parameter_main_flow{i}={P_tem,H_tem};
```

```
    end
end

if Number_of_variables_refrigeration>0
    for i=1:Number_of_variables_refrigeration
        P_tem=x(4*i-3+2*Number_of_variables_mail_flow+1)*100;
        aaaaa=4*i-2+2*Number_of_variables_mail_flow+1;
        T_tem_1=x(4*i-2+2*Number_of_variables_mail_flow+1)*300;
        T_tem_2=x(4*i-1+2*Number_of_variables_mail_flow+1)*300;
        H_tem_1=Thermal_Property('H','T',T_tem_1,'P',P_tem,Refrigerant);
        H_tem_1=Thermal_Property('H','T',T_tem_1,'P',P_tem,Refrigerant);
        H_tem_2=Thermal_Property('H','T',T_tem_2,'P',P_tem,Refrigerant);
        H_tem_2=Thermal_Property('H','T',T_tem_2,'P',P_tem,Refrigerant);
        if_splitting_or_not=x(4*i+2*Number_of_variables_mail_flow+1);
        outlet_parameter_refrigeration{i}={P_tem,H_tem_1,H_tem_2,if_splitting_or_not};
    end
end
```

A9. Code for main problem setting

```
function Efficiency_global=MAIN_PROBLEM(x)

global cycle_number
global outlet_parameter_main_flow
global outlet_parameter_refrigeration

global Start_point_main_flow
global End_point_main_flow
global Stage_main_flow

global Start_point_refrigeration
global End_point_refrigeration
global Stage_refrigeration

global Main_fluid

global Approach_temperature

cycle_number=cycle_number+1;
INITIALIZATION(x);

% 1. Please set the Number of the thermal cycle in the form of
% 'Number_THERMALCYCLE=2;'.
%Number_THERMALCYCLE=2;

% 2. Please set the working fluid for each thermal cycle in the form of
% 'Fluid{i}='FLUID';'.
%Fluid{1}='NITROGEN';
%Fluid{2}='HELIUM';

% 3. Please set if the thermal cycle produce liquid product in the form of
% 'If_product{i}=1;' for producing liquid and 'If_product{i}=0;' for no liquid product.
If_product{1}=1;
If_product{2}=0;

% 4. Please set if the stream split in the thermal cycle in the form of
% 'If_split{i}=1;' for yes and 'If_split{i}=0;' for no.
%If_split{1}=0;
%If_split{2}=1;

% 5. Please set the stages of each thermal cycle in the form of
% 'Number_stage{i}=2;'.
%Number_stage{1}=3;
%Number_stage{2}=4;

% 6. Please set the mass flow rate of each thermal cycle in the form of
% 'Mass_flow{i}=1;'.
%Mass_flow{1}=1;
%Mass_flow{2}=1;

% 7. Please edit the state pressure and temperature of each thermal cycle
% in the form of
```

```
%%%%%%%%%%%%%%%%%%%%%%%%%%%%%%%%%%%%%%%%%%%%%%%%%%%%%%%%%%%%%%%%%%%%%%%%%%%%
%%%              for i=1:Number_THERMALCYCLE                                %%%
%%%                  Number_code{i}=1+2^(Number_stage{i}-1);                %%%
%%%                  for j=1:Number_code{i}                                 %%%
%%%                      P{j}=[];                                           %%%
%%%                      T{j}=[];                                           %%%
%%%                  end                                                    %%%
%%%                  Pressure{i}=P;                                         %%%
%%%                  Temperature{i}=T;                                      %%%
%%%              end                                                        %%%
%%%%%%%%%%%%%%%%%%%%%%%%%%%%%%%%%%%%%%%%%%%%%%%%%%%%%%%%%%%%%%%%%%%%%%%%%%%%


% 8. Please edit other state parameters of each thermal cycle
% in the form of
%%%%%%%%%%%%%%%%%%%%%%%%%%%%%%%%%%%%%%%%%%%%%%%%%%%%%%%%%%%%%%%%%%%%%%%%%%%%
%%%              for i=1:Number_THERMALCYCLE                                %%%
%%%                  Number_code{i}=1+2^(Number_stage{i}-1);                %%%
%%%                  for j=1:Number_code{i}                                 %%%
%%%                      T_split{j}=[];                                     %%%
%%%                      Q{j}=[];                                           %%%
%%%                  end                                                    %%%
%%%                  Temperature_splitting{i}=T;                            %%%
%%%                  Coefficient_splitting{i}=Q;                            %%%
%%%              end                                                        %%%
%%%%%%%%%%%%%%%%%%%%%%%%%%%%%%%%%%%%%%%%%%%%%%%%%%%%%%%%%%%%%%%%%%%%%%%%%%%%


% 9. Please edit the objective function
% in the below form 'Objective=[];'

[W_main_flow Heat_total_main_flow M_liquid_product_main_flow Output_heat_flow_main_flow]=...

THERMALCYCLE(Start_point_main_flow,End_point_main_flow,Stage_main_flow,If_product{1},outlet_pa
rameter_main_flow);
[W_refrigeration Heat_total_refrigeration M_liquid_product_refrigeration
Output_heat_flow_refrigeration]=...

THERMALCYCLE(Start_point_refrigeration,End_point_refrigeration,Stage_refrigeration,If_product{
2},outlet_parameter_refrigeration);

Mass_refrigerant=-
Start_point_main_flow{1}*Heat_total_main_flow/Heat_total_refrigeration;%%%Mass flow update
Start_point_refrigeration{1}=Mass_refrigerant;
[W_refrigeration Heat_total_refrigeration M_liquid_product_refrigeration
Output_heat_flow_refrigeration]=...

THERMALCYCLE(Start_point_refrigeration,End_point_refrigeration,Stage_refrigeration,If_product{
2},outlet_parameter_refrigeration);
W_total=W_main_flow+W_refrigeration;
approach_temperature_real=sub_approach_temperature_capture(Output_heat_flow_main_flow,Output_h
eat_flow_refrigeration);
c=Approach_temperature;
if approach_temperature_real<Approach_temperature
    Efficiency_global=Approach_temperature-approach_temperature_real;
else
    Efficiency_global=M_liquid_product_main_flow*Exergy_liquid(Main_fluid)/W_total;

end

function E=Exergy_liquid(Fluid)

global P_ambient
global T_ambient

H_ambient=Thermal_Property('H','T',T_ambient,'P',P_ambient,Fluid);
H_ambient=Thermal_Property('H','T',T_ambient,'P',P_ambient,Fluid);

S_ambient=Thermal_Property('S','T',T_ambient,'P',P_ambient,Fluid);
S_ambient=Thermal_Property('S','T',T_ambient,'P',P_ambient,Fluid);

H=Thermal_Property('H','P',P_ambient,'Q',0,Fluid);
H=Thermal_Property('H','P',P_ambient,'Q',0,Fluid);
```

```
S=Thermal_Property('S','P',P_ambient,'Q',0,Fluid);
S=Thermal_Property('S','P',P_ambient,'Q',0,Fluid);

E=(H-H_ambient)-T_ambient*(S-S_ambient);
```

A10. Code for output controling

```
function [state, options,optchanged] = OUTPUT(options,state,flag)

%global Output_Objective_trend
global Output_Objective_data
%global Output_EHTF_trend
global Output_EHTF_data
global Output_Optimal_vector
%global Output_Composite_curves
%global Output_Captial_cost
%global Output_Liuqid_product
%global Output_Heat_flow
%global Output_State_parameter

optchanged = false;

switch flag
 case 'init'
        %disp('Starting the algorithm');
    case {'iter','interrupt'}
        %disp('Iterating ...')
        [unused,best] = min(state.Score);
        %a=state.Best;
        %b=state.Score;
        %c=state.Expectation;
        d=state.Population(best,:);
        [Efficiency_storage EHTF_value]=EHTF_output(d);

        if Output_Objective_data
            output_1=fopen('exergy_efficiency.txt','a');
            fprintf(output_1,'\n%12.6g', -unused);
            fclose(output_1);
        end

        if Output_EHTF_data
            output_2=fopen('EHTF_value.txt','a');
            fprintf(output_2,'\n%12.6g', EHTF_value);
            fclose(output_2);
        end

        if Output_Optimal_vector
            output_3=fopen('Detail_vector.txt','a');
            fprintf(output_3,'\n%E\t %E\t %E\t %E\t %E\t %E\t %E\t %E\t %E\t %E\t %E\t %E\t\n',d);
            fclose(output_3);
        end

    case 'done'
        %disp('Performing final task');
end
```

A11. Code for power transfer process calcuation

```
function [W work_unit_output_flow_1 work_unit_output_flow_2] =
Power_transfer(input_flow,output_pressure)
%STREAM_SPLITTING Summary of this function goes here
%   This function is used to simulate a flow splitting

a=length(input_flow); %% The elements of the input flow contains: (1)mass flow rate
(2)pressure (KPa) (3)enthalpy
                      %%(4)fluid name (5)splitting coefficient (0<x<1)
if a<4
    error ('incorrect fluid information');
end

if ~ischar(input_flow{4})
```

```
    error ('incorrect fluid name');
end

%%%%%%%%%%%%%%%%%%%%%%%%%%%%%%%%%%%%%%%%%%%%%%%%%%%%%%%%%%%%%%%%%%%%%%%%%%%%%%%%%%%%%%%%%%%%%%%
%%%
%%%%%%%%%%%%%%%%%%%%%%%%%%%Section 1 %% calculating the power
consumption%%%%%%%%%%%%%%%%%%%%%%%
%%%%%%%%%%%%%%%%%%%%%%%%%%%%%%%%%%%%%%%%%%%%%%%%%%%%%%%%%%%%%%%%%%%%%%%%%%%%%%%%%%%%%%%%%%%%%%%
%%%
if_throttle_valve=1; %%%%%1 for valve and 0 for liquid turbine

global P_ambient

work_unit_output_flow_2=[];
input_pressure=input_flow{2};

input_flow{2};
input_flow{3};

    D_input_flow=Thermal_Property('D','P',input_flow{2},'H',input_flow{3},input_flow{4});
    D_input_flow=Thermal_Property('D','P',input_flow{2},'H',input_flow{3},input_flow{4});

    D_liquid=Thermal_Property('D','P',P_ambient,'Q',0,input_flow{4});
    D_liquid=Thermal_Property('D','P',P_ambient,'Q',0,input_flow{4});

if abs(input_pressure-output_pressure)/input_pressure<0.01
    W=0;
    for i=1:4
    work_unit_output_flow_1{i}=input_flow{i};
    end


else if input_pressure>output_pressure  %%Expansion process
        if D_input_flow<D_liquid*0.3  %% Gas turbine
            [W work_unit_output_flow_1]=Component_turbine(input_flow,output_pressure);
        else if if_throttle_valve%%liquid turbine or throttle valve
                [W work_unit_output_flow_1
work_unit_output_flow_2]=Component_throttlevalve(input_flow,output_pressure);
            else
                [W work_unit_output_flow_1
work_unit_output_flow_2]=Component_cryoturbine(input_flow,output_pressure);
            end
        end
    else  %%compression process
        if D_input_flow<D_liquid*0.3 %% compressor
            [W work_unit_output_flow_1]=Component_compressor(input_flow,output_pressure);
        else %% pump
            [W work_unit_output_flow_1]=Component_pump(input_flow,output_pressure);
        end
    end
end
```

A12. Code for starting the program

```
function START

global optimisation_mode
global Initial_solution
global Lower_condition
global Upper_condition

CONTROL_PARAMETER;
LengthofOptimization=length(Lower_condition);
optionsold = optimset('display','iter',...
'MaxFunEvals',5000,'largescale','on','Diagnostics','on','DiffMaxChange',5e-2,'TolX',1e-
2,'TolFun',5e-2,'TolCon',1e-2);
options =
gaoptimset(optionsold,'InitialPopulation',Initial_solution,'PopulationSize',100,'Generations',
200,'OutputFcns',@OUTPUT);
if ~optimisation_mode
    Efficiency_global=MAIN_PROBLEM(Initial_solution);
    if Efficiency_global<0
```

```
        disp('Valid solution');
        Objective=-Efficiency_global
    end

else

[initial_vector_liquefaction_opt,fval,exitflag,output]=ga(@MAIN_PROBLEM,LengthofOptimization,[
],[],[],[],Lower_condition,Upper_condition,[],options);
end
```

A13. Code for stream structure calcualtion

```
function [W M_liquid_product heat_flow_1 heat_flow_2 heat_flow_3 heat_flow_4] =
stream_splitting(input_flow,output_flow,ifproduct)
%STREAM_SPLITTING Summary of this function goes here
%   This function is used to simulate a flow splitting

global min_splitting_coefficieny
global max_splitting_coefficieny %%if the flow splitting coefficient is too high or too low
than the splitting should not be taken place.
%%ifproduct=1;%%%%%%%set if the liquid is the product
global P_ambient

M_liquid_product=0;

a=length(input_flow); %% The elements of the input flow contains: (1)mass flow rate
(2)pressure (KPa) (3)enthalpy
                      %%(4)fluid name
b=length(output_flow);%%(1)output pressure (2)output enthalpy 1 (3)output enthalpy 2
(4)splitting coefficient (0<x<1)else
                      %%no splitting

output_pressure=output_flow{1};
output_enthalpy_1=output_flow{2};
if b>2
    output_enthalpy_2=output_flow{3};
else
    output_enthalpy_2=0;
end

if a<4
    error ('incorrect fluid information');
end

if ~ischar(input_flow{4})
    error ('incorrect fluid name');
end

if b>3
        if output_flow{4}>min_splitting_coefficieny &&
output_flow{4}<max_splitting_coefficieny
            splitting_or_not=1;%%stream splitting
        else
            splitting_or_not=0;
        end
else
        splitting_or_not=0;
end

 [W work_unit_output_flow_1 work_unit_output_flow_2] =
Power_transfer(input_flow,output_pressure);



    if ~isempty(work_unit_output_flow_2)
        if output_pressure<P_ambient*1.01 && ifproduct
            M_liquid_product=work_unit_output_flow_2{1};
            work_unit_output_flow_2=[];
        end
    end

 if ~isempty(work_unit_output_flow_1) && isempty(work_unit_output_flow_2)&& splitting_or_not
```

```
    work_unit_output_flow_1{1}=output_flow{4}*work_unit_output_flow_1{1};
    work_unit_output_flow_2{1}=(1-output_flow{4})*work_unit_output_flow_1{1};
    work_unit_output_flow_2{2}=work_unit_output_flow_1{2};
    work_unit_output_flow_2{3}=work_unit_output_flow_1{3};
    work_unit_output_flow_2{4}=work_unit_output_flow_1{4};
 end

  if ~isempty(work_unit_output_flow_2) && isempty(work_unit_output_flow_1)&& splitting_or_not
    work_unit_output_flow_1{1}=output_flow{4}*work_unit_output_flow_2{2};
    work_unit_output_flow_1{2}=work_unit_output_flow_2{2};
    work_unit_output_flow_1{3}=work_unit_output_flow_2{3};
    work_unit_output_flow_1{4}=work_unit_output_flow_2{4};
    work_unit_output_flow_2{1}=(1-output_flow{4})*work_unit_output_flow_2{1};
 end

Q_output_flow_1=Thermal_Property('Q','P',output_pressure,'H',output_enthalpy_1,input_flow{4});
Q_output_flow_1=Thermal_Property('Q','P',output_pressure,'H',output_enthalpy_1,input_flow{4});
Q_output_flow_2=Thermal_Property('Q','P',output_pressure,'H',output_enthalpy_2,input_flow{4});
Q_output_flow_2=Thermal_Property('Q','P',output_pressure,'H',output_enthalpy_2,input_flow{4});

if ~isempty(work_unit_output_flow_1)
    if (Q_output_flow_1>0) && (Q_output_flow_1<1)   %%%%%%%%% check if output flow is two
phase flow
        H_liquid=Thermal_Property('H','P',input_flow{2},'Q',0,input_flow{4})-1000;
        H_liquid=Thermal_Property('H','P',input_flow{2},'Q',0,input_flow{4})-1000;

        H_gas=Thermal_Property('H','P',input_flow{2},'Q',1,input_flow{4})+1000;
        H_gas=Thermal_Property('H','P',input_flow{2},'Q',1,input_flow{4})+1000;

        heat_flow_1{1}=work_unit_output_flow_1{1}*(1-Q_output_flow_1);
        heat_flow_1{2}=work_unit_output_flow_1{2};
        heat_flow_1{3}=work_unit_output_flow_1{3};
        heat_flow_1{4}=H_liquid;
        heat_flow_1{5}=work_unit_output_flow_1{4};

        heat_flow_2{1}=work_unit_output_flow_1{1}*Q_output_flow_1;
        heat_flow_2{2}=work_unit_output_flow_1{2};
        heat_flow_2{3}=work_unit_output_flow_1{3};
        heat_flow_2{4}=H_gas;
        heat_flow_2{5}=work_unit_output_flow_1{4};
    else
        heat_flow_1{1}=work_unit_output_flow_1{1};
        heat_flow_1{2}=work_unit_output_flow_1{2};
        heat_flow_1{3}=work_unit_output_flow_1{3};
        heat_flow_1{4}=output_enthalpy_1;
        heat_flow_1{5}=work_unit_output_flow_1{4};
        heat_flow_2=[];
    end
else
    heat_flow_1=[];
    heat_flow_2=[];
end

if ~isempty(work_unit_output_flow_2)
    if (Q_output_flow_2>0) && (Q_output_flow_2<1)   %%%%%%%%% check if output flow is two
phase flow
        H_liquid=Thermal_Property('H','P',input_flow{2},'Q',0,input_flow{4})-1000;
        H_liquid=Thermal_Property('H','P',input_flow{2},'Q',0,input_flow{4})-1000;

        H_gas=Thermal_Property('H','P',input_flow{2},'Q',1,input_flow{4})+1000;
        H_gas=Thermal_Property('H','P',input_flow{2},'Q',1,input_flow{4})+1000;

        heat_flow_3{1}=work_unit_output_flow_2{1}*(1-Q_output_flow_2);
        heat_flow_3{2}=work_unit_output_flow_2{2};
        heat_flow_3{3}=work_unit_output_flow_2{3};
        heat_flow_3{4}=H_liquid;
        heat_flow_3{5}=work_unit_output_flow_2{4};

        heat_flow_4{1}=work_unit_output_flow_2{1}*Q_output_flow_2;
        heat_flow_4{2}=work_unit_output_flow_2{2};
        heat_flow_4{3}=work_unit_output_flow_2{3};
        heat_flow_4{4}=H_gas;
        heat_flow_4{5}=work_unit_output_flow_2{4};
    else
```

```
        heat_flow_3{1}=work_unit_output_flow_2{1};
        heat_flow_3{2}=work_unit_output_flow_2{2};
        heat_flow_3{3}=work_unit_output_flow_2{3};
        heat_flow_3{4}=output_enthalpy_2;
        heat_flow_3{5}=work_unit_output_flow_2{4};
        heat_flow_4=[];
    end
else
    heat_flow_3=[];
    heat_flow_4=[];
end
```

A14. Code for approach temperature calculation

```
function approach_temperature=sub_approach_temperature_capture(Z1,Z2)

N_plot=0;

global ifplot

if ifplot
    N=50;
else
    N=50;
end

approach_temperature=100;
A1=length(Z1);
A2=length(Z2);
A=A1+A2;
for i=1:A1
    y{i}=Z1{i};
    a=Z1{i};
    T_in_1=ST(a{2},a{3},a{5});
    T_in_2=ST(a{2},a{4},a{5});
    b={a{1},a{2},T_in_1,T_in_2,a{5}};
end

for i=(A1+1):A
    y{i}=Z2{i-A1};
    a=Z2{i-A1};
    T_in_1=ST(a{2},a{3},a{5});
    T_in_2=ST(a{2},a{4},a{5});
    b={a{1},a{2},T_in_1,T_in_2,a{5}};

end

for i=1:A
    Tempy=y{i};
    [Q_(i) y_update]= temperature_ordering(y{i});
    y_update_{i}=y_update;
end

Q_all_HR=0;
Q_all_HA=0;

k1=0;
k2=0;
for i=1:A
[Q_all_HR Q_all_HA y_HR y_HA]=heat_source_grouping(Q_all_HR,Q_all_HA,Q_(i),y_update_{i});

if ~isempty(y_HR)
    k1=k1+1;
    y_HR_{k1}= y_HR;
    y_HR;
end

if ~isempty(y_HA)
    k2=k2+1;
    y_HA_{k2}= y_HA;
    y_HA;
end
```

```
end

if abs((Q_all_HR+Q_all_HA)/Q_all_HR)>0.01
    approach_temperature=-5;
    return;
else
    for i=1:A
        approach_temperature=mass_sign(y{i});
        if approach_temperature<0
            return
        end
    end

    for Q=0:Q_all_HR/N:Q_all_HR
        if ifplot
            N_plot=N_plot+1;
            Heat_all(N_plot)=Q;
            Temp_temperature_High(N_plot)=sub_temperature_capture(Q,y_HR_)-273.15*0;
            Temp_temperature_Low(N_plot)=sub_temperature_capture(Q,y_HA_)-273.15*0;
        end
        Temp_temperature_HR=sub_temperature_capture(Q,y_HR_);
        Temp_temperature_HA=sub_temperature_capture(Q,y_HA_);
        Approach_temperature_temp=Temp_temperature_HR-Temp_temperature_HA;
        if Approach_temperature_temp<approach_temperature
            approach_temperature=Approach_temperature_temp;
            if approach_temperature<0
                T_high=Temp_temperature_HR;
                T_low=Temp_temperature_HA;
            return
            end
        end
    end
end

if ifplot

plot(Heat_all,Temp_temperature_High,'-.c^',...
         Heat_all,Temp_temperature_Low,'-.k>','LineWidth',3);
end

approach_temperature=approach_temperature;

function [Q y_update]=temperature_ordering(y2)

    if ~isempty(y2)
            M_1=y2{1};
            P_1=y2{2};
            H_1_in=y2{3};
            H_1_out=y2{4};
            fluid_1=y2{5};

            T_1_in=ST(P_1,H_1_in,fluid_1);
            T_1_out=ST(P_1,H_1_out,fluid_1);

            Q=M_1*(H_1_in-H_1_out);

            if T_1_in<T_1_out
                y_update{1}=M_1;
                y_update{2}=T_1_in;
                y_update{3}=T_1_out;
                y_update{4}=P_1;
                y_update{5}=P_1;
                y_update{6}=fluid_1;
            else
                y_update{1}=M_1;
                y_update{2}=T_1_out;
                y_update{3}=T_1_in;
                y_update{4}=P_1;
                y_update{5}=P_1;
                y_update{6}=fluid_1;
            end

    else
        Q=[];
```

```
        y_update=y2;
    end

function [Q_all_HR Q_all_HA y_HR y_HA]=heat_source_grouping(Q_all_HR,Q_all_HA,Q,y)

if ~isempty(Q)
    if Q>0
        Q_all_HR=Q_all_HR+Q;
        y_HR=y;
        y_HA=[];
    else
        Q_all_HA=Q_all_HA+Q;
        y_HR=[];
        y_HA=y;
    end
else
    y_HR=[];
    y_HA=[];
end

function T_out=mass_sign(y)

T_out=100;

if ~isempty(y)
    if y{1}<0
        T_out=-5;
    end
end

%%%%%%%%%%%%%%%%%%%%%%%%%%%%%%%%%%%%%%%%%%%%%%%%%%%%%%%%%%%%%%%%%%%%%%%%%%%%
%%%%%%%%%%%%%%%%%%%%%%%%%%%%%%%%%%%%%%%%%%%%%%%%%%%%%%%%%%%%%%%%%%%%%%%%%%%%
function T_in=ST(P_in,H_in,fluid)

length_fluid=length(fluid);
if length_fluid==3
    if fluid=='CO2'
        IFCO2=1;
    else
        IFCO2=0;
    end
else
    IFCO2=0;
end

if length_fluid==6
    if fluid=='OXYGEN'
        IFO2=1;
    else
        IFO2=0;
    end
else
    IFO2=0;
end
%%%%%%%%%%%%%%%%%%%%%%%%%%%%%%%%%%%%%%%%%%%%%%%%%%%%%%%%%%%%%%%%%%%%%%%%%%%%

if IFCO2
    if P_in>100 && P_in<102
        if H_in>1.3278e+006
            Cp=Thermal_Property('C','P',P_in,'H',1.3278e+006,fluid);
            Cp=Thermal_Property('C','P',P_in,'H',1.3278e+006,fluid);
            T_in=1050+(H_in-1.3278e+006)/Cp;
        elseif H_in>4.3987e+005
            T_in=Thermal_Property('T','P',P_in,'H',H_in,fluid);
            T_in=Thermal_Property('T','P',P_in,'H',H_in,fluid);
        elseif H_in>4.2285e+005
            Cp=Thermal_Property('C','P',P_in,'H',4.3987e+005,fluid);
            Cp=Thermal_Property('C','P',P_in,'H',4.3987e+005,fluid);
            T_in=217+(H_in-4.3987e+005)/Cp;
        elseif H_in>-1.5059e+005
            T_in=195;
        else
            T_in=195+(H_in+1.5059e+005)/1240;
        end
```

```
    else
        T_in=Thermal_Property('T','P',P_in,'H',H_in,fluid);
        T_in=Thermal_Property('T','P',P_in,'H',H_in,fluid);
    end

elseif IFO2
    if P_in>100 && P_in<102
        if  H_in>9.2654e+005
            Cp=Thermal_Property('C','P',P_in,'H',9.2654e+005,fluid);
            Cp=Thermal_Property('C','P',P_in,'H',9.2654e+005,fluid);
            T_in=950+(H_in-9.2654e+005)/Cp;
        else
            T_in=Thermal_Property('T','P',P_in,'H',H_in,fluid);
            T_in=Thermal_Property('T','P',P_in,'H',H_in,fluid);
        end
    else
        T_in=Thermal_Property('T','P',P_in,'H',H_in,fluid);
        T_in=Thermal_Property('T','P',P_in,'H',H_in,fluid);
    end
else
        T_in=Thermal_Property('T','P',P_in,'H',H_in,fluid);
        T_in=Thermal_Property('T','P',P_in,'H',H_in,fluid);
end
```

A15. Code for process temperature capture

```
function Temp_temperature=sub_temperature_capture(Q,y1)

global minimum_temperature_grid

A1=length(y1);

Q_all=Q;

Tempa=y1{1};
T_min=Tempa{2};
T_max=Tempa{3};

for i=2:A1
[T_min T_max]=max_min_temperature(y1{i},T_min,T_max);
end

a=T_min;
b=T_max;

    while T_max-T_min > minimum_temperature_grid

            x = (T_max+T_min)/2;
            QQ=0;
            for i=1:A1
                QQ=QQ+Enthalpy_capture(y1{i},x);
            end


            if QQ<Q_all
                T_min = x;
            else
                T_max = x;
            end

    end
        Temp_temperature=(T_min+T_max)/2;


function Enthalpy=Enthalpy_capture(y2,x)

         if ~isempty(y2)

            M_1=y2{1};
            T_1_low=y2{2};
            T_1_high=y2{3};
            P_1_low=y2{4};
```

```
            P_1_high=y2{5};
            fluid_1=y2{6};

            if x<T_1_low
                [S_1_temp H_1_temp]=SH(T_1_low,P_1_low,fluid_1);

            elseif x<T_1_high
            P_1_temp=P_1_low+(P_1_high-P_1_low)*(x-T_1_low)/(T_1_high-T_1_low);
            [S_1_temp H_1_temp]=SH(x,P_1_temp,fluid_1);

            else
            [S_1_temp H_1_temp]=SH(T_1_high,P_1_high,fluid_1);

            end

            [S_1_low H_1_low]=SH(T_1_low,P_1_low,fluid_1);

            Enthalpy=M_1*(H_1_temp-H_1_low);

         else
            Enthalpy=0;
         end

function [T_min T_max]=max_min_temperature(y2,T_min,T_max)

    if ~isempty(y2)
    if y2{2}<T_min
        T_min=y2{2};
    end
    if y2{3}>T_max
        T_max=y2{3};
    end
    end

function [T_min T_max]=max_min(y1,y2,y3,y4,y5,y6,y7,y8,y9,y10,y11,y12,y13,y14,y15)

    if ~isempty(y1)
        T_min=y1{2};
        T_max=y1{3};
        return
    else if ~isempty(y2)
            T_min=y2{2};
            T_max=y2{3};
            return
        else if ~isempty(y3)
                T_min=y3{2};
                T_max=y3{3};
                return
            else if ~isempty(y4)
                    T_min=y4{2};
                    T_max=y4{3};
                    return
                else if ~isempty(y5)
                        T_min=y5{2};
                        T_max=y5{3};
                        return
                    else if ~isempty(y6)
                            T_min=y6{2};
                            T_max=y6{3};
                            return
                        else if ~isempty(y7)
                                T_min=y7{2};
                                T_max=y7{3};
                                return
                            else if ~isempty(y8)
                                    T_min=y8{2};
                                    T_max=y8{3};
                                    return
                                else if ~isempty(y9)
                                        T_min=y9{2};
                                        T_max=y9{3};
                                        return
                                    else if ~isempty(y10)
                                            T_min=y10{2};
```

```
                                            T_max=y10{3};
                                            return
                                        else if ~isempty(y11)
                                                T_min=y11{2};
                                                T_max=y11{3};
                                                return
                                            else if ~isempty(y12)
                                                    T_min=y12{2};
                                                    T_max=y12{3};
                                                    return
                                                else if ~isempty(y13)
                                                        T_min=y13{2};
                                                        T_max=y13{3};
                                                        return
                                                    else if ~isempty(y14)
                                                            T_min=y14{2};
                                                            T_max=y14{3};
                                                            return
                                                        else
                                                            T_min=y15{2};
                                                            T_max=y15{3};
                                                        end
                                                    end
                                                end
                                            end
                                        end
                                    end
                                end
                            end
                        end
                    end
                end
            end
        end
    end

%%%%%%%%%%%%%%%%%%%%%%%%%%%%%%%%%%%%%%%%%%%%%%%%%%%%%%%%%%%%%%%%%%%%%%
%%%%%%%%%%%%%%%%%%%%%%%%%%%%%%%%%%%%%%%%%%%%%%%%%%%%%%%%%%%%%%%%%%%%%%
    function [S_in H_in]=SH(T_in,P_in,fluid)

length_fluid=length(fluid);
if length_fluid==3
    if fluid=='CO2'
        IFCO2=1;
        T_limit=217;
    else
        IFCO2=0;
        T_limit=20;
    end
else
    T_limit=20;
    IFCO2=0;
end

if length_fluid==6
    if fluid=='OXYGEN'
        IFO2=1;
    else
        IFO2=0;
    end
else
    IFO2=0;
end
%%%%%%%%%%%%%%%%%%%%%%%%%%%%%%%%%%%%%%%%%%%%%%%%%%%%%%%%%%%%%%%%%%%%%%%%%%%

if IFCO2
    if T_in>1050
        S_1050=Thermal_Property('S','T',1050,'P',P_in,fluid);
        S_1050=Thermal_Property('S','T',1050,'P',P_in,fluid);

        H_1050=Thermal_Property('H','T',1050,'P',P_in,fluid);
        H_1050=Thermal_Property('H','T',1050,'P',P_in,fluid);

        Cp=Thermal_Property('C','T',1050,'P',P_in,fluid);
```

```
        Cp=Thermal_Property('C','T',1050,'P',P_in,fluid);

        S_in=S_1050+Cp*(log(T_in/1050));
        H_in=H_1050+Cp*(T_in-1050);
    elseif T_in>T_limit
        S_in=Thermal_Property('S','T',T_in,'P',P_in,fluid);
        S_in=Thermal_Property('S','T',T_in,'P',P_in,fluid);

        H_in=Thermal_Property('H','T',T_in,'P',P_in,fluid);
        H_in=Thermal_Property('H','T',T_in,'P',P_in,fluid);
    elseif T_in>195.15
            Cp=Thermal_Property('C','T',T_limit,'P',P_in,fluid);
            Cp=Thermal_Property('C','T',T_limit,'P',P_in,fluid);

            H_limit=Thermal_Property('H','T',T_limit,'P',P_in,fluid);
            H_limit=Thermal_Property('H','T',T_limit,'P',P_in,fluid);

            S_limit=Thermal_Property('S','T',T_limit,'P',P_in,fluid);
            S_limit=Thermal_Property('S','T',T_limit,'P',P_in,fluid);

            S_in=S_limit+Cp*(log(T_in/T_limit));
            H_in=H_limit+Cp*(T_in-T_limit);
    elseif T_in>194.85
                Cp=Thermal_Property('C','T',T_limit,'P',P_in,fluid);
                Cp=Thermal_Property('C','T',T_limit,'P',P_in,fluid);

                H_limit=Thermal_Property('H','T',T_limit,'P',P_in,fluid);
                H_limit=Thermal_Property('H','T',T_limit,'P',P_in,fluid);

                S_limit=Thermal_Property('S','T',T_limit,'P',P_in,fluid);
                S_limit=Thermal_Property('S','T',T_limit,'P',P_in,fluid);

                S_tem=S_limit+Cp*(log(195.15/T_limit));
                H_tem=H_limit+Cp*(195.15-T_limit);

                C=573000/(195.15-194.85);
                S_in=S_tem+C*(log(T_in/195.15));
                H_in=H_tem+C*(T_in-195.15);
    else
                Cp=Thermal_Property('C','T',T_limit,'P',P_in,fluid);
                Cp=Thermal_Property('C','T',T_limit,'P',P_in,fluid);

                H_limit=Thermal_Property('H','T',T_limit,'P',P_in,fluid);
                H_limit=Thermal_Property('H','T',T_limit,'P',P_in,fluid);

                S_limit=Thermal_Property('S','T',T_limit,'P',P_in,fluid);
                S_limit=Thermal_Property('S','T',T_limit,'P',P_in,fluid);

                S_tem=S_limit+Cp*(log(195.15/T_limit));
                H_tem=H_limit+Cp*(195.15-T_limit);

                C=573000/(195.15-194.85);
                S_tem_1=S_tem+C*(log(194.85/195.15));
                H_tem_1=H_tem+C*(194.85-195.15);

                C2=1.24*1000;
                S_in=S_tem_1+C2*(log(T_in/194.85));
                H_in=H_tem_1+C2*(T_in-194.85);
    end
elseif IFO2
    if T_in<950
        S_in=Thermal_Property('S','T',T_in,'P',P_in,fluid);
        S_in=Thermal_Property('S','T',T_in,'P',P_in,fluid);

        H_in=Thermal_Property('H','T',T_in,'P',P_in,fluid);
        H_in=Thermal_Property('H','T',T_in,'P',P_in,fluid);
    else
        H_0=Thermal_Property('H','T',950,'P',P_in,fluid);
        H_0=Thermal_Property('H','T',950,'P',P_in,fluid);

        S_0=Thermal_Property('S','T',950,'P',P_in,fluid);
        S_0=Thermal_Property('S','T',950,'P',P_in,fluid);

        Cp=Thermal_Property('C','P',P_in,'H',H_0,fluid);
```

```
        Cp=Thermal_Property('C','P',P_in,'H',H_0,fluid);

        H_in=H_0+(T_in-950)*Cp;
        S_in=S_0+Cp*(log(T_in/950));
    end
else
        S_in=Thermal_Property('S','T',T_in,'P',P_in,fluid);
        S_in=Thermal_Property('S','T',T_in,'P',P_in,fluid);

        H_in=Thermal_Property('H','T',T_in,'P',P_in,fluid);
        H_in=Thermal_Property('H','T',T_in,'P',P_in,fluid);
end
```

A16. Code for thermal property calculation

```
function Output=Thermal_Property(Object,Property_A,Value_A,Property_B,Value_B,Fluid)
switch Fluid
    case 'AIR'
        if Property_A=='P'
            if Value_A>3500 && Value_A<3800
                a1=refpropm(Object,Property_A,3500,Property_B,Value_B,Fluid);
                a1=refpropm(Object,Property_A,3500,Property_B,Value_B,Fluid);
                a2=refpropm(Object,Property_A,3800,Property_B,Value_B,Fluid);
                a2=refpropm(Object,Property_A,3800,Property_B,Value_B,Fluid);
                Output=a1-(a1-a2)/(3500-3800)*(3500-Value_A);
            else
                Output=refpropm(Object,Property_A,Value_A,Property_B,Value_B,Fluid);
                Output=refpropm(Object,Property_A,Value_A,Property_B,Value_B,Fluid);
            end
        elseif Property_B=='P'
            if Value_B>3500 && Value_B<3800
                a1=refpropm(Object,Property_A,Value_A,Property_B,3500,Fluid);
                a1=refpropm(Object,Property_A,Value_A,Property_B,3500,Fluid);
                a2=refpropm(Object,Property_A,Value_A,Property_B,3800,Fluid);
                a2=refpropm(Object,Property_A,Value_A,Property_B,3800,Fluid);
                Output=a1-(a1-a2)/(3500-3800)*(3500-Value_B);
            else
                Output=refpropm(Object,Property_A,Value_A,Property_B,Value_B,Fluid);
                Output=refpropm(Object,Property_A,Value_A,Property_B,Value_B,Fluid);
            end
        else
            Output=refpropm(Object,Property_A,Value_A,Property_B,Value_B,Fluid);
            Output=refpropm(Object,Property_A,Value_A,Property_B,Value_B,Fluid);
        end
    case 'NITROGEN'
        Output=refpropm(Object,Property_A,Value_A,Property_B,Value_B,Fluid);
        Output=refpropm(Object,Property_A,Value_A,Property_B,Value_B,Fluid);
    otherwise
        Output=refpropm(Object,Property_A,Value_A,Property_B,Value_B,Fluid);
        Output=refpropm(Object,Property_A,Value_A,Property_B,Value_B,Fluid);
end
```

A17. Code for thermal cycle calculation

```
function [W_total Heat_amount M_product
Output_heat_flow]=THERMALCYCLE(Start_point,End_point,Stage_number,if_product,outlet_parameter)


Input_flow{1}=Start_point; %%%%In the form of {1.0,500,2.5e5,'Nitrogen'};

N=length(outlet_parameter);

for i=1:N
    Output_paramether{i,:}=outlet_parameter{i};
end

Output_paramether_end=End_point; %%%In the form of {500,2.5e5,2.5e5,1};
k=1;
M_product=0;
```

```
Flow_number_start=1;
N=Stage_number;
W_total=0;
Flow_number_end=1;

Heat_amount=0;

for i=1:N
    tem_flow_number=k;
    for j=Flow_number_start:Flow_number_end
        x=i;
        y=j;
        if i~=N
            [W M_liquid_product heat_flow_1 heat_flow_2 heat_flow_3 heat_flow_4] =
stream_splitting(Input_flow{j},Output_paramether{j,:},if_product);
        else
            [W M_liquid_product heat_flow_1 heat_flow_2 heat_flow_3 heat_flow_4] =
stream_splitting(Input_flow{j},Output_paramether_end,if_product);
        end
        W_total=W+W_total;
        M_product=M_product+M_liquid_product;

        if ~isempty(heat_flow_1)
            Output_heat_flow{k,:}=heat_flow_1;
            Heat_amount=Heat_amount+heat_flow_1{1}*(heat_flow_1{4}-heat_flow_1{3});
            k=k+1;
            Input_flow{k}={heat_flow_1{1},heat_flow_1{2},heat_flow_1{4},heat_flow_1{5}};
        end
        if ~isempty(heat_flow_2)
            Output_heat_flow{k,:}=heat_flow_2;
            Heat_amount=Heat_amount+heat_flow_2{1}*(heat_flow_2{4}-heat_flow_2{3});
            k=k+1;
            Input_flow{k}={heat_flow_2{1},heat_flow_2{2},heat_flow_2{4},heat_flow_2{5}};
        end
        if ~isempty(heat_flow_3)
            Output_heat_flow{k,:}=heat_flow_3;
            Heat_amount=Heat_amount+heat_flow_3{1}*(heat_flow_3{4}-heat_flow_3{3});
            k=k+1;
            Input_flow{k}={heat_flow_3{1},heat_flow_3{2},heat_flow_3{4},heat_flow_3{5}};
        end
        if ~isempty(heat_flow_4)
            Output_heat_flow{k,:}=heat_flow_4;
            Heat_amount=Heat_amount+heat_flow_4{1}*(heat_flow_4{4}-heat_flow_4{3});
            k=k+1;
            Input_flow{k}={heat_flow_4{1},heat_flow_4{2},heat_flow_4{4},heat_flow_4{5}};
        end

    end
    Flow_number_start=tem_flow_number+1;
    Flow_number_end=k;

end
```

Appendix B Economic Model

The expressions of purchase the main components costs and amortization factor are presented below.

- Cryogenic pumps [176]

$$I_P = 3540W^{0.71} \tag{B1}$$

Where W is the power consumption of the cryogenic pump (Unit: kW) and I_P is the purchase cost of the cryogenic pump (Unit: USD).

- Combustion chamber [176, 205]

$$I_{CB} = 9728\dot{m}\left[1+\exp\left(0.018T_O - 26.4\right)\right] \tag{B2}$$

Where $\dot{m}$ is mass flowrate of air (Unit: kg/s; In the following calculation the mass flowrate of oxygen and blending gas is used as it is a oxy-combustion process) and T_O is the combustor outlet temperature (Unit: °C). I_{CB} is the purchase cost of the combustion chamber (Unit: USD).

- Compressor [175, 176, 205]

$$I_{CP} = \left(\frac{75\dot{m}}{0.9-\eta_{CP}}\right)\left(\frac{P_O}{P_I}\right)\ln\left(\frac{P_O}{P_I}\right) \tag{B3}$$

Where $\dot{m}$ is mass flowrate of the working fluid (Unit: kg/s), η_{CP} is the isentropic efficiency of the compressor, P_I and P_O are respectively the inlet and outlet pressures of the compressor and I_{CP} is the purchase cost of the compressor (Unit: USD).

- Expanders (including high pressure turbines and low pressure turbine) [176]:

$$I_{EP} = 6000W^{0.7} \tag{B4}$$

Where W is the power output of the expander (Unit: kW) and I_{EP} is the purchase cost of the expander (Unit: USD).

- Gas Turbine [176, 205]

$$I_{GT} = \left(\frac{1536\dot{m}}{0.92-\eta_{GT}}\right)\ln\left(\frac{P_I}{P_O}\right)\left[1+\exp\left(0.036T_I - 26.4\right)\right] \tag{B5}$$

Where $\dot{m}$ is mass flowrate of the working fluid (Unit: kg/s), η_{GT} is the isentropic efficiency of the gas turbine, P_I and P_O are respectively the inlet and outlet pressures of the gas turbine, T_I is the inlet temperature of the gas turbine and I_{GT} is the purchase cost of the gas turbine (Unit: USD).

- Electric generator [176]

$$I_{GEN} = 60W^{0.95} \tag{B6}$$

Where W is the generated power of the electric generator (Unit: kW) and I_{GEN} is the purchase cost of the electric generator (Unit: USD).

- Counter flow heat exchanger [174]

$$I_{HX} = 130\left(\frac{A_{HX}}{0.093}\right)^{0.78} \tag{B7}$$

Where A_{HX} is the heat exchanger area (Unit: m^2) and I_{HX} is the purchase cost of the counter flow heat exchanger (Unit: USD). A_{HX} is calculated from:

$$A_{HX} = \frac{\dot{Q}}{h\Delta T} \tag{B8}$$

Where $\dot{Q}$ is the heat load (Unit: W), h is heat transfer coefficient (Unit: $W/(m^2 \cdot K)$) and ΔT is the average temperature difference between the hot and cold fluids:

- Annuity factor [176, 206]

$$f = \left[\frac{q^{(k+CP)}-1}{(q-1)q^{k+CP}} - \frac{q^{CP}-1}{(q-1)q^{CP}}\right]^{-1} \tag{B9}$$

Where k is the amortization period (Unit: year) and CP is the construction period (Unit: year). q is calculated as:

$$q = \left(1+\frac{in}{100}\right)\left(1+\frac{ri}{100}\right) \tag{B10}$$

Where in is interest rate (Unit: %/year) and ri is the rate of inflation (Unit: %/year).

Appendix C Publications

JOURNAL PAPER:

1)H. Chen, T.N. Cong, W. Yang, C. Tan, ***Y. Li,*** and Y. Ding, Progress in electrical energy storage system: A critical review. Progress in Natural Science 19 (2009) 291-312.

2)***Y. Li***, H. Chen, and Y. Ding, Fundamentals and applications of cryogen as a thermal energy carrier: A critical assessment. International Journal of Thermal Sciences 49 (2010) 941-949.

3)***Y. Li***, H. Chen, X. Zhang, C. Tan and Y. Ding, Renewable energy carriers: Hydrogen or liquid air/nitrogen? Applied Thermal Engineering 30 (2010) 1985-1990.

4)***Y. Li***, Y. Jin, H. Chen, C. Tan and Y. Ding, An integrated system for thermal power generation, electrical energy storage and CO_2 capture. International Journal of Energy Research 35 (2011) 1158-1167.

5)H. Chen, Y. Ding, ***Y. Li***, X. Zhang and C. Tan, Air fuelled zero emission road transportation: A comparative study. Applied Energy 88 (2011) 337-342.

6)***Y. Li***, X. Wang, Y. Jin and Y. Ding, An integrated solar-cryogen hybrid power system. Renewable Energy 37 (2012) 76-81.

7)***Y. Li*** and Y. Ding, An optimal design methodology for large-scale gas liquefaction. Applied Energy, under review.

8)***Y. Li***, X. Wang and Y. Ding, A cryogen based peak-shaving technology: systematic approach and techno-economic analysis. International Journal of Energy Research, accepted.

PATENT:

9)Y. Ding, ***Y. Li***, Y. Jin, H. Chen and C. Tan, An integrated power system for electricity generation, energy storage and CO_2 capture, filed in May 2010, Chinese Patent.

Bibliography

1. Chen H, Cong TN, Yang W, Tan C, Li Y, Ding Y: **Progress in electrical energy storage system: A critical review**. *Progress in Natural Science* 2009, **19**(3):291-312.
2. **Metered half-hourly electricity demands** [http://www.nationalgrid.com/uk/Electricity/Data/Demand+Data/]
3. Makansi J, Abboud J: **Energy Storage: The missing link in the electricity value chain**. In: Editor|. City|: Publisher|; Year|:Pages|. [|Series Editor (Series Editor^Editors|): *Series Title*|, vol Series Volume|]|.
4. Stodola N, Modi V: **Penetration of solar power without storage**. *Energy Policy* 2009, **37**(11):4730-4736.
5. Kabisama HW: **Electrical power engineering**: New York ; London : McGraw-Hill; 1993.
6. EIA: **Electric Power Annual Report**. In: Editor|. City|: Publisher|; Year|:Pages|. [|Series Editor (Series Editor^Editors|): *Series Title*|, vol Series Volume|]|.
7. Hamidi V, Li F, Robinson F: **Demand response in the UK's domestic sector**. *Electric Power Systems Research* 2009, **79**(12):1722-1726.
8. Ricky Rambharat B, Brockwell AE, Seppi DJ: **A threshold autoregressive model for wholesale electricity prices**. *Journal of the Royal Statistical Society: Series C (Applied Statistics)* 2005, **54**(2):287-299.
9. Veziroglu TN, Sahin S: **21st Century's energy: Hydrogen energy system**. *Energy Conversion and Management* 2008, **49**(7):1820-1831.
10. Alnaser WE: **Estimation of energy from tide, wave and sea water currents in Bahrain**. *Renewable Energy* 1993, **3**(2-3):235-238.
11. REN21: **Renewables 2007 Global Status Report** In: Editor|. City|: Publisher|; Year|:Pages|. [|Series Editor (Series Editor^Editors|): *Series Title*|, vol Series Volume|]|.
12. H.M.Government: **Meeting the Energy Challenge: a white paper on energy**. In: Editor|. City|: Publisher|; Year|:Pages|. [|Series Editor (Series Editor^Editors|): *Series Title*|, vol Series Volume|]|.
13. Verbruggen A: **Renewable and nuclear power: A common future?** *Energy Policy* 2008, **36**(11):4036-4047.
14. Weisser D, Garcia RS: **Instantaneous wind energy penetration in isolated electricity grids: concepts and review**. *Renewable Energy* 2005, **30**(8):1299-1308.
15. Meisen P: **Linking Renewable Energy Resources Around the World: A Compelling Global Strategy**. *Power Engineering Review, IEEE* 1996, **16**(7):18-.
16. Vazquez S, Lukic SM, Galvan E, Franquelo LG, Carrasco JM: **Energy Storage Systems for Transport and Grid Applications**. *Industrial Electronics, IEEE Transactions on* 2010, **57**(12):3881-3895.
17. Walawalkar R, Apt J, Mancini R: **Economics of electric energy storage for energy arbitrage and regulation in New York**. *Energy Policy* 2007, **35**(4):2558-2568.
18. van der Linden S: **Bulk energy storage potential in the USA, current developments and future prospects**. *Energy* 2006, **31**(15):3446-3457.
19. Kondoh J, Ishii I, Yamaguchi H, Murata A, Otani K, Sakuta K, Higuchi N, Sekine S, Kamimoto M: **Electrical energy storage systems for energy networks**. *Energy Conversion and Management* 2000, **41**(17):1863-1874.
20. Hall PJ, Bain EJ: **Energy-storage technologies and electricity generation**. *Energy Policy* 2008, **36**(12):4352-4355.

21. Ibrahim H, Ilinca A, Perron J: **Energy storage systems--Characteristics and comparisons**. *Renewable and Sustainable Energy Reviews* 2008, **12**(5):1221-1250.
22. Morisson V, Rady M, Palomo E, Arquis E: **Thermal energy storage systems for electricity production using solar energy direct steam generation technology**. *Chemical Engineering and Processing: Process Intensification* 2008, **47**(3):499-507.
23. You Y, Hu EJ: **A medium-temperature solar thermal power system and its efficiency optimisation**. *Applied Thermal Engineering* 2002, **22**(4):357-364.
24. Vaivudh S, Rakwichian W, Chindaruksa S: **Heat transfer of high thermal energy storage with heat exchanger for solar trough power plant**. *Energy Conversion and Management* 2008, **49**(11):3311-3317.
25. *Proceedings of the High efficency integration of thermodynamic solar plant with natural gas combined cycle: 2007*.
26. Smith EM: **Storage of electrical energy using supercritical liquid air**. *ARCHIVE: Proceedings of the Institution of Mechanical Engineers 1847-1982 (vols 1-196)* 1977, **191**(1977):289-298.
27. Kooichi C, Hidefumi A: **Evaluation of energy storage method using liquid air**. *Heat Transfer—Asian Research* 2000, **29**(5):347-357.
28. Ahern JE: **Applications of the 2nd Law of Thermodynamics to Cryogenics - a Review**. *Energy* 1980, **5**(8-9):891-897.
29. Hoyeon K: **Review on economical efficiency of LNG cold energy use in South Korea**. In: *23rd World Gas Conference,: 2006; Amsterdam*; 2006.
30. Fyke A, Li D, Crane P, Scott DS: **Recovery of thermomechanical exergy from cryofuels**. *International Journal of Hydrogen Energy* 1997, **22**(4):435-440.
31. Ordonez CA: **Liquid nitrogen fueled, closed Brayton cycle cryogenic heat engine**. *Energy Conversion and Management* 2000, **41**(4):331-341.
32. Zalba B, Marín JM, Cabeza LF, Mehling H: **Review on thermal energy storage with phase change: materials, heat transfer analysis and applications**. *Applied Thermal Engineering* 2003, **23**(3):251-283.
33. Cornot-Gandolphe S, Appert O, Dickel R, Chabrelie M-F, Rojey A: **The challenges of turther cost reductions for new supply options (pipeline, LNG, GTL)**. In: *22nd World Gas Conference: 2003; Tokyo, Japan*; 2003.
34. Bai FF, Mang ZX: **Integration of low-level waste heat recovery and Liquefied Nature Gas cold energy utilization**. *Chinese Journal of Chemical Engineering* 2008, **16**(1):95-99.
35. Shin JY, Jeon YJ, Maeng DJ, Kim JS, Ro ST: **Analysis of the dynamic characteristics of a combined-cycle power plant**. *Energy* 2002, **27**(12):1085-1098.
36. Saleh B, Koglbauer G, Wendland M, Fischer J: **Working fluids for low-temperature organic Rankine cycles**. *Energy* 2007, **32**(7):1210-1221.
37. Chen Y, Lundqvist P, Johansson A, Platell P: **A comparative study of the carbon dioxide transcritical power cycle compared with an organic rankine cycle with R123 as working fluid in waste heat recovery**. *Applied Thermal Engineering* 2006, **26**(17-18):2142-2147.
38. Jha AR: **Cryogenic Technology and Applications**: Butterworth-Heinemann; 2006.
39. Cammarata G, Fichera A, Guglielmino D: **Optimization of a liquefaction plant using genetic algorithms**. *Applied Energy* 2001, **68**(1):19-29.
40. Maytal BZ: **Maximizing production rates of the Linde-Hampson machine**. *Cryogenics* 2006, **46**(1):49-54.
41. Mehmet K, Ibrahim D, Marc AR: **Performance analysis of gas liquefaction cycles**. *International Journal of Energy Research* 2008, **32**(1):35-43.

42. Remeljej CW, Hoadley AFA: **An exergy analysis of small-scale liquefied natural gas (LNG) liquefaction processes**. *Energy* 2006, **31**(12):2005-2019.
43. Chang H-M, Chung MJ, Kim MJ, Park SB: **Thermodynamic design of methane liquefaction system based on reversed-Brayton cycle**. *Cryogenics* 2009, **49**(6):226-234.
44. Li QY, Ju YL: **Design and analysis of liquefaction process for offshore associated gas resources**. *Applied Thermal Engineering* 2010, **In Press, Corrected Proof**.
45. Kirillov NG: **Analysis of Modern Natural Gas Liquefaction Technologies**. *Chemical and Petroleum Engineering* 2004, **40**(7):401-406.
46. Mehmet K, gbreve, lu: **Exergy analysis of multistage cascade refrigeration cycle used for natural gas liquefaction**. *International Journal of Energy Research* 2002, **26**(8):763-774.
47. Brostow AA, Agrawal R, Herron DM, Roberts MJ: **Process for nitrogen liquefaction**. In. *Volume US 6298688* Editor|. City|: Publisher|; Year|:Pages|. [|Series Editor (Series Editor^Editors|): *Series Title*|, vol Series Volume|]|.
48. Chang H-M, Chung MJ, Lee S, Choe KH: **An efficient multi-stage Brayton-JT cycle for liquefaction of natural gas**. *Cryogenics* 2010, **In Press, Corrected Proof**.
49. Finn AJ, Johnson GL, Tomlinson TR: **Developments in natural gas liquefaction**. *Hydrocarbon Processing* 1999, **78**(4):47-59.
50. Krasae-in S, Stang JH, Neksa P: **Development of large-scale hydrogen liquefaction processes from 1898 to 2009**. *International Journal of Hydrogen Energy* 2010, **35**(10):4524-4533.
51. Nogal FD, Kim J-K, Perry S, Smith R: **Optimal Design of Mixed Refrigerant Cycles**. *Industrial & Engineering Chemistry Research* 2008, **47**(22):8724-8740.
52. Li Y, Chen H, Zhang X, Tan C, Ding Y: **Renewable energy carriers: Hydrogen or liquid air/nitrogen?** *Applied Thermal Engineering* 2010, **30**(14-15):1985-1990.
53. Lee GC, Smith R, Zhu XX: **Optimal Synthesis of Mixed-Refrigerant Systems for Low-Temperature Processes**. *Industrial & Engineering Chemistry Research* 2002, **41**(20):5016-5028.
54. Vaidyaraman S, Maranas CD: **Synthesis of Mixed Refrigerant Cascade Cycles**. *Chemical Engineering Communications* 2002, **189**(8):1057 - 1078.
55. Mokarizadeh Haghighi Shirazi M, Mowla D: **Energy optimization for liquefaction process of natural gas in peak shaving plant**. *Energy* 2010, **35**(7):2878-2885.
56. *Proceedings of the Liquefaction technology; developments through history: 2009.* Elsevier.
57. Yooh J-i, Lee H-s, Oh S-t, Lee S-g, Choi K-h: **Characteristics of cascade and C3MR cycle on natural gas liquefaction process**. *World academy of secience engineering and technology* 2009, **59**.
58. Jensen JB, Skogestad S, Pantelides WMaC: **Optimal operation of a mixed fluid cascade LNG plant**. In: *Computer Aided Chemical Engineering*. *Volume Volume 21*y Editor|. City|: Publisher|; Year|:Pages|. [|Series Editor (Series Editor^Editors|): *Series Title*|, vol Series Volume|]|.
59. Miller J, Luyben WL, Blouin S: **Economic Incentive for Intermittent Operation of Air Separation Plants with Variable Power Costs**. *Industrial & Engineering Chemistry Research* 2008, **47**(4):1132-1139.
60. Atrey MD: **Thermodynamic analysis of Collins helium liquefaction cycle**. *Cryogenics* 1998, **38**(12):1199-1206.

61. Syed MT, Sherif SA, Veziroglu TN, Sheffield JW: **Second law analysis of hydrogen liquefiers operating on the modified Collins cycle**. *International Journal of Energy Research* 2001, **25**(11):961-978.
62. Kuz'menko IF, Morkovkin IM, Gurov EI: **Concept of Building Medium-Capacity Hydrogen Liquefiers with Helium Refrigeration Cycle**. *Chemical and Petroleum Engineering* 2004, **40**(1):94-98.
63. *Proceedings of the Conceptual design of a high efficiency large capacity hydrogen liquefier: 2002; Madison, Wisconsin (USA).* AIP.
64. Valenti G, Macchi E: **Proposal of an innovative, high-efficiency, large-scale hydrogen liquefier**. *International Journal of Hydrogen Energy* 2008, **33**(12):3116-3121.
65. Bracha M, Lorenz G, Patzelt A, Wanner M: **Large-scale hydrogen liquefaction in Germany**. *International Journal of Hydrogen Energy* 1994, **19**(1):53-59.
66. Nandi TK, Sarangi S: **Performance and optimization of hydrogen liquefaction cycles**. *International Journal of Hydrogen Energy* 1993, **18**(2):131-139.
67. Yin QS, Li HY, Fan QH, Jia LX: **ECONOMIC ANALYSIS OF MIXED-REFRIGERANT CYCLE AND NITROGEN EXPANDER CYCLE IN SMALL SCALE NATURAL GAS LIQUEFIER**. *AIP Conference Proceedings* 2008, **985**(1):1159-1165.
68. **Liquid expanders in LNG liquefaction plants**. *World Pumps* 2002, **2002**(431):16-16.
69. Kanoglu M: **Cryogenic turbine efficiencies**. *Exergy, An International Journal* 2001, **1**(3):202-208.
70. Qiang W, Li YZ, Xi C: **Exergy analysis of liquefied natural gas cold energy recovering cycles**. *International Journal of Energy Research* 2005, **29**(1):65-78.
71. Bisio G, Tagliafico L: **On the recovery of LNG physical exergy**. *35th Intersociety Energy Conversion Engineering Conference & Exhibit (Iecec), Vols 1 and 2, Technical Papers* 2000:309-317.
72. Bisio G, Tagliafico L: **On the recovery of LNG physical exergy by means of a simple cycle or a complex system**. *Exergy, An International Journal* 2002, **2**(1):34-50.
73. Deng SM, Jin HG, Cai RX, Lin RM: **Novel cogeneration power system with liquefied natural gas (LNG) cryogenic exergy utilization**. *Energy* 2004, **29**(4):497-512.
74. Qiang W, Li YZ, Jiang W: **Analysis of power cycle based on cold energy of liquefied natural gas and low-grade heat source**. *Applied Thermal Engineering* 2004, **24**(4):539-548.
75. Szargut J, Szczygiel I: **Utilization of the cryogenic exergy of liquid natural gas (LNG) for the production of electricity**. *Energy* 2009, **34**(7):827-837.
76. Zhang N, Lior N, Liu M, Han W: **COOLCEP (cool clean efficient power): A novel CO2-capturing oxy-fuel power system with LNG (liquefied natural gas) coldness energy utilization**. *Energy* 2010, **35**(2):1200-1210.
77. Kim TS, Ro ST: **Power augmentation of combined cycle power plants using cold energy of liquefied natural gas**. *Energy* 2000, **25**(9):841-856.
78. Kaneko K, Ohtani K, Tsujikawa Y, Fujii S: **Utilization of the cryogenic exergy of LNG by a mirror gas-turbine**. *Applied Energy* 2004, **79**(4):355-369.
79. Bisio G, Pisoni C: **Thermodynamic analysis of solar energy utilization combined with the exploitation of the LNG physical exergy**. *Journal of Solar Energy Engineering-Transactions of the Asme* 1995, **117**(4):333-335.

80. Najjar YSH: **A Cryogenic Gas-Turbine Engine Using Hydrogen for Waste Heat-Recovery and Regasification of Lng**. *International Journal of Hydrogen Energy* 1991, **16**(2):129-134.
81. Saxe M, Alvfors P: **Advantages of integration with industry for electrolytic hydrogen production**. *Energy* 2007, **32**(1):42-50.
82. Dispenza C, Dispenza G, La Rocca V, Panno G: **Exergy recovery during LNG regasification: Electric energy production - Part one**. *Applied Thermal Engineering* 2008, **In Press, Corrected Proof**.
83. Dispenza C, Dispenza G, Rocca VL, Panno G: **Exergy recovery during LNG regasification: Electric energy production - Part two**. *Applied Thermal Engineering* 2008, **In Press, Corrected Proof**.
84. Otsuka T: **Evolution of an LNG Terminal: Senboku Terminal of Osaka Gas**. In: *23rd World Gas Conference: 2006; Amsterdam*; 2006.
85. Lu T, K.S W: **Analysis and optimization of a cascading power cycle with liquefied natural gas (LNG) cold energy recovery**. *Applied Thermal Engineering* 2008, **In Press, Corrected Proof**.
86. Miyazaki T, Kang YT, Akisawa A, Kashiwagi T: **A combined power cycle using refuse incineration and LNG cold energy**. *Energy* 2000, **25**(7):639-655.
87. Shi X, Che D: **A combined power cycle utilizing low-temperature waste heat and LNG cold energy**. *Energy Conversion and Management* 2009, **50**(3):567-575.
88. Hisazumi Y, Yamasaki Y, Sugiyama S: **Proposal for a high efficiency LNG power-generation system utilizing waste heat from the combined cycle**. *Applied Energy* 1998, **60**(3):169-182.
89. Zhang N, Lior N: **A novel Brayton cycle with the integration of liquid hydrogen cryogenic exergy utilization**. *Proceedings of the ASME Advanced Energy Systems Division* 2005, **45**:541-551.
90. Zhang N, Lior N: **Proposal and analysis of a novel zero CO2 emission cycle with liquid natural gas cryogenic exergy utilization**. *Journal of Engineering for Gas Turbines and Power-Transactions of the Asme* 2006, **128**(1):81-91.
91. Zhang N, Lior N: **A novel near-zero CO2 emission thermal cycle with LNG cryogenic exergy utilization**. *Energy* 2006, **31**(10-11):1666-1679.
92. Zhang N, Lior N: **A novel Brayton cycle with the integration of liquid hydrogen cryogenic exergy utilization**. *International Journal of Hydrogen Energy* 2008, **33**(1):214-224.
93. Zhang N, Lior N: **Two novel oxy-fuel power cycles integrated with natural gas reforming and CO2 capture**. *Energy* 2008, **33**(2):340-351.
94. Najjar YSH, Zaamout MS: **Cryogenic power conversion with regasification of LNG in a gas turbine plant**. *Energy Conversion and Management* 1993, **34**(4):273-280.
95. Barbir F: **Transition to renewable energy systems with hydrogen as an energy carrier**. *Energy* 2009, **34**(3):308-312.
96. Salgi G, Donslund B, Alberg Østergaard P: **Energy system analysis of utilizing hydrogen as an energy carrier for wind power in the transportation sector in Western Denmark**. *Utilities Policy* 2008, **16**(2):99-106.
97. Wietschel M, Seydel P: **Economic impacts of hydrogen as an energy carrier in European countries**. *International Journal of Hydrogen Energy* 2007, **32**(15):3201-3211.
98. Pelc R, Fujita RM: **Renewable energy from the ocean**. *Marine Policy* 2002, **26**(6):471-479.

99. M.F.Merriam: **Wind, waves and tides**. *Annual Reviews Energy* 1978, **3**(3):27.
100. John T, George S, Margaret M, Pin-Ching M, Ben K, Maria G, J ER, Dan B: **Renewable hydrogen production**. *International journal of energy research* 2008, **32**(29):379-407.
101. Wurster R, Bent S: **Hydrogen and fuel cells, emerging technologies and applications**. *International Journal of Hydrogen Energy* 2007, **32**(18):5109-5110.
102. Holladay JD, Hu J, King DL, Wang Y: **An overview of hydrogen production technologies**. *Catalysis Today* 2009, **139**(4):244-260.
103. Gardner D: **Hydrogen production from renewables**. *Renewable Energy Focus*, **9**(7):34-37.
104. Granovskii M, Dincer I, Rosen MA: **Exergetic life cycle assessment of hydrogen production from renewables**. *Journal of Power Sources* 2007, **167**(2):461-471.
105. Levene JI, Mann MK, Margolis RM, Milbrandt A: **An analysis of hydrogen production from renewable electricity sources**. *Solar Energy* 2007, **81**(6):773-780.
106. USDE: **'National Hydrogen Energy Roadmap', based on the results of the national hydrogen roadmap workshop**. In: Editor|. City|: Publisher|; Year|:Pages|. [|Series Editor (Series Editor^Editors|): *Series Title*|, vol Series Volume|]|.
107. Reider R, Edeskuty FJ: **Hydrogen safety problems**. *International Journal of Hydrogen Energy* 1979, **4**(1):41-45.
108. Solomon BD, Banerjee A: **A global survey of hydrogen energy research, development and policy**. *Energy Policy* 2006, **34**(7):781-792.
109. Sakintuna B, Lamari-Darkrim F, Hirscher M: **Metal hydride materials for solid hydrogen storage: A review**. *International Journal of Hydrogen Energy* 2007, **32**(9):1121-1140.
110. Hasan MMF, Zheng AM, Karimi IA: **Minimizing Boil-Off Losses in Liquefied Natural Gas Transportation**. *Industrial & Engineering Chemistry Research* 2009, **48**(21):9571-9580.
111. Lin W, Zhang N, Gu A: **LNG (liquefied natural gas): A necessary part in China's future energy infrastructure**. *Energy* 2010, **35**(11):4383-4391.
112. Tsujikawa Y, Sawada T: **Characteristics of hydrogen-fueled gas turbine cycle with intercooler, hydrogen turbine and hydrogen heater**. *International Journal of Hydrogen Energy* 1985, **10**(10):677-683.
113. Najjar YSH: **Hydrogen fueled and cooled gas turbine engine**. *International Journal of Hydrogen Energy* 1990, **15**(11):827-832.
114. White CM, Steeper RR, Lutz AE: **The hydrogen-fueled internal combustion engine: a technical review**. *International Journal of Hydrogen Energy* 2006, **31**(10):1292-1305.
115. Jin H, Ishida M: **A novel gas turbine cycle with hydrogen-fueled chemical-looping combustion**. *International Journal of Hydrogen Energy* 2000, **25**(12):1209-1215.
116. Zhang X, Han W, Hong H, Jin H: **A chemical intercooling gas turbine cycle with chemical-looping combustion**. *Energy* 2009, **34**(12):2131-2136.
117. Cormos C-C: **Evaluation of iron based chemical looping for hydrogen and electricity co-production by gasification process with carbon capture and storage**. *International Journal of Hydrogen Energy* 2010, **35**(6):2278-2289.
118. Ishida M, Jin H: **A new advanced power-generation system using chemical-looping combustion**. *Energy* 1994, **19**(4):415-422.
119. Hotza D, Diniz da Costa JC: **Fuel cells development and hydrogen production from renewable resources in Brazil**. *International Journal of Hydrogen Energy* 2008, **33**(19):4915-4935.

120. Dicks AL, Diniz da Costa JC, Simpson A, McLellan B: **Fuel cells, hydrogen and energy supply in Australia**. *Journal of Power Sources* 2004, **131**(1-2):1-12.
121. Song C: **Fuel processing for low-temperature and high-temperature fuel cells: Challenges, and opportunities for sustainable development in the 21st century**. *Catalysis Today* 2002, **77**(1-2):17-49.
122. Bennaceur K, Clark B, Franklin M. Orr J, T.S.Ramakrishnan, Roulet C, Stort E: **Hydrogen: A future energy carrier?** *Oilfield Review* 2005.
123. Sharma A, Chen CR, Murty VVS, Shukla A: **Solar cooker with latent heat storage systems: A review**. *Renewable and Sustainable Energy Reviews*, **In Press, Corrected Proof**.
124. Koca A, Oztop HF, Koyun T, Varol Y: **Energy and exergy analysis of a latent heat storage system with phase change material for a solar collector**. *Renewable Energy* 2008, **33**(4):567-574.
125. Sutthivirode K, Namprakai P, Roonprasang N: **A new version of a solar water heating system coupled with a solar water pump**. *Applied Energy* 2009, **86**(9):1423-1430.
126. Shukla A, Buddhi D, Sawhney RL: **Solar water heaters with phase change material thermal energy storage medium: A review**. *Renewable and Sustainable Energy Reviews* 2009, **13**(8):2119-2125.
127. Jiang J, Prausnitz JM: **Equation of state for thermodynamic properties of chain fluids near-to and far-from the vapor--liquid critical region**. *The Journal of Chemical Physics* 1999, **111**(13):5964-5974.
128. Lemmon EW, Huber ML, McLinden MO: **NIST Standard Reference Database 23: Reference Fluid Thermodynamic and Transport Properties-REFPROP**. In: *National Institute of Standards and Technology, Standard Reference Data Program*, 8.0 edition|. Edited Editor|. City|: Publisher|; Year|:Pages|. [|Series Editor (Series Editor^Editors|): *Series Title*|, vol Series Volume|]|.
129. **Pinch technology: basics for the beginners** [http://www.cheresources.com/pinchtech3.shtml]
130. Linnhoff B: **Thermodynamic analysis in the design of process networks**. *Ph.D.* University of Leeds, Department of Chemical Engineering; 1979.
131. Linnhoff B, Flower JR: **Synthesis of heat exchanger networks: I. Systematic generation of energy optimal networks**. *AIChE Journal* 1978, **24**(4):633-642.
132. Linnhoff B, Mason DR, Wardle I: **Understanding heat exchanger networks**. *Computers & Chemical Engineering* 1979, **3**(1-4):295-302.
133. Linnhoff B, Flower JR: **Synthesis of heat exchanger networks: II. Evolutionary generation of networks with various criteria of optimality**. *AIChE Journal* 1978, **24**(4):642-654.
134. Ebrahim M, Kawari A: **Pinch technology: an efficient tool for chemical-plant energy and capital-cost saving**. *Applied Energy* 2000, **65**(1-4):45-49.
135. Kemp IC: **Pinch Analysis and Process Integration - A User Guide on Process Integration for the Efficient Use of Energy (2nd Edition)**. In: Editor|. City|: Publisher|; Year|:Pages|. [|Series Editor (Series Editor^Editors|): *Series Title*|, vol Series Volume|]|.
136. Aspelund A, Berstad DO, Gundersen T: **An Extended Pinch Analysis and Design procedure utilizing pressure based exergy for subambient cooling**. *Applied Thermal Engineering* 2007, **27**(16):2633-2649.
137. Castro P, Matos H, Fernandes MC, Pedro Nunes C: **Improvements for mass-exchange networks design**. *Chemical Engineering Science* 1999, **54**(11):1649-1665.

138. Relvas S, Matos HA, Fernandes MC, Castro P, Nunes CP: **AquoMin: A software tool for Mass-Exchange Networks targeting and design**. *Computers & Chemical Engineering* 2008, **32**(6):1085-1105.
139. Emhamed AM, Lelkes Z, Rev E, Farkas T, Fonyo Z, Fraser DM: **NEW HYBRID METHOD FOR MASS EXCHANGE NETWORK OPTIMIZATION**. In. *Volume 194* Editor|. City|: Publisher|; Year|:Pages|. [|Series Editor (Series Editor^Editors|): *Series Title*|, vol Series Volume|]|.
140. Tan YL, Manan ZA, Foo DCY: **Retrofit of Water Network with Regeneration Using Water Pinch Analysis**. *Process Safety and Environmental Protection* 2007, **85**(4):305-317.
141. Hallale N: **A new graphical targeting method for water minimisation**. *Advances in Environmental Research* 2002, **6**(3):377-390.
142. Prakash R, Shenoy UV: **Targeting and design of water networks for fixed flowrate and fixed contaminant load operations**. *Chemical Engineering Science* 2005, **60**(1):255-268.
143. Agrawal V, Shenoy UV: **Unified conceptual approach to targeting and design of water and hydrogen networks**. *AIChE Journal* 2006, **52**(3):1071-1082.
144. Fonseca A, Sá V, Bento H, Tavares MLC, Pinto G, Gomes LACN: **Hydrogen distribution network optimization: a refinery case study**. *Journal of Cleaner Production* 2008, **16**(16):1755-1763.
145. Zhelev TK, Ntlhakana JL: **Energy-environment closed-loop through Oxygen Pinch**. *Computers & Chemical Engineering* 1999, **23**(Supplement 1):S79-S83.
146. Zhelev TK, Bhaw N: **Combined water-oxygen pinch analysis for better wastewater treatment management**. *Waste Management* 2000, **20**(8):665-670.
147. Tantimuratha L, Kokossis AC, Müller FU: **The heat exchanger network design as a paradigm of technology integration**. *Applied Thermal Engineering* 2000, **20**(15-16):1589-1605.
148. Bogataj M, Bagajewicz MJ: **Synthesis of non-isothermal heat integrated water networks in chemical processes**. *Computers & Chemical Engineering* 2008, **32**(12):3130-3142.
149. Mussati SF, Barttfeld M, Aguirre PA, Scenna NJ: **A disjunctive programming model for superstructure optimization of power and desalting plants**. *Desalination* 2008, **222**(1-3):457-465.
150. Manninen J, Zhu XX: **Level-by-level flowsheet synthesis methodology for thermal system design**. *AIChE Journal* 2001, **47**(1):142-159.
151. Lewin DR, Wang H, Shalev O: **A generalized method for HEN synthesis using stochastic optimization - I. General framework and MER optimal synthesis**. *Computers & Chemical Engineering* 1998, **22**(10):1503-1513.
152. Lewin DR: **A generalized method for HEN synthesis using stochastic optimization -- II.: The synthesis of cost-optimal networks**. *Computers & Chemical Engineering* 1998, **22**(10):1387-1405.
153. Morton W: **Optimization of a heat exchanger network superstructure using nonlinear programming**. *Proceedings of the Institution of Mechanical Engineers, Part E: Journal of Process Mechanical Engineering* 2002, **216**(2):89-104.
154. Chen D, Yang S, Luo X, Wen Q, Ma H: **An Explicit Solution for Thermal Calculation and Synthesis of Superstructure Heat Exchanger Networks**. *Chinese Journal of Chemical Engineering* 2007, **15**(2):296-301.

155. Lotfi R, Boozarjomehry RB: **Superstructure Optimization in Heat Exchanger Network (HEN) Synthesis Using Modular Simulators and a Genetic Algorithm Framework**. *Industrial & Engineering Chemistry Research* 2010, **49**(10):4731-4737.
156. Mussati SF, Aguirre PA, Scenna NJ: **Optimization of alternative structures of integrated power and desalination plants**. *Desalination* 2005, **182**(1-3):123-129.
157. Futterer E, Gruhn G, Lohe B, Noronha S, Rücker A: **Exergy as an objective function to MINLP problems in process synthesis**. *Chemical Engineering & Technology* 1996, **19**(3):203-208.
158. *Proceedings of the The MATLAB genetic algorithm toolbox: 1995.*
159. Prakotpol D, Srinophakun T: **GAPinch: genetic algorithm toolbox for water pinch technology**. *Chemical Engineering and Processing* 2004, **43**(2):203-217.
160. Eurostat: **Energy statistics - supply, transformation, consumption**. In: Editor|. City|: Publisher|; Year|:Pages|. [|Series Editor (Series Editor^Editors|): *Series Title*|, vol Series Volume|]|.
161. Steenhof PA: **Decomposition of electricity demand in China's industrial sector**. *Energy Economics* 2006, **28**(3):370-384.
162. Lan Y, Bin L, Zongxin W: **Present and future power generation in China**. *Nuclear Engineering and Design* 2007, **237**(12-13):1468-1473.
163. EIA: **Electric Power Annual**. In: Editor|. City|: Publisher|; Year|:Pages|. [|Series Editor (Series Editor^Editors|): *Series Title*|, vol Series Volume|]|.
164. Division TUNS: **Energy Statistics Database**. In: Editor|. City|: Publisher|; Year|:Pages|. [|Series Editor (Series Editor^Editors|): *Series Title*|, vol Series Volume|]|.
165. Ashok S: **Peak-load management in steel plants**. *Applied Energy* 2006, **83**(5):413-424.
166. Larjola J: **Electricity from industrial waste heat using high-speed organic Rankine cycle (ORC)**. *International Journal of Production Economics* 1995, **41**(1-3):227-235.
167. Hung TC, Shai TY, Wang SK: **A review of organic rankine cycles (ORCs) for the recovery of low-grade waste heat**. *Energy* 1997, **22**(7):661-667.
168. Khaliq A, Kumar R, Dincer I: **Exergy Analysis of an Industrial Waste Heat Recovery Based Cogeneration Cycle for Combined Production of Power and Refrigeration**. In. *Volume 131* Editor|. City|: Publisher|; Year|:Pages|. [|Series Editor (Series Editor^Editors|): *Series Title*|, vol Series Volume|]|.
169. Khaliq A, Kumar R, Dincer I: **Performance analysis of an industrial waste heat-based trigeneration system**. *International Journal of Energy Research* 2009, **33**(8):737-744.
170. Chen H, Goswami DY, Stefanakos EK: **A review of thermodynamic cycles and working fluids for the conversion of low-grade heat**. *Renewable and Sustainable Energy Reviews* 2010, **14**(9):3059-3067.
171. Shi XJ, Che DF: **Thermodynamic analysis of an LNG fuelled combined cycle power plant with waste heat recovery and utilization system**. *International Journal of Energy Research* 2007, **31**(10):975-998.
172. Pfaff I, Kather A: **Comparative thermodynamic analysis and integration issues of CCS steam power plants based on oxy-combustion with cryogenic or membrane based air separation**. *Energy Procedia* 2009, **1**(1):495-502.
173. Kerry FG: **Industrial gas handbook: gas separation and purification**. Boca Raton: CRC Press; 2007.

174. Cheddie DF, Murray R: **Thermo-economic modeling of an indirectly coupled solid oxide fuel cell/gas turbine hybrid power plant**. *Journal of Power Sources* 2010, **195**(24):8134-8140.
175. Sayyaadi H, Babaelahi M: **Thermoeconomic optimization of a cryogenic refrigeration cycle for re-liquefaction of the LNG boil-off gas**. *International Journal of Refrigeration* 2010, **33**(6):1197-1207.
176. Silveira JL, Tuna CE: **Thermoeconomic analysis method for optimization of combined heat and power systems. Part I**. *Progress in Energy and Combustion Science* 2003, **29**(6):479-485.
177. Lazzaretto A, Macor A: **Direct Calculation of Average and Marginal Costs From the Productive Structure of an Energy System**. *Journal of Energy Resourse and Technology* 1995, **117**(3):171-178.
178. De Lima AC, Guimaraes SC, Camacho JR, Bispo D: **Electric energy demand analysis using fuzzy decision-making system**. *Melecon 2004: Proceedings of the 12th Ieee Mediterranean Electrotechnical Conference, Vols 1-3* 2004:811-814.
179. Rabl A, Norford LK: **Peak load reduction by preconditioning buildings at night**. *International Journal of Energy Research* 1991, **15**(9):781-798.
180. Graus W, Worrell E: **Trend in efficiency and capacity of fossil power generation in the EU**. *Energy Policy* 2009, **37**(6):2147-2160.
181. Denton MJ, Rassenti SJ, Smith VL, Backerman SR: **Market power in a deregulated electrical industry**. *Decision Support Systems* 2001, **30**(3):357-381.
182. Harumi W, Koichi C, Osamu Y: **Cold heat reused air liquefaction/vaporization and storage gas turbine electric power system**. In: *United States Patent*. *Volume US 6,920,795 B2* Editor|. City|: Publisher|; Year|:Pages|. [|Series Editor (Series Editor^Editors|): *Series Title*|, vol Series Volume|]|.
183. Vandor D: **System and method for liquid air production, power storage and power release**. In. *Volume US 8,020,404,B2* Editor|. City|: Publisher|; Year|:Pages|. [|Series Editor (Series Editor^Editors|): *Series Title*|, vol Series Volume|]|.
184. Davison J: **Performance and costs of power plants with capture and storage of CO2**. *Energy* 2007, **32**(7):1163-1176.
185. Yang H, Xu Z, Fan M, Gupta R, Slimane RB, Bland AE, Wright I: **Progress in carbon dioxide separation and capture: A review**. *Journal of Environmental Sciences* 2008, **20**(1):14-27.
186. Geoffrey PH, Serge SOA: **Thermodynamic and related analysis of natural gas combined cycle power plants with and without carbon sequestration**. *International Journal of Energy Research* 2007, **31**(12):1180-1201.
187. Pyong Sik P, Young Duk L, Kook Young A: **Characteristic evaluation of a CO2-capturing repowering system based on oxy-fuel combustion and exergetic flow analyses for improving efficiency**. *International Journal of Energy Research* 2010:In press.
188. Chen H, Ding Y, Peters T, Berger F: **A method of storing energy and a cryogenic energy storage system**. In. *Volume PCT/GB2007/000667* Editor|. City|: Publisher|; Year|:Pages|. [|Series Editor (Series Editor^Editors|): *Series Title*|, vol Series Volume|]|.
189. Castle WF: **Air separation and liquefaction: recent developments and prospects for the beginning of the new millennium**. *International Journal of Refrigeration* 2002, **25**(1):158-172.

190. Weisberg AH, Aceves SM, Espinosa-Loza F, Ledesma-Orozco E, Myers B: **Delivery of cold hydrogen in glass fiber composite pressure vessels**. *International Journal of Hydrogen Energy* 2009, **34**(24):9773-9780.
191. Richard; D, A. G, M. C, Jean-Pierre T, Nicolas P: **Air separation Unit: Flexibility & Energy Storage**. In: *2nd Oxyfuel Combustion Conference: 2011; Queensland, Australia*; 2011.
192. K Hossain A, Badr O: **Prospects of renewable energy utilisation for electricity generation in Bangladesh**. *Renewable and Sustainable Energy Reviews* 2007, **11**(8):1617-1649.
193. Lior N: **Energy resources and use: The present (2008) situation and possible sustainable paths to the future**. *Energy* 2010, **35**(6):2631-2638.
194. *Proceedings of the Solar Power – Photovoltaics or Solar Thermal Power Plants?: 2001; Brussels.*
195. Zhai XQ, Wang RZ: **Experimental investigation and performance analysis on a solar adsorption cooling system with/without heat storage**. *Applied Energy* 2010, **87**(3):824-835.
196. García-Rodríguez L, Blanco-Gálvez J: **Solar-heated Rankine cycles for water and electricity production: POWERSOL project**. *Desalination* 2007, **212**(1-3):311-318.
197. Horn M, Führing H, Rheinländer J: **Economic analysis of integrated solar combined cycle power plants: A sample case: The economic feasibility of an ISCCS power plant in Egypt**. *Energy* 2003, **29**(5-6):935-945.
198. Michael F, Borislav B: **High temperature metal hydrides as heat storage materials for solar and related applications**. *International Journal of Molecular Sciences* 2009(10):325-344.
199. Winter CJ, Sizmann RL, Vant-Hull LL: **Solar power plants: Fundamentals, technology, systems economics**. Berlin: Springer-Verlag; 1991.
200. Li Y, Chen H, Ding Y: **Fundamentals and applications of cryogen as a thermal energy carrier: A critical assessment**. *International Journal of Thermal Sciences* 2010, **49**(6):941-949.
201. Chen H, Ding Y: **An Overview of Air Liquefaction and Separation Process**. In: Editor|. City|: Publisher|; Year|:Pages|. [|Series Editor (Series Editor^Editors|): *Series Title*|, vol Series Volume|]|.
202. Srinophakun T, Laowithayangkul S, Ishida M: **Simulation of power cycle with energy utilization diagram**. *Energy Conversion and Management* 2001, **42**(12):1437-1456.
203. Fernández-García A, Zarza E, Valenzuela L, Pérez M: **Parabolic-trough solar collectors and their applications**. *Renewable and Sustainable Energy Reviews*, **14**(7):1695-1721.
204. Berstad DO, Stang JH, Nekså P: **Comparison criteria for large-scale hydrogen liquefaction processes**. *International Journal of Hydrogen Energy* 2009, **34**(3):1560-1568.
205. Gorji-Bandpy M, Goodarzian H, Biglari M: **The Cost-effective Analysis of a Gas Turbine Power Plant**. *Energy Sources, Part B: Economics, Planning, and Policy* 2011, **5**(4):348-358.
206. Nelson DB, Nehrir MH, Wang C: **Unit sizing and cost analysis of stand-alone hybrid wind/PV/fuel cell power generation systems**. *Renewable Energy* 2006, **31**(10):1641-1656.